Acidic Organocatalysts toward Ring-Opening Polymerization Leading to Well-Defined Polyesters

A Dissertation for the Degree of Doctor of Engineering

KOSUKE MAKIGUCHI

Hokkaido University

March, 2014

Acknowledgements

The study presented in this dissertation has been performed under the direction of Professor Toyoji Kakuchi, Division of Biotechnology and Macromolecular Chemistry, Faculty of Engineering, Hokkaido University, from 2009 to 2014. The author wishes to offer his immeasurable gratitude to his sincere appreciation to Professor Toyoji Kakuchi, for his kind instruction, helpful advice, and unstinting encouragement during the course of this work.

The author is also deeply grateful to Professor Toshifumi Satoh, Division of Biotechnology and Macromolecular Chemistry, Faculty of Engineering, Hokkaido University, for his helpful and valuable suggestions with continuous encouragement throughout this work. The author is further indebted to Associate Professor Ryosuke Sakai, Department of Material Chemistry, Asahikawa National College of Technology, Associate Professor Sin-ichiro Sato, Division of Biotechnology and Macromolecular Chemistry, Faculty of Engineering, Hokkaido University, and Drs. Ryohei Kakuchi, Hideki Misaka, and Keita Fuchise for their practical guideline and fruitful discussions. The author would like to express special thanks to Messrs. Yoshitaka Ogasawara, Seiya Kikuchi, and Tatsuya Saito for their fine contributions to this dissertation work. The author would also like to acknowledge Dr. Harumi Kaga, National Institute of Advanced Industrial Science and Technology (AIST), and Dr. Frédéric Peruch, Laboratoire de Chimie des Polymères Organiques, University of Bordeaux, for making a number of helpful suggestions and supporting research life in AIST and Bordeaux. The author owes his deep gratitude to members in Professor Kakuchi's laboratory and Professor Satoh's laboratory for their friendship, accommodating help and creating cheerful and active environment in the laboratory.

The author is very grateful to the Research Fellowships of the Japan Society for the Promotion of Science (JSPS) for Young Scientists during 2012–2014.

Finally, the author would like to express deep appreciation to his family for their understanding, support, and continuous encouragement throughout his research and daily life.

March, 2014

Kosuke Makiguchi

Contents

Chapter 1

General Introduction

1.1 Organocatalyst for the Ring-opening Polymerization (ROP)

In recent years, the metal-free syntheses of organic compounds have attracted much attention along with the increasing concerns for green chemistry. Since List used L-proline as the first organocatalyst in 2000, as shown Figure 1.1,[1, 2] many metal catalysts were replaced by organocatalysts in organic syntheses. In particular, MacMillan investigated that imidazolidinone, which is a non-metallic chiral catalyst, showed a comparable ability to metallic chiral catalysts for providing a high enantioselectivity in asymmetric reactions, and Maruoka created chiral phase transfer catalysts consisting of a quaternary ammonium compound leading to a high reaction efficiency.[3, 4] Furthermore, the futures such as chemical stability, low toxicity, tunable structure, etc., were preferred for other synthetic strategies and many reactions were carried out using organocatalysts. To date, organocatalytic synthesis has been expanded to polymer synthesis due to its reliable ability.[5 ,6]

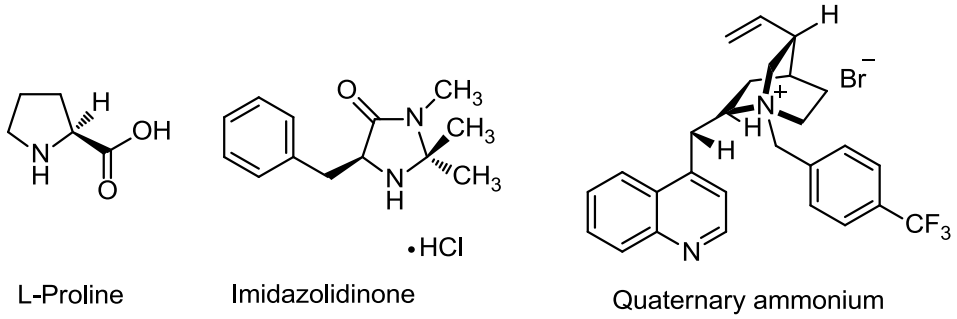

Figure 1.1. Primitive organocatalysts for organic reactions.

Organocatalytic polymerizations were mainly provided by Hedrick and Waymouth. Since Hedrick reported that 4-dimethylaminopyridine (DMAP) was effective for the ring-opening polymerization (ROP) of the lactide (LA), which is one of the most researched cyclic esters.[7] The resultant polymer, polylactide (PLA), has a biodegradability and biocompatibility, thus it

is useful to use organocatalysts in the synthetic route from the view point of environmental friendly methods. Whereas several reports regarding the organocatalytic polymerization of other monomers, such as hererocyclic monomers (cyclic carbonate,[8-10] morpholinedione,[11] epoxide, [12-19] lactam,[20] siloxane,[21, 22] phosphate,[23-27] carboxyanhydride,[28] and cyclopropane[29, 30]), and vinyl monomers (acrylate, methacrylate, and acryl amide)[31-39] were evaluated, as shown in Figure 1.2, the organocatalytic ROP of cyclic esters has aroused significant interest.

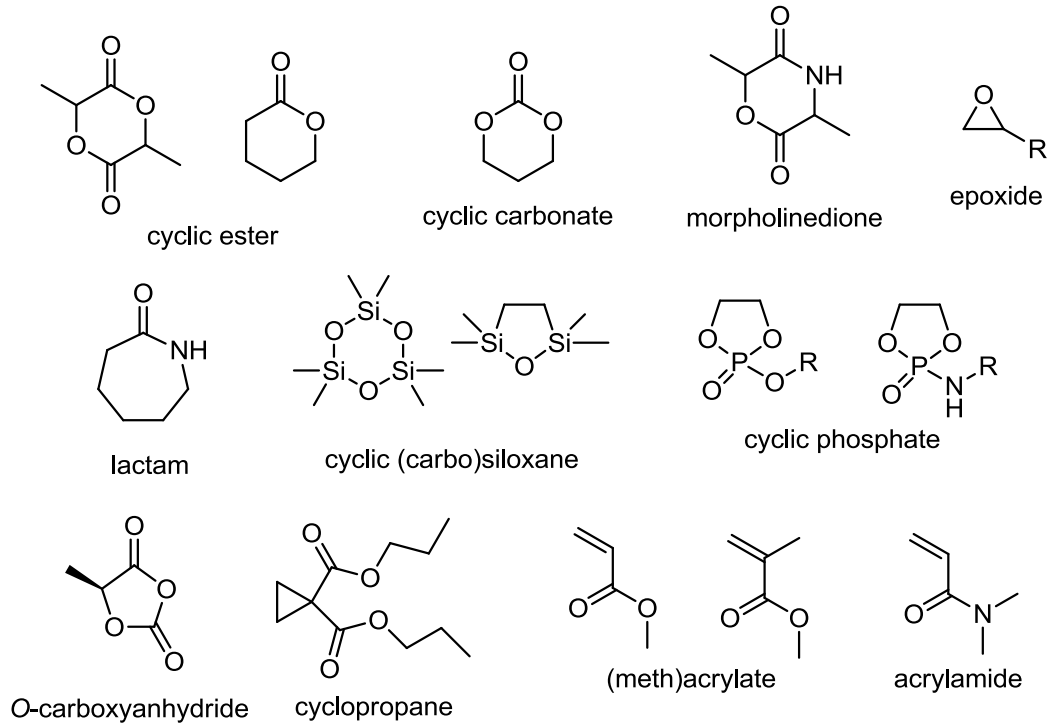

Figure 1.2. Applicable monomers for organocatalytic polymerization.

For the ROP of cyclic esters, the fundamental reaction is the Fischer esterification, as shown in Scheme 1.1. The reaction was absolutely simple, thus number of researchers tried to adopt the organocatalytic or organometallic transesterification reaction for the polymerization reaction. The most important part is the activation of the carbonyl group and/or alcoholic OH group. Before the organocatalytic ROP was investigated, metal catalysts having a Lewis acidic metal center were utilized for activating the monomer and/or initiator.[40-45] Tin or

aluminum-centered catalysts were widely utilized for the ROP of cyclic esters.[46-51] The mechanisms were classified as (a) coordination-insertion, (b) monomer activation, or (c) anionic initiation/propagation mechanisms, as shown in Scheme 1.2. Schemes 1.2a and 1.2b commonly went through the Lewis acidic activation of the carbonyl group of the monomer, and then the nucleophilic part of the catalysts or additional alcohol acted as an initiator and attacked the monomer. On the other hand, alkali metals, such as lithium, sodium and potassium, could generate an alkali metal alkoxide having a strong nucleophilicity, which simply promoted the anionic polymerization of the lactide, as shown in Scheme 1.2c.

Scheme 1.1. Schematic model of Fishcer esterification reaction

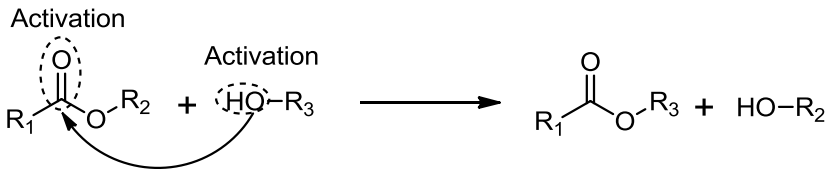

Scheme 1.2. Metal-catalyzed ring-opening polymerization of lactide via (a) coordination-insertion mechanism, (b) monomer activation mechanism, and (c) anionic initiation mechanism

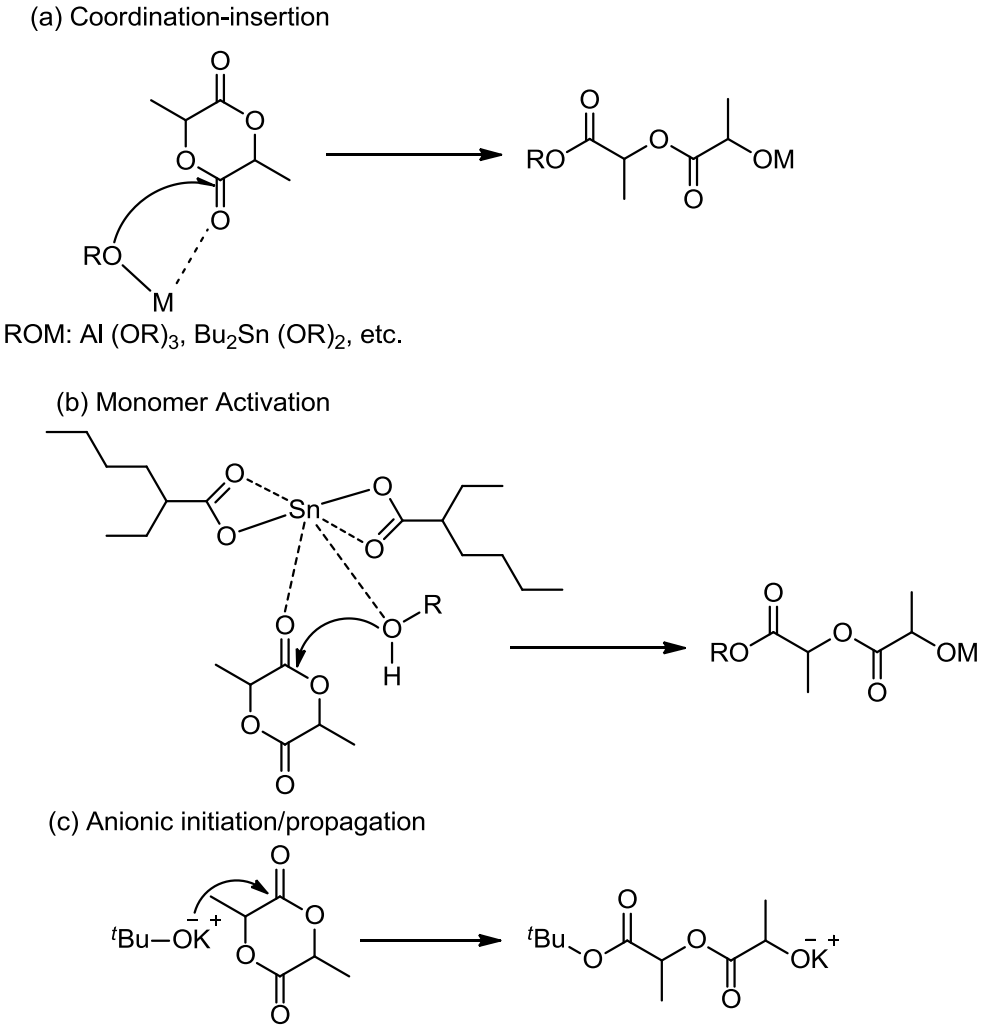

For achieving the organocatalytic ROP, the catalysts were designed to exert the appropriate ability by tuning their elcectrophilicity/nucleophilicity and/or acidity/basicity.[8-10, 52-55] As described below, the primitive strategy generatd active species by the nucleophilicity or basicity of the catalysts because the early type electrophilic/acidic organocatalysts had a weak ability compared to metal catalysts and were incapable of driving the polymerization reactions.

1.2 Organic Base-Catalyzed ROP

For the organocatalyzed-ROP, organic bases were the main focus due to their highly catalytic ability. In the presence of an alcohol initiator, the polymerization proceeded via the basic activation of the initiator/propagating chain-end or nucleophilic monomer activation, as shown in Scheme 1.3.[53]

Scheme 1.3. Organic base-catalyzed ring-opening polymerization of lactide via (a) monomer activation mechanism and (b) initiator/chain-end activation mechanism

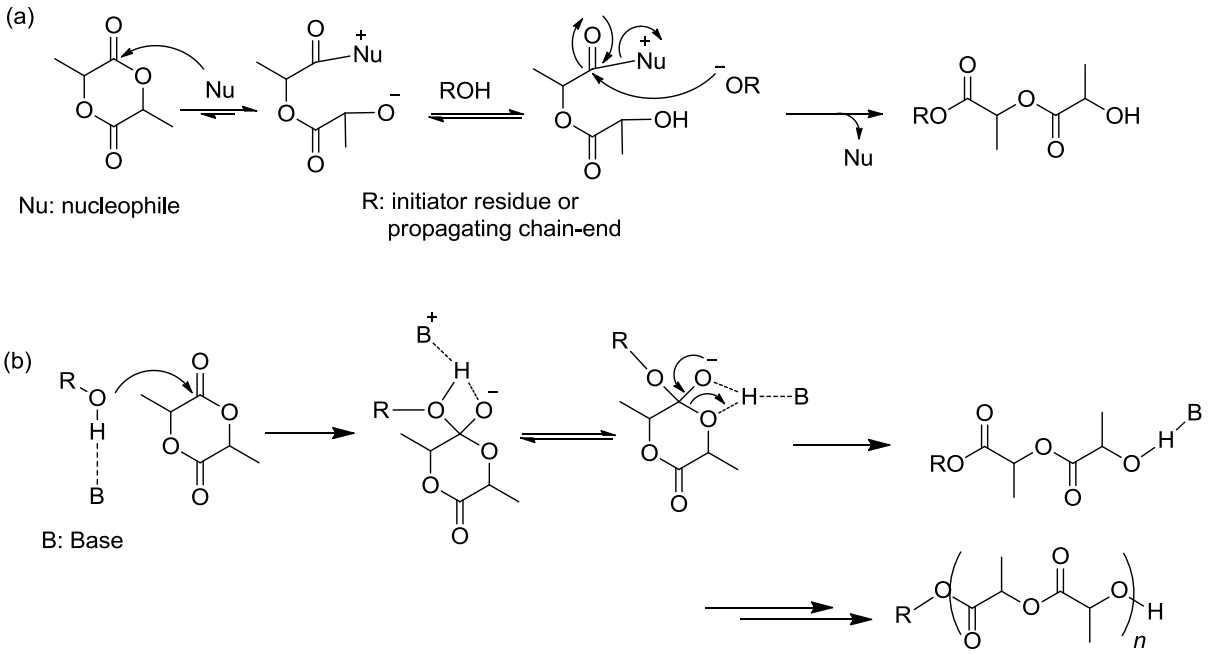

Figures 1.3 and 1.4 show the representative organic base catalysts. Since Hedrick et al. reported that DMAP and 4-pyrrolidinopyridine (PPY)[7] were effective for the ROP of LA leading to the polymer production with predictable molecular weights and narrow polydispersities, many reports have been published. For the nucleophilic monomer activation (Scheme 1.3a), *N*-heterocyclic carbenes (NHCs) were the most established catalysts.[56] The

NHC could activate the carbonyl group of the monomer via nucleophilic activation, and subsequent protonation of the zwitterionic alkoxide by the initiating or propagating alcohol (ROH) leads to the formation of a ring-opened adduct. Therefore, the reaction is repeated to produce the linear polylactide (PLA) (Scheme 1.4a).[57, 58] In addition, the zwitterionic chain ends afford the cyclic PLA in the absence of an initiator, as shown in Scheme 1.4b.[59, 60] Thanks to its high nucleophilicity, the NHCs also showed a catalytic ability for the ROPs of the cyclic monomers, such as δ-valerolactone (δ-VL),[61] ε-caprolactone (ε-CL),[61, 62] β-butyrolactone (β-BL),[63-67] and trimethylene carbonate (TMC),[8, 10] meaning that the strong nucleophilic monomer activation was a reliable method. In addition, the phopshines have the nucleophilic monomer activation property and the polymerization was controlled by changing the substituent on the phosphine by controlling the potential reactivity of the monomer.[68]

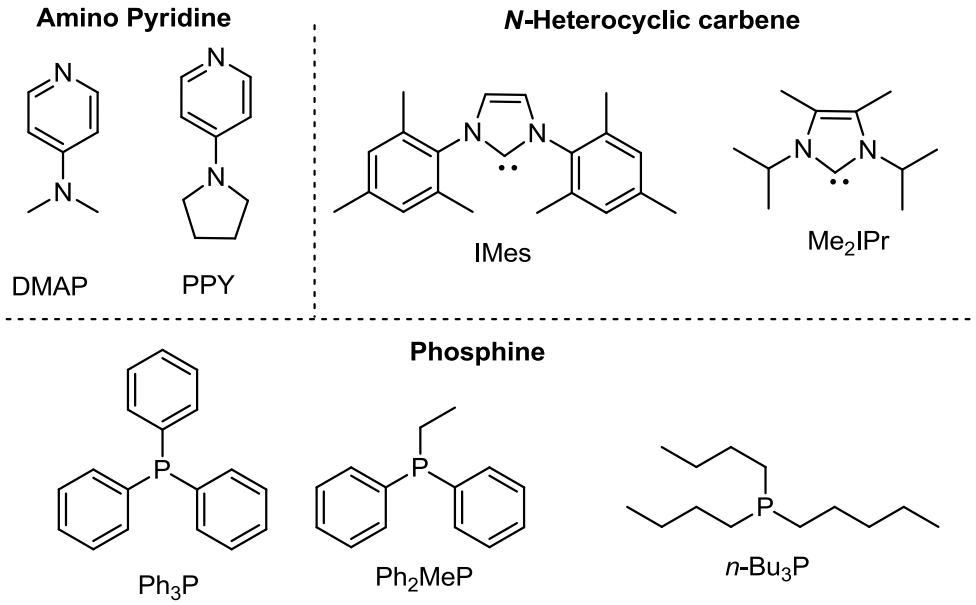

Figure 1.3. Representatives of nucleophilic organocatalysts.

Scheme 1.4. Synthesis of (a) linear polylactide via nucleophilic monomer activation and (b) cyclic polylactide via zwitterionic polymerization

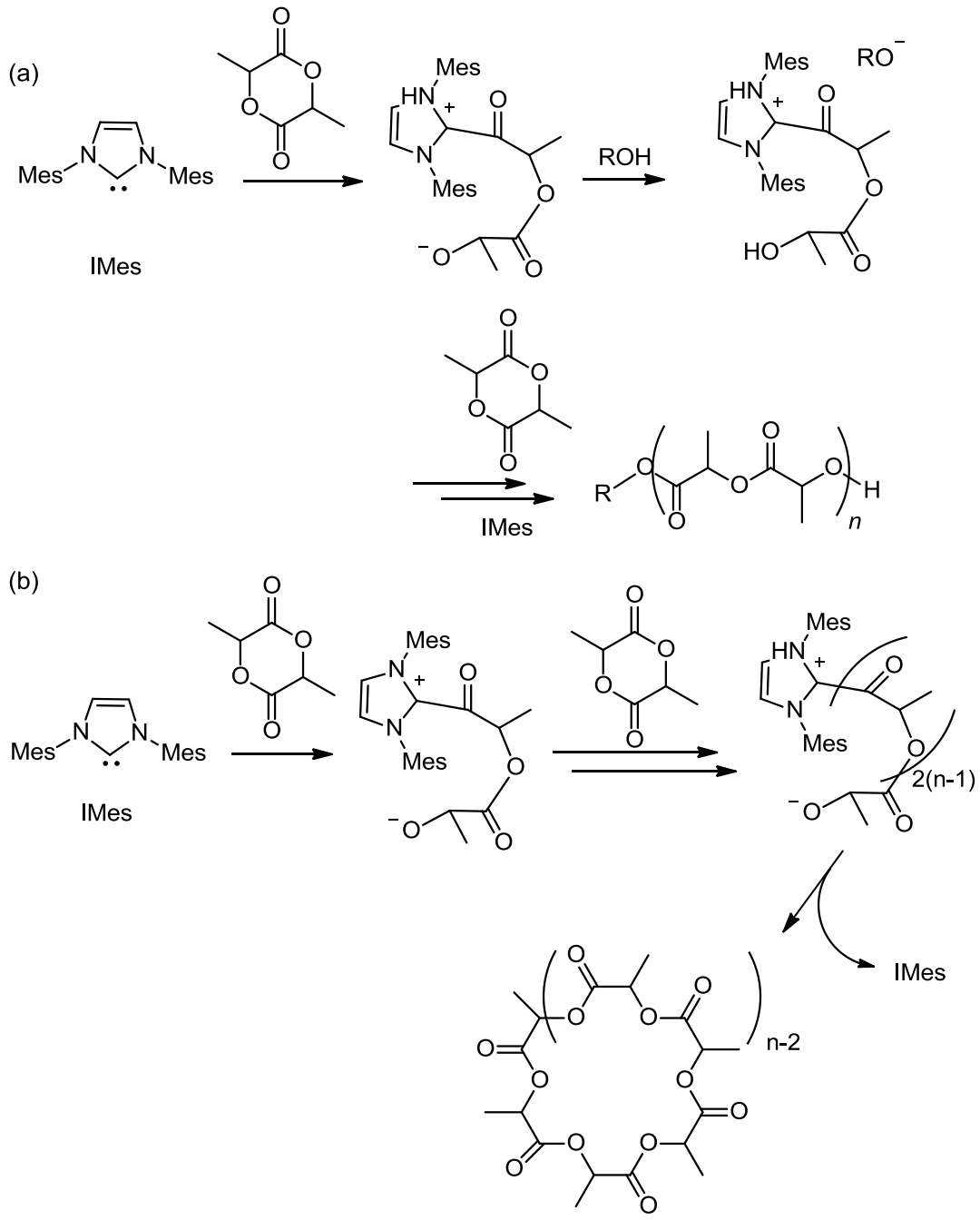

To control the polymerization, the basic activation of the initiator and propagating chain-end was one of the effective strategies (Scheme 1.3b). The catalysts having a low nucleophilicity and high Brønsted basicity were applicable for the basic activated-ROP. The cyclic amidine and cyclic/acyclic guanidine, which are categorized as super bases, have a

relatively high basicity leading to the controlled/living polymerization of LA.[69-71] Regarding the versatility of these catalysts, only 1,5,7-triazabicyclo[4.4.0]dec-5-ene (TBD) promoted the ROPs of the lactones such as *δ*-VL and *ε*-CL ,[8-10, 70, 71] whereas 1,8-diazabicyclo[5.4.0]undec-7-ene (DBU) and *N*-methyl-TBD (MTBD) were insufficient to polymerize these monomers.[71] These findings implied that TBD had two activation sites for the monomer and initiator; the proton donor site in the molecule to activate these monomers accompanied by basic activation of the OH group in the initiator/propagating chain-end lead to production of the polymers via bifunctional activation (see the section below). On the other hand, the basicity of DBU and MTBD was not enough to catalyze the ROP of the lactones.

More basic catalysts, i.e., phosphazene bases, could afford a wide range of well-defined polyesters (PLA and polylactones) due to strong activation of the propagating chain-end. 2-*tert*-Butylimino-2-diethylamino-1,3-dimethylperhydro-1,3,2diazaphosphorine (BEMP), *tert*-butylimino-tris(dimethylamino)phosphorane (P_1-*t*-Bu), and 1-*tert*-butyl-2,2,4,4,4-pentakis(dimethylamino)-2Λ^5,4Λ^5-catenadi(phosphazene) (P_2-*t*-Bu) were used for the polymerization of LA, *δ*-VL, *ε*-CL, and TMC.[8-10, 72, 73]

Furthermore, for the ROP of *β*-BL, amidine, guanidine and BEMP could produce the polymeric material. Unfortunately, these bases have the potential ability to initiate the polymerization and the crotonylation occurred during the early stage of the polymerization leading to production of a polymer having a catalyst residue at the α-chain-end and an acrylic group at the ω-chain-end in some cases, as shown in Scheme 1.5a.[74-76] On the other hand, phosphazene bases, such as P_1-*t*-Bu, P_2-*t*-Bu, and 1-*tert*-butyl-4,4,4-tris(dimethylamino)-2,2-bis[tris(dimethylamino)phosphoranylidenamino]-2Λ^5,4Λ^5-catenadi(phosphazene) (P_4-*t*-Bu), were applicable for the ROP of *β*-BL via activation of the carboxylic acid chain-end, as shown in Scheme 1.5b.[77, 78]

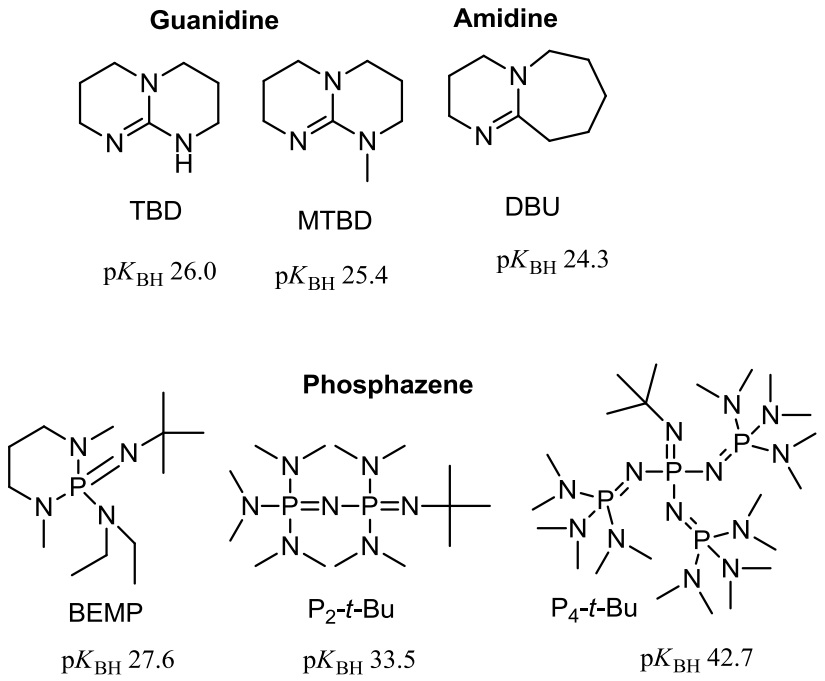

Figure 1.3. Representatives of basic organocatalysts.

Scheme 1.5. Ring-opening polymerization of β-butyrolactone using super bases

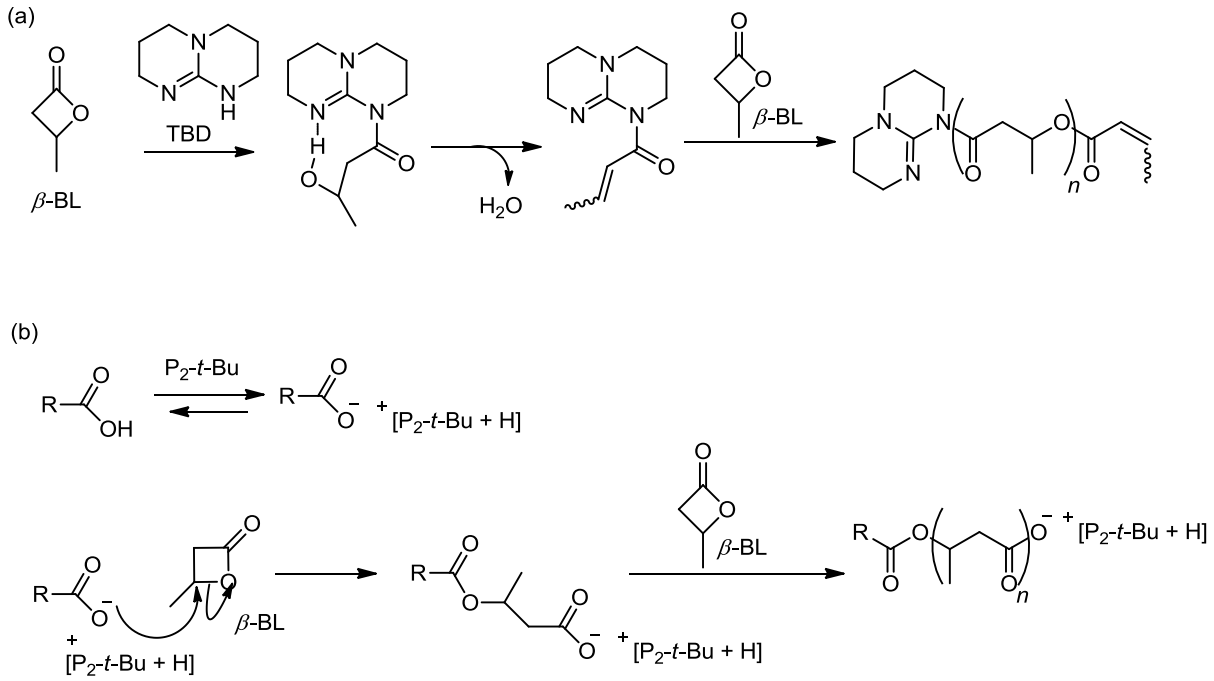

1.3 Bifunctional Organocatalysts for the ROP

The combination of monomer activation and chain-end activation constructed a new paradigm for the ROP. Thiourea/amine was the first reported catalyst to introduce this concept.[79, 80] Thiourea worked as an H-bond donor to electrophilically activate the carbonyl group of the monomer and the additional amine acted as an H-bond acceptor to enhance the nucleophilicity of the propagating chain-end, as shown in Scheme 1.6. Thiourea/amine type catalysts have two activation sites in one molecule (tethered structure), and cinchona alkaloid and imidodiphosphoric acid were also classified as proton donor/proton acceptor type.[81-83] The H-bond donor and acceptor also worked as separate molecules, thus a wide-range of combinations of two molecules were screened, e.g., a variety of tertiary amines were evaluated as co-catalysts for thiourea, and the result showed that (-)-sparteine and tris[2-(dimethylamino)ethyl]amine (Me_6TREN) has the ideal ability by a chelate effect.[80, 84] With the increasing investigation of the H-bond acceptors, various H-bond donors, such as an amide,[85, 86] sulfon amide,[87] phenol,[88, 89] and fluorinated alcohol[90], have also been reported, and these H-bond donors with (-)-sparteine produced a well-defined PLA. In particular, the combination of DBU and thiourea showed the ability for the polymerization of δ-VL and ε-CL. These polymerizations could not be achieved by only DBU or thiourea, meaning that a complementary use was important to carry out the polymerization.[71]

Scheme 1.6. Bifunctional thiourea/amine-catalyzed ring-opening polymerization of *rac*-lactide

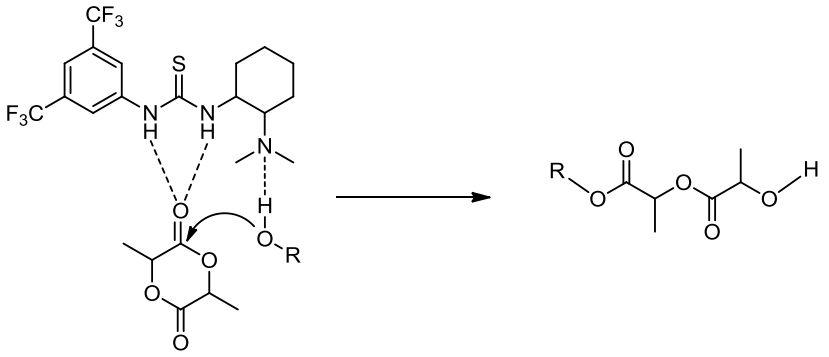

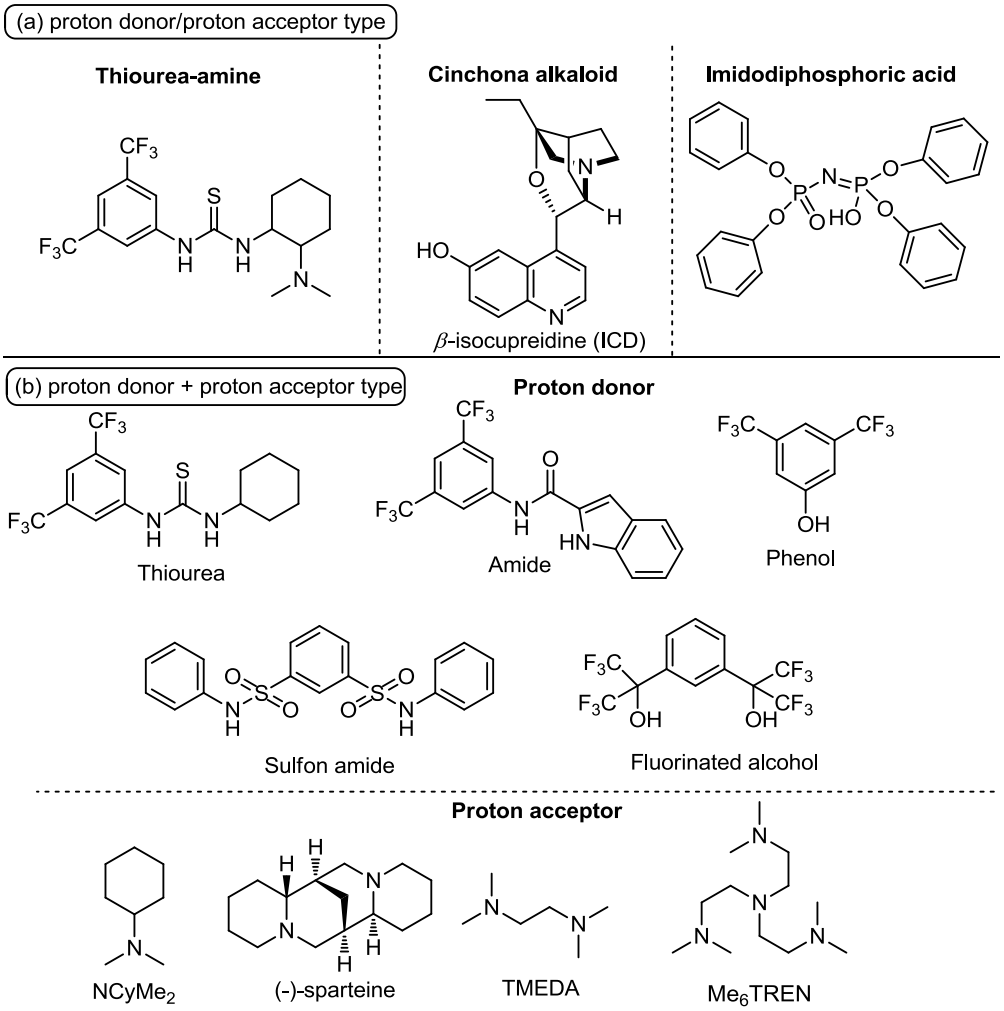

Figure 1.4. Representatives of bifunctional organocatalysts; (a) proton donor/proton acceptor type and (b) proton dononor + proton accepter type.

1.4 Organic Acid-Catalyzed ROP

In contrast to the previously reported organic base-catalyzed ROP, organic acids have attracted much attention due to its simple activation mechanism. In advance of the development of the organic acid-catalyzed ROP, Endo et al. reported that hydrogen chloride (HCl)[91] with a diethyl ether complex induced the acidic monomer activation, which has a high activity for the ROP of lactones and cyclic carbonates, as shown in Scheme 1.7.[92] The concept was comparable to the successful polymerization of LA with a highly controlled molecular weight of the resultant polymers. The end-functionalized polyesters were successfully produced by the HCl-catalyzed ROP of lactones with initiators having functional substituent, such as a bromide, acrylate, etc.[93] It is hard to introduce these functional groups to the resultant polymers via the organic base catalyzed-ROP. Inspired by the HCl-catalyzed system, several organic acid compounds were investigated, as shown in Figure 1.5. The carboxylic acids or amino acids-catalyzed ROP of δ-VL was previously reported.[94, 95] However, the polymerization was conducted under extremely hard conditions (temperature, 120 °C; 10 mol % of catalysts relative to monomer required) because of the weak acidity. Hence, an organic acid-catalyzed system is now being developed.

Scheme 1.7. HCl-catalyzed ring-opening polymerization of cyclic ester via monomer activation mechanism

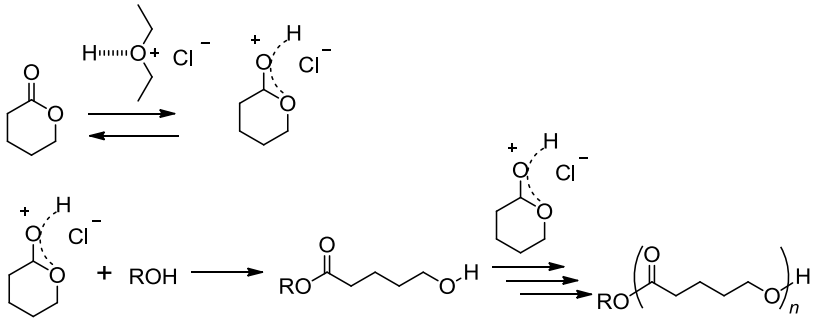

For expanding the scope and limit of the organic acid-catalyzed ROP, Bourissou et al. reported that sulfonic acid could be used for the ROP of LA and ε-CL.[96-100] Methane sulfonic acid (MsOH) and trifluoromethane sulfonic acid (TfOH) were evaluated; the results showed that MsOH promoted the controlled polymerization of ε-CL at room temperature due to its relatively strong acidity (pK_a -2 in CH_2Cl_2)[98] and TfOH successfully proceeded the polymerization of LA, which was a slightly polymerized monomer using an organic acid, by enhancing the monomer activation due to its extremely strong acidity (pK_a -13 in CH_2Cl_2)[96]. Although suitable catalysts were investigated for the ROP of cyclic monomers thanks to the high monomer activation ability, there are some problems regarding the versatility of these catalysts. For instance, the TfOH-catalyzed ROP of ε-CL and TMC were insufficient to control the polymerization because its high acidity caused a chain-end deactivation leading to only an oligomer production.[101] For the catalytic ability of MsOH, the MsOH-catalyzed ROP of TMC proceeded in two pathways, i.e., a monomer activation mechanism and chain-end activation mechanism, as shown in Scheme 1.8, thus the chain-end activation must be avoided by lowering the instantaneous monomer concentration via the multifeed or continuous addition of the monomer.[102] In addition to Bourissou's work, Takasu et al. examined the ROP of ε-CL using nonafluorobutanesulfonimide (Nf_2NH) and nonafluorobutanesulfonic acid (NfOH) as a catalyst.[103] Although the polymerization proceeded under moderate conditions, the molecular weights of the obtained polymer were limited to ca. 10000 g mol^{-1} and the polydespersiy indices were relatively wide values. Thus the organic acid-catalyzed ROP still remains to be optimized.

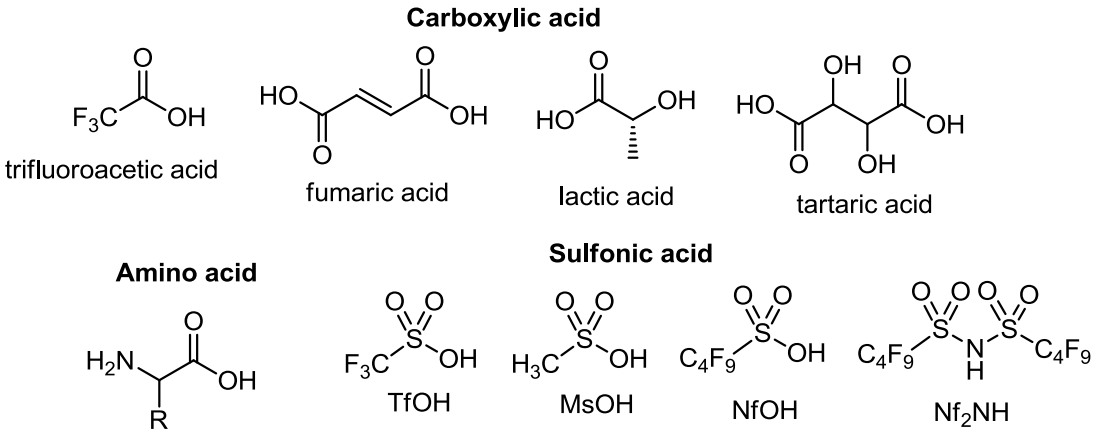

Figure 1.5. Representatives of acidic organocatalysts.

Scheme 1.8. MsOH-catalyzed ring-opening polymerization of TMC via (a) monomer activation and chain end activation mechanism

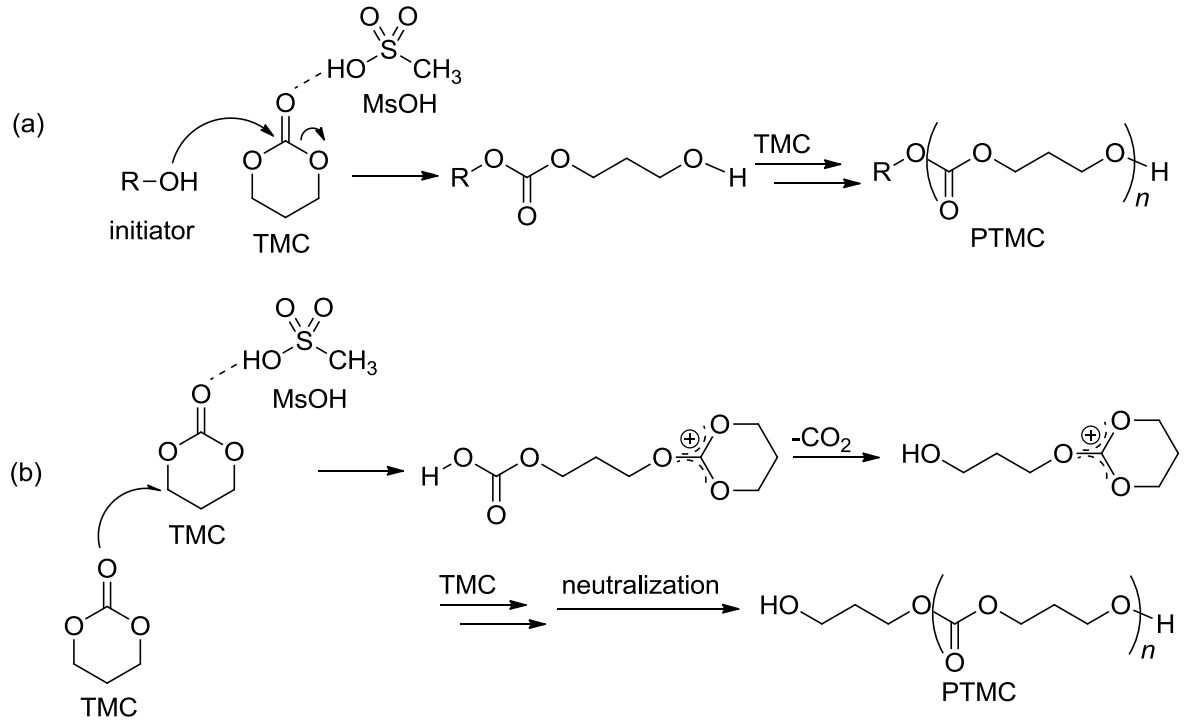

For generating suitable polymerization conditions, it is important to select the appropriate acidity of the catalysts. On the other hand, it is useful to create a simultaneous activation as demonstrated by bifunctional catalysts, mentioned above. For the organic acid-catalyzed

system, the use of the Brønsted base part in the organic acid compounds has attracted attention.[104, 105] Notably, the combination of methanol and phosphoryl oxygen (P=O) in phosphate formed the strongest conjugate base compared to that of the sulfonyl oxygen (S=O) in sulfonate and carboxylic oxygen (C=O) in carboxylate, as shown in Figure 1.6.[104] Therefore, the OH proton of the initiator/chain-end could be easily captured and the initiating/propagating property was activated leading to "dual activation", which consisted of the acidic monomer activation and basic initiator/chain-end activation (the system is different from the "bifunctional activation" mechanism). However, phosphoric acids have not been utilized for the ROP despite their reliable properties.

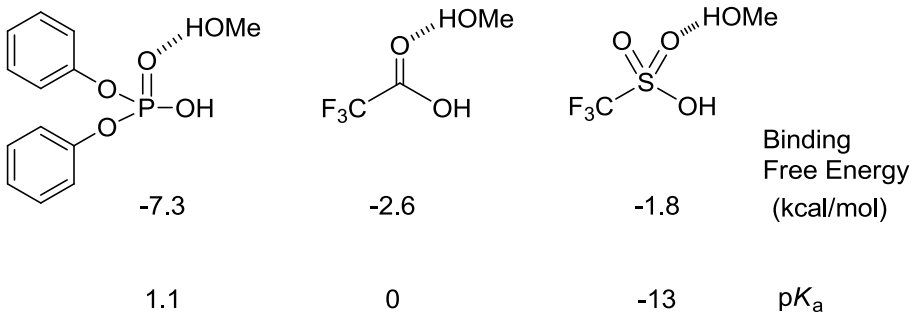

Figure 1.6. Energetics of adducts between methanol and various acids as calculated at the B3PW91/6-31G(d,p) level of theory.[104]

1.5 Stereocontrol Polymerization of rac-Lactide (rac-LA) Using Organocatalyst

In the field of organic reactions, organocatalysts have been attracted much attention due to their high enantioselectivity for asymmetric reactions. For the organocatalyzed ROP, the use of organocatalysts for the stereoselective and enantiomer-selective polymerization was less reported though the metal-mediated polymerization of *rac*-LA was widely validated.[106, 107] For the stereocontrol synthesis of a polymer, PLA is an attractive target, which is generally composed of a random sequence of D-lactide (DLA) and L-lactide (LLA) leading to an atactic polymer. However, the sequence controlled PLA having a regulated tacticity exhibited preferred physical properties, e.g., the isotactic PLA had a melting point (T_m) of 180 °C whereas the atactic PLA has no T_m because it is an amorphous material.[108, 109] To obtain the stereoregulated PLA, there are two ways for controlling the monomer reaction order. One is the "chain-end control" mechanism, as shown in scheme 1.9.[110, 111] In this route, the propagating chain-end consisting of LLA preferentially reacted with the extra LLA, thus the obtained polymer was composed of only LLA, although a stereoerror subsequently occurs leading to the production of isotactic stereoblock PLA. In general, the catalysts had an achiral ligand, which contributed to creating a selective reaction pathway due to its bulkiness.

Scheme 1.9. Synthesis of isotactic and stereoblock polylactide by ring-opening polymerization of *rac*-lactide via "chain-end control" mechanism

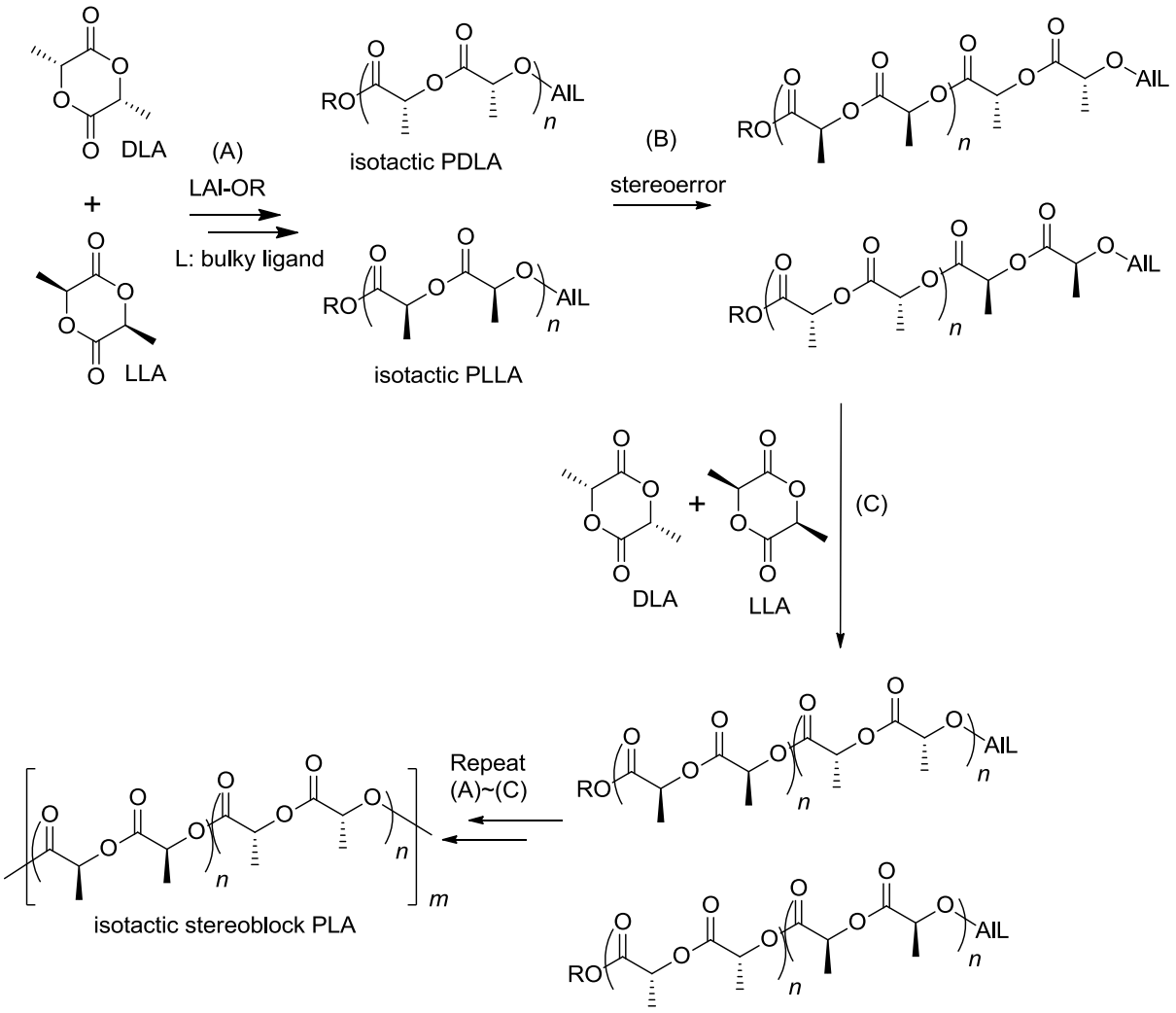

Notably, P_2-*t*-Bu has the ability to enable the production of the highly stereoregulated PLA via the ROP of *rac*-LA at -78 °C with the isotactic probability (P_m) of 0.95.[73] The residual monomer was not enantioriched meaning that each polymerization of DLA and LLA simultaneously proceeded. In addition, NHC,[112] thiourea/amine[80] and guanidine[69] also produced the isotactic enriched PLA, thus the organocatalytic stereocontrol polymerization has made advancements.

In contrast to the "chain-end control" mechanism, the polymerization of *rac*-LA proceeded via the "enantiomorphic-site control" mechanism, which leads to the enantiomer-selective polymerization, as shown in Scheme 1.10. For instance, the selective activation of the monomer and/or propagating chain-end was derived from chiral catalysts, resulting in the preferential polymerization of DLA due to the rate difference between the DLA and LLA polymerizations. Ideally, the subsequential polymerization of LLA afforded the stereoblock PLA. For the organometallic polymerization, Al centered catalysts having a chiral ligand, such as *N*,*N*'-disalicylalethylenediamine (SALEN) or a saturated version of SALEN (SALAN), led to the enantiomer-selective polymerization.[113-117] The most successful example was reported using the Spaskky's Al-SALEN catalyst (selectivity factor, k_D/k_L of 20).[113] For applying the mechanism in the presence of racemic Al catalysts each having a chirality, DLA and LLA simultaneously polymerized and both isotactic PLAs were produced.[116] In the field of organocatalytic ROP, only the cinchona alkaloid showed an enantiomer-selective future with a k_L/k_D up to 4.4.[81] Thus the organocatalytic enantiomer-selective polymerization is still a remaining task.

Scheme 1.10. Synthesis of isotactic polylactide by ring-opening polymerization of *rac*-lactide via "enantiomorphic-site control" (kinetic resolution) mechanism

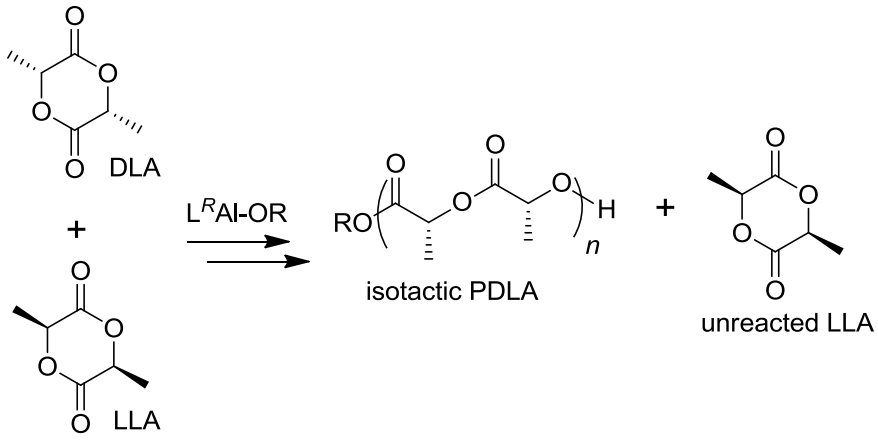

1.6 Objectives and Outline of the Thesis

As mentioned above, organocatalysts have been widely used in the field of polymer synthesis in the last decade. In particular, the organocatalytic synthesis of aliphatic polyesters via ring-opening polymerization (ROP) is an ongoing topic along with a growing concern for green chemistry. Organic bases have attracted much attention and developed this field. Although the weak nucleophilic/basic catalysts were sufficient to polymerize only LA, the strong nucleophilicity/basicity could expand the applicable monomers such as δ-VL and ε-CL. In addition, weak amines along with an H-bond donor could polymerize LA. However, the use of these compounds is complicated because of their extreme air and moisture sensitivity. On the other hand, organic acid-catalyzed ROP is now developing due to its simple polymerization mechanism. Sulfonic acids easily promoted the ROP of lactones via a monomer activation mechanism in contrast to the organic base-catalyzed ROP. Consequently, the greatest concern is how to achieve a high acidity, thus the use of the initiator/chain-end activation tended to be ignored.

Thus the objective of the thesis was expanding the scope and limit of the organic acid-catalyzed ROP of cyclic monomers, such as LA, lactones, cyclic carbonates, and their derivatives. For achieving a well-controlled polymerization, the author focused on the activation mechanism and tuning of the catalytic system, i.e., the main concern was designing a system to achieve monomer activation and initiator/chain-end activation by enhancing the acidity, adding a cocatalyst, and introducing the substituent. In addition, the enantiomer-selective polymerization was also discussed as an expansion of the substituent effect. An outline of the thesis is shown in chart 1:

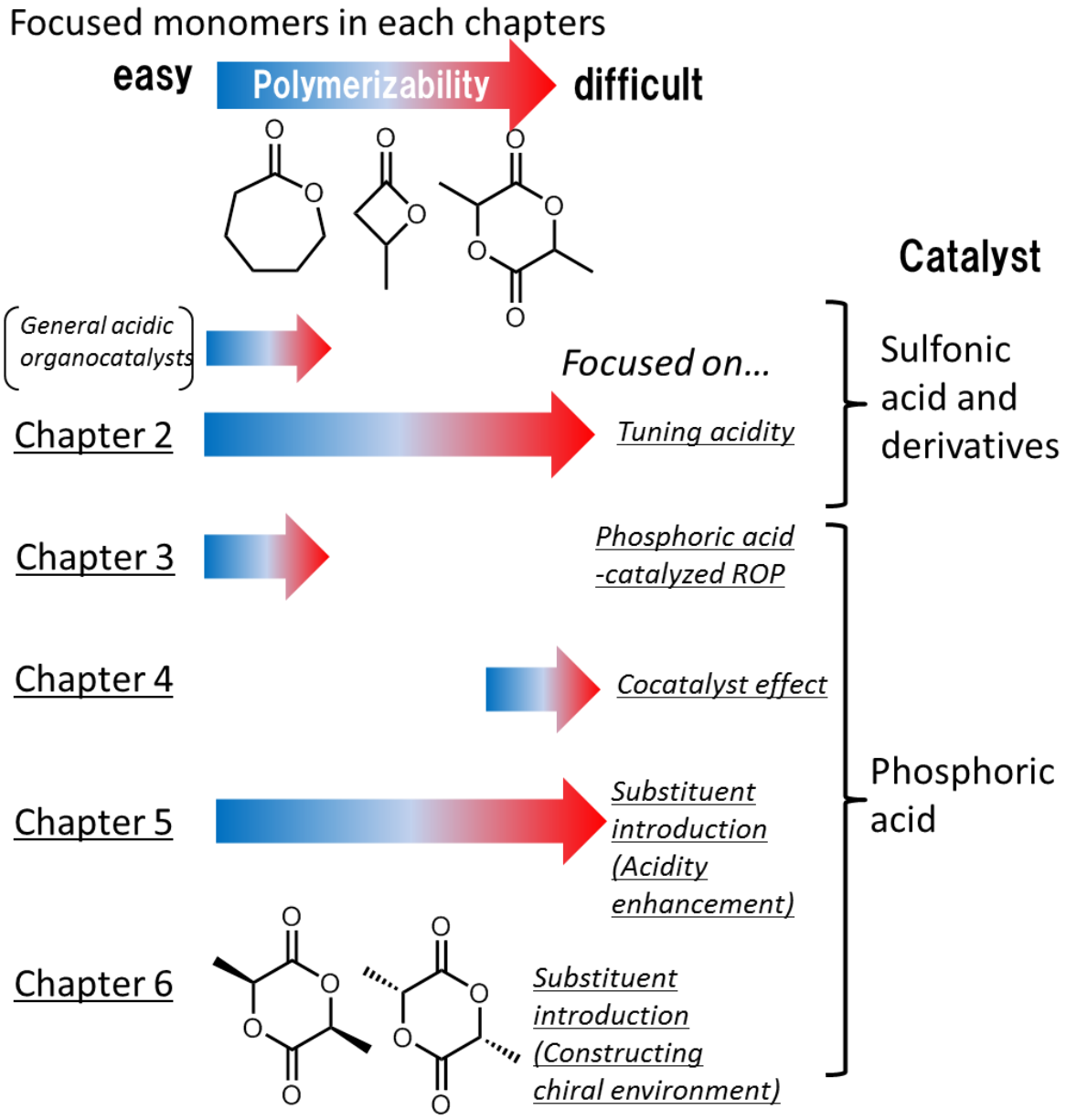

Chart 1.1. Objectives and outline of the thesis.

An outline of the thesis is as follows:

Chapter 2 describes that super Brønsted acid-catalyzed ROPs of cyclic esters, as shown in Scheme 1.11. The highly acidic catalysts, such as pentafluorophenylbis(triflyl)methane ($C_6F_5CHTf_2$) and triflimide ($HNTf_2$), were the focus and their acidities were situated between those of methanesulfonic acid (MSA) and trifluoromethane sulfonic acid (TfOH). The controlled/living polymerizations of δ-valerolactone (δ-VL) and ε-caprolactone (ε-CL) using these catalysts were confirmed with an extremely low loading amount of the catalysts compared to that of MSA. In addition, the $HNTf_2$-catalyzed ROP was applicable for other cyclic esters, such as *rac*-lactide (*rac*-LA) and β-butyrolactone (β-BL), which were only slightly polymerized using other acidic catalysts. An NMR analysis showed that the polymerization proceeded with monomer activation. In addition, the alcohol initiating system produced various end-functionalized polyesters having functional moieties, such as a clickable and polymerizable group, at the α-position of the polymer chain-end. Furthermore, the diblock copolymers were produced using the above-mentioned features; the one-pot diblock copolymerization by sequential monomer addition, introduction of poly(ethylene glycol) segment using macroinitiator, and connecting two polymer segments at each polymer chain-end via the click reaction, successfully occured.

Scheme 1.11. Synthesis of polyesters via controlled/living ring-opening polymerization of cyclic esters using super Brønsted acid as a highly active organocatalyst

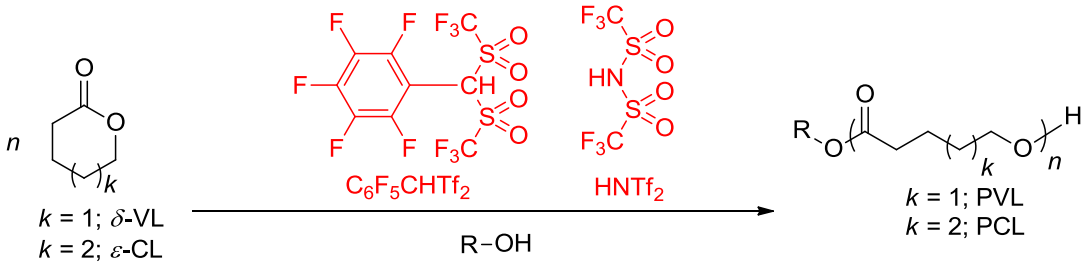

Chapter 3 describes the ROP of δ-VL, ε-CL, and trimethylene carbonate (TMC) using diphenyl phosphate (DPP), which is one of the weak acidic catalysts, as shown in Scheme 1.12. The polymerizations were well-controlled and proceeded in a living nature affording high molar mass polymers (up to 27500 for polyester; up to 9640 for polycarbonate) with narrow polydispersity indices (<1.13). In addition, DPP exhibited a high functional group tolerance due to its low acidity, thus the functionalized initiators and monomers were adopted for the DPP-catalyzed polymerization affording end-functionalized, main chain-modified, and side chain-functionalized polymers. Furthermore, the diblock copolymers consisting of polyesters and polycarbonates were successfully produced by the one-pot synthesis regardless of the monomer addition order. These preferred characteristics were derived from the dual activation ability of DPP, which was assigned from the NMR measurements; all the carbonyl carbon signals of the monomer and OH proton signal of the polymer chain-end model were downfield shifted in the presence of DPP.

Scheme 1.12. Synthesis of well-defined polyesters and polycarbonates via controlled/living ring-opening polymerization using diphenyl phosphate as an efficient organocatalyst

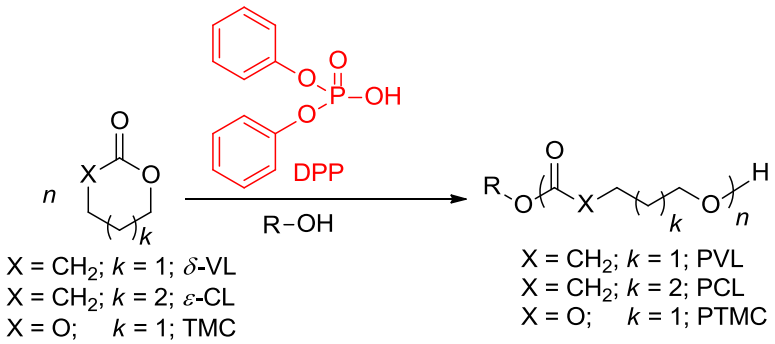

Chapter 4 describes the controlled/living ROP of L-lactide (LLA) that proceeded using DPP/4-dimethylaminopyridine (DMAP), as shown in Scheme 1.13, which was formed by additional DMAP *in situ*. The author confirmed that DPP with DMAP successfully proceeded the polymerization of LLA with a controlled molecular weight (2860 – 19200 g mol^{-1}) and narrow polydispersity indices (<1.13). Additionally, functional initiators were utilized for producing the end-functionalized PLLAs. The suitable catalysts ratio of [DPP]/[DMAP] was 1/2, whereas the polymer was not obtained using DPP alone. In addition, the NMR measurement showed the carbonyl carbon signal of LLA downfield shifted with a 1:1 mixture of DPP/DMAP, and the OH proton signal of the chain-end model compound of PLLA was shifted in the presence of DMAP. Thus the activation mechanism was a bifunctional activation; the monomer was activated by the DPP/DMAP complex and the chin-end was activated by additional DMAP. The dual activation system was easily changed to the bifunctional activation system *in situ*, thus the block copolymers were successfully produced by the first DPP-catalyzed ROP of the lactone or cyclic carbonate and the second DPP/DMAP-catalyzed ROP of LLA.

Scheme 1.13. Synthesis of well-defined poly(L-lactide) via ring-opening polymerization via bifunctional activation using diphenyl phosphate and 4-dimethylaminopyridine

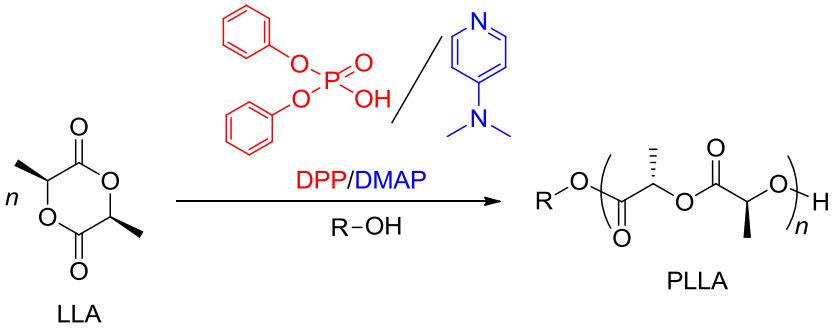

Chapter 5 describes the ROP of *β*-BL using bis(4nitrophenyl) phosphate (BNPP) as the organocatalyst, which has a strong acidity compared to that of DPP, as shown in Scheme 1.14. The controlled/living ROP of *β*-BL was achieved using BNPP, whereas that using DPP was insufficient due to its low acidity. For the BNPP-catalyzed ROP of *β*-BL, the dual activation property was confirmed by the NMR measurement of the *β*-BL and the chain-end model of poly(*β*-butyrolactone) (PBL). The polymerization conditions were optimized for the ROP of *β*-BL resulting in the well-defined PBL with a molecular weight up to 10700 g mol^{-1} and the relatively narrow polydispersities of 1.19-1.39. Additionally, functional initiators were utilized for producing the end-functionalized PBLs. Furthermore, the BNPP-catalyzed ROPs of LLA, *ε*-CL, and TMC successfully proceeded and the diblock copolymers of PBL with polyesters or polycarbonates were prepared by the one-pot sequential addition of another monomer.

Scheme 1.14. Synthesis of poly(*β*-butyrolactone) via ring-opening polymerization using bis(4-nitrophenyl) phosphate

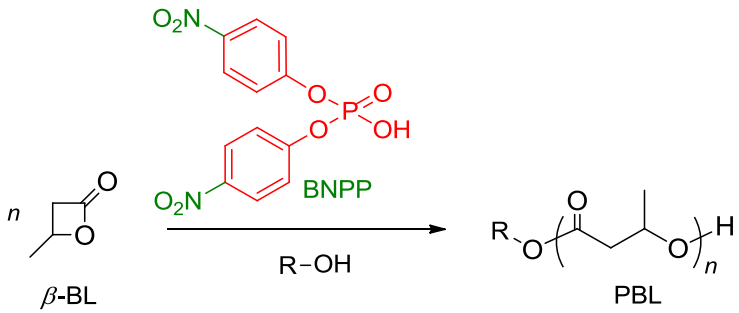

Chapter 6 describes enantiomer-selective polymerization of *rac*-LA using chiral phosphoric acid as the catalyst, as shown in Scheme 1.15. In the polymerization, the high enantiomer-selectivity was achieved using (*R*)-3,3'-bis(pentafluorophenyl)-1,1'-binaphtyl-2,2'-diyl-hydrogenphosphate (*R*)-**1a** at 75 °C. The D-lactide (DLA) was preferentially polymerized via kinetic resolution with the maximum selectivity factor (k_D/k_L) of 28.3. The chiral environment was constructed by the binaphtyl backbone with 3,3'-substituents, and the electron withdrawing group of the substituent (G) strongly influenced the k_D/k_L compared to the steric hindrance. The obtained polymer was a well-defined polylactide with a controlled molecular weight (~7290 g mol^{-1}) and narrow polydispersity index (1.09-1.11), which indicated that the controlled/living polymerization had occured. The selective polymerization of DLA was derived from the dual activation mechanism, i.e., enantiomer-selective monomer activation with chain-end activation, which was determined by the NMR and IR analyses. Thus the chiral phosphoric acid constructed a new pathway for the enantiomer-selective polymerization.

Scheme 1.15. Chiral phosphoric acid-catalyzed enantiomer-selective ring-opening polymerization of *rac*-lactide

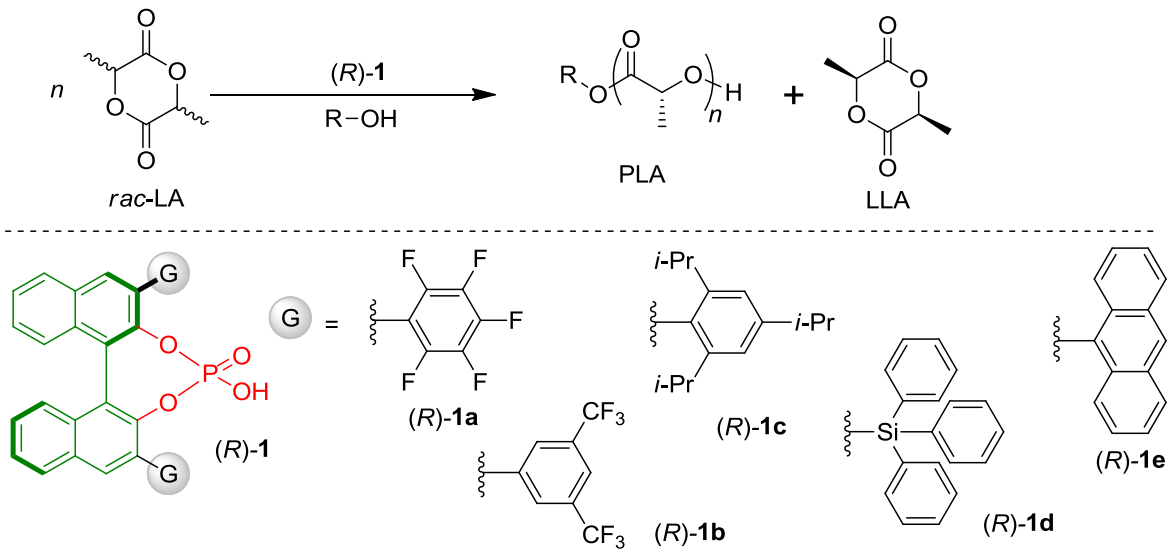

1.7 References and Notes

1. List, B.; Lerner, R. A.; Barbas III, C. F. *J. Am. Chem. Soc.* **2000,** *122,* 2395-2396.
2. Ahrendt, K. A.; Borths, C. J.; MacMallin, D. W. C. *J. Am. Chem. Soc.* **2000**, *122*, 4243-4244.
3. W. S. Jen; D. W. C. MacMillan *J. Am. Chem. Soc.* **2000**, *122*, 9874-9875.
4. K. Maruoka; T. Ooi *Chem. Rev.* **2003**, *103,* 3013-3028.
5. Kiesewetter, M. K.; Shin, E. J.; Hedrick, J. L.; Waymouth, R. M. *Macromolecules* **2010,** *43*, 2093-2107.
6. Kamber, N. E.; Jeong, W.; Waymouth, R. M.; Pratt, R. C.; Lohmeijer, B. G. G.; Hedrick, J. L. *Chem. Rev.* **2007,** *107*, 5813-5840.
7. Nederberg, F.; Connor, E. F.; Moller, M.; Glauser, T.; Hedrick, J. L. *Angew. Chem. Int. Ed.* **2001**, *40*, 2712-2715.
8. Nederberg, F.; Lohmeijer, B. G. G.; Leibfarth, F.; Pratt, R. C.; Choi, J.; Dove, A. P.; Waymouth, R. M.; Hedrick, J. L. *Biomacromolecules* **2007**, *8*, 153-160.
9. Guillaume, S. M.; Carpentier, J.-F. *Catal. Sci. Technol.* **2012**, *2*, 898-906.
10. Helou, M.; Miserque, O.; Brusson, J.-M.; Carpentier, J.-F.; Guillaume, S. M. *Chem. Eur. J.* **2010**, *16*, 13805-13813.
11. Pratt, R. C.; Dove, A. P.; Lohmeijer, B. G. G.; Culkin, D. A.; Waymouth, R. M.; Hedrick, J. L. *Polym. Prepr. (Am. Chem. Soc.,Di*V. *Polym. Chem.*) **2005**, *46*, 902.
12. Esswein, B.; Möller, M. *Angew. Chem. Int. Ed.* **1996**, *35*, 623-625.
13. Esswein, B.; Steidl, N. M.; Möller, M. *Macromol. Rapid Commun.* **1996**, *17*, 143-148.
14. Esswein, B.; Molenberg, A.; Möller, M. *Macromol. Symp.* **1996**, *107*, 331-340.
15. Rexin, O.; Mülhaupt, R. *J. Polym. Sci., Polym. Chem.* **2002**, *40*, 864-873.

16. Hans, M.; Keul, H.; Möller, M. *Polymer* **2009**, *50*, 1103-1108.

17. Schmalz, H.; Lanzerdörfer, M. G.; Abetz, V.; Müller, A. H. E. *Macromol. Chem. Phys.* **2003**, *204*, 1056-1071.

18. Misaka, H.; Sakai, R.; Satoh, T.; Kakuchi, T. *Macromolecules* **2011**, *44*, 9099–9107.

19. Misaka, H.; Tamura, E.; Makiguchi, K.; Kamoshida, K.; Sakai, R.; Satoh, T.; Kakuchi, T. *J. Polym. Sci., Part A, Polym. Chem.,* **2012**, *50*, 1941-1952.

20. Memenger, Jr. W.; Campbell, G. C.; Davidson, F. *Macromolecules* **1996**, *29*, 6475-6480.

21. Rodriguez, M.; Marrot, S.; Kato, T.; Sterin, S.; Fleury, E.; Baceiredo, A. *J. Organomet. Chem.* **2007**, *692*, 705-708.

22. Lohmeijer, B. G.; Dubois, G.; Leibfarth, F.; Pratt, R. C.; Nederberg, F.; Nelson, A.; Waymouth, R. M.; Wade, C.; Hedrick, J. L. *Org. Lett.* **2006**, *8*, 4683-4686.

23. Iwasaki, Y.; Yamaguchi, E. *Macromolecules* **2010**, *43*, 2664–2666.

24. Zhang, S.; Li, A.; Zou,J.; Lin, L. Y.; Wooley, K. L. *Macro Lett.* **2012**, *1*, 328−333.

25. Clément, B.; Grignard, B.; Koole, L.; Jérôme, C.; Lecomte, P. *Macromolecules* **2012**, *45*, 4476−4486.

26. Steinbach, T.; Schröder, R.; Ritzc, S.; Wurm, F. R. *Polym. Chem.* **2013**, *4*, 4469-4479.

27. Zhang, S.; Wang, H.; Shen, Y.; Zhang, F.; Seetho, K.; Zou, J.; Taylor, J.-S. A.; Dove, A. P.; Wooley, K. L. *Macromolecules*, **2013**, *46*, 5141–5149.

28. du Boullay, O. T.; Marchal, E.; Martin-Vaca, B.; Cossio, F. P.; Bourissou, D. *J. Am. Chem. Soc*. **2006**,*128*, 16442–16443.

29. Illy, N.; Boileau, S.; Buchmann, W.; Penelle, J.; Barbier, V. *Macromolecules* **2010**, *43*, 8782-8789.

30. Illy, N.; Boileau, S.; Penelle, J.; Barbier, V. *Macromol. Rapid. Commun.* **2009**, *30*, 1731-1735.

31. Kakuchi, R.; Chiba, K.; Fuchise, K.; Sakai, R.; Satoh, T.; Kakuchi, T. *Macromolecules*, **2009, *42***, 8747-8750.

32. Fuchise, K.; Kakuchi, R.; Narumi, A.; Sakai, R.; Satoh, T.; Kawaguchi, S.; Kakuchi, T. *Macromolecules* **2010**, *43*, 5589-5594.

33. Kakuchi, T.; Chen, Y.; Kitakado, J.; Mori, K.; Fuchise, K.; Satoh, T. *Macromolecules* **2011**, *44*, 4641-4647.

34. Hsu, J.-C.; Chen, Y.; Kakuchi, T.; Chen, W.-C. *Macromolecules* **2011**, *44*, 5168-5177.

35. Chen, Y.; Fuchise, K.; Narumi, A.; Kawaguchi, S.; Satoh, T.; Kakuchi, T. *Macromolecules* **2011, *44***, 9091-9098.

36. Chen, Y.; Takada, K.; Fuchise, K.; Satoh, T.; Kakuchi, T. *J. Polym. Sci., Part A, Polym. Chem.,* **2012***, 50,* 3277-3285.

37. Takada, K.; Fuchise, K.; Chen, Y.; Satoh, T.; Kakuchi, T. *J. Polym. Sci., Part A, Polym. Chem.,***2012***, 50,* 3560-3566.

38. Fuchise, K.; Chen, Y.; Takada, K.; Satoh, T.; Kakuchi, T. *Macromol. Chem. Phys.,* **2012**, *213,* 1604-1611.

39. Fuchise, K.; Chen, Y.,; Satoh, T.; Kakuchi, T. *Polym. Chem.*, **2013**, *4*, 4278-4291.

40. Albertson, A.-C.; Varma, I. K. *Biomacromolecules* **2003**, *4*, 1466-1486

41. Wu, J.; Lin, C.-C. *Coord.Chem. Rev.* **2006**, *250*, 602-626.

42. Guillaume, S. M.; Carpentier, J.-F. *Catal. Sci. Technol.* **2012**, *2*, 898-906.

43. Ajellal, N.; Carpentier, J. F.; Guillaume, C.; Guillaume, S. M.; Helou, M.; Poirier, V.; Sarazina, Y.; Trifonov, A.; *Dalton Trans.* **2010**, *39*, 8363-8376.

44. Labet, M.; Thielemans, W. *Chem. Soc. Rev,* **2009**, *38*, 3484-3504.

45. Dechy-Cabaret, O.; Martin-Vaca, B.; Bourissou, D. *Chem. Rev.* **2004**, *104*, 6147-6176.

46. Eguiburu, J. L.; Fernandez-Berridi, M. J.; Cossío, F. P.; San Román, J. *Macromolecules* **1999,** *32,* 8252-8258

47. Dubois, P.; Jacobs, C.; Jérôme, R,; Teyssié, P. *Macromolecules* **1991**, *24*, 2266-2270.

48. Degée, P., Dubois, Ph.; Jérôme, R. *Macromol. Chem. Phys.***1997**, *198*, 1973-1984.

49. von Schenck, H.; Ryner, M.; Albertsson, A. -C. Svensson, M. *Macromolecules* **2002**, *35,* 1556-1562.

50. Kowalski, A.; Duda, A.; Penczek, S. *Macromolecules* **2000**, *33,* 7359-7370.

51. Kricheldorf, H. R.; Kreiser-Saunders, I.; Stricker, A. *Macromolecules* **2000**, *33*, 702-709.

52. Kamber, N. E.; Jeong, W.; Waymouth, R. M.; Pratt, R. C.; Lohmeijer, B. G. G.; Hedrick, J. L. *Chem. Rev.* **2007,** *107*, 5813-5840.

53. Kiesewetter, M. K.; Shin, E. J.; Hedrick, J. L.; Waymouth, R. M. *Macromolecules* **2010,** 43, *5*, 2093-2107.

54. Dove, A. P. *Macro Lett.* **2012**, *1*, 1409-1412.

55. Thomas, C.; Bibal, B.; *Green Chem.* **2013**, in press (DOI: 10.1039/C3GC41806E)

56. Févre,M.; Pinaud, J.; Gnanou, Y.; Vignolle, J.; Taton, D. *Chem. Soc. Rev.* **2013**, *42*, 2142-2172.

57. Nyce, G. W.; Glauser, T.; Connor, E. F.; Mock, A.; Waymouth, R. M.; Hedrick, J. L. *J. Am. Chem. Soc.* **2003**, *125*, 3046-3056.

58. Dove, A. P.; Pratt, R. C.; Lohmeijer, B. G. G.; Culkin, D. A.; Hagberg, E. C.; Nyce, G. W.; Waymouth, R. M.; Hedrick, J. L. *Polymer* **2006**, *47*, 4018-4025.

59. Culkin, D. A. ; Jeong, W.; Csihony, S.; Gomez, E. D.; Balsara, N. P.; Hedrick, J. L.; Waymouth. R. M. *Angew. Chem. Int. Ed.* **2007**, *46*, 2627-2630.

60. Jeong, W.; Shin, E. J.; Culkin, D. A.; Hedrick, J. L.; Waymouth, R. M. *J. Am. Chem. Soc,* **2009**, *131*, 4884-4891.

61. Shin, E. J.; Brown, H. A.; Gonzalez, S.; Jeong, W.; Hedrick, J. L.; Waymouth, R. M. *Angew. Chem.* **2001**, *123*, 1-5.

62. Kamber, N. E.; Jeong, W.; Gonzalez, S.; Hedrick, J. L.; Waymouth, R. M. *Macromolecules* **2009**, *42*, 1634-1639.

63. Jeong, W.; Hedrick, J. L.; Waymouth, R. M. *J. Am. Chem. Soc.* **2007**, *129*, 8414-8415.

64. Connor, E. F.; Nyce, G. W.; Myers, M.; Mock, A.; Hedrick, J. L.; *J. Am. Chem. Soc.* **2002**, *124*, 914-915.

65. Coulembier, O.; Lohmeijer, B. G. G.; Dove, A. P.; Pratt, R. C.; Mespouille, L.; Culkin, D. A.; Benight, S. J.; Dubois, Ph.; Waymouth, R. M.; Hedrick, J. L. *Macromolecules* **2009,** *39*, 5617-5628.

66. Coulembier, O.; Delva, X.; Hedrick, J. L.; Waymouth, R. M.; Dubois, P. *Macromolecules* **2007,** *40,* 8560-8567.

67. Coulembier, O.; Mespouille, L.; Hedrick, J. L.; Waymouth, R. M.; Dubois, P. *Macromolecules* **2006,** *39,* 4001-4008.

68. Myers, M.; Connor, E. F.; Glauser, T.; Mock, A.; Nyce, G.; Hedrick, J. L. *J. Polym. Sci., Part A: Polym. Chem.* **2002**, *40*, 844-851.

69. Zhang, L.; Pratt, R. C.; Nederberg, F.; Horn, H. W.; Rice, J. E.; Waymouth, R. M.; Wade, C. G.; Hedrick, J. L. *Macromolecules* **2010**, *43*, 1660-1664.

70. Pratt, R. C.; Lohmeijer, B. G. G.; Long, D. A.; Waymouth, R. M.; Hedrick, J. L. *J. Am. Chem. Soc.* **2006**, *128*, 4556-4557.

71. Lohmeijer, B. G. G.; Pratt, R. C.; Leibfarth, F.; Logan, J. W.; Long, D. A.; Dove, A. P.; Nederberg, F.; Choi, J.; Wade, C.; Waymouth, R. M.; Hedrick, J. L. *Macromolecules* **2006**, *39*, 8574-8583.

72. Zhang, L.; Nederberg, F.; Pratt, R. C.; Waymouth, R. M.; Hedrick, J. L.; Wade, C. G. *Macromolecules* **2007**, *40*, 4154-4158.

73. Zhang, L.; Nederberg, F.; Messman, J. M.; Pratt, R. C.; Hedrick, J. L.; Wade, C. G. *J. Am. Chem. Soc.* **2007**, *129*, 12610-12611.

74. Jaffredo, C. G.; Carpentier, J.-F.; Guillaume, S. M. *Polym. Chem.*, **2013**, *4*, 3837-3850.

75. Jaffredo, C. G.; Carpentier, J. –F.; Guillaume, S. M. *Macromol. Rapid Commun,* **2012**, *33*, 1938-1944.

76. Jaffredo, C. G.; Carpentier, J. –F.; Guillaume, S. M. *Macromolecules* **2013**, *46*, 6765-6776.

77. Kawalec, M.; Coulembier, O.; Gerbaux, P.; Sobota, M.; Winter, J. D.; Dubois, P.; Kowalczuk, M.; Kurcok, P. *React. Funct. Polym.* **2012**, *72*, 509-520.

78. De Winter, J.; Coulembier, O.; Gerbaux, P.; Dubois, P. *Macromolecules* **2010**, *43*, 10291–10296.

79. Dove, A. P.; Pratt, R. C.; Lohmeijer, B. G. G.; Waymouth, R. M.; Hedrick, J. L. *J. Am. Chem. Soc.* **2005**, *127*, 13798-13799.

80. Pratt, R. C.; Lohmeijer, B. G. G.; Long, D. A.; Lundberg, P. N. P.; Dove, A. P.; Li, H. B.; Wade, C. G.; Waymouth, R. M.; Hedrick, J. L. *Macromolecules* **2006**, *39*, 7863-7871.

81. Miyake, G. M.; Chen, E. Y. X. *Macromolecules*, **2011**, *44*, 4116-4124.

82. Kan, S.; Jin, Y.; He, X.; Chen, J.; Wu, H.; Ouyang, P.; Guo, K.; Li, Z.; *Polym. Chem.,* **2013**, *4*, 5432-5439.

83. He, X.; Ji, Y.; Jin, Y.; Kan, S.; Xia, H.; Chen, J.; Liang, B.; Wu, H.; Guo, K.; Li, Z. *J. Polym. Sci., Part A, Polym. Chem.,* **2013 (**DOI: 10.1002/pola.27082).

84. Coady, D. J.; Engler, A. C.; Horn, H. W.; Bajjuri, K. M.; Fukushima, K.; Jones, G. O.; Nelson, A.; Rice, J. E.; Hedrick, J. L. *Macro Lett.,* **2012**, *1*, 19-22.

85. Koeller, S.; Kadota,J.; Deffieux, A.; Peruch,F.; Massip, S.; L*é*ger, J. –M.; Desvergne, J. –P.; Bibal, B. *J. Am. Chem. Soc.*, **2009**, *131*, 15088-15089.

86. Koeller, S.; Kadota, J.; Peruch, F.; Deffieux, A.; Pinaud, N.; Pianet, I.; Massip, S.; Léger, J.-M.; Desvergne, J.-P.; Bibal, B. *Chem. Eur. J.* **2010**, *16*, 4196-4205.

87. Alba, A.; Schopp, A.; De Souza Delgado, A. –P.; Cherif-Cheikh R.; Martin-Vaca B.; Bourissou, D. *J. Polym. Sci., Part A, Polym. Chem.,* **2010***, 48,* 959-965.

88. Thomas, C.; Peruch, F.; Deffieux, A.; Milet, A.; Desvergne, J. –P.; Bibal, B. *Adv. Synth. Catal.* **2011**, *353*, 1049-1054.

89. Thomas, C.; Peruch, F.; Bibal, B. *RSC Adv.* **2012**, ***2***, 12851-12856.

90. Coulembier, O.; Sanders, D. R.; Nelson, A.; Hollenbeck, A. N.; Horn, H. W.; Rice, J. E.; Fujiwara, M.; Dubois, P.; Hedrick, J. L. *Angew. Chem. Int. Ed.* **2009**, *48*, 5170-5173.

91. Shibasaki, Y.; Sanada, H.; Yokoi, M.; Sanda, F.; Endo, T. *Macromolecules* **2000**, *33*, 4316-4320.

92. Kim, M. S.; Seo, K. S.; Khang, G.; Lee, H. B. *Macromol. Rapid Commun.* **2005**, 26, (8), 643-648.

93. Lou, X. D.; Detrembleur, C.; Jerome, R. *Macromolecules* **2002**, *35*, 1190-1195.

94. Sanda, F.; Sanada, H.; Shibasaki, Y.; Endo, T. *Macromolecules* **2002**, *35*, 680-683.

95. Casas, J.; Persson, P. V.; Iversen, T.; Cordova, A. *Adv. Synth. Catal.* **2004**, *346*, 1087-1089.

96. Bourissou, D.; Martin-Vaca, B.; Dumitrescu, A.; Graullier, M.; Lacombe, F. *Macromolecules* **2005**, *38*, 9993-9998.

97. Basko, M.; Bednarek, M. *React. Funct. Polym.* **2012**, *72*, 213-220.

98. Jaipuri, F. A.; Bower, B. D.; Pohl, N. L. *Tetrahedron: Asymmetry* **2003**, *14*, 3249-3252.

99. Couffin, A.; Martin-Vaca, B.; Bourissou, D.; Navarro, C.; *Polym. Chem.* **2014**, *5*, 161-168.

100. Basko, M.; Duda, A.; Kazmierski, S.; Kubisa, P. *J. Polym. Sci., Part A: Polym. Chem.* **2013**, *51*,4873-488

101. Gazeau-Bureau, S.; Delcroix, D.; Martin-Vaca, B.; Bourissou, D.; Navarro, C.; Magnet, S. *Macromolecules* **2008**, *41*, 3782-3784.

102. Delcroix, D.; Martin-Vaca, B.; Bourissou, D.; Navarro, C. *Macromolecules* **2010**, *43*, 8828-8835.

103. Oshimura, M.; Tang, T.; Takasu, A. *J. Polym. Sci., Part A: Polym. Chem.* **2011**, *49*, 1210-1218.

104. Coady, D. J.; Horn, H. W.; Jones, G. O.; Sardon, H.; Engler, A. C., Waymouth, R. M.; Rice, J. E.; Yang, Y. Y.; Hedrick, J. L. *Macro Lett*. **2013**, *2*, 306−312.

105. Sardon, H.; Engler, A. C.; Chan, J. M. W.; García, J. M.; Coady, D. J.; Pascual, A.; Mecerreyes, D.; Jones, G. O.; Rice, J. E.; Horn, H. W.; Hedrick J. L. *J. Am. Chem. Soc.* **2013**, *135*, 16235-16241.

106. Thomas, C. M. *Chem. Soc. Rev.* **2010**, *39*, 165-173.

107. Stanford, M. J.; Dove, A. P. *Chem. Soc. Rev.* **2010**, *39*, 486-494.

108. Tsuji, H. *Macromol. Biosci.* **2005**, *5*, 569-597.

109. Tsuji, H. In *Polyesters*; Doi, Y.; Steinbüchel, A., Eds.; Wiley-VCH: Weinheim, **2002**; Vol. 4, pp 129-177.

110. Nomura, N.; Ishii, R.; Akakura M.; Aoi, K. *J. Am. Chem. Soc.* **2002**, *124*, 5938-5939.

111. Hormnirun, P. ; Marshall, E. L., Gibson, V. C.; White, A. J. P.; Williams, D. J. *J. Am. Chem. Soc.* **2004**, *126*, 2688-2689.

112. Dove, A. P.; Li, H.; Pratt, R. C.; Lohmeijer, B. G. G.; Culkin, D. A.; Waymouth, R. M.; Hedrick, J. L. *Chem. Commun.***2006**, 2881-2883.

113. Spassky, N.; Wisniewski, M.; Pluta, C.; Le Borgne, A. *Macromol. Chem. Phys.* **1996**, *197*, 2627-2637.

114. Zhong, Z.; Dijkstra, P. J.; Feijen, J. *Angew. Chem., Int. Ed.* **2002**, *41*, 4510- 4513.

115. Ovitt, T. M.; Coates, G. W. *J. Polym. Sci., Part A: Polym. Chem.* **2000**, *38*, 4686-4692.

116. Radano, C. P.; Baker G. L.; Smith, M. R. *J. Am. Chem. Soc.* **2000**, *122*, 1552-1553.

117. Ovitt, T. M.; Coates, G. W. *J. Am. Chem. Soc.* **2002**, *124*, 1316-1326.

Chapter 2

Synthesis of Polyesters via Controlled/Living Ring-Opening Polymerization of Cyclic Esters Using Super Brønsted Acid as a Highly Acticve Organocatalyst

2.1 Introduction

Organocatalytic polymerizations have been developed as some of the important methods for polymer synthesis from the viewpoint of producing metal-free products.[1-3] In particular, precisely controlled polymerization methods, such as living polymerization systems using organocatalysts, are required for synthesizing complex macromolecular architectures with well-defined structures.[4, 5] For example, Kakuchi along with Waymouth, Gnanou, and Taton,[6,7] reported the organocatalyzed group transfer polymerization (GTP) of (meth)acrylates and acrylamides, in which a loaded amount of organocatalysts, such as phosphazene,[8] triflimide ($HNTf_2$),[9, 10] and pentafluorophenylbis(triflyl)methane ($C_6F_5CHTf_2$)[11] was significantly low compared to those for the GTPs using conventional Lewis acids and nucleophilic catalysts.[12] In addition, there have been many efforts to utilize various types of organocatalysts for the ring opening polymerizations (ROPs) of cyclic monomers.[1,2]

Organocatalytic ROPs of cyclic esters are useful to synthesize biodegradable aliphatic polyesters. Organocatalysts promoted the controlled/living ROPs in association with alcohols as initiators, in which the polymerization rates were accelerated by activating the monomers and/or activating initiators/polymer chain-ends. For example, Hedrick and Waymouth et al. reported that the controlled/living ROPs of cyclic esters, such as lactide (LA), ε-caprolactone (ε-CL), and δ-valerolactone (δ-VL), were achieved using nucleophilic organocatalysts, such as NHC,[13-16] 4-dimethylaminopyridine,[17] and phosphine,[18] through the nucleophilic activation of the monomers. In addition, strong basic catalysts, such as guanidine,[19-21] amidine,[20] and phosphazene,[21-23] performed the controlled/living ROPs of cyclic esters by activation of the hydroxyl groups in the initiators or polymer chain-ends through hydrogen bonding. Thus, the suitable combination of a monomer and a catalyst is very important for the ROPs of cyclic esters using nucleophilic and basic organocatalysts leading to well-defined polyesters.

On the other hand, acid-catalyzed ROPs proceeded only through the monomer activation using proton donor catalysts. For example, Endo et al. reported that hydrogen chloride (HCl), one of the most established ROP-acid catalysts, provided an excellent catalytic activity for the ROP of δ-VL and ε-CL using an alcohol initiator to afford polyesters with controlled molecular weights ($M_{n,}$ ~15000) and narrow polydispersity indices (<1.17).[24] In addition, organic acids, such as carboxylic acids (e.g., tartaric acid, lactic acid, citric acid, and fumaric acid),[25, 26] amino acids (e.g., L-proline)[26] and organic sulfonic acids (e.g., methane sulfonic acid)[27] performed the controlled/living ROPs of δ-VL and/or ε-CL to afford well-defined polyesters. Although these organic acids were effective for the ROPs of δ-VL and ε-CL, their mild and weak acidity are insufficient for the activation of LA resulting in no polymerization.

The simplest way to enhance the activation of LA is the use of a strong organic acid, such as a very strong Brønsted acid, i.e., a super Brønsted acid.[28] In fact, Bourissou et al. reported that the ROP of LA was achieved using trifluoromethane sulfonic acid (TfOH) that has a strong acidity of pK_a = -0.96 (in AcOH) as an organocatalyst at ambient temperature.[29] In order to expand the scope of the organic acid catalyst, the authoer newly focused on $C_6F_5CHTf_2$ (pK_a = 1.5 in AcOH) and $HNTf_2$ (pK_a = 0.67 in AcOH), which possesses weak acidity compared to TfOH. Thus, it is important to elucidate the relation between the acidity of organocatalysts and cyclic monomers in order to realize the ROPs of cyclic esters. In this chapter, the $C_6F_5CHTf_2$ and $HNTf_2$-catalyzed ROPs of cyclic esters, such as δ-VL, ε-CL, 1,5-dioxepan-2-one (DXO), *rac*-lactide (*rac*-LA), and β-butyrolactone (β-BL) were conducted, as shown in Scheme 2.1. This chapter describes (1) the characterization of the obtained polyesters and kinetic studies using 3-phenyl-1-propanol (PPA) as the conventional initiator, (2) the synthesis of end-functionalized polyesters using functional initiators, such as propargyl alcohol (PGA), 6-azido-1-hexanol (AHA), *N*-(2-hydroxyethyl)maleimide (HEMI), 5-hexen-1-

ol (HEA), and 2-hydroxyethyl methacrylate (HEMA), and (3) the synthesis of diblock copolymers by the $HNTf_2$-catalyzed ROP of ε-CL, DXO, *rac*-LA, and δ-VL.

Scheme 2.1. Super Brønsted acid-catalyzed ring-opening polymerizations (ROPs) of δ-valerolactone (δ-VL), ε-caprolactone (ε-CL), *rac*-lactide (*rac*-LA), and β-butyrolactone (β-BL) using 3-phenyl-1-propanol (PPA), propargyl alcohol (PGA), *N*-(2-hydroxyethyl)maleimide (HEMI), 5-hexen-1-ol (HEA), and 2-hydroxyethyl methacrylate (HEMA)

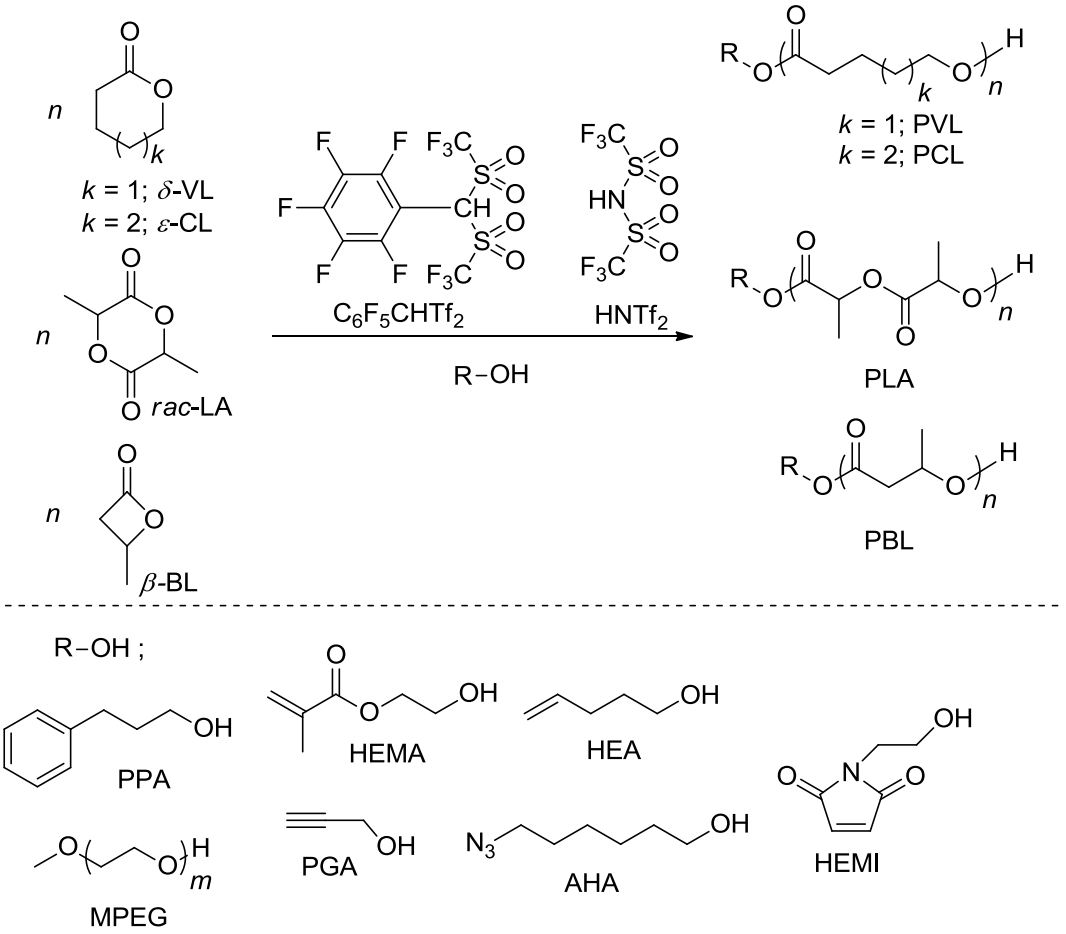

2.2 Results and Discussion

2.2.1 Super Brønsted Acid-Catalyzed ROPs of *δ*-Valerolactone (*δ*-VL) and *ε*-Caprolactone (*ε*-CL). In order to prepare polyesters with narrow molecular weight distribution in high polymer yield, the author tried to optimize the synthetic conditions for the ring-opening polymerizations (ROPs) of *ε*-caprolactone (*ε*-CL) and *δ*-valerolactone (*δ*-VL) using pentafluorophenylbis(triflyl)methane ($C_6F_5CHTf_2$). First, the author carried out the polymerization of *ε*-CL uisng 3-phenyl-1-propanol (PPA) as the initiator. All polymerizations homogeneously proceeded and were quenched with immobilized base. Just before quenching the polymerizations, aliquots of the polymerization mixture were taken and the monomer conversion was directly determined by the ^{1}H NMR spectra. Finally, the obtained polymers were purified by reprecipitation using CH_2Cl_2 as the good solvent and cold methanol as the poor solvent. Table 2.1 summarizes a few typical experimental results in CH_2Cl_2 at room temperature. Shorter polymerization time, a smaller ratio of $[C_6F_5CHTf_2]_0/[PPA]_0$, and higher monomer concentration ($[M]_0$) were suitable for controlling the ROP of *ε*-CL (Table 2.1, runs 1-3); the optimized condition of $[M]_0 = 3.0\ mol\cdot L^{-1}$ and $[C_6F_5CHTf_2]_0/[PPA]_0 = 0.1$ produced a polymer in a monomer conversion of 97.2 % for the polymerization time of 7 h (Table 2.1, run 3). The same condition was suitable for the ROP of *δ*-VL to afford a polymer in a monomer conversion of 94.1 % for the polymerization time of 2 h (Table 2.1, run 5). In addition, same polymerization conditions were applicable for triflimide ($HNTf_2$)-catalyzed ROPs of *ε*-CL and *δ*-VL, as listed in Table 2.1, runs 7-10.

The chemical structures of the obtained polymers were assigned to poly(*ε*-caprolactone) (PCL) and poly(*δ*-valerolactone) (PVL) having the PPA residue by ^{1}H NMR measurement (Figures 2.1a and 2.1b, respectively). The characteristic peaks due to the initiator of PPA were observed in the range from 7.14 to 7.35 ppm, 2.69 ppm, and 1.96 ppm, which were

attributable to the phenyl protons, the benzyl protons, and the ester methylene protons, respectively. In addition, the peak due to the hydroxy methylene protons at the polymer chain end was clearly observed at 3.61 ppm. For PVL, the peaks due to the phenyl protons, the benzyl protons, the ester methylene protons, and the hydroxy methylene protons appeared in the ranges of 7.13 - 7.37, 2.69, 1.97, and 3.65 ppm, respectively. These results implied that both polymers included the PPA residue.

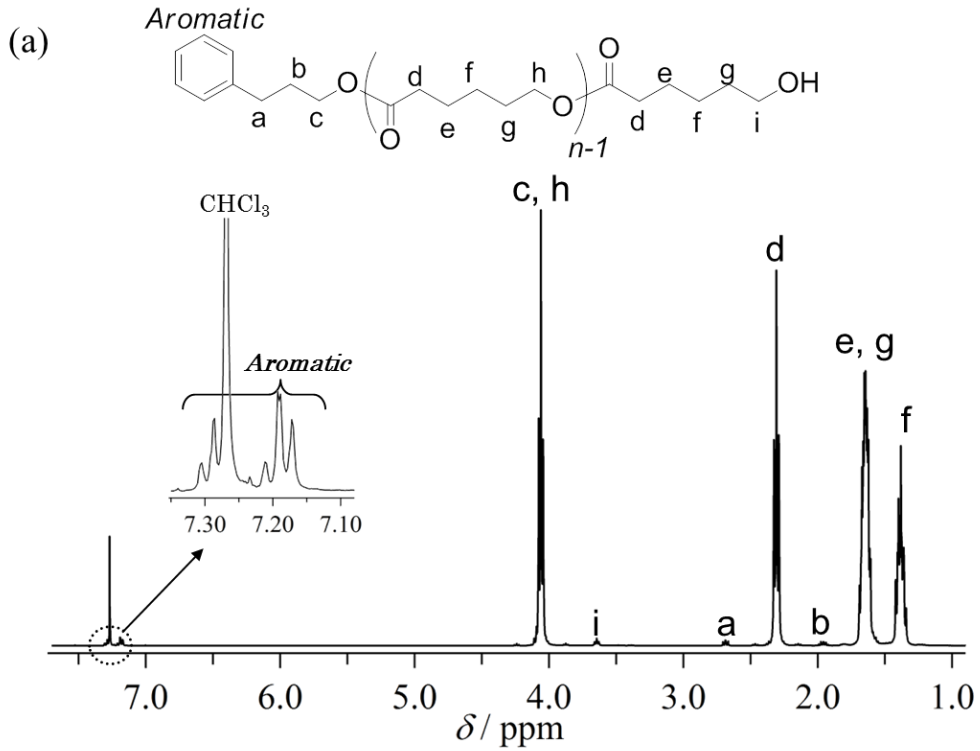

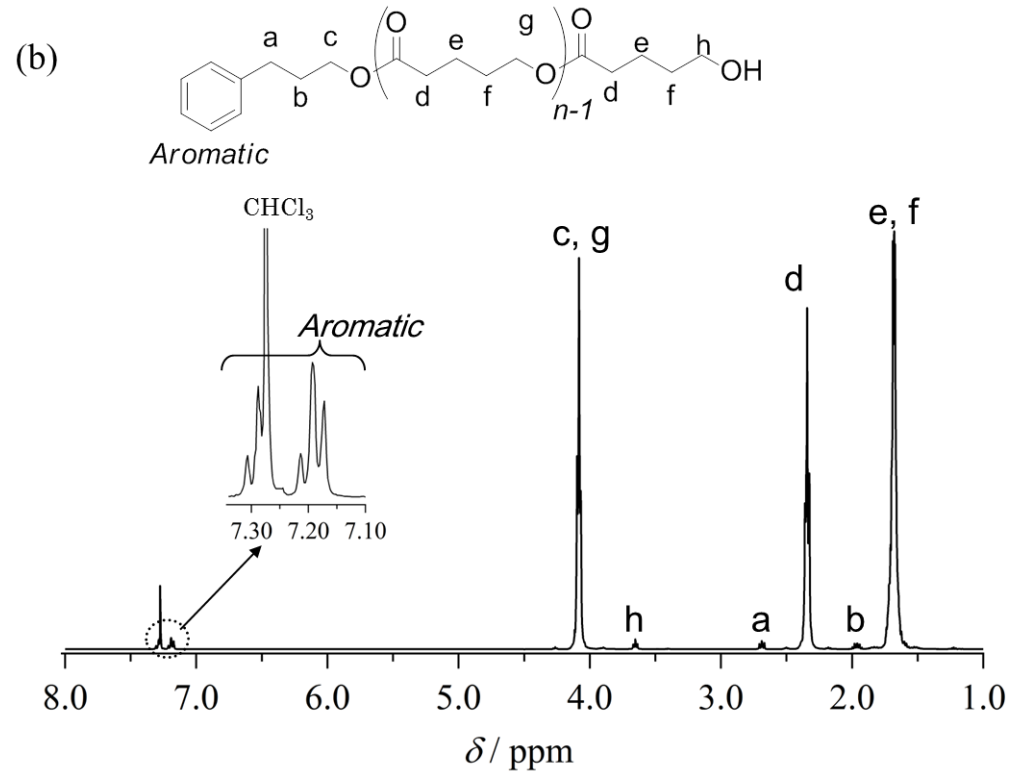

Figure 2.1. ^{1}H NMR spectra of (a) PCL and (b) PVL initiated from PPA in $CDCl_3$ (Table 2.1, runs 3 and 5).

The number average molecular weight ($M_{n,NMR}$) value agreed fairly well with the calculated one ($M_{n,calcd}$), which was determined by the ^{1}H NMR measurement and calculated by the initial ratio of [ε-CL or δ-VL]$_0$/[PPA]$_0$ and monomer conversions, respectively; for example, the $M_{n,NMR}$ and $M_{n,calcd}$ values for the PCL (Table 2.1, run 3) were 5690 g mol^{-1} and 5680 g mol^{-1}, respectively, and those for the PVL (Table 2.1, run 5) were 4940 g mol^{-1} and 4850 g mol^{-1}, respectively. In addition, SEC traces of the obtained PCL and PVL showed monomodal shapes, as shown in Figure 2.2, and the molecular weight distributions (M_w/M_ns) were relatively low, 1.12 for PCL and 1.17 for PVL. Polymers with different molecular weights were synthesized by changing the initial ratio of the monomer and initiator, e.g., high molar mass polymers were obtained corresponding to [M]$_0$/[PPA]$_0$ = 100 (Table 2.1, runs 4 and 6).

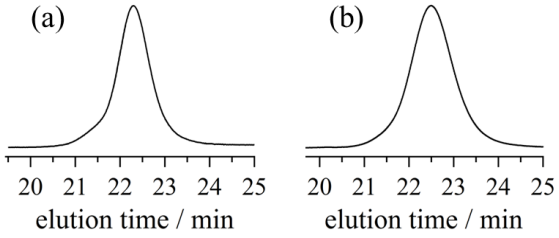

Figure 2.1. SEC traces of (a) PCL and (b) PVL initiated from PPA (Table 2.1, runs 3 and 5) (eluent, $CHCl_3$; flow rate, 0.8 mL min^{-1}).

Furthermore, the catalytic performance of $HNTf_2$ was confirmed by the polymerization of other cyclic monomers, such as 1,5-dioxepan-2-one (DXO), *rac*-lactide (*rac*-LA), and *β*-butyrolactone (*β*-BL) using PPA as the conventional initiator at room temperature. The monomer conversions for all the polymerizations were high, which was directly determined by the ^1H NMR spectrum of an aliquot of the polymerization mixtures in $CDCl_3$ (Table 2.2). The polymerization rate of DXO was similar to that of *ε*-CL, whereas that of *rac*-LA was extremely low. $M_{n,NMR}$ fairly agreed with the $M_{n,calcd}$; for example, the $M_{n,NMR}$ values were 11400 g mol^{-1} for $[DXO]_0/[PPA]_0 = 100$, 6490 g mol^{-1} for $[rac\text{-LA}]_0/[PPA]_0 = 50$, and 3580 for $[\beta\text{-BL}]_0/[PPA]_0 = 40$, that corresponded to the respective $M_{n,calcd}$ values of 11300, 6430, and 3540 g mol^{-1}. All the SEC traces of the obtained polymers showed a monomodal distribution, as shown in Figure 2.3, and their M_w/M_ns were relatively narrow at 1.14 – 1.28, as listed in Table 2.2.

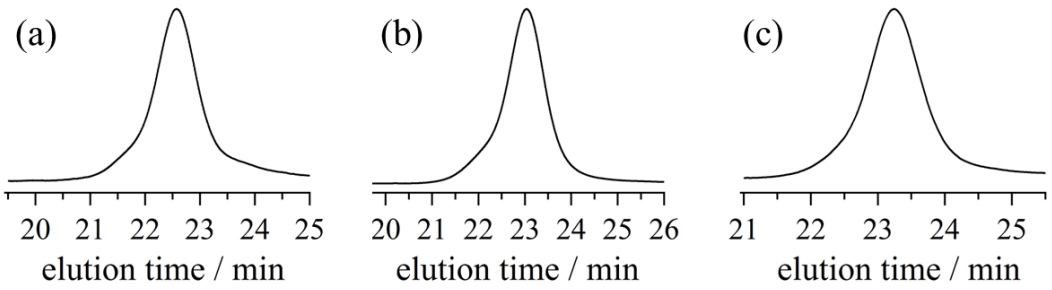

Figure 2.3. SEC traces of (a) PDXO, (b) PLA, and (c) PBL initiated from PPA (Table 2.2, runs 11, 14 and 15) (eluent, $CHCl_3$; flow rate, 0.8 mL min^{-1}).

Table 2.1. Ring-opening polymerization (ROP) of ε-caprolactone (ε-CL) and δ-valerolactone (δ-VL) using 3-phenyl-1-propanol (PPA) and super Brønsted acids[a]

run	monomer (M)	catalyst (cat.)	$[M]_0$ /$[PPA]_0$	$[M]_0$ (mol L^{-1})	$[cat.]_0$ /$[PPA]_0$	time (h)	conv. (%)[b]	$M_{n,calcd.}$[c] (g mol^{-1})	$M_{n,NMR}$[b] (g mol^{-1})	M_w/M_n[d]
1	ε-CL	$C_6F_5CHTf_2$	50	1.0	1.0	11	91.6	5360	4160	1.58
2			50	1.0	0.1	24	78.7	4630	4460	1.22
3			50	3.0	0.1	7	97.2	5680	5690	1.12
4			100	3.0	0.1	45	94.7	11000	11100	1.11
5	δ-VL	$C_6F_5CHTf_2$	50	3.0	0.1	2	94.1	4850	4940	1.17
6			100			8	93.9	9540	9700	1.18
7	ε-CL	$HNTf_2$	50	3.0	0.1	7	90.1	5280	5380	1.14
8			100			22	95.0	11000	11300	1.19
9	δ-VL	$HNTf_2$	50	3.0	0.1	2	91.3	4700	4200	1.12
10			100			9	92.6	9400	9600	1.09

[a] temperature, r.t.; solvent, CH_2Cl_2. [b] Determined by ^1H NMR in $CDCl_3$. [c] Calculated from ($[M]_0/[PPA]_0$) × conv. × (M.W. of monomer) + (M. W. of PPA). [d] Determined by SEC in $CHCl_3$ using PSt standards.

Table 2.2. ROP of cyclic monomers using PPA and $HNTf_2$ [a]

run	monomer (M)	$[M]_0$ /$[PPA]_0$	$[M]_0$ (mol L^{-1})	[cat.] /$[PPA]_0$	time (h)	conv. (%)[b]	$M_{n,calcd.}$ [c] (g mol^{-1})	$M_{n,NMR}$ [b] (g mol^{-1})	M_w/M_n [d]
11	DXO	50	3.0	0.1	7	95.8	5700	5820	1.14
12		100			16	95.8	11300	11400	1.16
13	*rac*-LA	30	1.0	3.0	192	91.0	4070	4480	1.15
14		50			423	87.3	6430	6490	1.17
15	*β*-BL	40	0.4	0.12	14	99.1	3540	3580	1.19
16		60			18	99.1	5260	5470	1.28

[a] temperature, r.t.; solvent, CH_2Cl_2 for DXO and *rac*-LA, toluene for *β*-BL. [b] Determined by ^1H NMR in $CDCl_3$. [c] Calculated from $([M]_0/[PPA]_0) \times$ conv. $\times$ (M.W. of monomer) + (M. W. of PPA). [d] Determined by SEC in $CHCl_3$ using PSt standards.

2.2.2 Controlled/Living Nature of Super Brønsted Acid-Catalyzed ROP. To confirm the controlled/living nature of the $C_6F_5CHTf_2$ and $HNTf_2$-catalyzed ROPs, the kinetic experiments were conducted. Figures 2.4 and 2.5 showed the kinetic experiments for [*δ*-VL]$_0$/[PPA]$_0$/[$C_6F_5CHTf_2$]$_0$ = 50/1/0.1 and [*rac*-LA]$_0$/[PPA]$_0$/[$HNTf_2$]$_0$ = 50/1/3 as the representatives. The molecular weight linearly increased with the increasing monomer conversion, and the monomer consumption steadily increased with polymerization time followed by first-order kinetics. In addition, the $M_{n,NMR}$ values (circles) fairly agreed with the $M_{n,calcd}$ values (linear lines) based on the [M]$_0$/[PPA]$_0$ ratio. These results indicated that the $C_6F_5CHTf_2$ and $HNTf_2$-catalyzed ROPs proceeded through a controlled/living manner without any side reactions. Additionally, $HNTf_2$ sufficiently promoted the ROPs of *rac*-LA. For the Brønsted acid-ROP of cyclic esters, trifluoromethane sulfonic acid (TfOH) effectively controlled the living ROP of *rac*-LA, but not *ε*-CL,[19] while $C_6F_5CHTf_2$ was effective for *δ*-VL and *ε*-CL, but not *rac*-LA.[26] Thus, the acidity of $HNTf_2$, which is situated between TfOH and $C_6F_5CHTf_2$, is suitable for the controlled/living ROP of cyclic esters.

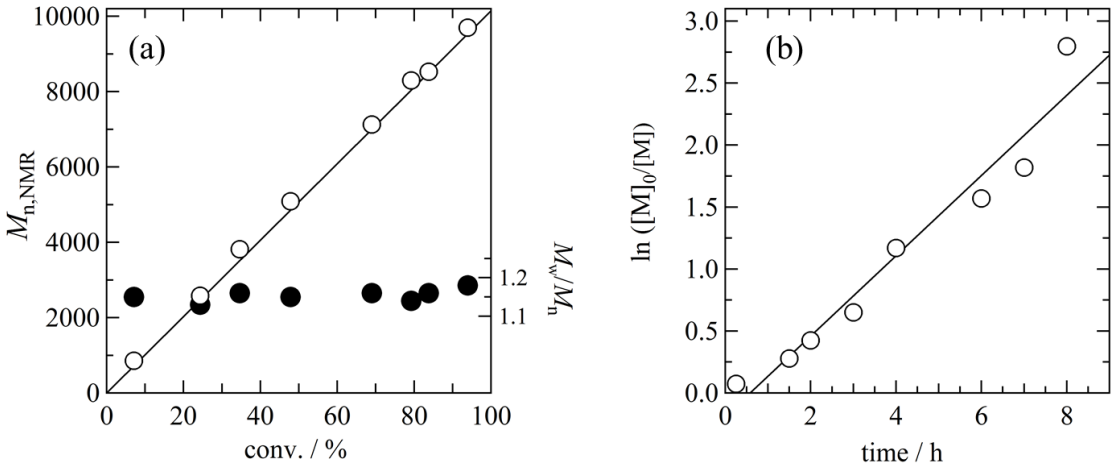

Figure 2.4. (a) Kinetic plots for the polymerization of *δ*-VL and (b) dependence of molecular weight (M_n) and polydispersity (M_w/M_n) on the monomer conversion (conv.) ([*δ*-VL]$_0$/[PPA]$_0$/[$C_6F_5CHTf_2$]$_0$ = 50/1/0.1).

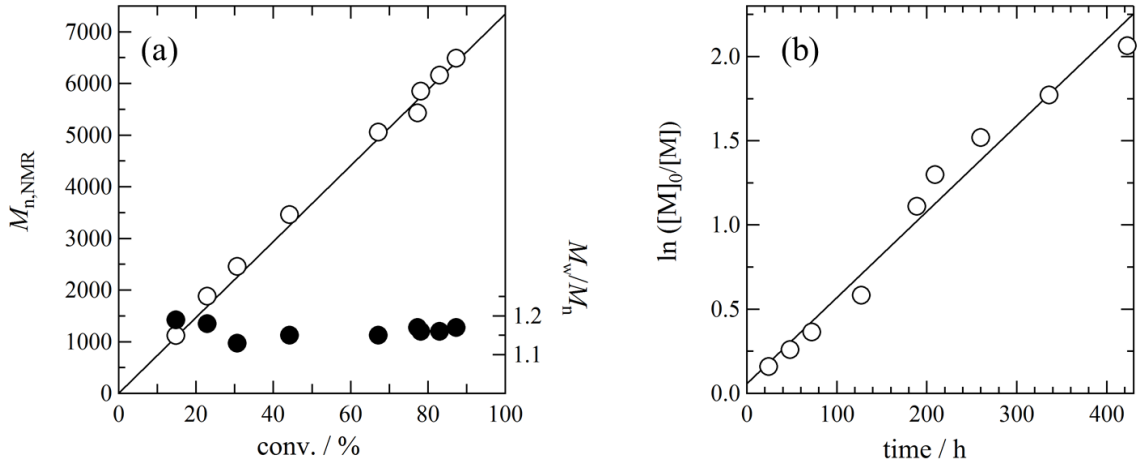

Figure 2.5. (a) Kinetic plots for the polymerization of *rac*-LA and (b) dependence of molecular weight (M_n) and polydispersity (M_w/M_n) on the monomer conversion (conv.) ([*rac*-LA]$_0$/[PPA]$_0$/[$HNTf_2$]$_0$ = 50/1/3).

Previously, Penczek et al. reported that the Brønsted acid-catalyzed ROP of cyclic esters proceeded through the activated monomer mechanism, leading to well defined polyesters connected to an initiator residue at the α-chain-end.[30] In fact, all the results using the ^{1}H NMR, SEC measurements strongly indicated that the obtained polymers, which were produced using $C_6F_5Tf_2$ and $HNTf_2$, possessed the 3-phenylpropoxy group as the α-chain-end, i.e., PPA acted as the initiating agent for the $C_6F_5CHTf_2$ and $HNTf_2$-catalyzed ROP system. Thus, the author concluded that these ROPs using the PPA initiator proceeded through the activated monomer mechanism, as shown in Scheme 2.2.

Further evidence was obtained from instrumental analysis. In fact, a change in the carbonyl carbon of the monomer in the absence/presence of $HNTf_2$ ([M]/[$HNTf_2$] = 1.0) was observed in the ^{13}C NMR measurement as shown in Figure 2.5; the chemical shifts of 176.17, 174.01, 168.20, and 167.35 ppm shifted a downfield to 181.06, 178.03, 171.48, and 168.67 ppm for ε-CL, DXO, β-BL, and *rac*-LA, respectively. The difference in the chemical shifts between

before and after adding $HNTf_2$ was in the order of ε-CL $\geq$ DXO > β-BL > *rac*-LA, which was fairly reflected in the order of polymerization rate, ε-CL $\geq$ DXO > β-BL > *rac*-LA. On the other hand, the ^{1}H NMR spectrum of PPA is measured in the absence/presence of $HNTf_2$. The hydroxyl proton signal shifts from 1.70 to 1.41 ppm, as shown in Figures 2.5, which indicated that OH alcoholic proton was deactivated by $HNTf_2$ in the same result as Bourissou's report.[27] These results strongly supported the fact that the $HNTf_2$-catalyzed ROP of cyclic esters using an alcohol initiator proceeded through the monomer activation mechanism.

Scheme 2.2. An activated monomer mechanism for the $C_6F_5CHTf_2$ and $HNTf_2$-catalyzed ROPs of ε-CL and δ-VL using PPA

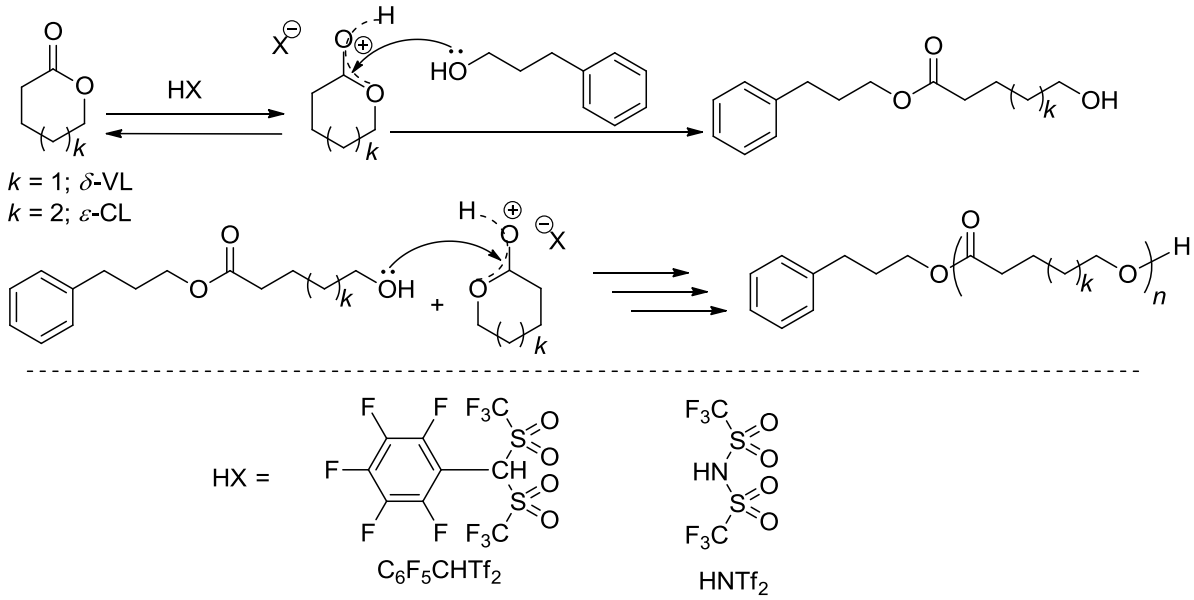

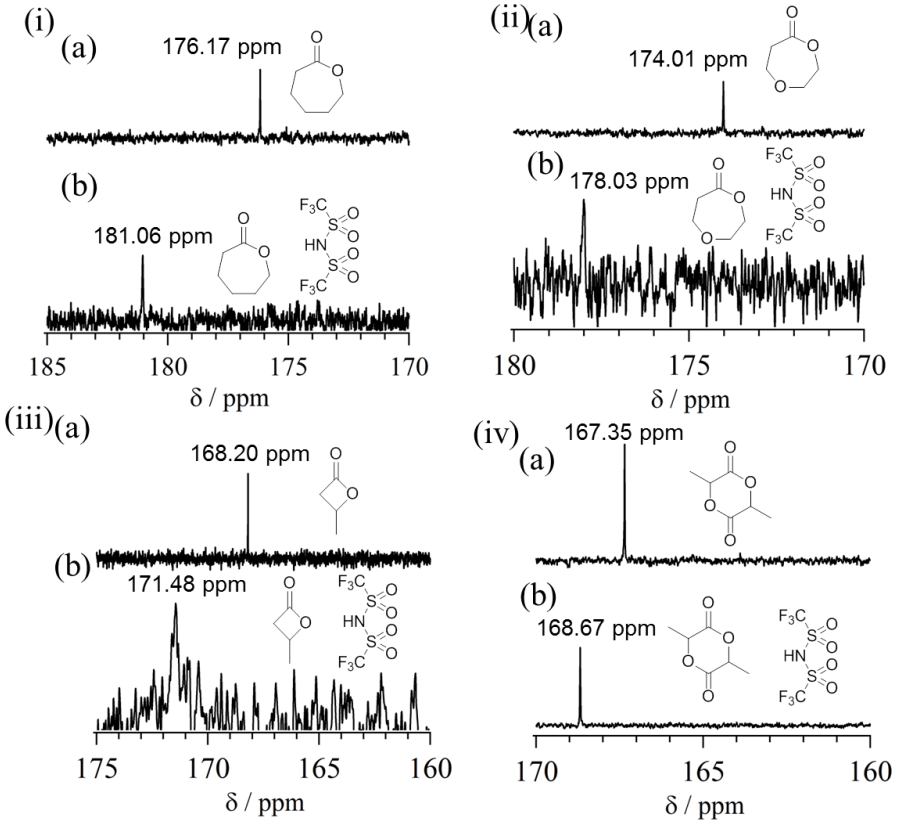

Figure 2.4. ^{13}C NMR spectra of the carbonyl carbon signals for (i) the *ε*-CL system, (ii) the DXO system, (iii) the *β*-BL system, and (iv) the *rac*-LA system, in $CDCl_3$; (a) *ε*-CL, DXO, *β*-BL, and *rac*-LA and (b) 1:1 mixtures of *ε*-CL, DXO, *β*-BL, and *rac*-LA with $HNTf_2$.

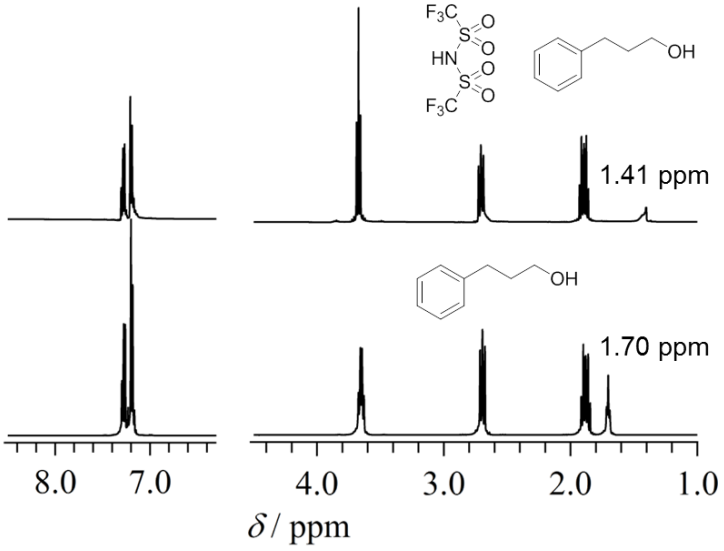

Figure 2.5. ^{1}H NMR spectra of the hydroxyl proton signals of (a)PPA, and (b) the 1:1 mixture of PPA with $HNTf_2$ in $CDCl_3$.

2.2.3 Synthesis of End-Functionalized Polyesters. Controlled/living polymerization systems provide the precise synthesis of well-defined macromolecular architectures. For the $C_6F_5CHTf_2$ and $HNTf_2$-catalyzed ROP of cyclic esters, PPA acted as the initiator to afford polyesters possessing the PPA moiety through the monomer activation mechanism. Thus, the author utilized the controlled/living characteristics for the $C_6F_5CHTf_2$ and $HNTf_2$-catalyzed ROP of cyclic esters for producing end-functionalized polyesters, which are typical applications based on controlled/living polymerization systems. For end-functionalized polyesters, clickable functional groups, such as azido, alkyne, and alkene, are useful moieties for further modifications,[31, 32] and vinyl groups act as macromonomers.[5, 33] To synthesize end-functionalized polyesters, the author used propargyl alcohol (PGA), 6-azido-1-hexanol (AHA), *N*-(2-hydroxyethyl)maleimide (HEMI), 5-hexen-1-ol (HEA), and 2-hydroxyethyl methacrylate (HEMA) as functional initiators (FIs) for the ROPs, as shown in Scheme 2.1. Tables 2.3 and 2.4 summarized the results. All ROPs of cyclic monomers initiated from FIs were well-controlled to afford the corresponding polymers with narrow molecular weight distributions, whose $M_{n,NMR}$ agreed with predictable $M_{n,calcd}$, as shown in Tables 2.3 and 2.4. For example, for the polymerization of ε-CL using AHA, the $M_{n,NMR}$ value of the PCL was 5790 g mol^{-1}, which agreed with the $M_{n,calcd}$ value of 5710 g mol^{-1} (Table 2.3, run 23). The NMR and IR spectra provided evidence for the existence of the azido group in PCL, as shown in Figures 2.6 and 2.7, respectively. In addition, the obtained polymers possessed these functional groups at the α-chain end by confirming with the ^{1}H NMR analysis. However, the ROP of *rac*-LA using AHA was exceptional because of high acidic conditions and longer polymerization time such that the M_w/M_n of 1.94 for the obtained polymer was broad due to decomposition of the azido group (Table 2.4, run 42).

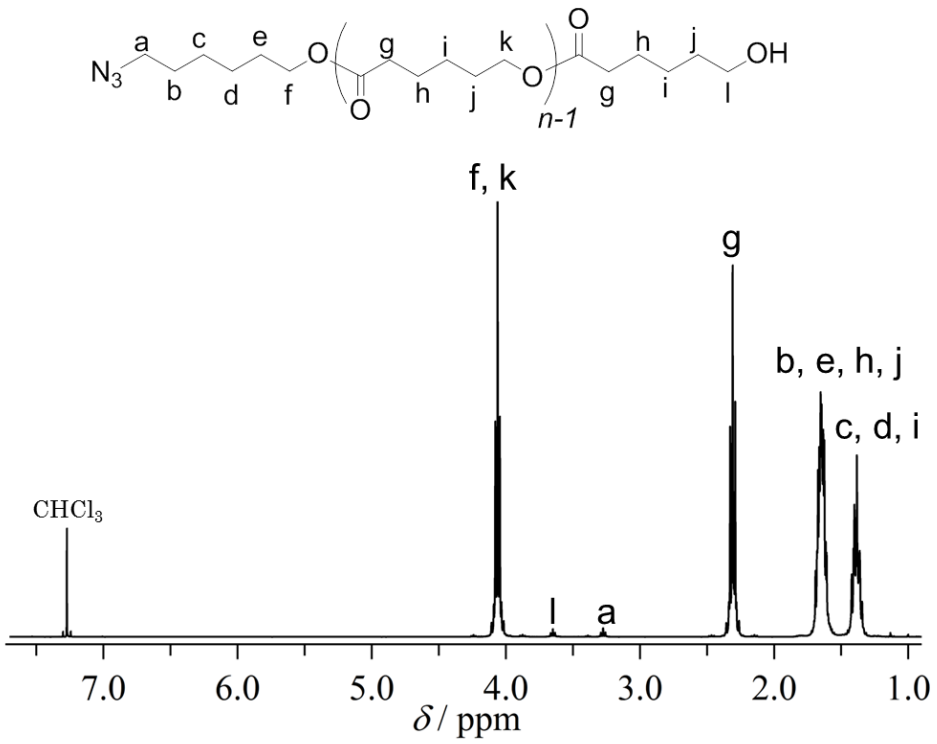

Figure 2.6. ^{1}H NMR spectrum of the obtained PCL functionalized by AHA (Table 2.3, run 23) in $CDCl_3$.

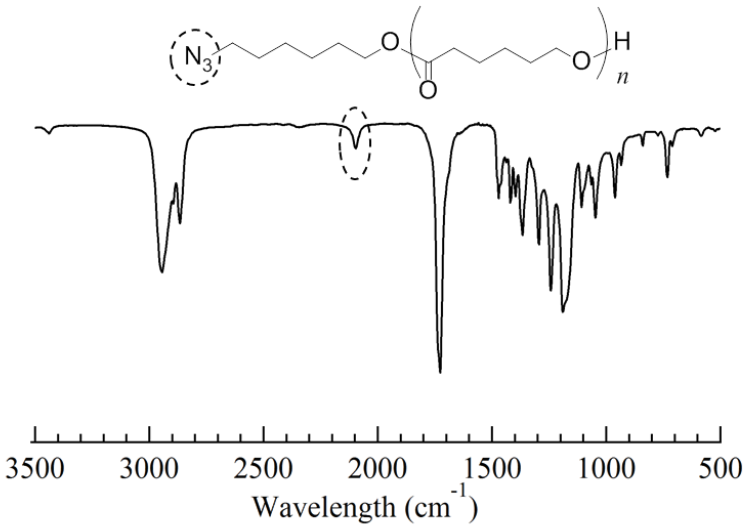

Figure 2.7. IR spectrum of the obtained PCL functionalized by AHA (Table 2.3, run 23).

Table 2.3. Synthesis of end-functionalized polyesters by the $C_6F_5CHTf_2$-catalyzed ROPs of *δ*-VL and *ε*-CL using functional initiators (FIs) [a]

run	monomer (M)	functional initiator (FI)	time (h)	conv. (%)[b]	$M_{n,calcd}$ [c] (g mol^{-1})	$M_{n,NMR}$ [b] (g mol^{-1})	M_w/M_n [d]
17		PGA		95.2	4820	5070	1.19
18		AHA		94.9	4890	4920	1.19
19	*δ*-VL	HEMI	2	91.0	4700	4820	1.15
20		HEMA		90.0	4640	4850	1.18
21		HEA		91.0	4620	5150	1.13
22		PGA		96.0	5540	5670	1.14
23		AHA		97.6	5710	5790	1.13
24	*ε*-CL	HEMI	7	97.3	5690	5830	1.14
25		HEMA		87.5	5130	5260	1.14
26		HEA		88.2	5130	5180	1.13

[a] $[M]_0$, 3.0 mol · L^{-1}; $[M]_0/[FI]_0/[C_6F_5CHTf_2]_0$, 50/1/0.1; temp., r.t.; solvent, CH_2Cl_2. [b] Determined by ^{1}H NMR in $CDCl_3$. [c] Calculated from $([M]_0/[FI]_0) \times$ conv. $\times$ (M. W. of *δ*-VL or *ε*-CL) + (M. W. of FI). [d] Determined by SEC in $CHCl_3$ using PSt standards.

Table 2.4. Synthesis of end-functionalized polymers by the $HNTf_2$-catalyzed ROP of cyclic monomers using various functional initiators [a]

run	monomer (M)	functional initiator (FI)	$[M]_0$ (mol L^{-1})	$[HNTf_2]_0$ /$[FI]_0$	time (h)	conv. (%) [b]	$M_{n,calcd}$ (g mol^{-1}) [c]	$M_{n,NMR}$ (g mol^{-1}) [b]	M_w /M_n [d]
27		AHA				92.0	4700	4700	1.12
28		PGA				96.2	4870	4970	1.17
29	δ-VL	HEMI	3.0	0.1	2	91.0	4700	6300	1.11
30		HEA				94.9	4850	5130	1.17
31		HEMA				92.4	4760	4950	1.18
32		AHA				96.5	5650	5750	1.15
33		PGA				87.4	5040	5210	1.13
34	ε-CL	HEMI	3.0	0.1	7	98.0	5740	5760	1.17
35		HEA				98.5	5720	5740	1.19
36		HEMA				98.3	5740	5910	1.16
37		AHA				96.7	5760	5830	1.17
38		PGA				96.0	5630	5710	1.18
39	DXO	HEMI	3.0	0.1	7	97.5	5800	5780	1.19
40		HEA				97.5	5790	5770	1.17
41		HEMA				97.9	5790	5980	1.16
42		AHA				80.8	5970	n.d.[e]	1.94 [f]
43 [g]		PGA				93.2	6770	6810	1.19
44	*rac*-LA	HEMI	1.0	3.0	385	90.6	6670	7040	1.19
45		HEA				98.1	6940	7170	1.24
46		HEMA				97.7	6910	7170	1.22
47		AHA				99.6	3570	3760	1.32
48		PGA				99.1	3470	3590	1.24
49	β-BL	HEMI	0.4	0.12	14	98.6	3540	3750	1.23
50		HEA				98.7	3500	3540	1.23
51		HEMA				98.7	3530	3740	1.31

[a] Temperature, room temp.; solvent, CH_2Cl_2; $[M]_0/[FI]_0$, 50. [b] Determined by ^1H NMR in $CDCl_3$. [c] Calculated from $([M]_0/[FI]_0) \times$ conv. $\times$ (M.W. of monomer) + (M. W. of FI). [d] Determined by SEC in $CHCl_3$ using PSt standards. [e] Not determined. [f] Azido was degraded as indicated by IR and MALDI-TOF MS. [g] time, 412 h.

2.2.4. Synthesis of Diblock Copolyesters

The author synthesized diblock copolymers using a macroinitiator, block copolymerization, and click reaction, based on the $HNTf_2$-catalyzed ROP, which could be polymerized wide range of monomers compared with $C_6F_5CHTf_2$-catalyzed ROP. First, the author carried out the synthesis of diblock copolymers consisting of poly(ethylene glycol) (PEG) and polyesters by the $HNTf_2$-catalyzed ROP of *δ*-VL, *ε*-CL, and DXO using methoxy poly(ethylene glycol) (MPEG; $M_{n,NMR}$ = 4,980 g mol^{-1}, M_w/M_n = 1.13) as the macroinitiator, as shown in Scheme 2.1. Table 2.5 summarizes the polymerization results. The obtained polymers consisted of PEG with PVL, PCL, and PDXO, which were confirmed by their ^{1}H NMR spectra, i.e., poly(ethylene glycol)-*block*-poly(*δ*-valerolactone) (PEG-*b*-PVL), poly(ethylene glycol)-*block*-poly(*ε*-caprolactone) (PEG-*b*-PCL), and poly(ethylene glycol)-*block*-poly(1,5-dioxepan-2-one) (PEG-*b*-PDXO). After the block copolymerization of *δ*-VL, *ε*-CL, and DXO using MPEG, the SEC traces shifted to the higher molecular weight region while keeping a narrow polydispersity, such as from 1.13 to 1.19 for *δ*-VL, from 1.13 to 1.17 for *ε*-CL, and from 1.13 to 1.12 for DXO, as shown in Figure 2.8. In addition, the $M_{n,NMR}$s of the PEG-polyesters obtained from *δ*-VL, *ε*-CL, and DXO were 9790, 10600, and 10200 g mol^{-1}, which well agreed with the $M_{n,calcd}$s of 9660, 10000, and 10200 g mol^{-1}, respectively.

Table 2.5. Synthesis of diblock copolyesters by the $HNTf_2$-catalyzed ROP of *δ*-VL, *ε*-CL, and DXO using MPEG [a]

run	monomer (M)	time (h)	conv. (%)[b]	$M_{n,calcd}$ [c] (g mol^{-1})	$M_{n,NMR}$ [b] (g mol^{-1})	M_w/M_n [d]
52	*δ*-VL	22	93.1	9660	9790	1.19
53	*ε*-CL	48	87.9	10000	10600	1.17
54	DXO	116	89.0	10200	10200	1.12

[a] Temperature, room temp.; solvent, CH_2Cl_2; $[M]_0/[MPEG]_0/[HNTf_2]_0$; 50/1/0.1; $[M]_0$, 2.0 mol L^{-1}. [c] Calculated from $([M]_0/[OH]_0) \times$ conv. $\times$ (M.W. of monomer) + 5,000 as molecular weight of MPEG. [b] Determined by ^{1}H NMR in $CDCl_3$. [d] Determined by SEC in DMF containing 0.01 mol·L^{-1} LiCl using PSt standards.

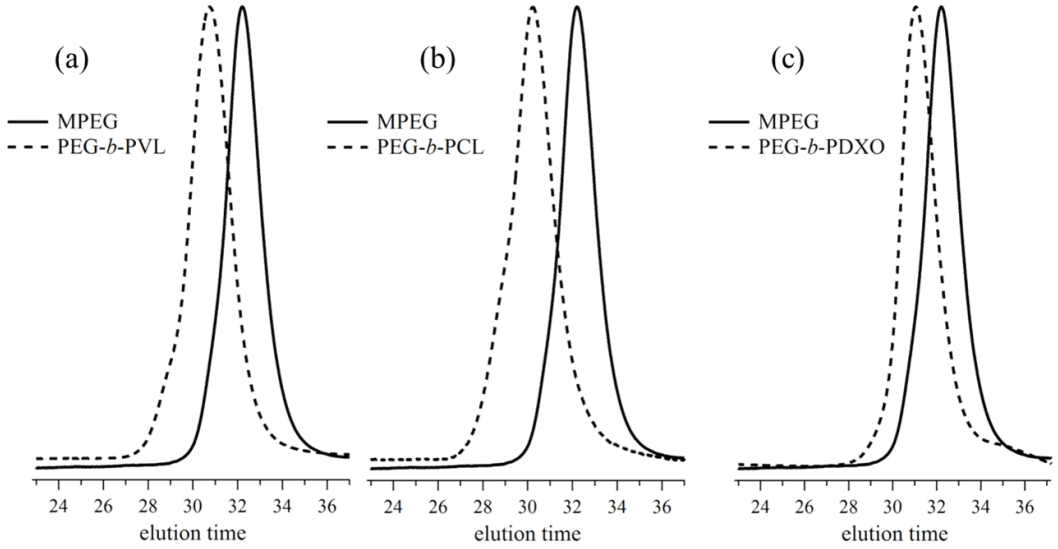

Figure 2.8. SEC traces of MPEG (solid line) and (a) PEG-*b*-PVL, (b) PEG-*b*-PCL, and (c) (a) PEG-*b*-PDXO (dashed line) (solvent, DMF containing 0.01 mol·L^{-1} LiCl; flow rate, 0.4 mL·min^{-1}).

Furthermore, the author attempted to prepare the diblock copolyesters consisting of PVL and PCL by the $HNTf_2$-catalyzed block copolymerization of *δ*-VL and *ε*-CL without quenching. For the ROPs of *ε*-CL and *δ*-VL as the first and second monomers, respectively, under the condition of $[\varepsilon\text{-CL}, \delta\text{-VL}]_0/[PPA]_0/[HNTf_2]_0 = 50/1/0.1$, the SEC trace shifted to a higher molecular weight region from 5900 to 10200 g mol^{-1}, which agreed with the $M_{n,calcd}$ values, and the polydispersity was as low as 1.16, as shown in Figure 2.9a. A similar result was obtained for the ROP of *ε*-CL and *δ*-VL as the first and second monomers, respectively, as shown in Figure 2.8b. These results mean that the well-defined diblock copolyesters consisting of PVL and PCL, poly(*δ*-valerolactone)-*block*-poly(*ε*-caprolactone) (PVL-*b*-PCL) and poly(*ε*-caprolactone)-*block*-poly(*δ*-valerolactone) (PCL-*b*-PVL), were synthesized depending on the order of the monomer addition.

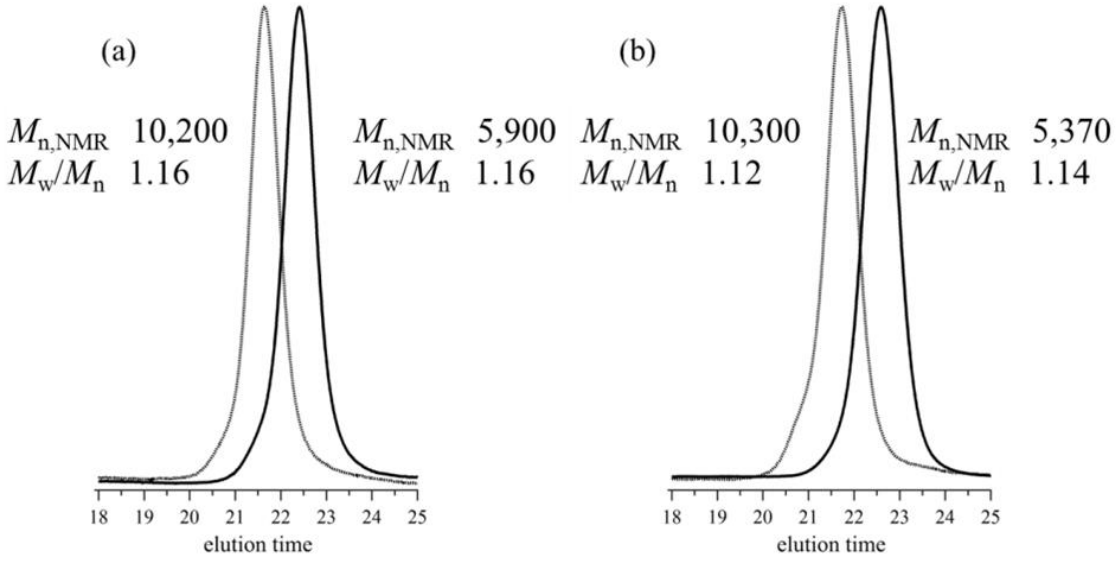

Figure 2.9. (a) SEC traces of first PCL sequence (solid line) and PCL-*b*-PVL (dashed line) and (b) SEC traces of first PVL sequence (solid line) and PVL-*b*-PCL (solvent, $CHCl_3$; flow rate, 0.8 $mL \cdot min^{-1}$).

Diblock copolyesters with a PLA segment were only slightly prepared by the block copolymerization of *rac*-LA as the second monomer without quenching because the ROP rate of *rac*-LA was low, resulting in broadening of the polydispersity by transesterification. Thus, the block copolyester with PLA was synthesized by the click reaction of the azido-functionalized poly(ε-caprolactone) (PCL-N_3) and the alkyne-functionalized polylactide (PLA-C≡CH), as shown in Scheme 2.3. The click reaction of the PCL-N_3 ($M_{n,NMR}$, 5750; M_w/M_n, 1.15) and PLA-C≡CH ($M_{n,NMR}$, 6810; M_w/M_n, 1.19) was carried out using the CuBr/2,2'-bipyridine (bpy) catalyst in THF under the condition of $[PCL\text{-}N_3]_0/[PLA\text{-}C{\equiv}CH]_0/[CuBr]_0/[bpy]_0$ = 1.1/1/4.8/2.8. The SEC trace of the obtained polymer shifted to a high molecular weight region and its polydispersity was 1.19, as shown in Figure 2.10. The FT-IR spectrum of the polymer obtained after click reaction showed the disappearance of the azido peak (2090 cm^{-1}). In addition, the methylene proton peak adjacent to the azido group (3.3 ppm) of PCL shifted to a low magnetic field (4.35 ppm) relative to the formation of 1,2,3-

triazole after click reaction. These results indicated that the polymer obtained after the click reaction was the block copolyester, poly(ε-caprolactone)-*block*-polylactide (PCL-*b*-PLA) with an $M_{n,NMR}$ of 12,700.

Scheme 2.3. Synthesis of PCL-*b*-PLA by the click reaction using PCL-N_3 and PLA-C≡CH

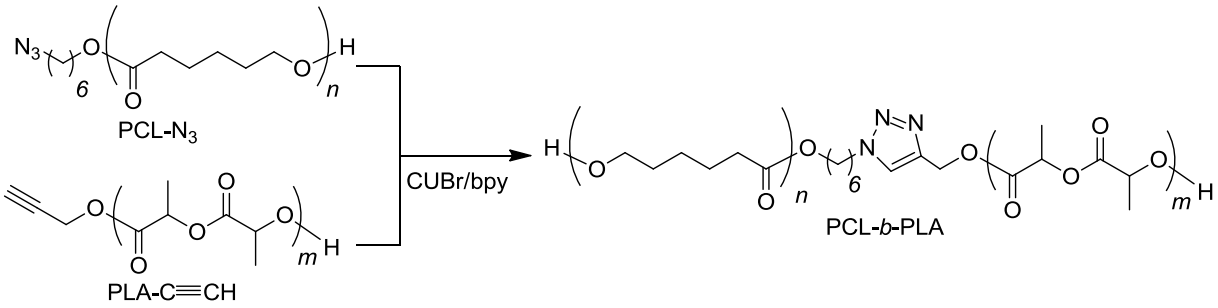

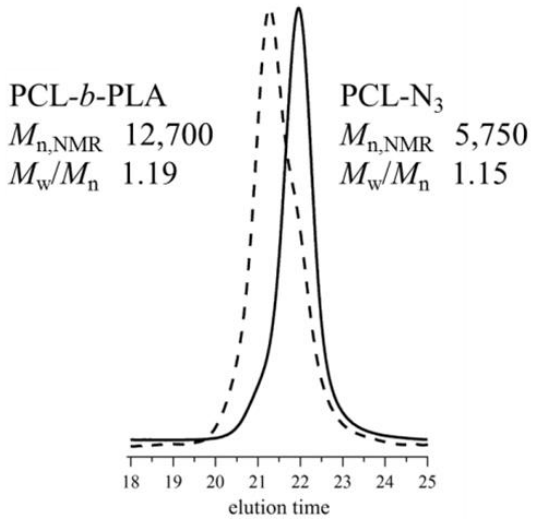

Figure 2.10. SEC traces of first PCL-N_3 sequence (solid line) and PCL-*b*-PLA (dashed line) (solvent, $CHCl_3$; flow rate, 0.8 mL·min^{-1}).

2.3 Conclusions

In this chapter, the author revealed that low loading amount of super Brønsted acids such as pentafluorophenylbis(triflyl)methane ($C_6F_5CHTf_2$) and triflimide ($HNTf_2$) acted as an organocatalyst to control the ring-opening polymerizations (ROPs) of *ε*-caprolactone (*ε*-CL) and *δ*-valerolactone (*δ*-VL) with hydroxy compounds as the initiator, affording the well-defined poly(*ε*-caprolactone)s (PCLs) and poly(*δ*-valerolactone)s (PVLs) with narrow polydispersities. The living nature of these polymerizations was confirmed by kinetic experiment, indicating the conclusion that the $C_6F_5CHTf_2$ and $HNTf_2$-catalyzed ROP of *ε*-CL and *δ*-VL using the PPA initiator proceeded through the activated monomer mechanism. The mechanism was also revealed NMR analyses. $HNTf_2$ was also efficiently catalyzed the ROPs of 1,5-dioxepan-2-one (DXO), *β*-butyrolactone (*β*-BL) and *rac*-lactide (*rac*-LA) due to its high acidity compared with $C_6F_5CHTf_2$. In addition, the Brønsted acid/alcohol system efficiently produced end-functionalized polyesters using propargyl alcohol, 6-azido-1-hexanol, *N*-(2-hydroxyethyl)maleimide, 5-hexen-1-ol, and 2-hydroxyethyl methacrylate and diblock copolymers using the macroinitiator, the sequential addition polymerization, and the click reaction.

2.4 Experimental Section

Materials. Toluene (>99.5 %; water content, <0.001 %) was purchased from Kanto Chemical Co., Inc., and distilled over sodium benzophenone ketyl under an argon atmosphere. Dichloromethane (CH_2Cl_2, >99.5 %; water content, <0.001 %, Kanto Chemical Co., Inc.), *δ*-valerolactone (*δ*-VL; 99 %, Kanto Chemical Co., Inc.), and *ε*-caprolactone (*ε*-CL; 99 %, Tokyo Kasei Kogyo Co., Ltd. (TCI)) were distilled over CaH_2 under an argon atmosphere. 1,5-Dioxepan-2-one (DXO; >98%, TCI) was dried by azeotropic distillation with toluene. The racemic lactide (*rac*-LA; >98%, TCI) was purified by two recrystallizations from dry toluene prior to use. Pentafluorophenylbis(triflyl)methane ($C_6F_5CHTf_2$, Tokyo Kasei Kogyo Co., Ltd. (TCI)), triflimide ($HNTf_2$, 95 %, Aldrich) and a weak base anion exchange resin, Amberlyst A21 (Organo Co., Ltd.), were used as received. 3-Phenyl-1-propanol (PPA; >98%, TCI) and propargyl alcohol (PGA; >98%, TCI) were distilled over CaH_2 under an argon atmosphere. 5-Hexen-1-ol (HEA; >98%, TCI) and 2-hydroxyethyl methacrylate (HEMA; >95%, TCI) were distilled under reduced pressure. 6-Azido-1-hexanol (AHA)[34] and *N*-(2-hydroxyethyl)maleimide (HEMI)[35] were synthesized using previously reported methods. Methoxy poly(ethylene glycol) (MPEG; average M_n, 5,000, Aldrich) was dried by azeotropic distillation with toluene. Copper(I) bromide (CuBr; >99.0 %, Aldrich), and bypiridine (bpy; >99.0 %, Aldrich) were purchased and used as received.

Instruments. The number-average molecular weights ($M_{n,NMR}$s) were determined from the ^{1}H NMR spectra recorded using a JEOL JNM-A400II instrument. The polymerization was carried out in an MBRAUN stainless steel glove box equipped with a gas purification system (molecular sieves and copper catalyst) in a dry argon atmosphere (H_2O, O_2 < 1 ppm). The moisture and oxygen contents in the glove box were monitored by an MB-MO-SE 1 and an MB-OX-SE 1, respectively. The size exclusion chromatography (SEC) was performed at

40 °C in $CHCl_3$ (0.8 mL·min^{-1}) using a Jasco GPC-900 system equipped with a set of two Shodex KF-805L columns (linear, 8 mm × 300 mm). The SEC in DMF containing lithium chloride (0.01 mol·L^{-1}) was performed at 40 °C using a Jasco high performance liquid chromatography (HPLC) system (PU-980 Intelligent HPLC pump, CO-965 column oven, RI-930 Intelligent RI detector, UV-2075 Plus Intelligent UV/VIS detector, and Shodex DEGAS KT-16) equipped with a Shodex Asahipak GF-310 HQ column (linear, 7.6 mm × 300 mm) and a Shodex Asahipak GF-7M HQ column (linear, 7.6 mm × 300 mm) at the flow rate of 0.4 mL·min^{-1}. The polydispersity (M_w/M_n) of the polymers was calculated on the basis of a polystyrene calibration. Matrix-assisted laser desorption ionization time-of-flight mass spectrometry (MALDI-TOF MS) of the obtained polymers was performed using an Applied Biosystems Voyager-DE STR-H equipped with a 337-nm nitrogen laser (3 ns pulse width). One hundred shots were accumulated for the spectra at a 25 kV acceleration voltage in the reflector mode and calibrated using polystyrene (average M_n 3,600, Waters Associates) as the internal standard. Samples for the MALDI-TOF MS were prepared by mixing the polymer (1.0 mg), a matrix (2,5-dihydroxybenzoic acid, 15 mg), and a cationizing agent (sodium trifluoroacetate, 1.0 mg) in 1 mL of THF. The MALDI target was spotted with 0.5 μL of solution and allowed to air-dry.

Polymerization of *ε*-caprolactone. A typical procedure for the polymerization is as follows: *ε*-CL (0.16 mL, 1.5 mmol) was added to a stock solution of PPA (30 μL, 30 μmol) in CH_2Cl_2 at room temperature in the glove box. A stock solution of $HNTf_2$ (30 μL, 3.0 μmol) in CH_2Cl_2 was added to the monomer solution to initiate the polymerization under an argon atmosphere. During the polymerization, the author obtained a small portion of the polymerization mixture and then a small amount of triethylamine was added to the mixtures for determining the monomer conversion based on the ^{1}H NMR measurements. After 7 h, the

polymerization was quenched by the addition of Amberlyst A21. The polymer was isolated by reprecipitation in cold methanol. Yield, 63 %; $M_{n,NMR}$, 5,380 g·mol^{-1}; M_w/M_n, 1.14; ^{1}H NMR ($CDCl_3$) δ (ppm), 1.38 (m, 2H × *n*, (-$CH_2CH_2CH_2CH_2CH_2$-)$_n$), 1.55-1.63 (m, 4H × *n*, (-$COCH_2CH_2CH_2CH_2CH_2O$-)$_n$), 1.96 (q, 2H, *J* = 6.8 Hz, ArCH_2CH_2-), 2.31 (t, 2H × n, *J* = 5.6 Hz, (-$COCH_2$-)$_n$), 2.69 (t, 2H, *J* = 7.6 Hz, ArCH_2-), 3.65 (t, 2H, *J* = 6.8 Hz,-CH_2CH_2OH), 4.06 (t, 2H × *n*, *J* = 6.8 Hz, (-CH_2O-)$_n$), 4.11 (m, 2H,Ar$CH_2CH_2CH_2$-) 7.15-7.32 (m, 5H, aromatic).

Synthesis of PCL-block-PLA by azide/alkyne click reaction

To a mixture of azido-functionalized poly(ε-caprolactone) (PCL-N_3: $M_{n,NMR}$ 5,750, M_w/M_n 1.15; 42 mg, 7.2 μmol), CuBr (4.4 mg, 31 μmol), and 2,2'-bipyridine (bpy, 2.8 mg, 18 μmol) were added a degassed solution of the alkyne-functionalized poly(lactide) (PLA-C≡CH: $M_{n,NMR,}$ 6,810, M_w/M_n 1.19; 44 mg, 7.7 μmol) in THF (2 mL) under an argon atmosphere. After 2 days, the reaction mixture was passed through the silica gel column and evaporated to remove the solvent and reagents. The clicked polymer was isolated by dialysis against CH_2Cl_2. Yield, 87% (before dialysis); 24 % (after dialysis); $M_{n,NMR}$, 12,700 g·mol^{-1}; M_w/M_n, 1.15; ^{1}H NMR ($CDCl_3$) δ (ppm), 1.30-1.47 (m, 4H, (-$CH_2CH_2CH_2CH_2N$<, 2H × *n*, (-$CH_2CH_2CH_2CH_2CH_2$-)$_n$), 1.49-1.70 (m, 4H -$CH_2CH_2CH_2(CH_2)_2N$<, 4H × *n*, (-$COCH_2CH_2CH_2CH_2CH_2O$-)$_n$, 3H × *m*, (-CH_3)$_m$), 2.31 (m, 2H × *n*, (-$COCH_2$-)$_n$), 3.65 (t, 2H, *J* = 6.0 Hz, -CH_2CH_2OH), 4.03-4.11 (m, 2H, -$CH_2(CH_2)_5N$<), 4.06 (m, t, 2H × *n*, *J* = 8.0 Hz, (-CH_2O-)$_n$), 4.36 (t, 2H, *J* = 8.0 Hz, -CH_2N<) 5.09-5.30 (m, 2H, -OCH_2C<, 1H × *m*, (-$CH(CH_3)O$-)$_m$), 7.52 (s, 1H, triazole ring).

2.5 References and Notes

1. Kamber, N. E.; Jeong, W.; Waymouth, R. M.; Pratt, R. C.; Lohmeijer, B. G. G.; Hedrick, J. L. *Chem. Rev.* **2007,** *107*, 5813-5840.

2. Kiesewetter, M. K.; Shin, E. J.; Hedrick, J. L.; Waymouth, R. M. *Macromolecules* **2010,** 43, *5*, 2093-2107.

3. Dove, A. P. *Macro Lett.* **2012**, *1*, 1409-1412.

4. Sanda, F.; Sanada, H.; Shibasaki, Y.; Endo, T. *Macromolecules* **2002**, *35*, 680-683.

5. Kakwere, H.; Perrier, S. *J. Polym. Sci., Part A: Polym. Chem.* **2009,** *47*, 6396-6408.

6. Scholten, M. D.; Hedrick, J. L.; Waymouth, R. M. *Macromolecules* **2008,** *41,* 7399-7404.

7. Raynaud, J.; Gnanou, Y.; Taton, D. *Macromolecules* **2009,** *42*, 5996-6005.

8. Kakuchi, T.; Chen, Y.; Kitakado, J.; Mori, K.; Fuchise, K.; Satoh, T. *Macromolecules* **2011**, *44*, 4641-4647.

9. Kakuchi, R.; Chiba, K.; Fuchise, K.; Sakai, R.; Satoh, T.; Kakuchi, T. *Macromolecules*, **2009,** ***42***, 8747-8750.

10. Fuchise, K.; Kakuchi, R.; Narumi, A.; Sakai, R.; Satoh, T.; Kawaguchi, S.; Kakuchi, T. *Macromolecules* **2010**, *43*, 5589-5594.

11. Takada, K.; Fuchise, K.; Chen, Y.; Satoh, T.; Kakuchi, T. *J. Polym. Sci., Part A, Polym. Chem.,***2012***, 50,* 3560-3566.

12. Fuchise, K.; Chen, Y.; Satoh, T.; Kakuchi, T. *Polym. Chem.*, **2013**, *4*, 4278-4291.

13. Connor, E. F.; Nyce, G. W.; Myers, M.; Mock, A.; Hedrick, J. L.; *J. Am. Chem. Soc.* **2002**, *124*, 914-915.

14. Nyce, G. W.; Glauser, T.; Connor, E. F.; Mock, A.; Waymouth, R. M.; Hedrick, J. L. *J. Am. Chem. Soc.* **2003**, *125*, 3046-3056.

15. Dove, A. P.; Pratt, R. C.; Lohmeijer, B. G. G.; Culkin, D. A.; Hagberg, E. C.; Nyce, G. W.; Waymouth, R. M.; Hedrick, J. L. *Polymer* **2006**, *47*, 4018-4025.

16. Kamber, N. E.; Jeong, W.; Gonzalez, S.; Hedrick, J. L.; Waymouth, R. M. *Macromolecules* **2009**, *42*, 1634-1639.

17. Nederberg, F.; Connor, E. F.; Moller, M.; Glauser, T.; Hedrick, J. L. *Angew. Chem. Int. Ed.* **2001**, *40*, 2712-2715.

18. Myers, M.; Connor, E. F.; Glauser, T.; Mock, A.; Nyce, G.; Hedrick, J. L. *J. Polym. Sci., Part A: Polym. Chem.* **2002**, *40*, 844-851.

19. Pratt, R. C.; Lohmeijer, B. G. G.; Long, D. A.; Waymouth, R. M.; Hedrick, J. L. *J. Am. Chem. Soc.* **2006**, *128*, 4556-4557.

20. Lohmeijer, B. G. G.; Pratt, R. C.; Leibfarth, F.; Logan, J. W.; Long, D. A.; Dove, A. P.; Nederberg, F.; Choi, J.; Wade, C.; Waymouth, R. M.; Hedrick, J. L. *Macromolecules* **2006**, *39*, 8574-8583.

21. Zhang, L.; Pratt, R. C.; Nederberg, F.; Horn, H. W.; Rice, J. E.; Waymouth, R. M.; Wade, C. G.; Hedrick, J. L. *Macromolecules* **2010**, *43*, 1660-1664.

22. Zhang, L.; Nederberg, F.; Pratt, R. C.; Waymouth, R. M.; Hedrick, J. L.; Wade, C. G. *Macromolecules* **2007**, *40*, 4154-4158.

23. Zhang, L.; Nederberg, F.; Messman, J. M.; Pratt, R. C.; Hedrick, J. L.; Wade, C. G. *J. Am. Chem. Soc.* **2007**, *129*, 12610-12611.

24. Shibasaki, Y.; Sanada, H.; Yokoi, M.; Sanda, F.; Endo, T. *Macromolecules* **2000**, *33*, 4316-4320.

25. Sanda, F.; Sanada, H.; Shibasaki, Y.; Endo, T. *Macromolecules* **2002**, *35*, 680-683.

26. Casas, J.; Persson, P. V.; Iversen, T.; Cordova, A. *Adv. Synth. Catal.* **2004**, *346*, 1087-1089.

27. Gazeau-Bureau, S.; Delcroix, D.; Martin-Vaca, B.; Bourissou, D.; Navarro, C.; Magnet, S. *Macromolecules* **2008**, *41*, 3782-3784.

28. Hasegawa, A.; Ishihara, K.; Yamamoto, H. *Angew. Chem. Int. Ed.* **2003**, *42*, 5731-5733.

29. Bourissou, D.; Martin-Vaca, B.; Dumitrescu, A.; Graullier, M.; Lacombe, F. *Macromolecules* **2005**, *38*, 9993-9998.

30. Penczek S. *J. Polym. Sci., Part A: Polym. Chem.* **2000**, *38*, 1919-1933.

31. Misaka, H.; Kakuchi, R.; Zhang, C. H.; Sakai, R.; Satoh, T.; Kakuchi, T. *Macromolecules* **2009,** *42*, 5091-5096.

32. Xie, M.; Shi, J.; Ding, L.; Li, J.; Han, H.; Zhang, Y. *J. Polym. Sci., Part A: Polym. Chem.* **2009**, *47*, 3022-3033.

33. Ito, K. *Prog. Polym. Sci.* **1998,** *23*, 581-620.

34. Speers, A. E.; Adam, G. C.; Cravatt, B. F. *J. Am. Chem. Soc.* **2003**, *125*, 4686-4687.

35. Heath, W. H.; Palmieri, F.; Adams, J. R.; Long, B. K.; Chute, J.; Holcombe, T. W.; Zieren, S.; Truitt, M. J.; White, J. L.; Willson, C. G. *Macromolecules* **2008**, *41*, 719−726.

Chapter 3

Synthesis of Well-Defined Polyesters and Polycarbonates via Controlled/Living Ring-Opening Polymerization Using Diphenyl Phosphate as an Efficient Organocatalyst

3.1 Introduction

As revealed in chapter 2, very strong Brønsted acids, such as pentafluorophenylbis(triflyl)methane ($C_6F_5CHTf_2$), and triflimide ($HNTf_2$),[1] were efficiently controlled the ring-opening polymerization (ROP) of various cyclic esters, and their acidity strongly affected the polymerization characteristics of these monomers. Although a loaded amount of strong Brønsted acids toward monomer was very low in comparison with other acid catalysts due to the extremely strong acidity of catalysts, this property caused undesirable reactions, such as transesterification, resulting in broadening of the molecular weight distributions of the obtained polyesters. In addition, Bourrissou et al. reported that the trifluoromethane sulfonic acid (TfOH)-catalyzed ROP of ε-caprolactone (ε-CL) produced only oligomer because the high acidity of catalysts deactivated the propagating chain-end during the polymerization whereas the lower acidic catalyst, methane sulfonic acid (MsOH), could afford well-defined poly(ε-caprolactone) (PCL).[2] Thus, it is interesting to elucidate the scope and limit of applicable acid catalysts in connection with suitable cyclic monomers for the ROP. The author focused on diphenyl phosphate (DPP) as the weak acid organocatalyst because DPP is commercially available, has a low toxicity, and is chemically stable.[3]

To expand the scope of applicable monomers for the organocatalytic ROP, in addition to cyclic esters, the author focused on cyclic carbonates and their polymers of aliphatic polycarbonates from the viewpoint of biodegradable polymeric materials. The ROP of cyclic carbonates, such as trimethylene carbonate (TMC), has been studied using nucleophilic and basic organocatalysts, such as a tertiary amine,[4-6] guanidine,[5-7] amidine,[5, 7] phosphazene,[5, 6] *N*-heterocyclic carbene,[7] and thiourea/amine,[5, 7] in which these organocatalysts activated the monomers and/or the initiating/propagating groups. However, the polymerization conditions required a relatively high polymerization temperature (50-150 °C), and the obtained polymers

had relatively wide polydispersity indices, except for some reports.[8, 9] In addition, Bourissou et al. reported the ROP of TMC using acidic organocatalysts, such as TfOH and MsOH;[10] TfOH triggered a undesirable decarboxylation of the carbonate group due to the extremely strong acidity of TfOH, resulting in broadening of the molecular weight distributions of the obtained polymers, while MSA was effective for affording poly(trimethylene carbonate)s (PTMCs) with controlled molecular weights ($M_{n,}$ ~8640) and narrow polydispersity indices (<1.12).

In this chapter, the author describes that DPP was used as the organocatalyst for the ROPs of δ-valerolactone (δ-VL), ε-CL, and TMC using PPA as the initiator (Scheme 1). This chapter describes 1) the characterization and optimization of the DPP-catalyzed ROPs of δ-VL, ε-CL, and TMC, 2) the characterization of the obtained polymers and polymerization mechanism of the DPP-catalyzed ROP of cyclic esters and cyclic carbonates using ^{1}H NMR, SEC, and MALDI-TOF MS analyses, 3) syntheses of end-functionalized PVLs, PCLs, and PTMCs using functional initiators, such as 2-hydroxyethyl methacrylate (HEMA), 4-vinylbenzyl alcohol (VBA), propargyl alcohol (PGA), and 6-azido-1-hexanol (AHA) and side-chain or main-chain modified polymers using analogue monomers, and 4) the syntheses of diblock copolymers consisting of PVL, PCL, and PTMC, as shown in Scheme 3.1.

Scheme 3.1. Synthesis of poly(δ-valerolactone) (PVL), poly(ε-caprolactone) (PCL), and poly(trimethylene carbonate) (PTMC) using 3-phenyl-1-propanol (PPA), 2-hydroxyethyl methacrylate (HEMA), 4-vinylbenzyl alcohol (VBA), propargyl alcohol (PGA), and 6-azido-1-hexanol (AHA) as the initiator and diphenyl phosphate (DPP) as a catalyst

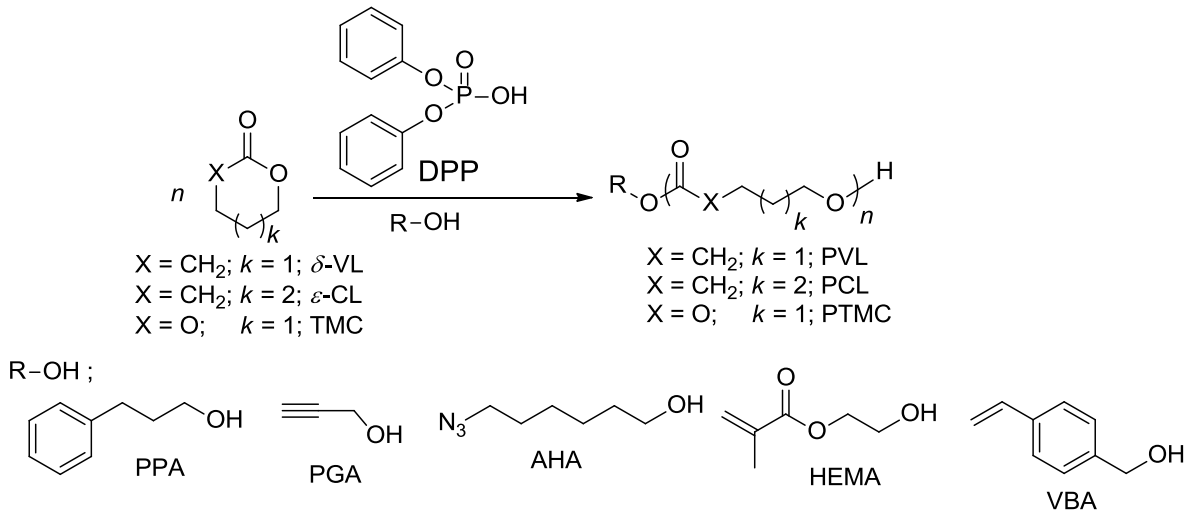

3.2 Results and Discussion

3.2.1 ROPs of *δ*-VL, *ε*-CL, and Trimethylene Carbonate (TMC) Catalyzed by Diphenyl Phosphate (DPP). In order to use diphenyl phosphate (DPP) as the acid catalyst for the ring-opening polymerizations (ROPs) of *δ*-valerolactone (*δ*-VL), *ε*-caprolactone (*ε*-CL), and trimethylene carbonate (TMC), the author first carried out the polymerizations of *δ*-VL, *ε*-CL, and TMC using 3-phenyl-1-propanol (PPA) as the initiator in toluene at room temperature at the $[M]_0/[PPA]_0/[DPP]_0$ ratio of 50/1/1 (Table 3.1, runs 1, 5, and 11, respectively). All polymerizations homogeneously proceeded and were quenched with immobilized base, and the obtained polymers were purified by reprecipitation using CH_2Cl_2 as the good solvent and cold methanol as the poor solvent. The conversion of *δ*-VL was 95.0 % for the polymerization time of 1 h, that of *ε*-CL was 97.1 % for 8 h, and that of TMC was 97.9 % for 36 h, which were directly determined by the ^{1}H NMR spectra of aliquots of the polymerization mixtures in $CDCl_3$. The consumption rate of *δ*-VL was faster than that of *ε*-CL, which agreed with other systems for the polymerizations of *δ*-VL and *ε*-CL.

The chemical structures of the obtained polymers were assigned to poly(*δ*-valerolactone) (PVL), poly(*ε*-caprolactone) (PCL), and poly(trimethylene carbonate) (PTMC) by the ^{1}H NMR measurement (Figure 3.1). The characteristic peaks due to the initiator of PPA were observed as the peaks due to the phenyl protons, the benzyl protons, and the methylene protons adjacent to the ester linkage that appeared in the range from 7.15 to 7.34 ppm, 2.68 ppm, and 1.93 ppm, respectively, and the peak due to the methylene protons adjacent to the *ω*-chain end of the hydroxyl group was clearly observed at 3.61 ppm. In addition, the peaks for PCL appeared in the ranges of 7.15 - 7.34, 2.63, 1.93, and 3.65 ppm, respectively, and the peaks for PTMC appeared in the ranges of 7.16 - 7.37, 4.13-4.32, 2.71, 1.97-2.11 ppm, respectively. Furthermore, no decarboxynation had occurred in the ROP of TMC because

there was no signal at 3.47 ppm due to the ether linkages formed by the decarboxylation, as shown in Figure 3.1c. These results implied that all polymerizations were initiated from PPA. More importantly, the number average molecular weight ($M_{n,NMR}$) of the obtained polymer estimated from the ^{1}H NMR measurement fairly agreed with that ($M_{n,calcd}$) calculated from the initial ratio of $[M]_0/[PPA]_0$ and monomer conversions; the $M_{n,NMR}$ and $M_{n,calcd}$ values for PVL were 5170 g mol^{-1} and 4890 g mol^{-1}, respectively, and those for PCL were 5920 g mol^{-1} and 5680 g mol^{-1}, respectively, and those for PTMC were 5220 g mol^{-1} and 5130 g mol^{-1}. These results indicated that the obtained polyesters should possess a PPA residue as the initiating end group.

Additionally, a MALDI-TOF MS measurement provided direct evidence that the ROPs of δ-VL, ε-CL, and TMC initiated by PPA proceeded in controlled/living nature. Figures 3.3-3.5 showed the MALDI-TOF MS spectra of the obtained PVL, PCL, and PTMC respectively. For example, one series of peaks perfectly agreed with the molecular weight of PVL possessing the PPA residue and the hydroxyl chain end (Figure 3.2). In addition, the author confirmed that PCL and PTMC showed results similar to MALDI-TOF MS spectra (Figures 3.3 and 3.4). These results mean that the DPP-catalyzed ROPs of δ-VL, ε-CL, and TMC proceeded in a living manner without any side reactions, such as backbiting, decarboxylation, and transesterification reactions, and PPA was obviously the initiator.

(a)

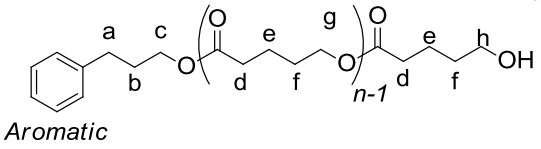
a
c
O
e
g
O
e
h
OH
b
O
d
f
O
d
f
n-1
Aromatic

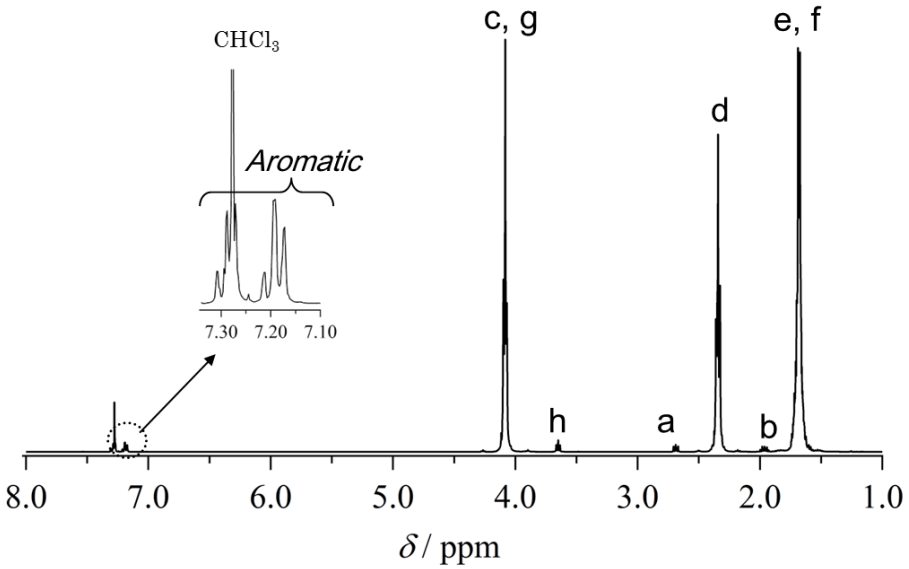
CHCl3
Aromatic
7.30 7.20 7.10
c, g
e, f
d
h
a
b
8.0 7.0 6.0 5.0 4.0 3.0 2.0 1.0
δ / ppm

(b)

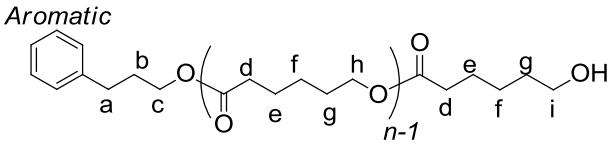
Aromatic
b
O
d
f
h
O
e
g
OH
a
c
O
e
g
O
d
f
i
n-1

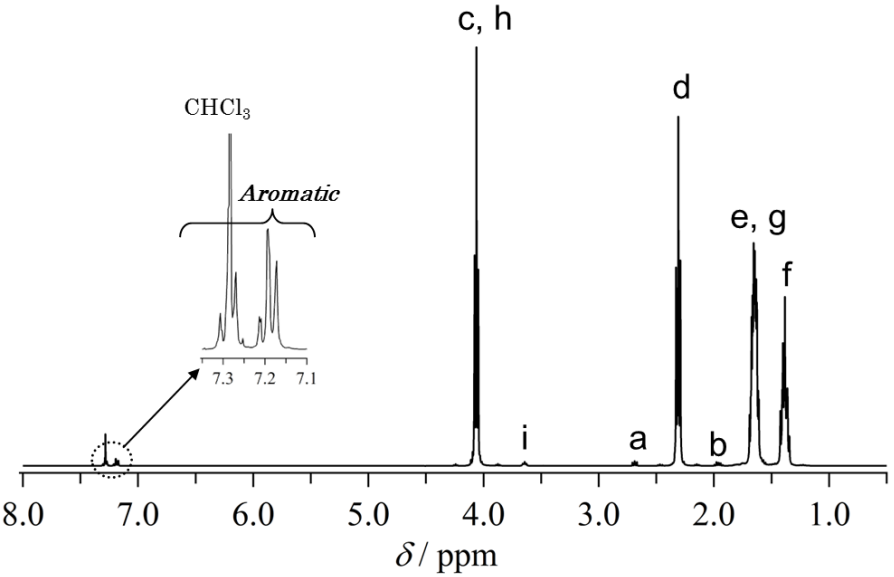
c, h
d
CHCl3
Aromatic
e, g
f
7.3 7.2 7.1
i
a
b
8.0 7.0 6.0 5.0 4.0 3.0 2.0 1.0
δ / ppm

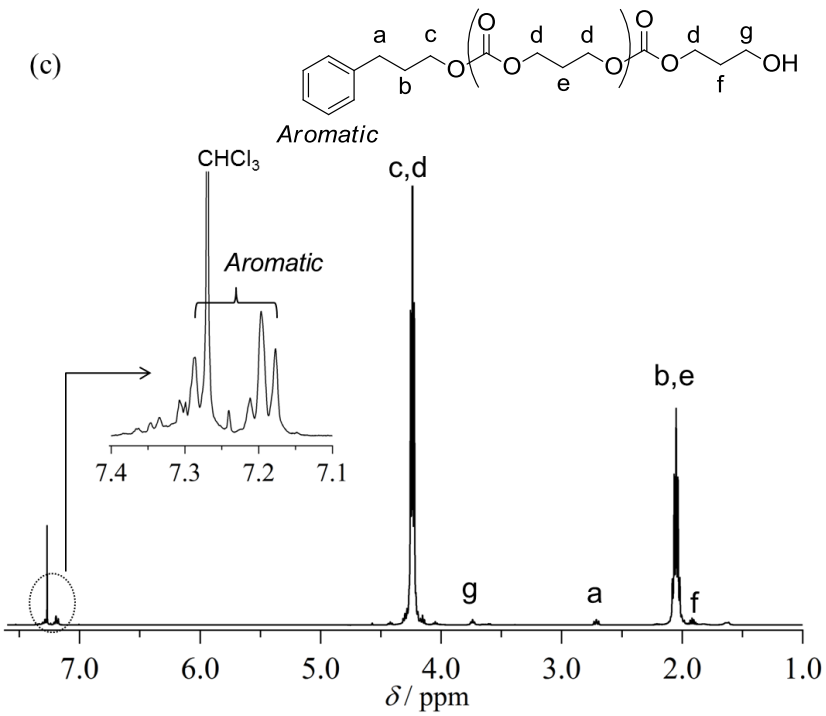

Figure 3.1. ^{1}H NMR spectra of (a) PVL, (b) PCL, and (c) PTMC initiated from 3-phenyl-1-propanol (PPA) in $CDCl_3$ (Table 1, runs 1, 5, and 11).

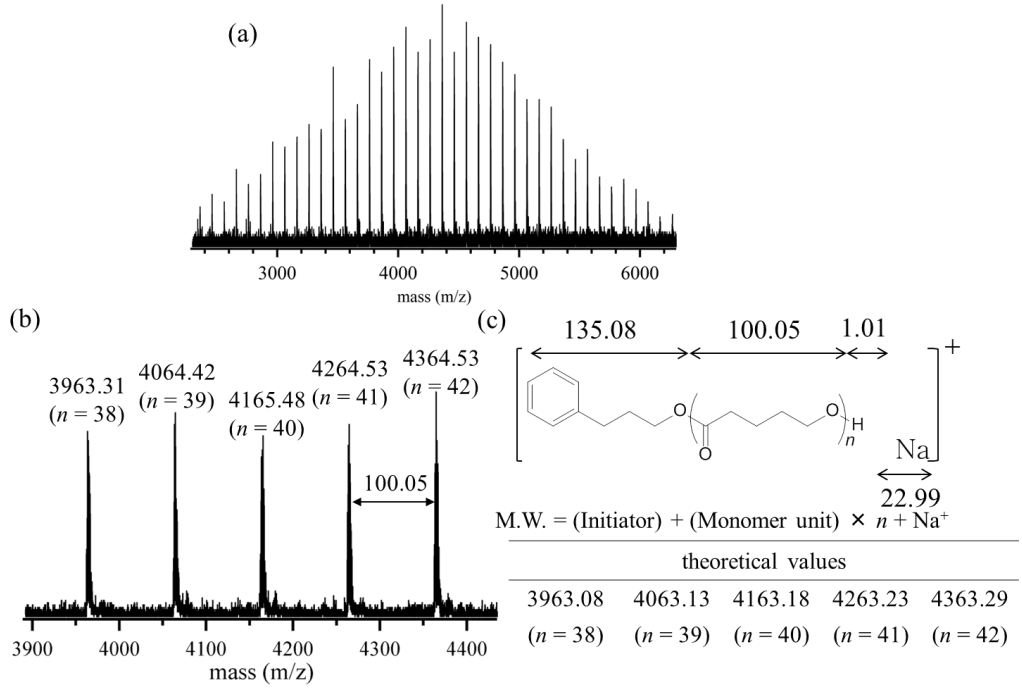

Figure 3.2. (a) MALDI-TOF MS spectrum in reflector mode of the obtained PVL (Table 3.1, run 1), (b) expanded spectrum, and (c) calculated molecular weights.

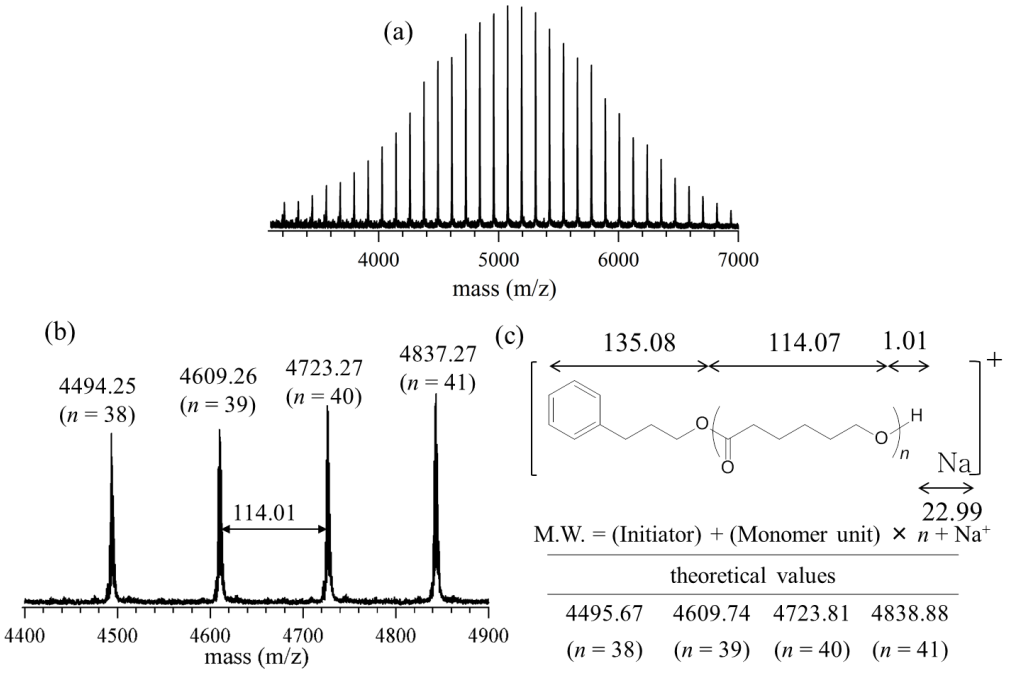

Figure 3.3. (a) MALDI-TOF MS spectrum in reflector mode of the obtained PCL (Table 3.1, run 5), (b) expanded spectrum, and (c) calculated molecular weights.

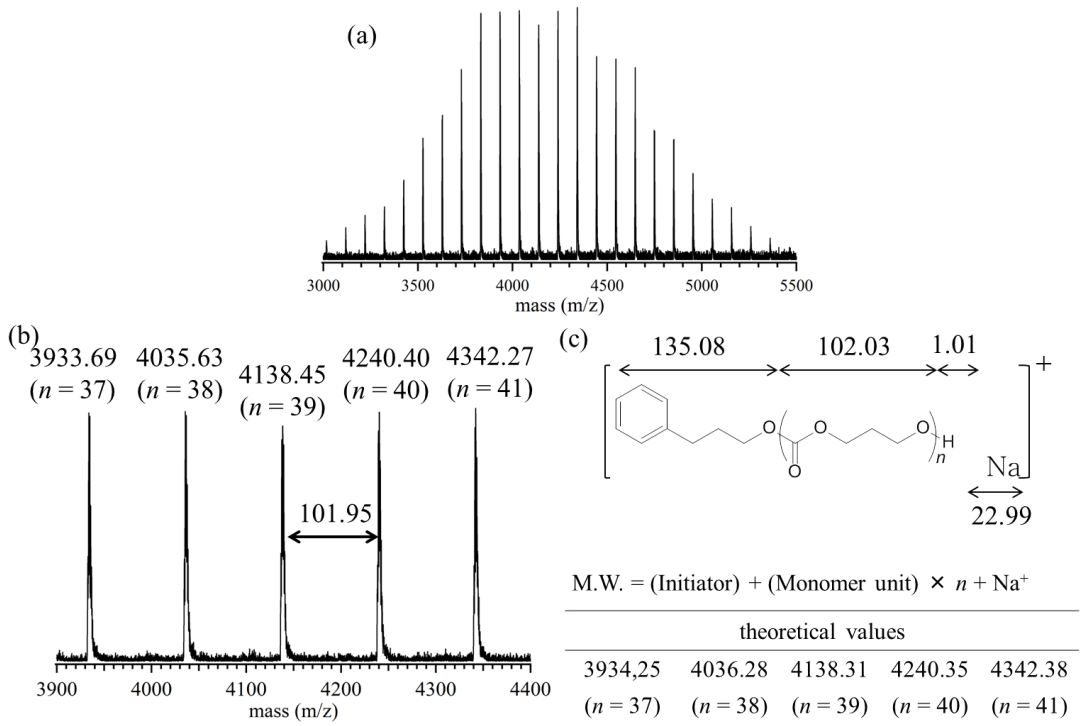

Figure 3.4. (a) MALDI-TOF MS spectrum in reflector mode of the obtained PTMC (Table 3.1, run 11), (b) expanded spectrum, and (c) calculated molecular weights.

To confirm that the polymerization system proceeded in a controlled/living fashion, the author carried out the ROPs of δ-VL, ε-CL, and TMC with varying $[M]_0/[PPA]_0$ ratios (Table 3.1). The molecular weights of the resultant polymers linearly increased with the increasing initial ratio of $[M]_0/[PPA]_0$, whose values fairly agreed with the molecular weights predicted from the initial ratios of $[M]_0/[PPA]_0$ and the monomer conversions. Their polydispersities were narrow, as shown in Figure 3.5, and their indices (M_w/M_n) were as low as 1.07 – 1.09 even though relatively high molecular weights, e.g., the M_w/M_n value was 1.08 for the PVL with a $M_{n,NMR}$ of 27500 g mol^{-1} (Table 3.1, run 4). For PCL, the molecular weight distributions were low with M_w/M_n values of 1.08 – 1.11, as shown in Figure 3.5. However, the characteristics for the ROP of ε-CL apparently differed from those of δ-VL, which was caused by the difference in the polymerization rate between δ-VL and ε-CL. In particular, the monomer conversion was required to be low for the synthesis of PCLs with relatively high molecular weights because the excess polymerization time induced the intra- and intermolecular esterification process leading to broad polydispersed PCLs. Thus, the author obtained a PCL of 1.07 and 21600 g mol^{-1} for the monomer conversion of 61.6 %. The molecular weights of the resultant PTMCs also increased with the increasing $[TMC]_0/[PPA]_0$, and the $M_{n,NMR}$ values fairly agreed with the $M_{n,calcd}$ ones. In addition, their SEC traces are narrow, and the M_w/M_n values are as low as 1.09 – 1.13 even for the relatively high molecular weights; for example, the M_w/M_n was 1.13 for the PTMC with the $M_{n,NMR}$ of 9640 g mol^{-1} (Table 3.1, run 12).

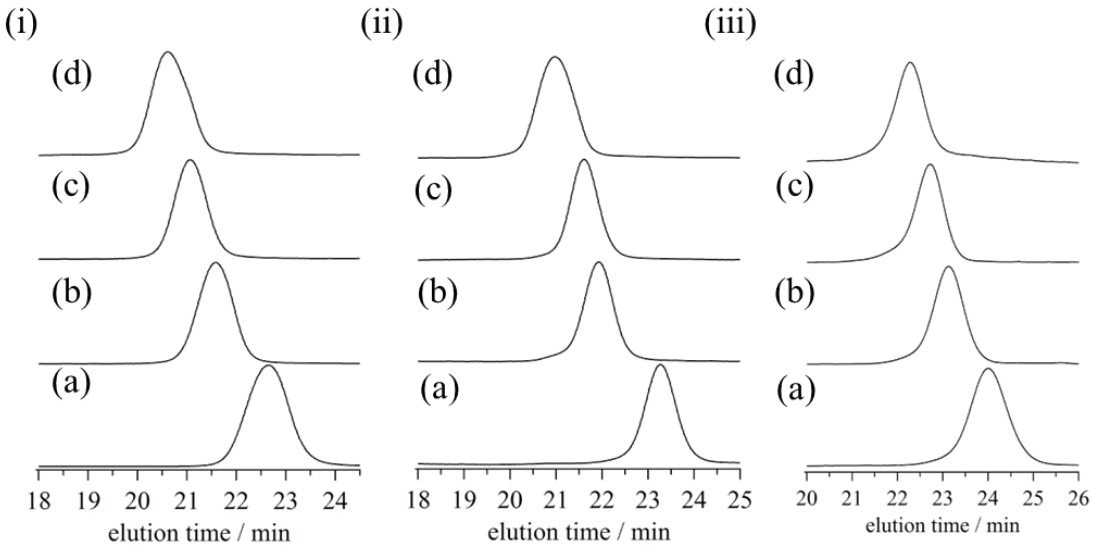

Figure 3.5. SEC traces of (i) PVLs obtained with $[\delta\text{-VL}]_0/[\text{PPA}]_0$ of (a) 50, (b) 100, (c) 150, and (d) 300, (ii) PCLs obtained with $[\varepsilon\text{-CL}]_0/[\text{PPA}]_0$ of (a) 50, (b) 100, (c) 150, and (d) 300, and (iii) PTMCs obtained with $[\text{TMC}]_0/[\text{PPA}]_0$ of (a) 20, (b) 30, (c) 50, and (d) 100 (eluent, $CHCl_3$; flow rate, 0.8 $mL \cdot min^{-1}$).

Table 3.1. Ring-opening polymerizations (ROPs) of δ-valerolactone (δ-VL), ε-caprolactone (ε-CL), and trimethylene Carbonate (TMC) using 3phenyl-1-propanol (PPA) and diphenyl phosphate (DPP) [a]

run	monomer (M)	$[M]_0/[PPA]_0$	time (h)	conv. (%) [b]	$M_{n,theo.}$ [c] (g mol^{-1})	$M_{n,NMR}$ [b] (g mol^{-1})	M_w/M_n [d]
1	δ-VL	50	1	95.0	4890	5170	1.09
2		100	2.5	94.8	9630	10000	1.07
3		150	4	94.6	14300	14800	1.07
4		300	6	90.7	27400	27500	1.08
5	ε-CL	50	8	97.1	5680	5920	1.07
6		100	24	95.1	11000	11500	1.07
7		150	29	80.4	13900	15200	1.06
8		300	43	61.6	21200	21600	1.07
9	TMC	20	6	91.1	1990	2100	1.10
10		30	16	99.6	3190	3000	1.09
11		50	36	97.9	5130	5220	1.09
12 [e]		100	24	95.1	9850	9640	1.13

[a] $[M]_0$, 1.0 mol·L^{-1}; $[DPP]_0/[PPA]_0$, 1.0; solvent, toluene; temperature, r.t. [b] Determined by ^{1}H NMR in $CDCl_3$ [c] Calculated from $([M]_0/[PPA]_0) \times$ conv. $\times$ (M.W. of monomer) + (M. W. of PPA). [d] Determined by SEC in $CHCl_3$ using PSt standards. [e] temperature, 70 °C, $[TMC]_0$, 0.5 mol·L^{-1}.

3.2.2 Controlled/Living Nature of DPP-Catalyzed ROP. The kinetic and post-polymerization experiments were carried out to confirm the controlled/living nature for the DPP-catalyzed ROPs of *δ*-VL, *ε*-CL, and TMC. For the kinetic plots, a distinct first-order relationship between the reaction time and monomer conversion was observed, meaning that the monomer consumption rate was constant during the polymerization. In addition, the molecular weight of the obtained PVL, PCL, and PTMC linearly increased with the reaction time, and the monomer conversion was as high as ≈ 95 %, as shown in Figures 3.6-3.8, respectively. More importantly, the $M_{n,NMR}$ values of the obtained PVLs, PCLs, and PTMCs fairly agreed with those calculated by the initial ratio of $[M]_0/[PPA]_0$ and the monomer conversion. From the SEC results, the M_w/M_ns of the obtained polymers showed low values ranging from 1.07 to 1.12 for PVLs, those from 1.07 to 1.17 for PCLs, and those from 1.06 to 1.15 for PTMCs, respectively.

The chain extension experiment also supported the controlled/living nature of the DPP-catalyzed ROPs. Figure 3.9 showed SEC trace for the chain extension experiment. A PVL with $M_{n,NMR}$ = 5120 g mol^{-1} and M_w/M_n = 1.10 was first obtained from the polymerization with $[\delta\text{-VL}]_0/[PPA]_0/[DPP]_0$ = 50/1/1 and the monomer conversion of 97.5 %. A further polymerization was then carried out by the subsequent addition of 50 equivalents of *δ*-VL to afford a PVL with $M_{n,NMR}$ = 10100 g mol^{-1} and M_w/M_n = 1.10, indicating that the chain end group of the PVL truly possessed a living nature (Figure 3.9a). In addition, the post-polymerization of *ε*-CL was confirmed as the first polymerization with $M_{n,NMR}$ = 5550 g mol^{-1} and M_w/M_n = 1.07, and then the second one with $M_{n,NMR}$ = 11000 g mol^{-1} and M_w/M_n = 1.09 (Figure 3.9b). Furthermore, for the post-polymerization of TMC, the first PTMC ($M_{n,NMR}$ = 4820 g mol^{-1} and M_w/M_n = 1.09) was obtained along with the monomer conversion of 96.4 %. After the second polymerization by the subsequent addition of 50 equivalents of TMC toward PPA (in CH_2Cl_2; $[TMC]_0$ = 5.0 mol·L^{-1}), the PTMC with $M_{n,NMR}$ = 8920 g mol^{-1} and M_w/M_n =

1.09 was afforded, as shown in Figure 3.9c. Thus, the DPP-catalyzed ROPs of *δ*-VL, *ε*-CL, and TMC were revealed to possess a living nature and produce precisely controlled polymers at ambient temperature.

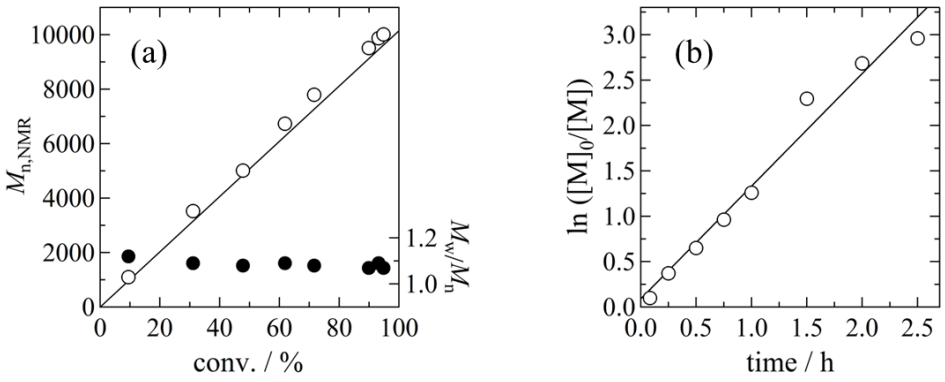

Figure 3.6. (a) Kinetic plots for the polymerization of *δ*-VL and (b) dependence of molecular weight (M_n) and polydispersity (M_w/M_n) on the monomer conversion (conv.) ([*δ*-VL]$_0$/[PPA]$_0$/[DPP]$_0$ = 100/1/1).

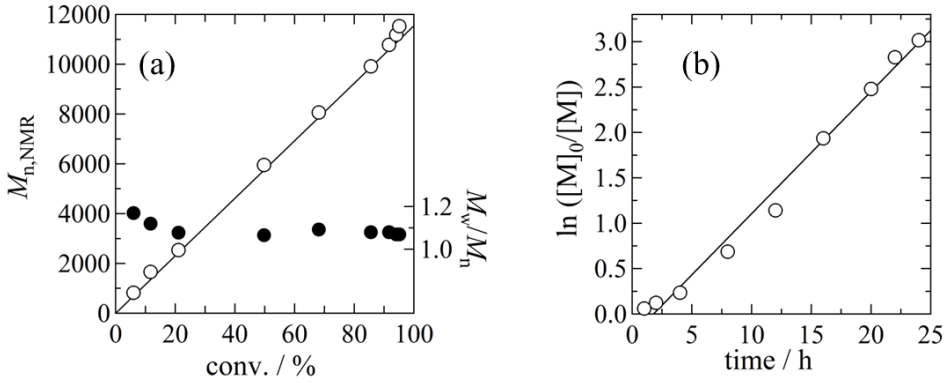

Figure 3.7. (a) Kinetic plots for the polymerization of *ε*-CL and (b) dependence of molecular weight (M_n) and polydispersity (M_w/M_n) on the monomer conversion (conv.) ([*ε*-CL]$_0$/[PPA]$_0$/[DPP]$_0$ = 100/1/1).

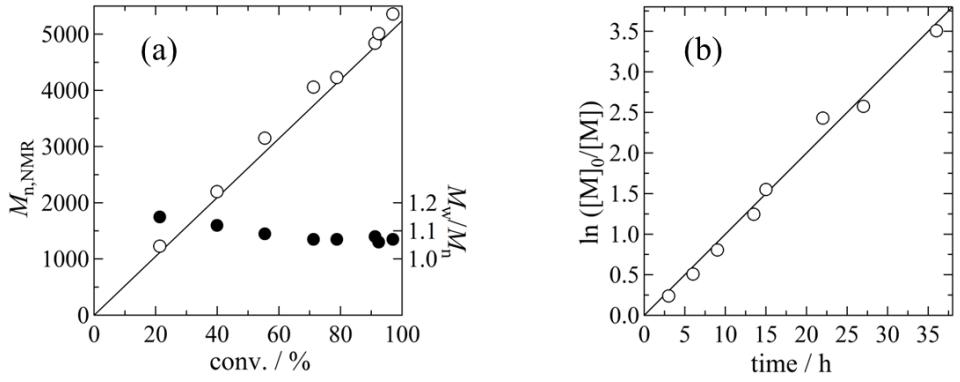

Figure 3.8. (a) Kinetic plots for the polymerization of TMC and (b) dependence of molecular weight (M_n) and polydispersity (M_w/M_n) on the monomer conversion (conv.) ($[TMC]_0/[PPA]_0/[DPP]_0$ = 50/1/1).

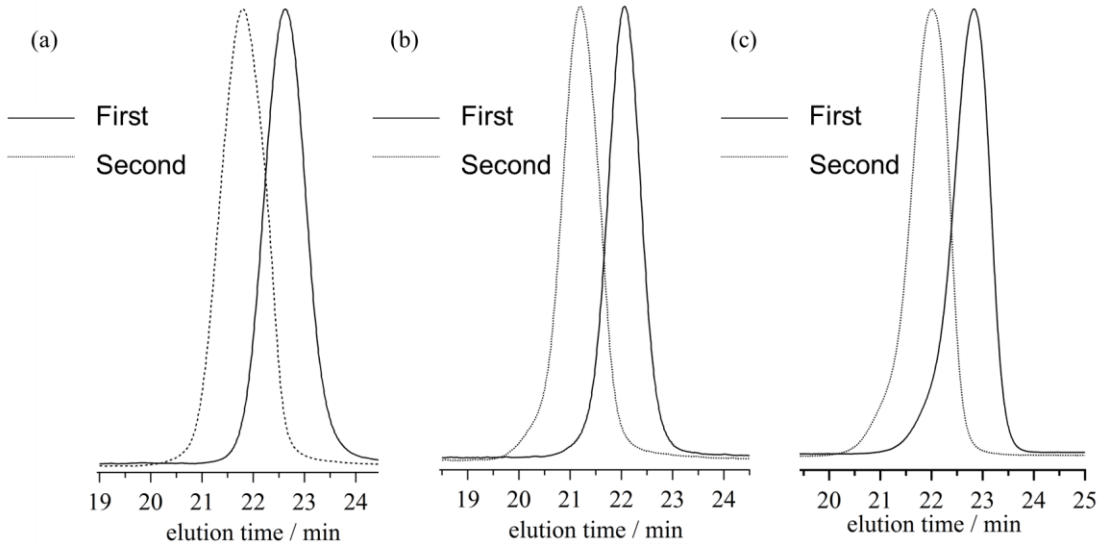

Figure 3.9. SEC traces of first sequence of (a) PVL, (b) PCL, and (c) PTMC (solid line) and post-polymerization (dashed line) (eluent, $CHCl_3$; flow rate, 0.8 mL·min^{-1}).

In order to clarify the catalytic performance of DPP, the ^{13}C NMR spectra of δ-VL, ε-CL, and TMC were measured in the absence/presence of DPP ([a cyclic monomer]/[DPP] = 1.0). The chemical shifts for the carbonyl carbon of 171.32 ppm for δ-VL, 176.17 ppm for ε-CL, and 148.41 ppm for TMC are observed downfield shift to 171.48, 176.31, and 148.69 ppm,

respectively, as shown in Figures 3.10a-c. In addition, the chemical shifts for the carbonyl carbon of the TMC were downfield with the increasing molar ratio of DPP and TMC ([DPP]/[TMC]), and the chemical shift reached the constant value of 148.85 ppm for [DPP]/[TMC] ≥ 2, as shown in Figure 3.10d. This result strongly indicated that DPP activates the carbonyl group of cyclic monomers.

In addition, the ^{1}H NMR spectrum is measured in the absence/presence of DPP using methyl 6-hydroxycaproate as a model for the polyester chain-end and ethyl 3-hydroxypropyl carbonate as a model for the polycarbonate chain-end; the hydroxyl proton signal shifts from 1.93 to 8.40 ppm for methyl 6-hydroxycaproate and that shifts from 1.71 to 8.34 ppm for ethyl 3-hydroxypropyl carbonate in the presence of DPP, as shown in Figures 3.11 and 3.12. These results strongly indicated that DPP has the dual activation ability for the monomer along with the polymer chain-end, as shown in Schemes 3.2a and 3.2b, respectively, resulting in that the DPP-catalyzed ROPs of δ-VL, ε-CL, and TMC proceeded through a living fashion to afford well-defined polymers via dual activation at initiation and propagation, as shown in Scheme 3.3.

Scheme 3.2. Activations of (a) ε-caprolactone (ε-CL) and trimethylene carbonate (TMC) by DPP, and (b) a PCL and a PTMC Chain-end by DPP

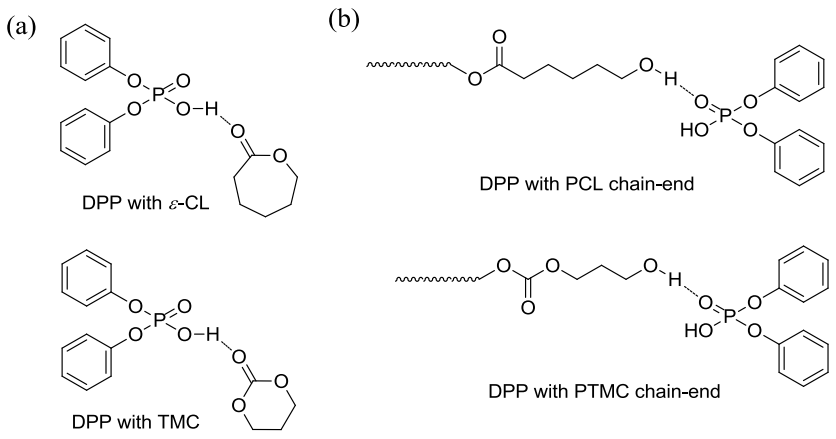

Scheme 3.3. A proposed mechanism for ring-opening polymerization of cyclic esters and cyclic carbonates with PPA using DPP

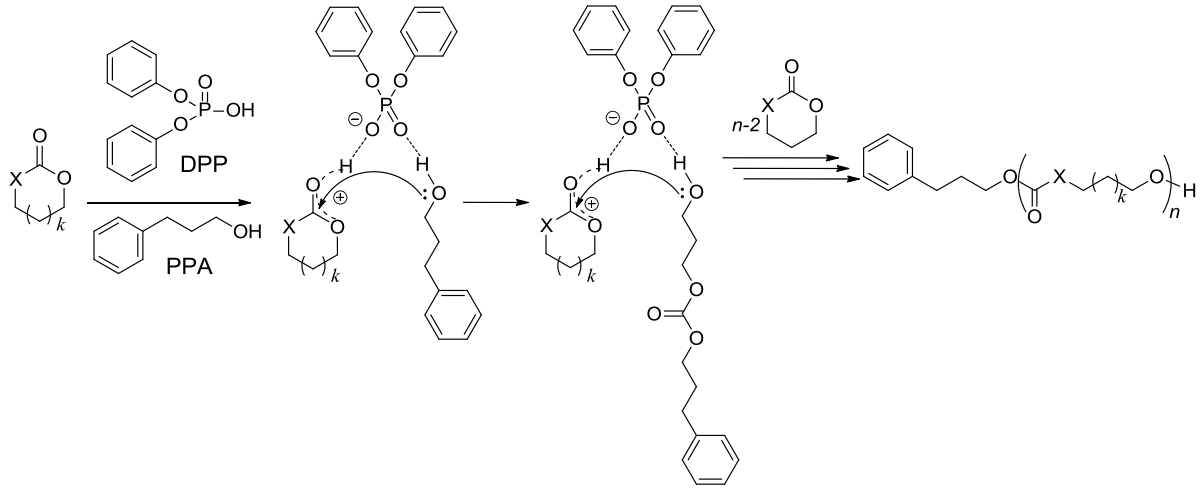

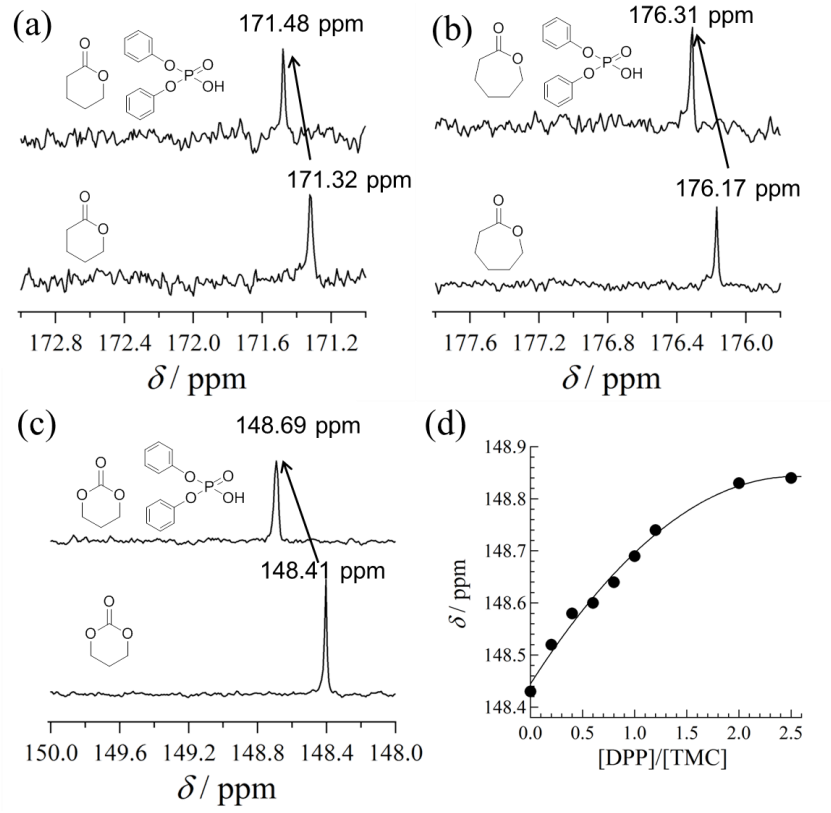

Figure 3.10. ^{13}C NMR spectra of the carbonyl carbon signals for (i) the *δ*-VL system, (ii) the *ε*-*ε*-CL system, and (iii) the TMC system, in $CDCl_3$; (a) *δ*-VL, *ε*-CL, and TMC and (b) 1:1 mixtures of *δ*-VL, *ε*-CL, and TMC with DPP. (vi) Titration of TMC with DPP in $CDCl_3$.

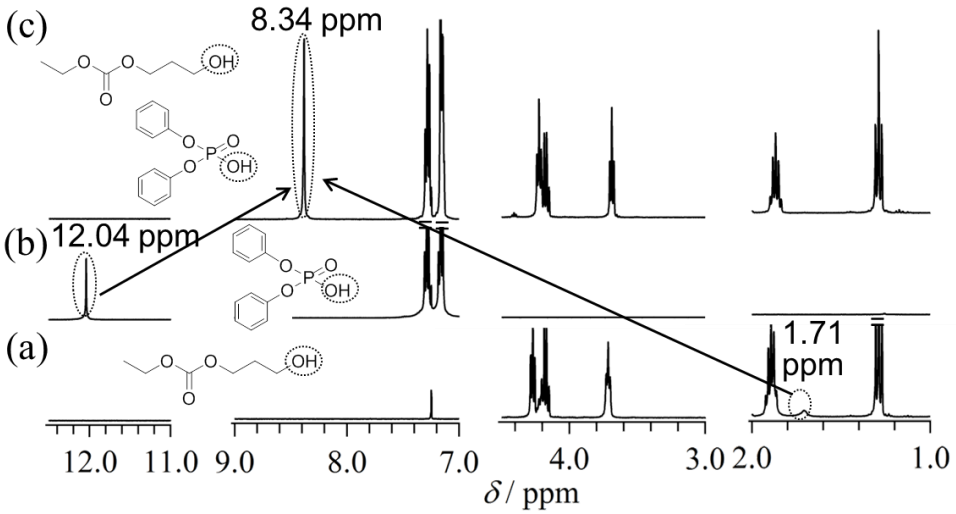

Figure 3.11. ^{1}H NMR spectra of the hydroxyl proton signals of (a) methyl 6-hydroxycaproate, (b) DPP, (c) the 1:1 mixture of methyl 6-hydroxycaproate with DPP in $CDCl_3$.

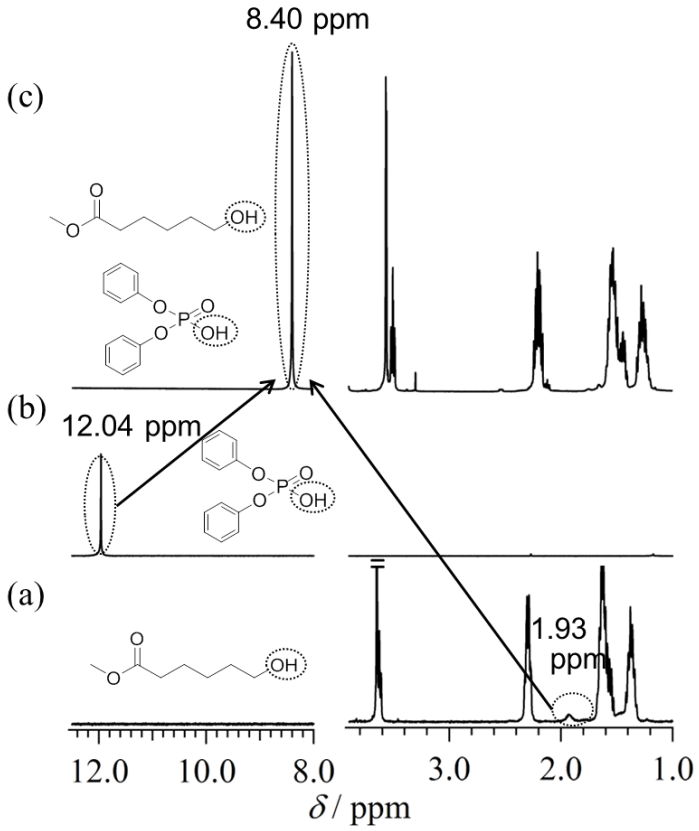

Figure 3.12. ^{1}H NMR spectra of the hydroxyl proton signals of (a) ethyl 3-hydroxypropyl carbonate, (b) DPP, (c) the 1:1 mixture of ethyl 3-hydroxypropyl carbonate with DPP in $CDCl_3$.

3.2.3 Synthesis of Functionalized Polymers. To provide an intrinsic advantage of the DPP-catalyzed ROPs of δ-VL, ε-CL, and TMC, the author focused on the synthesis of the end-functionalized PVLs, PCLs and PTMCs using functional initiators (FIs), such as 2-hydroxyethyl methacrylate (HEMA), 4-vinylbenzyl alcohol (VBA), propargyl alcohol (PGA), and 6-azido-1-hexanol (AHA), as shown in Scheme 3.1. HEMA and VBA are FIs with the methacrylate and 4-vinylbenzyl groups, respectively, leading to the end-functionalized polyesters as macromonomers,[11] and PGA and AHA are FIs with the acetylenic and azido groups, respectively, leading to the end-functionalized polyesters as click ready polymers.[12] Table 3.2 lists the synthetic results of the end-functionalized polyesters and polycarbonates. All the DPP-catalyzed ROPs of δ-VL, ε-CL, and TMC using HEMA, VBA, PGA, and AHA proceeded in a well-controlled manner to afford the corresponding PVLs, PCLs, and PTMCs with predictable molecular weights and narrow polydispersity indices. The $M_{n,NMR}$ values of the obtained polymers estimated by the ^{1}H NMR measurement agreed with the $M_{n,calcd}$ values calculated by the $[M]_0/[FI]_0$ and monomer conversions, e.g., for the polymerization using HEMA, the $M_{n,NMR}$ values of the PVL, PCL, and PTMC were 4550, 5260, and 4770 g mol^{-1}, respectively, which agreed with the $M_{n,calcd}$ values of 4530, 5250, and 4770 g mol^{-1}, respectively. In addition, the introduction of these functional groups at the α-end of the obtained PVLs, PCLs, and PTMCs were confirmed by the ^{1}H NMR and IR analyses. Thus, the author revealed that DPP was an efficient organocatalyst for the ROP of δ-VL, ε-CL, and TMC to afford well-defined polyester and polycarbonate-based materials.

Table 3.2. Synthesis of end-functionalized polyesters by the DPP-catalyzed ROP of *δ*-VL, *ε*-CL, and TMC using functional initiators (FI) [a]

run	monomer (M)	Functional initiator (FI)	time (h)	conv. (%) [b]	$M_{n,theo.}$ [c] (g mol^{-1})	$M_{n,NMR}$ [b] (g mol^{-1})	M_w/M_n [d]
13	*δ*-VL	HEMA	1	87.8	4530	4550	1.12
14		VBA		94.3	4860	5030	1.11
15		PGA		94.6	4790	4840	1.13
16		AHA		95.0	4900	4980	1.11
17	*ε*-CL	HEMA	5	89.7	5250	5260	1.08
18		VBA		84.9	4980	5220	1.08
19		PGA		84.9	4900	4980	1.11
20		AHA		91.7	5380	5470	1.08
21	TMC	HEMA	36	93.1	4880	4770	1.08
22		VBA		94.4	4950	5030	1.08
23		PGA		97.0	5010	5080	1.10
24		AHA		98.9	5190	5070	1.08

[a] $[M]_0$, 1.0 mol L^{-1}; $[M]_0/[FI]_0/[DPP]_0$, 50/1/1; temp., r.t.; solvent, toluene. [b] Determined by ^{1}H NMR in $CDCl_3$. [c] Calculated from $([M]_0/[FI]_0) \times$ conv. $\times$ (M. W. of monomer) + (M. W. of FI). [d] Determined by SEC in $CHCl_3$ using PSt standards.

In order to synthesize well-defined polycarbonates with functional groups in the side-chains, the DPP-catalyzed ROP was carried out using trimethylene carbonates having functional groups, such as 5,5-dimethyl-1,3-dioxan-2-one (DMC), 5,5-dibromomethyl-1,3-dioxan-2-one (DBTC), 5-benzyloxy-1,3-dioxan-2-one (BTMC), 5-methyl-5-allyloxycarbonyl-1,3-dioxan-2-one (MAC), and 5-methyl-5-propargyloxycarbonyl-1,3-dioxan-2-one (MPC), as shown in Scheme 3.4. All the polymerizations proceeded in a well-controlled manner to

afford the corresponding polycarbonates, and all results are listed in Table 3. In order to accelerate the polymerization rate, the polymerizations were carried out at 100 °C, resulting in monomer conversions of 83.3 – 90.4 % for the polymerization time of 5 – 14 h though with a slight increase in the polydispersity indices, M_w/M_n = 1.13 – 1.20, compared to the results for the polymerization at room temperature (Table 3.3). The $M_{n,NMR}$ of 6450, 12700, 10200, 9380, and 9030 g mol^{-1} for the polymers, respectively, fairly agreed with the $M_{n,calcd}$ of 5930, 12100, 9510, 9180, and 8970 g mol^{-1}, respectively. In addition, the polymer structures were confirmed as poly(trimetylene carbonate)s with functional groups in the side-chains without any undesired reactions, such as backbiting, decarboxylation, and transesterification reactions, by the ^{1}H NMR measurements; the peaks due to the polymer main chain were confirmed and the peaks due to side chains appeared at 1.00 ppm for PDMC, at 3.54 ppm for PDBTC, at 5,31 and 7.23-7.37 ppm for PBTMC, at 1.27, 4.64, 5.28, and 5.87 ppm for PMAC, and at 1.30, 2.54, and 4.72 ppm for PMPC.

These results for the synthesis of the PTMCs with functional groups in the side-chain and chain-end indicated that DPP performed as the ROP catalyst and was inactive for the functional groups in the initiators and monomers to afford well-defined polycarbonates.

Scheme 3.4. Synthesis of PTMCs with functional groups in side chain by ROP of functional TMC derivatives

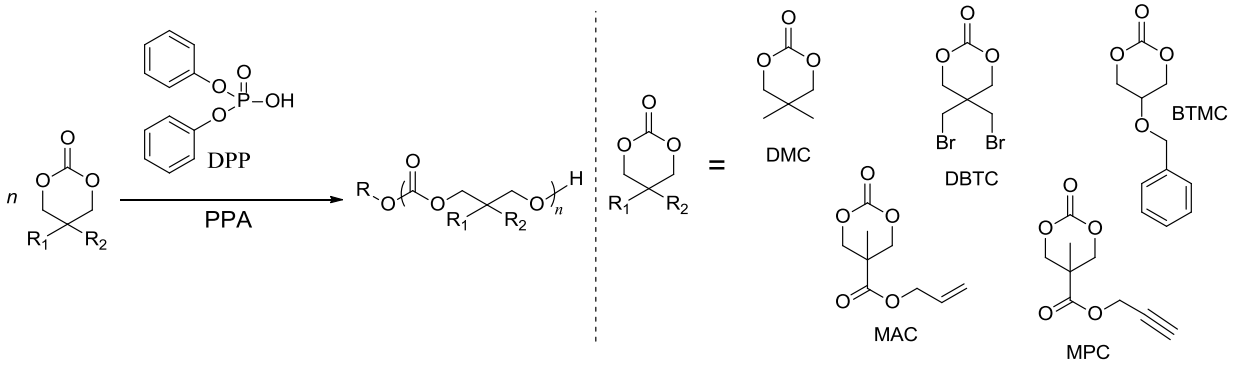

Table 3.3. ROP of DMC, DBTC, BTMC, MAC, and MPC using DPP and PPA [a]

run	monomer	time (h)	conv. (%) [b]	$M_{n,calcd}$ (g mol^{-1}) [c]	$M_{n,NMR}$ (g mol^{-1}) [b]	M_w/M_n [d]
25	DMC	5	89.0	5930	6450	1.19
26	DBTC	6	83.3	12100	12700	1.20
27 [e]	BTMC	14	90.0	9510	10200	1.20
28	MAC	10	90.4	9180	9380	1.15
29	MPC	14	89.2	8970	9030	1.13

[a] Temperature, 100 °C; solvent, toluene; $[M]_0$, 1.0 mol·L^{-1}; $[M]_0/[PPA]_0/[DPP]_0$, 50/1/1. [b] Determined by ^{1}H NMR in $CDCl_3$ [c] Calculated from $([M]_0/[PPA]_0) \times$ conv. × (M.W. of monomer) + (M.W. of PPA). [d] Determined by SEC in $CHCl_3$ using PSt standards. [e] $[BTMC]_0$, 0.5 mol·L^{-1}.

For the synthesis of well-defined polyester-ether, the author applied the DPP-catalyzed ROP for 1,5-dioxepan-2-one (DXO), which is one of cyclic esters having ether linkage in monomer unit, as shown in Scheme 3.5. The polymerization was conducted with initial ratio of $[DXO]_0/[PPA]_0$ of 50/1 (Table 3.4 run 32), and the monomer conversion determined from ^{1}H NMR was 95.4 % within 24 h. The $M_{n,NMR}$ of 5670 was farily agreed well with the $M_{n.calcd}$ of 5680, which was estimated from the initial rario of $[DXO]_0/[PPA]_0$ and monomer converision. The chemical structure of the obtained polymer was assigned to PDXO because the peaks derived from chain-end at 7.14-7.24, 4.09, 2.75, and 1.94 ppm and the main chain at 4.20, 3.73, 3.63, and 2.59 ppm were observed on ^{1}H NMR spectrum. Thus the results strongly indicated that the obtained polmyer was PDXO having PPA residue at the polymer chain-end. For controlling the molecular weight, the ROP of DXO was conducted varying the inital $[DXO]_0/[PPA]_0$ from 20 to 100 (Table 3.4, runs 30-33). The molecular weights of the PDXOs liniarly increased corrsponding to the increasing of $[DXO]_0/[PPA]_0$ and the $M_{n,NMR}$s of 2310,

3310, and 9980 agreed with $M_{n,calcd}$s of 2290, 3480, 10700, respectively. Thus DPP has the versatility for the synthesis of polyersters and polycarbonates having functional residue in the polymer chain-end and side chain, and main-chain modified polyester could be obtained.

Scheme 3.5. Synthesis of poly(1,5-dioxepan-2-one) (PDXO) using PPA and DPP

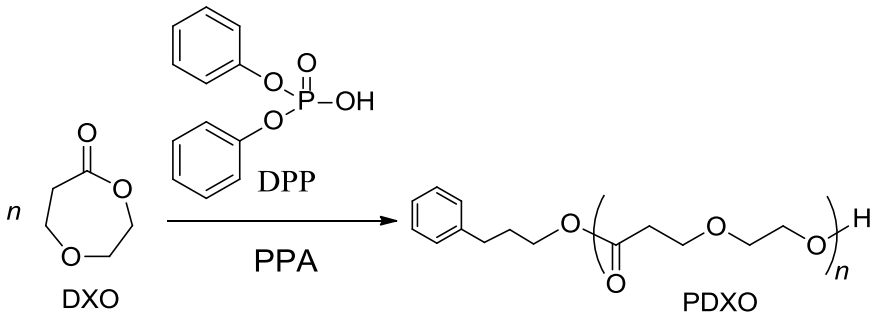

Table 3.4. ROP of DXO with PPA Using DPP [a]

run	$[DXO]_0/[PPA]_0/[DPP]_0$	time (h)	conv. (%) [b]	$M_{n,calcd}$ (g mol^{-1}) [c]	$M_{n,NMR}$ (g mol^{-1}) [b]	M_w/M_n [d]
30	20/1/1	7.5	95.3	2290	2310	1.08
31	30/1/1	17	95.9	3480	3310	1.05
32	50/1/1	24	95.4	5680	5670	1.04
33	100/1/1	54	90.6	10700	9980	1.05

[a] Temperature, room temp.; solvent, toluene; $[DXO]_0$ = 1.0 mol L^{-1}. [b] Determined by ^{1}H NMR in $CDCl_3$ [c] Calculated from $([DXO]_0/[PPA]_0)$ × conv. × (M.W. of DXO) + (M. W. of PPA). [d] Determined by SEC in THF using PSt standards.

3.2.4 Block Copolymerization of *δ*-VL, *ε*-CL, and TMC. The post-polymerization property indicated that the chain ends of PVL, PCL, and PTMC maintained the proper structures possessing a further polymerization ability. The polymerization characteristic can be used to synthesize diblock copolymers consisting of PVL, PCL, and PTMC, which are interesting biodegradable polymeric materials with two different mechanistic properties. First, the author carried out the polymerization of *δ*-VL at $[\delta\text{-VL}]_0/[\text{PPA}]_0/[\text{DPP}]_0 = 50/1/1$, and then the same mole of *ε*-CL was added to the reaction mixture. A monomodal SEC trace of the first *δ*-VL polymerization shifted to a higher molecular weight region while keeping the monodispersity after the second *ε*-CL polymerization, as shown in Figure 3.13, i.e., the molecular weight increased from 5250 to 10800 g mol^{-1} and the polydispersity slightly varied from 1.11 to 1.13. The block copolymer consisting of PVL and PCL, PVL-*b*-PCL, was confirmed by the ^1H NMR measurement. In addition, the author synthesized various diblock copolymers consisting of PCL, PVL, and PTMC regardless of monomer addition order, as listed in Table 3.5. Applying the cotrolled/living nature to the block copolymerization of *δ*-VL, *ε*-CL, and TMC, the well-defined block copolymers.

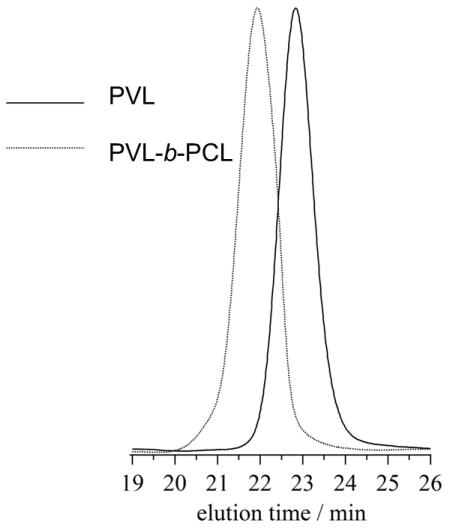

Figure 3.13. SEC traces of first sequence of (a) PVL (solid line) and (b) PVL-*b*-PCL (dashed line) (eluent, $CHCl_3$; flow rate, 0.8 mL·min^{-1}).

Table 3.5. Block copolymerization of δ-VL, ε-CL, and TMC using PPA and DPP [a]

	run	monomer (M)	solvent	time (h)	$[M]_0$ (mol L^{-1})	conv. (%) [b]	$M_{n,calcd}$ (g mol^{-1}) [c]	$M_{n,NMR}$ (g mol^{-1}) [b]	M_w/M_n [d]
34	First	δ-VL	toluene	1	1.0	96.1	4950	5250	1.11
	Second	ε-CL		7	1.0	96.0	10600	10800	1.13
35	First	ε-CL	toluene	7	1.0	91.5	5360	5520	1.07
	Second	δ-VL		1	1.0	95.0	10200	10800	1.07
36	First	TMC	toluene	36	1.0	97.0	5090	4920	1.11
	Second	ε-CL		7	1.0	94.2	10460	10500	1.12
37	First	ε-CL	toluene	8	1.0	99.4	5810	5800	1.11
	Second	TMC	toluene/CH_2Cl_2	36	0.9	96.8	10750	10800	1.19
38	First	TMC	toluene	36	1.0	97.2	5100	4990	1.09
	Second	δ-VL		4	1.0	93.3	9820	9760	1.14
39	First	δ-VL	toluene	1	1.0	95.0	4890	4950	1.13
	Second	TMC	toluene/CH_2Cl_2	36	0.9	95.2	9750	10000	1.17

[a] Initiator, 3-phenyl-1-propanol (PPA); $[M]_0/[PPA]_0/[DPP]_0$, 50/1/1.; temperature, room temp. [b] Determined by ^1H NMR in $CDCl_3$ [c] Calculated from $([M]_0/[PPA]_0) \times$ conv. $\times$ (M.W. of a monomer) + (M. W. of PPA). [d] Determined by SEC in $CHCl_3$ using PSt standards.

3.3 Conclusions

In this chapter, the author achieved the production of well controlled poly(δ-valerolactone)s (PVLs), poly(ε-caprolactone)s (PCLs), and poly(trimethylene carbonate)s (PTMCs) by the ring-opening polymerizations (ROPs) of δ-valerolactone (δ-VL), ε-caprolactone (ε-CL), and trimethylene carbonate (TMC) using diphenyl phosphate (DPP) as the organocatalyst and 3-phenyl-1-propanol (PPA) as the initiator. All the polymerizations proceeded in a living fashion via dual activation of monomer and propagating chain-end, and the molecular weights of the polymers were well controlled with narrow polydispersities. The dual activation system gave the high molar mass polymers, which were not obtained by the use of highly acidic catalysts. In addition, DPP had a tolerance to the functional groups in the initiators and monomers to afford well-defined polyesters and polycarbonates with functional groups in the side-chain, main-chain, and chain-end using functional monomres and functional initiators. Various diblock copolymers were synthesized by the block copolymerization of δ-VL, ε-CL, and TMC regardless of the monomer addition sequence. In conclusion, the author demonstrated a new catalytic activity of DPP, and various functionalized and diblock polymers were produced using the DPP-catalyzed ROP system.

3.4 Experimental Section

Materials. Toluene (> 99.5 %; water content, < 0.001 %) was purchased from Kanto Chemical Co., Inc., and distilled over sodium benzophenone ketyl under an argon atmosphere. Dichloromethane (CH_2Cl_2; >99.5 %, water content, <0.001 %, Kanto Chemical Co., Inc.), δ-valerolactone (δ-VL; 99 %, Kanto Chemical Co., Inc.) and ε-caprolactone (ε-CL; 99 %, Tokyo Kasei Kogyo Co., Ltd. (TCI)) were distilled over CaH_2 under reduced pressure. Trimethylene carbonate (TMC; >98%, TCI) was purified by recrystallization from dry toluene prior to use. Diphenylphosphate (DPP, TCI) was used as received. 3-Phenyl-1-propanol (PPA, TCI) and propargyl alcohol (PGA, TCI) was distilled over CaH_2 under an argon atmosphere. 2-Hydroxyethyl methacrylate (HEMA, TCI) was distilled under reduced pressure. A weak base anion exchange resin, Amberlyst® A21 (Organo Co., Ltd.), was used as received. Methyl 6-hydroxycaproate,[13] ethyl 3-hydroxypropyl carbonate,[14] 5,5-dimethyl-1,3-dioxan-2-one (DMC),[15] 5,5-dibromomethyl-1,3-dioxan-2-one (DBTC),[16] 5-benzyloxy-1,3-dioxan-2-one (BTMC),[17] 5-methyl-5-allyloxycarbonyl-1,3-dioxan-2-one (MAC),[8] 5-methyl-5-propargyloxycarbonyl-1,3-dioxan-2-one (MPC)[18, 19] 4-Vinylbenzyl alcohol (VBA),[20] and 6-azido-1-hexanol (AHA)[21] were synthesized using previously reported techniques.

Instruments. The number-average molecular weight ($M_{n,NMR}$) was determined from the ^1H NMR spectra recorded using a JEOL JNM-A400II instrument. The polymerization was carried out in an MBRAUN stainless steel glove box equipped with a gas purification system (molecular sieves and copper catalyst) in a dry argon atmosphere (H_2O, O_2 < 1 ppm). The moisture and oxygen contents in the glove box were monitored by an MB-MO-SE 1 and an MB-OX-SE 1, respectively. The size exclusion chromatography (SEC) was performed at 40 °C in $CHCl_3$ (0.8 mL·min^{-1}) using a Jasco GPC-900 system equipped with a set of two

Shodex K-805L columns (linear, 8 mm × 300 mm). The polydispersity (M_w/M_n) of the polymers was calculated on the basis of a polystyrene calibration. The preparative SEC was performed in $CHCl_3$ (3.5 mL·min^{-1}) at 23 °C using a JAI LC-9201 equipped with a JAI JAIGEL-3H column (20 mm × 600 mm; exclusion limit, 7×10^4) and a JAI RI-50s refractive index detector. The viscosity of the polymer solution was determined by SEC in THF (1.0 mL·min^{-1}) at 40 °C using an Agilent 1100 series instrument equipped with two Shodex KF-804 L columns (linear, 8 mm × 300 mm; exclusion limit, 4×10^5) and a Viscostar viscosity detector (Wyatt Technology). Matrix-assisted laser desorption ionization time-of-flight mass spectrometry (MALDI-TOF MS) of the obtained polymers was performed using an Applied Biosystems Voyager-DE STR-H equipped with a 337-nm nitrogen laser (3 ns pulse width). Two hundred shots were accumulated for the spectra at a 25 kV acceleration voltage in the reflector mode and calibrated using insulin (TAKARA BIO, Inc.) as the internal standard. Samples for the MALDI-TOF MS were prepared by mixing the polymer (1.0 mg·mL^{-1}) and a matrix (2,5-dihydroxybenzoic acid, 15 mg·mL^{-1}, 10 μL) in THF. For the measurement, a sample plate, which was coated by a solution (1.0 μL) of NaI as the cationic agent in acetone (1.0 mmol·L^{-1}), was used. [22]

Polymerization of *δ*-valerolactone. A typical procedure for the polymerization is as follows: *δ*-VL (0.270 mL, 3.00 mmol) was added to a stock solution of PPA (60.0 μL, 60.0 μmol) in toluene at 27 °C in the grove box. A toluene stock solution of DPP (60.0 μL, 60.0 μmol) was then added to the solution to initiate the polymerization under an argon atmosphere. After 1 h, the polymerization was quenched by the addition of Amberlyst® A21. Before the addition of the Amberlyst® A21, the author obtained a portion of the polymerization mixtures and then added a small amount of triethylamine to the mixtures for determining the monomer conversion that was directly determined from the ^{1}H NMR measurements of the

polymerization mixtures. The polymer was isolated by reprecipitation from CH_2Cl_2 in cold methanol/hexane. Yield, 49.8 %; $M_{n,NMR}$, 5170 g·mol^{-1}; M_w/M_n, 1.09; ^{1}H NMR ($CDCl_3$) δ (ppm), 1.66 (m, 2H × n, (-$CH_2CH_2CH_2O$-)$_n$), 1.69 (m, 2H × n, (-$COCH_2CH_2CH_2$-)$_n$), 1.93, (q, 2H, J = 6.2, Ar$CH_2CH_2CH_2$-), 2.34 (t, 2H × n, J = 6.5 Hz, (-$OCOCH_2CH_2$-)$_n$), 2.68 (t, 2H, J = 7.8 Hz, ArCH_2CH_2-), 3.61 (t, 2H, J = 6.8 Hz, -CH_2CH_2OH), 4.08 (t, 2H × n, J = 5.9, (-CH_2CH_2O-)$_n$), 4.12 (m, 2H, Ar$CH_2CH_2CH_2O$-) 7.15-7.34 (m, 5H, aromatic).

A similar condition for δ-VL was used for the polymerization of ε-CL. Yield, 75.8 %; $M_{n,NMR}$, 5920 g·mol^{-1}; M_w/M_n, 1.07; ^{1}H NMR ($CDCl_3$) δ (ppm), 1.38 (m, 2H × n, (-$CH_2CH_2CH_2CH_2CH_2$-)$_n$), 1.57 (m, 2H × n, (-$CH_2CH_2CH_2O$-)$_n$), 1.65 (m, 2H × n, (-$COCH_2CH_2CH_2$-)$_n$), 1.93, (q, 2H, J = 6.3, Ar$CH_2CH_2CH_2$-), 2.31 (t, 2H × n, J = 7.3 Hz, (-$OCOCH_2CH_2$-)$_n$), 2.63 (t, 2H, J = 7.3 Hz, ArCH_2CH_2-), 3.65 (t, 2H, J = 6.6 Hz, -CH_2CH_2OH) 4.06 (t, 2H × n, J = 6.9, (-CH_2CH_2O-)$_n$), 4.12 (m, 2H, Ar$CH_2CH_2CH_2O$-) 7.15-7.34 (m, 5H, aromatic).

A similar condition for δ-VL was used for the polymerization of TMC. Yield, 85.7 %; $M_{n,NMR}$, 5220 g·mol^{-1}; M_w/M_n, 1.09; ^{1}H NMR ($CDCl_3$) δ (ppm), 1.92 (q, 2H, J = 6.4, -CH_2CH_2OH), 1.97-2.11 (m, 2H, ArCH_2CH_2-; 2H × (*n-1*), (-OCH_2CH_2-)$_{n-1}$), 2.71 (t, 2H, J = 7.6, ArCH_2-), 3.74 (t, 2H, J = 6.0, -CH_2OH), 4.13-4.32 (m, 2H,Ar$CH_2CH_2CH_2$-; m, 4H × *n-1*, (-$OCH_2CH_2CH_2O$-)$_{n-1}$; m, 2H, -$CH_2CH_2CH_2OH$), 7.16-7.37 (m, 5H, aromatic).

Synthesis of End-functionalized Poly(trimethylene carbonate). A typical procedure for the polymerization is as follows: TMC (204 mg, 2.00 mmol) was added to a stock solution of DPP (40.0 μL, 40.0 μmol) in toluene at room temperature in the glove box. A toluene stock solution of **1a** (40.0 μL, 40.0 μmol) was then added to the solution of TMC and DPP to initiate the polymerization under an argon atmosphere. Before the polymerization was quenched by the addition of Amberlyst A21 after 36 h, a portion of the polymerization

mixture was added to a small amount of triethylamine to determine the monomer conversion, which was directly determined from the ^{1}H NMR measurement. The crude polymer was isolated by reprecipitation in cold methanol to give the end-functionalized poly(trimethylene carbonate) with the azido group (**2a**). Yield, 68.0 %; $M_{n,NMR}$, 5070 g·mol^{-1}; M_w/M_n, 1.08; ^{1}H NMR ($CDCl_3$) δ (ppm), 1.41 (m, 4H, $N_3CH_2CH_2CH_2CH_2$-), 1.65 (m, 4H, $N_3CH_2CH_2CH_2CH_2CH_2$-), 1.92 (q, 2H, J = 6.4, -CH_2CH_2OH), 1.97-2.16 (m, 2H × (*n-1*), (-OCH_2CH_2-)$_{n-1}$), 3.28 (t, 2H, J = 7.6, N_3CH_2-), 3.74 (t, 2H, J = 5.6, -CH_2OH), 4.05 (m, 2H, $N_3CH_2CH_2CH_2CH_2CH_2CH_2$-), 4.12-4.39 (m, 4H × (*n-1*), (-$OCH_2CH_2CH_2O$-)$_{n-1}$; m, 2H, -$CH_2CH_2CH_2OH$).

Block Copolymerization of Trimethylene Carbonate (TMC) and *δ*-Valerolactone (*δ*-VL) or *ε*-Caprolactone (*ε*-CL). A typical procedure for the polymerization is as follows: TMC (51.0 mg, 500 μmol) was added to a stock solution of DPP (10.0 μL, 10.0 μmol) in toluene at room temperature in a glove box. A toluene stock solution of PPA (10.0 μL, 10.0 μmol) was then added to the solution to initiate the polymerization under an argon atmosphere. After the first polymerization was stirred for 36 h, the block copolymerization was then started with 50 equiv. of *δ*-VL (45.3μL, 500 μmol). Before the polymerization was quenched by the addition of Amberlyst A21 after 4 h, a portion of the polymerization mixtures was added using a small amount of triethylamine to determine the monomer conversion, which was directly determined from the ^{1}H NMR measurement. The crude polymer was isolated by reprecipitation in cold methanol to give poly(trimethylene carbonate)-*block*-poly(*δ*-valerolactone) (PTMC-*b*-PVL). Yield, 34.5 %; $M_{n,NMR}$, 9760 g·mol^{-1}; M_w/M_n, 1.09; ^{1}H NMR ($CDCl_3$) δ (ppm), 1.59-1.78 (m, 4H × *m*, (-$COCH_2CH_2CH_2CH_2O$-)$_m$), 1.98-2.15 (m, 2H, $ArCH_2CH_2$-; m, 2H × *n*, (-OCH_2CH_2-)$_n$), 2.34 (t, 2H × *m*, J = 7.2 Hz, (-$COCH_2$-)$_m$), 2.71 (t, 2H, J = 7.6, $ArCH_2$-), 3.65 (m, 2H, -CH_2OH), 4.03-4.17 (m, 2H,$ArCH_2CH_2CH_2$-; m, 4H × *n*, (-OCH_2CH_2-)$_n$), 4.24 (t, 2H × (*m*-1), J = 6.0 Hz, (-CH_2O-)$_{m-1}$), 7.17-7.34 (m, 5H, aromatic).

A similar condition for the diblock ROP of TMC and *δ*-VL was used for the block copolymerization of TMC and *ε*-CL to give poly(trimethylene carbonate)-*block*-poly(*ε*-caprolactone) (PTMC-*b*-PCL). Yield, 52.1 %; $M_{n,NMR}$, 10500 g·mol^{-1}; M_w/M_n, 1.12; ^{1}H NMR ($CDCl_3$) *δ* (ppm), 1.34-1.45 (m, 2H × *m*, (-COCH$_2$CH$_2$C*H*$_2$CH$_2$CH$_2$O-)$_m$), 1.56-1.76 (m, 4H × *m*, (-COCH$_2$C*H*$_2$CH$_2$C*H*$_2$CH$_2$O-)$_m$), 1.98-2.13 (m, 2H, ArCH$_2$C*H*$_2$-; m, 2H × *n*, (-OCH$_2$C*H*$_2$-)$_n$), 2.31 (t, 2H × *m*, J = 7.6 Hz, (-COC*H*$_2$-)$_m$), 2.71 (t, 2H, J = 8.0, ArC*H*$_2$-), 3.65 (m, 2H, -C*H*$_2$OH), 4.02-4.15 (m, 2H,ArCH$_2$CH$_2$C*H*$_2$-; m, 4H × *n*, (-OC*H*$_2$CH$_2$-)$_n$), 4.24 (t, 2H × *m*, J = 6.4 Hz, (-C*H*$_2$O-)$_m$), 7.17-7.34 (m, 5H, aromatic).

3.5 References and Notes

1. Hasegawa, A.; Ishihara, K.; Yamamoto, H. *Angew. Chem. Int. Ed.* **2003**, *42*, 5731-5733.

2. Gazeau-Bureau, S.; Delcroix, D.; Martin-Vaca, B.; Bourissou, D.; Navarro, C.; Magnet, S. *Macromolecules* **2008**, *41*, 3782-3784.

3. Krasovec, F.; Jan, J. *Croat. Chem. Acta* **1963**, *35*, 183-193.

4. Mingfa, Y.; Tao, W.; Na, Q.; Yongkai, H.; Daping, Q. *Polym. Int.* **2012**, *61*, 1525-1531

5. Helou, M.; Miserque, O.; Brusson, J.-M.; Carpentier, J.-F.; Guillaume, S. M. *Chem. Eur. J.* **2010**, *16*, 13805-13813.

6. Guillaume, S. M.; Carpentier, J.-F. *Catal. Sci. Technol.* **2012**, *2*, 898-906.

7. Nederberg, F.; Lohmeijer, B. G. G.; Leibfarth, F.; Pratt, R. C.; Choi, J.; Dove, A. P.; Waymouth, R. M.; Hedrick, J. L. *Biomacromolecules* **2007**, *8*, 153-160.

8. Tempelaar, S.; Mespouille, L.; Dubois, P.; Dove, A. P. *Macromolecules* **2011**, *44*, 2084-2091.

9. Pratt, R. C.; Nederberg, F.; Waymouth, R. M.; Hedrick, J. L. *Chem. Commun.*, **2008**, *114*, 114-116.

10. Delcroix, D.; Martin-Vaca, B.; Bourissou, D.; Navarro, C. *Macromolecules* **2010**, *43*, 8828-8835.

11. Xie, M.; Shi, J.; Ding, L.; Li, J.; Han, H.; Zhang, Y. *J. Polym. Sci., Part A: Polym. Chem.* **2009**, *47*, 3022-3033.

12. Ito, K. *Prog. Polym. Sci.* **1998,** *23*, 581-620.

13. Bosone, E.; Farina, P. Guazzi, G.; Innocenti, S.; Marrotta, V.; Valcavi, U. *Synthesis* **1983**, *11*, 942-944.

14. Al-Azemi, T. F., Dib, H. H.; Al-Awadi, N. A., El-Dusouqui, O. M. E. *Tetrahedron* **2008**, *64*, 4216-4134.

15. Al-Azemi, T. F.; Dib, H. H.; Al-Awadi, N. A.; El-Dusouqui, O. M. E. *Tetrahedron*, **2008**, *64*, 4126-4134.

16. Zhang, X.; Zhong, Z,; Zhuo, R. *Macromolecules* **2011**, *44*, 1755-1759.

17. Ray, W. C.; Grinstaff, M. W. *Macromolecules* **2003**, *36*, 3557-3562.

18. Lu, C.; Shi, Q.; Chen, X.; Lu, T.; Xie, Z.; Hu, X.; Ma, J.; Jing, X. *J. Polym. Sci., Part A: Polym. Chem.* **2007**, *45*, 3204-3217.

19. Tempelaar, S.; Barker, I. A.; Truong, V. X.; Hall, D. J.; Mespouille, L.; Dubois, P.; Dove, A. P. *Polym. Chem.* **2013**, *4*, 174-183.

20. Abramo, J. G.; Chapin, E.C. *J. Org. Chem.* **1961**, *26*, 2671–2673.

21. Speers, A. E.; Adam, G. C.; Cravatt, B. F. *J. Am. Chem. Soc.* **2003**, *125*, 4686-4687.

22. Kristofer J.T.; Andreas H.; Matthijs deG.; Silvia V.; Jiaxiang Z.; Mark F. W.; Steven M. H. *Macromolecules* **2006**, *39*, 7967-7972.

Chapter 4

Ring-Opening Polymerization of L-lactide via Bifunctional Activation Using Diphenyl Phosphate and 4-Dimethylaminopyridine

4.1 Introduction

In chapter 3, diphenyl phosphate (DPP) effectively catalyzed the controlled/living ring-opening polymerizations (ROPs) of δ-valerolactone (δ-VL), ε-caprolactone (ε-CL), and trimethylene carbonate (TMC) using alcohol initiators leading to narrow polydispersed poly(δ-valerolactone) (PVL), poly(ε-caprolactone) (PCL), and poly(trimethylene carbonate) (PTMC), respectively, via "dual" activation mechanism (DPP has dual function even for monofunctional phosphate substituent). In addition, the DPP-catalyzed ROP was versatile for producing diblock copolymers consisting of PVL, PCL, and PTMC by the sequential addition of a second monomer without quenching. However, DPP exhibited little catalytic ability for the ROP of lactide (LA), meaning that the monomer activation property of DPP was extremely insufficient.

In organocatalytic polymerizations, a suitable combination of two different organocatalysts is known to perform the ROPs of lactones and LA, in which each organocatalysts component respectively activated monomers and initiators/polymer chain-ends, i.e., "bifunctional activation" mechanism.[1-10] For instance, the "bifunctional activation" of a monomer and an initiator was achieved by binary catalyst systems consisting of electrophiles and amines, such as thiourea/amine[2] and hexafluoro-2-propanol/amine.[9]

Furthermore, methanesulfonic acid (MSA) with DMAP was an efficient binary catalyst system for the controlled ROP of LA because the pyridinium salt formed from MSA and DMAP acted as an effective electrophile to activate LA along with the activation of an initiator/polymer chain-end by DMAP, i.e., the "bifunctional activation" mechanism, whereas MSA possessed no catalytic ability for the ROP of LA, whose characteristic is similar to that of DPP.[10] Thus, the design of a suitable electrophile consisting of DPP and an appropriate amine is necessary to achieve the "bifunctional activation" property for the controlled ROP of

LA. The author now report the ROP of L-lactide (LLA) using the DPP coupled with the 4-dimethylaminopyridine (DMAP) binary system, as shown in Scheme 4.1. This chapter describes (1) the DPP/DMAP-catalyzed ROP of LLA, (2) the activation of monomers and polymer chain-ends by DPP and DMAP, (3) the confirmation of the controlled/living nature by a structure analysis of the obtained polymer and kinetic experiment, (4) the synthesis of the end-functionalized poly(L-lactide)s (PLLAs) using functional alcohols as initiators, and (5) the synthesis of diblock copolymers by the DPP-catalyzed ROPs of TMC, δ-VL, and ε-CL combined with the DPP/DMAP-catalyzed ROP of LLA without quenching.

Shcme 4.1. Ring-opening polymerization (ROP) of L-Lactide (LLA) using an alcohol initiator and diphenyl phosphate (DPP) with 4-dimethylaminopyridine (DMAP)

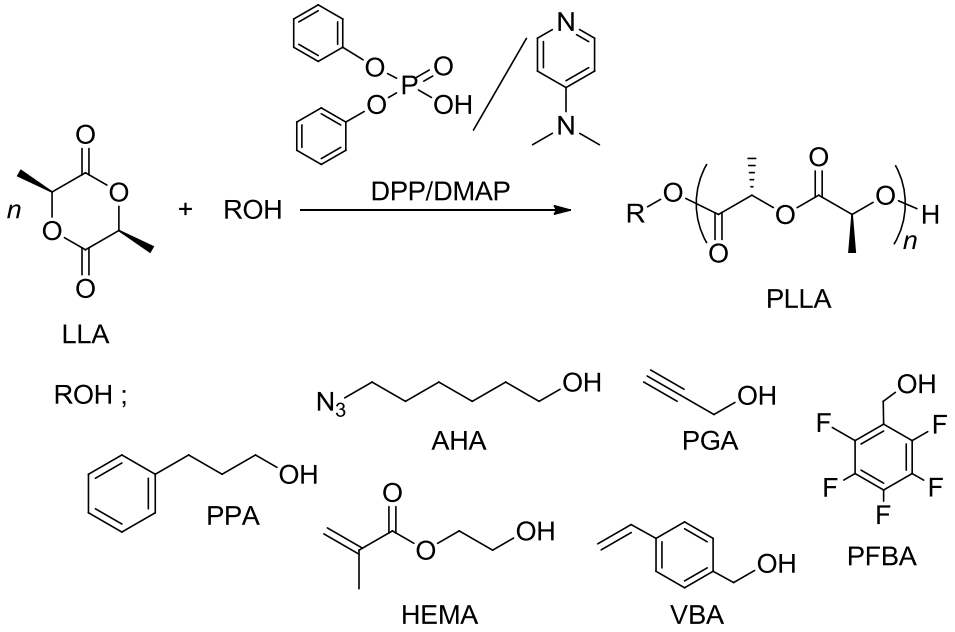

4.2 Results and Discussion

4.2.1 ROP of L-Lactide (LLA) catalyzed by DPP and Tertiary Amine (TA). As described in chapter 3, diphenyl phosphate (DPP)-catalyzed ring-opening polymerizations (ROPs) of cyclic monomers such as *δ*-valerolactone (*δ*-VL), *ε*-caprolactone (*ε*-CL), and trimethylene carbonate (TMC) successfully proceeded and the activation mechanism was assigned by the chemical shifts for the carbonyl carbon signal of the monomer and OH proton signal of chain-end model compounds in the presence of DPP. On the contrary, the catalytic ability of DPP was quietly insufficient for the ROP of L-lactide (LLA), resulting in the formation of an oligomer; in contrast to *δ*-VL, *ε*-CL, and TMC, no shift was observed in the ^{13}C NMR spectrum of LLA in the presence of DPP (referred to in a later section). Thus the author examined DPP coupled with tertiary amines, such as TMEDA, PMDETA, Me_6TREN, DABCO, Sp, and DMAP as co-catalysts for the ROP of LLA, as shown Scheme 4.2.[11] The results were listed in Table 4.1. Although the use of only DPP exhibited a low catalytic activity, the addition of DMAP was most effective for the production of well-defined poly(L-lactide) (PLLA) with a predicted molecular weight and low polydispersity in a high yield.

Shcme 4.2. ROP of LLA using 3-phenyl-1-propanol (PPA) and DPP with tertiary amines (TA)

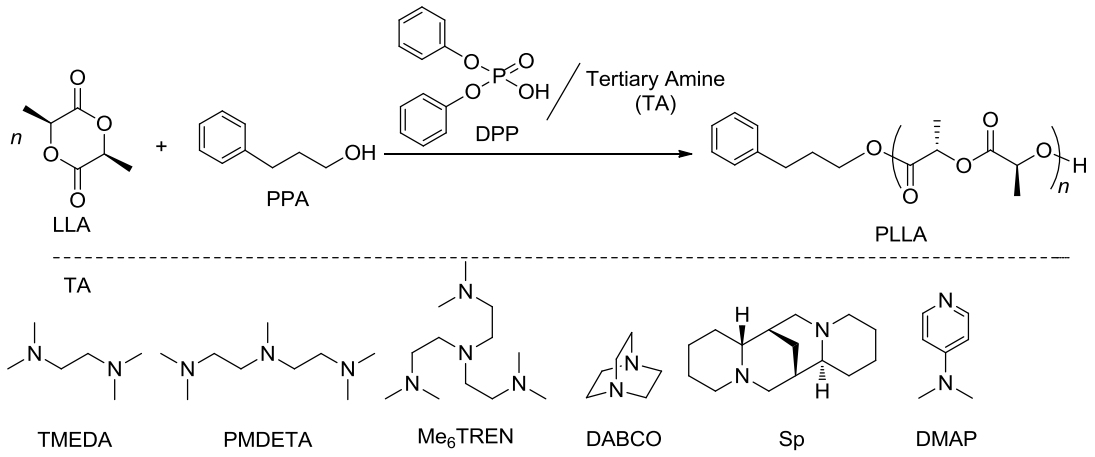

Table 4.1. Ring-opening polymerization (ROP) of L-lactide (LLA) using 3-phenyl-1-propanol (PPA), diphenyl phosphate (DPP), and tertiary amine (TA) [a]

run	tertiary amine (TA)	$[DPP]_0/[TA]_0$	conv. (%) [b]	$M_{n,calcd}$ (g mol^{-1}) [c]	$M_{n,NMR}$ (g mol^{-1}) [b]	M_w/M_n [d]
1	none	-	3.4	380	350	n.d.
2	TMEDA	1	9.1	790	810	1.20
3	TMEDA	2	14.3	1170	1260	1.16
4	PMDETA	1	3.2	370	350	n.d.
5	PMDETA	2	9.7	840	940	1.16
6	Me_6TREN	1	3.8	410	490	n.d.
7	Me_6TREN	2	8.6	760	820	1.14
8	DABCO	1	8.3	730	830	1.22
9	DABCO	2	18.3	1460	1600	1.17
10	Sp	1	52.4	3910	3840	1.25
11	Sp	2	59.3	4410	4330	1.11
12	DMAP	1	64.5	4790	5020	1.11
13	DMAP	2	90.2	6630	6650	1.11

[a] Temperature, room temp.; time, 48 h; solvent, CH_2Cl_2; $[LLA]_0/[PPA]_0/[DPP]_0$, 50/1/3; $[LLA]_0$, 3.0 mol·L^{-1}. [b] Determined by ^{1}H NMR in $CDCl_3$ [c] Calculated from $([LLA]_0/[PPA]_0) \times$ conv. × (M.W. of LLA) + (M. W. of PPA). [d] Determined by SEC in $CHCl_3$ using PSt standards.

In order to optimize the molar ratio of DPP and DMAP (DPP/DMAP) for the ROP of LLA, the author carried out polymerizations with the initial ratio of $[LLA]_0/[PPA]_0/[DPP]_0/[DMAP]_0$ = 50/1/3/3, 50/1/3/6, and 50/1/3/9. Table 4.2 lists the

polymerization results. For the DPP/DMAP of 1/1, the polymerization rate was low, resulting in the medium conv. of 64.5 % for the polymerization time of 48 h, whereas the observed molecular weight ($M_{n,NMR}$) of 5020 g mol^{-1} agreed with the calculated one ($M_{n,calcd}$) of 4790 g mol^{-1} and the polydipersity (M_w/M_n) was very low at 1.11. In addition, the polymerization with the DPP/DMAP of 1/2 produced a polymer with the low M_w/M_n of 1.11 (Figure 4.1) with the high conv. of 90.2 %, and the $M_{n,NMR}$ of 6650 g mol^{-1} strongly agreed with the $M_{n,calcd}$ of 6630 g mol^{-1}. On the other hand, the DPP/DMAP of 1/3 was relatively unsuitable to control the molecular weight, such as the higher $M_{n,NMR}$ of 8340 g mol^{-1} than the $M_{n,calcd}$ of 6830 g mol^{-1} and a relatively broad molecular weight distribution of M_w/M_n = 1.24, suggesting that DMAP was in excess based on the DPP/DMAP of 1/2, resulting in the insufficient control of the molecular weight and its distribution because an excess amount of DMAP caused undesirable side-reactions, such as transesterification and back biting together with the activation of polymer chain-ends. These results indicated that the suitable DPP/DMAP ratio was 1/2 for the controlled ROP of LLA.

The optimized polymerization condition, the $[DPP]_0/[DMAP]_0$ of 1/2, was used for the synthesis of polymers with various molecular weights. The polymerizations were carried out under the conditions of $[LLA]_0/[PPA]_0/[DPP]_0/[DMAP]_0$ = 20/1/1/2, 30/1/1/2, 100/1/5/10 and 150/1/5/10 (Table 4.2, runs 15 - 18, respectively) though the loading amounts of DPP and DMAP while maintaining the DPP/DMAP ratio of 1/2 increased or decreased to control the polymerization rate and polydsipersity. The molecular weights of the resultant polymers linearly increased with the increasing $[LLA]_0/[PPA]_0$, and the $M_{n,NMR}$ of 2860, 4190, 13400 and 19200 g mol^{-1} firmly agreed with the $M_{n,calcd}$ of 2850, 4030, 13000 and 18700 g mol^{-1}, respectively. In addition, the SEC traces of the obtained polymers exhibits monomodal shapes (Figure 4.1), strongly indicating that the DPP/DMAP-catalyzed ROP of LLA proceeded through a controlled/living mechanism without any side reactions.

Table 4.2. ROP of LLA with PPA using DPP and DMAP [a]

run	$[LLA]_0/[PPA]_0$ /$[DPP]_0/[DMAP]_0$	time (h)	conv. (%) [b]	$M_{n,calcd}$ (g mol^{-1}) [c]	$M_{n,NMR}$ (g mol^{-1}) [b]	M_w/M_n [d]
12	50/1/3/3	48	64.5	4790	5020	1.11
13	50/1/3/6	48	90.2	6630	6650	1.11
14	50/1/3/9	28	92.9	6830	8340	1.24
15	20/1/1/2	14	94.0	2850	2860	1.13
16	30/1/1/2	28	90.0	4030	4190	1.09
17	100/1/5/10	120	89.1	13000	13400	1.09
18	150/1/5/10	208	85.7	18700	19200	1.10

[a] Temperature, room temp.; solvent, CH_2Cl_2; $[LLA]_0$ = 3.0 mol·L^{-1}. [b] Determined by ^{1}H NMR in $CDCl_3$. [c] Calculated from $([LLA]_0/[PPA]_0)$ × conv. × (M.W. of LLA) + (M. W. of PPA). [d] Determined by SEC in $CHCl_3$ using PSt standards.

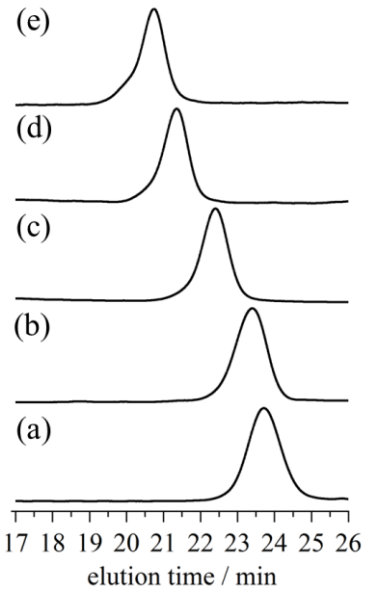

Figure 4.1. SEC traces of PLLA obtained with the $[LLA]_0/[PPA]_0$ of (a) 20, (b)30, (c) 50, (d) 100, and (e) 150 (eluent, $CHCl_3$; flow rate, 0.8 mL·min^{-1}) (Table 4.2, runs 13, and 15- 18).

The chemical structure of the obtained PLLA (Table 4.2, run 13) was revealed by the ^{1}H NMR and MALDI-TOF MS measurements. The peaks at 1.58 and 5.10-5.23 ppm due to the polymer main chain and at 1.97, 2.67, 4.15, and 7.15-7.31 ppm due to the initiator residue are observed in the ^{1}H NMR spectrum, as shown in Figure 4.2. Additionally, one series of peaks perfectly agreed with the molecular weight of the polymer from LLA possessing the PPA residue and the hydroxyl chain-end in the MALDI-TOF MS measurement, as shown in Figure 4.3; e.g., for the 35-mer, the measured value of 5202.47 corresponded to the calculated one of 5202.56, as shown in Figures 4.3b and 4.3c. These results indicated that the DPP/DMAP-catalyzed ROP of LLA should be the controlled/living polymerization system leading to well-defined PLLAs.

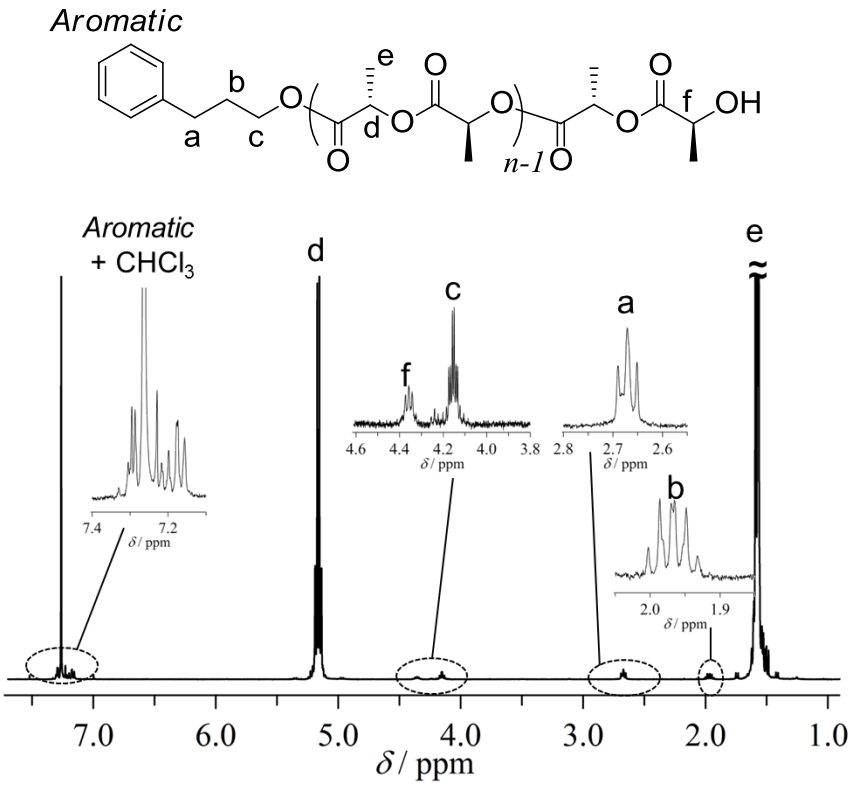

Figure 4.2. ^{1}H NMR spectrum of PLLA initiated from PPA in $CDCl_3$ (Table 4.2, run 13).

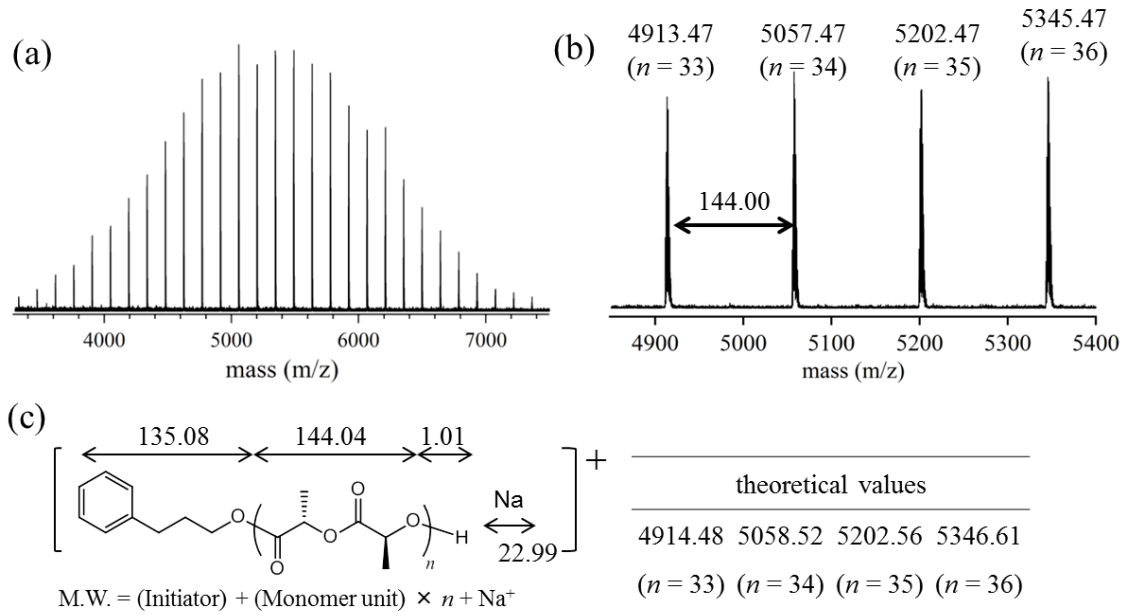

Figure 4.3. MALDI-TOF MS spectrum of PLLA initiated from PPA (Table 4.2, run 13).

4.2.2 Controlled/Living Nature of DPP/4-Dimethylaminopyridine (DMAP)-Catalyzed ROP of LLA. The livingness of the ROP of LLA was confirmed by chain extension and kinetic experiments. For the chain extension experiment, the first polymerization with $[LLA]_0/[PPA]_0/[DPP]_0/[DMAP]_0$ = 20/1/1/2 in toluene was carried out to afford the PLLA with the $M_{n,NMR}$ of 2760 g mol^{-1} and the M_w/M_n of 1.13 for the monomer conversion of 85.8 %. The second polymerization then proceeded by the subsequent addition of 20 equivalents of LLA to PPA (in CH_2Cl_2; $[LLA]_0$ = 4.0 mol·L^{-1}) to give the PLLA with the $M_{n,NMR}$ of 5530 g mol^{-1} and the M_w/M_n of 1.16, as shown in Figure 4.4. This result indicated that the chain end group of PLLA was definitely maintained and DPP/DMAP possesses a catalytic ability. In addition, the kinetic experiment showed a distinct first-order relationship between the reaction time and monomer conversion, meaning that the monomer consumption rate was constant during the polymerization, as shown in Figure 4.5. The $M_{n,NMR}$ of PLLA linearly increased with the reaction time, the $M_{n,NMR}$ values of the PLLA fairly agreed with the $M_{n,calcd}$ ones, and the M_w/M_n of PLLA showed low values ranging from 1.07 to 1.16.

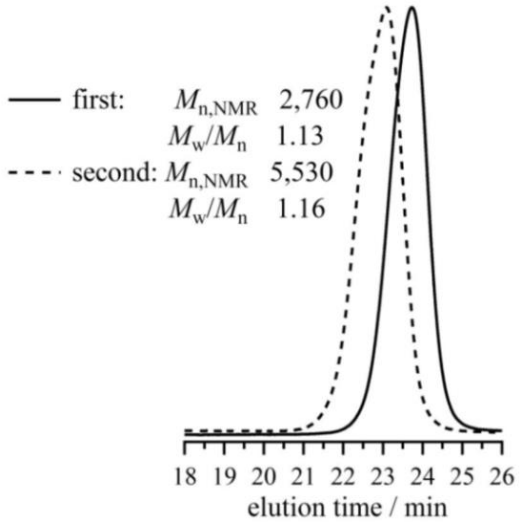

Figure 4.4. SEC traces of PLLAs obtained by the first polymerization (solid line) and the post-polymerization (dashed line) (eluent, $CHCl_3$; flow rate, 0.8 mL·min^{-1}).

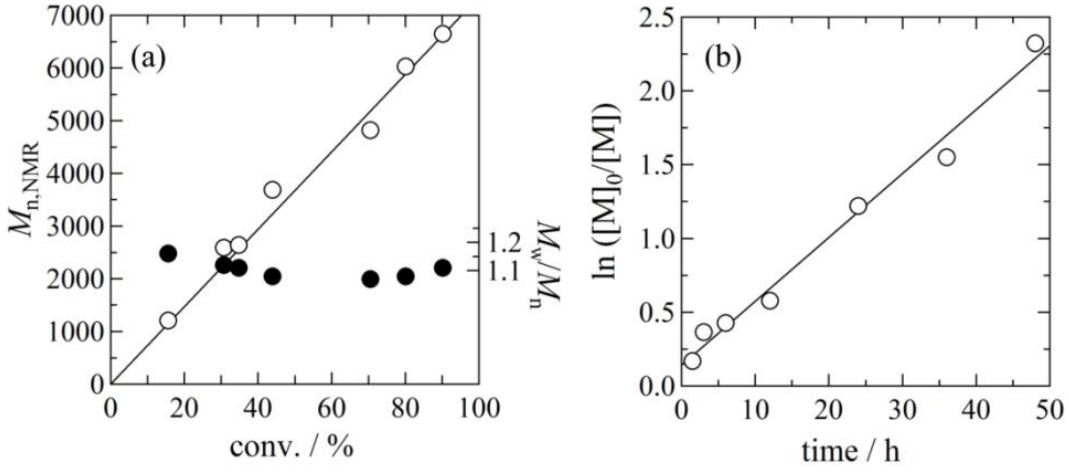

Figure 4.5. (a) Dependence of $M_{n,NMR}$ (○), M_w/M_n (●), and $M_{n,calcd}$ (solid line) on monomer conversion (conv.) and (b) kinetic plots for the polymerization of LLA at room temp. in CH_2Cl_2 with $[LLA]_0/[PPA]_0/[DPP]_0[DMAP]_0$ = 50/1/3/6, $[LLA]_0$ = 3.0 mol·L^{-1}.

As the author mentioned in chapter 2 and 3, NMR measurement strongly proved the activation mechanism. Thus the measurement was conducted for LLA in the presence/absence of catalysts. Interestingly, the carbonyl carbon of LLA shifts downfield from 167.34 to 168.06 ppm in the presence of an equimolar mixture of DPP and DMAP, as shown in Figure 4.6a and 4.6d, strongly suggesting that the DPP/DMAP as the electrophile should activate an LLA molecule, as shown in Scheme 4.3a. In addition, the hydroxyl proton signal of methyl (*S*)-(-)-lactate as a model for the PLLA chain-end shifts from 2.87 to 3.86 ppm in the presence of DMAP, as shown in Figure 4.7, which agreed with the well-known fact that DMAP activates the hydroxyl group in the polymer chain-end, as shown in Scheme 4.3b. These results strongly suggested that the DPP/DMAP system should catalyze the ROP of LLA through the "bifunctional activation" of the monomer and polymer chain-end to afford well-defined PLLAs. Thus, the DPP/DMAP-catalyzed ROP of LLA proceeded through a controlled/living mechanism to afford a well-defined PLLA, in which the equimolar DPP/DMAP activates the

carbonyl group in an LLA molecule and DMAP activates the hydroxyl group in the polymer chain-end, as shown in Scheme 4.4.

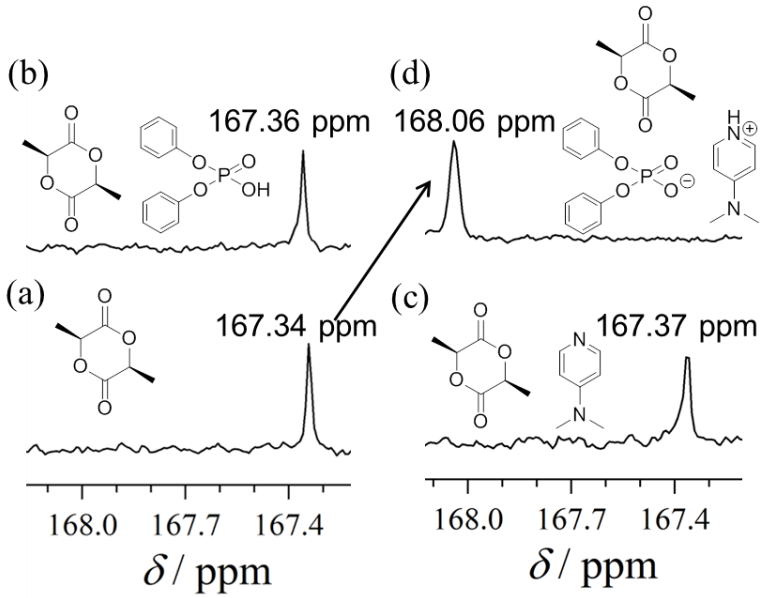

Figure 4.6. ^{13}C NMR spectra of the carbonyl carbon signals for (a) LLA, (b) 1:1 mixtures of LLA with DPP, (c) 1:1 mixtures of LLA with DMAP, and (d) the 1:1:1 mixture of LLA, DPP, and DMAP in $CDCl_3$.

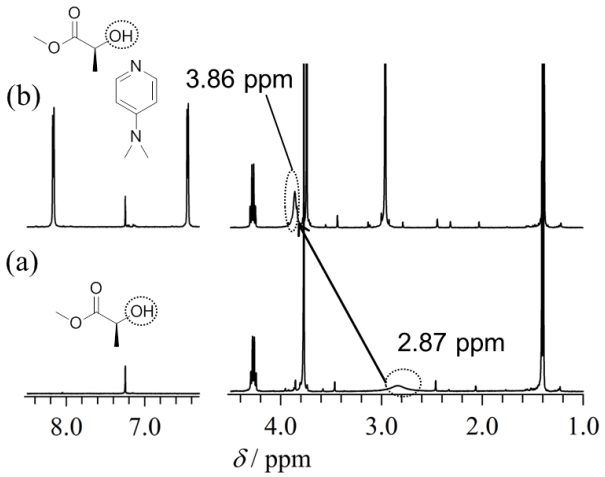

Figure 4.7. ^{1}H NMR spectra of the hydroxyl proton signals of (a) methyl (*S*)-(-)-lactate and (b) the 1:1 mixture of methyl (*S*)-(-)-lactate with DMAP in $CDCl_3$.

Scheme 4.3. Activations of (a) LLA by DPP/DMAP and (b) a poly(L-lactide) (PLLA) chain-end by DMAP

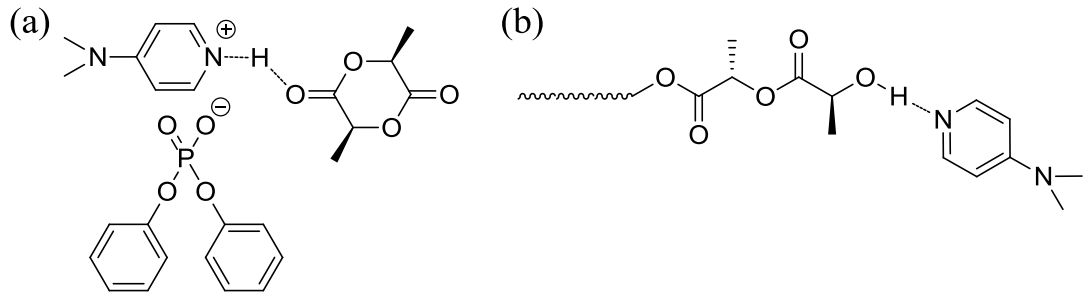

Scheme 4.4. A proposed mechanism for ROP of LLA with PPA using DPP and DMAP

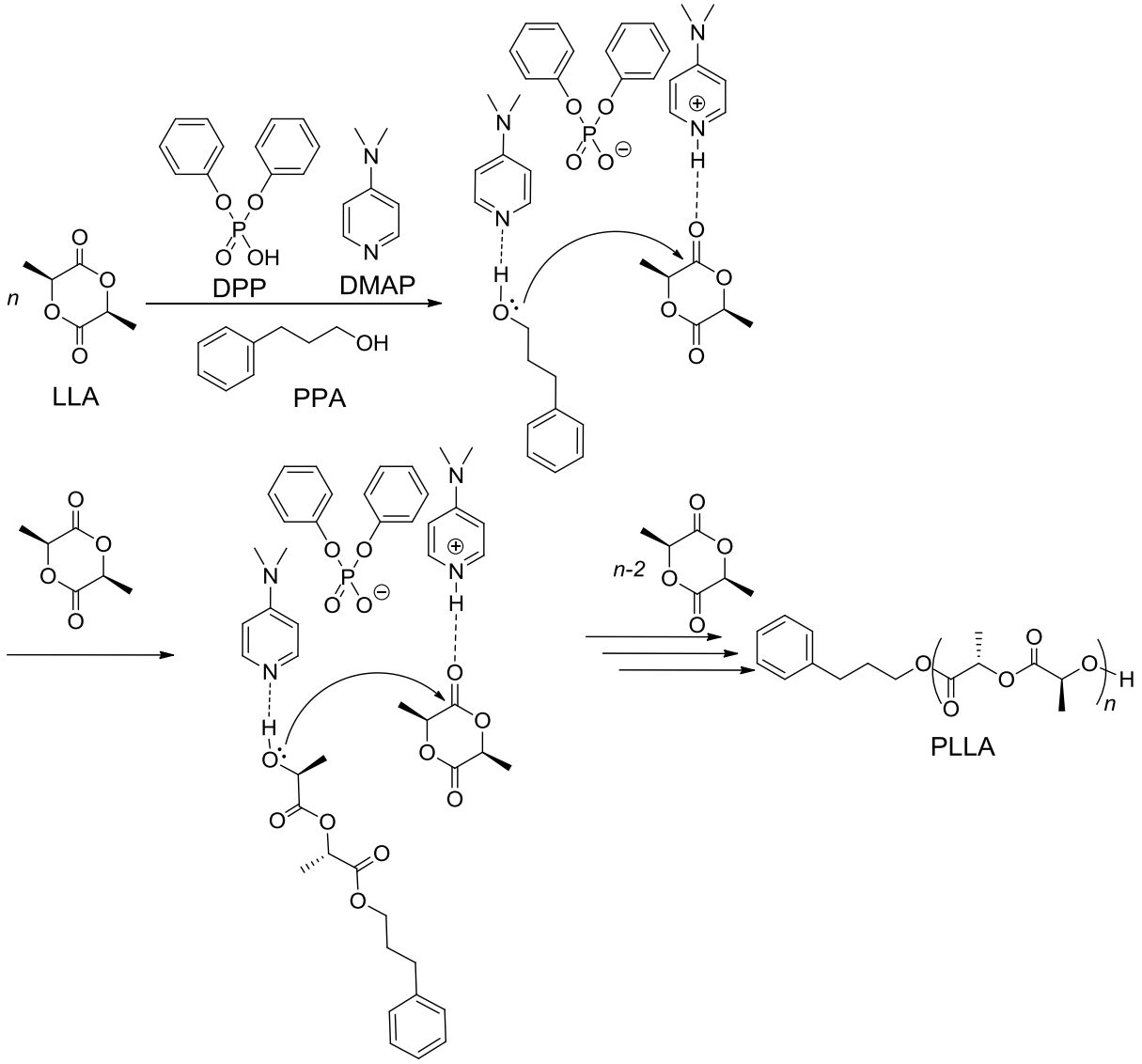

4.2.3 Synthesis of End-Functionalized Poly(L-lactide)s (PLLAs). The controlled/living polymerization system provides the precise synthesis of end-functionalized PLLAs because the DPP/DMAP-catalyzed ROP of LLA was initiated from PPA to afford PLLA possessing the PPA moiety as the end-functional group. Thus, the author utilized the system for producing end-functionalized PLLAs using functional initiators, such as 6-azido-1-hexanol (AHA), propargyl alcohol (PGA), 2,3,4,5,6-pentafluorobenzyl alcohol (PFBA), 2-hydroxyethyl methacrylate (HEMA), and 4-vinylbenzyl alcohol (VBA), as shown in Scheme 4.1. The end-functionalized PLLAs having clickable moieties, such as azido, ethynyl, and pentafluorophenyl groups, are applicable for further modification and those having methacryloyl and vinyl groups are useful as marcromonomers. All the DPP/DMAP-catalyzed ROPs of LLA using AHA, PGA, PFBA, HEMA, and VBA proceeded in a well-controlled manner to afford the corresponding PLLAs with predictable molecular weights and narrow molecular weight distributions of 1.10-1.12, and Table 4.3 lists the synthetic results. The $M_{n,NMR}$s of 7120 g mol^{-1} for AHA, 6800 g mol^{-1} for PGA, 6760 g mol^{-1} for PFBA, 6370 g mol^{-1} for HEMA, and 6940 g mol^{-1} for VBA fairly agreed with the $M_{n,calcd}$s of 7010, 6580, 6490, 6820, and 6690 g mol^{-1}, respectively. Furthermore, the structures of the functional chain-end groups were confirmed by the ^{1}H and^{13}C NMR spectra; the signal at 3.26 ppm due to the methylene protons linked to the azido group was observed for AHA-initiated PLLA, that at 2.50 ppm due to the ethynyl proton for PGA-initiated PLLA, those at 6.12 and 5.60 ppm due to the methacryloyl vinyl protons for HEMA-initiated PLLA, those at 5.79 and 5.34 ppm due to the styryl vinyl protons for VBA-initiated PLLA, and the signal at 54.1 ppm due to the benzyl carbon was confirmed for PFBA-initiated PLLA.

Table 4.3. DPP/DMAP-catalyzed ROP of LLA with the functional initiators (FIs) [a]

run	functional initiator (FI)	conv. (%) [b]	$M_{n,calcd}$ (g mol^{-1}) [c]	$M_{n,NMR}$ (g mol^{-1}) [b]	M_w/M_n [d]
19	AHA	95.3	7010	7120	1.11
20	PGA	90.5	6580	6800	1.11
21	PFBA	87.3	6490	6760	1.11
22	HEMA	92.9	6820	6370	1.12
23	VBA	95.3	7010	7120	1.11

[a] Temperature, room temp.; time, 48 h; solvent, CH_2Cl_2; $[LLA]_0/[FI]_0/[DPP]_0/[DMAP]_0$, 50/1/3/6; $[LLA]_0$, 3.0 mol·L^{-1}. [b] Determined by ^{1}H NMR in $CDCl_3$. [c] Calculated from $([LLA]_0/[FI]_0)$ × conv. × (M.W. of LLA) + (M. W. of FI). [d] Determined by SEC in $CHCl_3$ using PSt standards.

4.2.4 Synthesis of Block Copolymers via DPP-Catalyzed ROP and DPP/DMAP-Catalyzed ROP. DPP efficiently catalyzed the controlled/living ROPs of δ-VL, ε-CL, and TMC, and the bifunctional organocatalyst system of DPP and DMAP is effective for the controlled/living ROP of LLA. Thus, of interest is the synthesis of diblock copolymers consisting of the PLLA segment with the poly(δ-valerolactone) (PVL), poly(ε-caprolactone) (PCL), or poly(trimethylene carbonate) (PTMC) segments by tuning from the "dual activation" to "bifunctional activation" catalyst systems. The author examined synthetic procedures, such as the first DPP-catalyzed ROP of TMC and then the DPP/DMAP-catalyzed ROP of LLA (Scheme 4.5). When the polymerization of TMC was carried out with the condition of $[TMC]_0[PPA]_0/[DPP]_0$ = 20/1/1 for 2 h, the PTMC with the $M_{n,NMR}$ of 1040 g mol^{-1} was produced. After LLA, DPP, and DMAP were added with the $[LLA]_0/[PPA]_0/[DPP]_0/[DMAP]_0$ ratio of 20/1/3/6 without quenching, the diblock copolymer with the $M_{n,NMR}$ of 3580 g mol^{-1} was obtained. The SEC traces are unimodal, and the low polydispersity changed from 1.11 for the first ROP to 1.13 for the second ROP, as shown in Figure 4.8a. For the ^{1}H NMR spectra of the polymerization mixtures for the first and second ROPs, the proton signals due to PTMC and TMC are observed in Figure 4.8b and those due to the PTMC and PLLA segments along with TMC and LLA in Figure 4.8c. Importantly, the TMC conversion of 40.1 % for the first DPP-catalyzed ROP was the same as 40.6 % after the second DPP/DMAP-catalyzed ROP of LLA even though the LLA conversion was 92.5 %, indicating that TMC and LLA were selectively polymerized by tuning the organocatalyst of DPP and DMAP.

Scheme 4.5. Synthesis of poly(*δ*-valerolactone)-*block*-poly(L-lactide) (PVL-*b*-PLLA), poly(*ε*-caprolactone)-*block*-poly(L-lactide) (PCL-*b*-PLLA), and poly(trimethylene carbonate)-*block*-poly(L-lactide) (PTMC-*b*-PLLA) by DPP and DPP/DMAP-catalyzed ROP of *δ*-valerolactone (*δ*-VL), *ε*-caprolactone (*ε*-CL), and trimethylene carbonate (TMC) with LLA

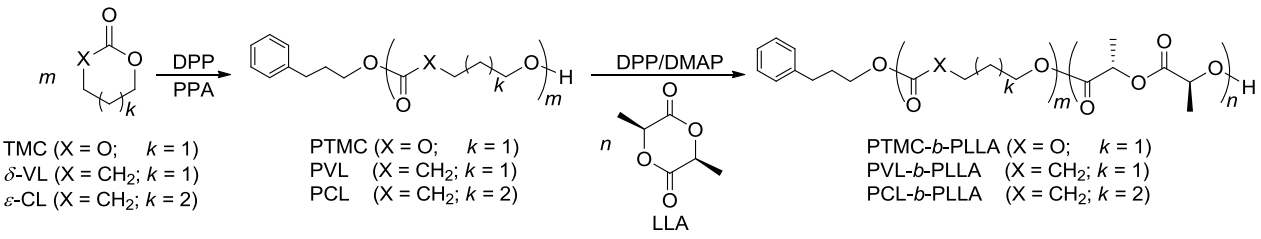

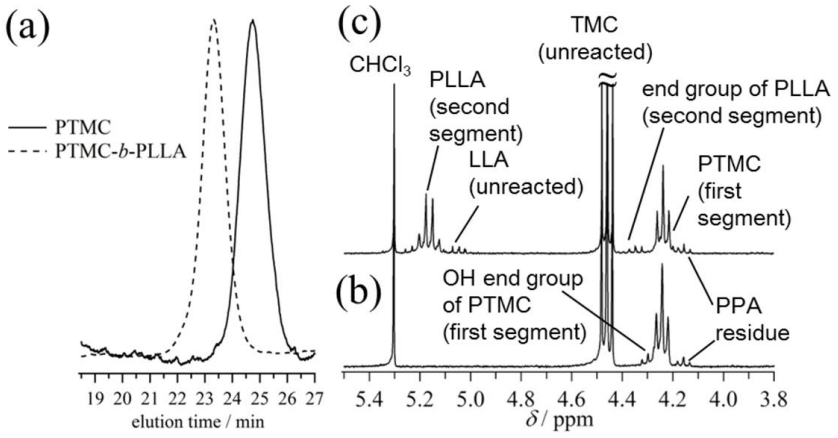

Figure 4.8. (a) SEC traces of PTMC obtained by the first DPP-catalyzed ROP of TMC (solid line) and PTMC-*b*-PLLA by the second DPP/DMAP-catalyzed ROP of LLA (eluent, $CHCl_3$; flow rate, 0.8 mL·min^{-1}), and ^{1}H NMR spectra ($CDCl_3$) of the polymerization mixtures for (b) the first DPP-catalyzed ROP of TMC and (c) the second DPP/DMAP-catalyzed ROP of LLA.

Finally, the author synthesized diblock copolymers consisting of the PVL, PCL, or PTMC segments with the PLLA segment by the DPP/DMAP-catalyzed ROP, as shown in Scheme 4.5. Table 4.4 lists the results of the diblock polymerizations. After the DPP-catalyzed ROPs of *δ*-VL, *ε*-CL, or TMC using PPA, LLA was continuously polymerized as the second

monomer by adding DMAP. The SEC trace of the first ROP shifted to the higher molecular weight region while maintaining a narrow polydispersity; the $M_{n,NMR}$ values increased from 4440 (M_w/M_n, 1.16) to 11600 g mol^{-1} (1.16) for the δ-VL/LLA system, from 5270 (1.14) to 12600 g mol^{-1} (1.12) for the ε-CL/LLA system, and from 5440 g mol^{-1} (1.10) to 11000 g mol^{-1} (1.10) for the TMC/LLA system, as shown in Figure 4.9. For the ^{1}H NMR measurement, the peaks due to the PPA residue and the PVL, PCL, or PTMC main chain were observed along with the appearance of the peaks due to PLLA as the second polymer segment at 1.47−1.78, 1.96, 2.34, 2.67, 4.03-4.15, 5.15, and 7.17-7.31 ppm for the δ-VL/LLA system, at 1.34−1.42, 1.54−1.69, 1.96, 2.31, 2.69, 4.01-4.14, 5.15, and 7.17-7.32 ppm for the ε-CL/LLA system, and at 1.57, 1.95-2.12, 2.76, 4.15, 4.24, 4.46, 5.11-5.21, and 7.13-7.29 ppm for the TMC/LLA system, respectively. In addition, only two peaks due to the carbonyl carbons of PVL and PLLA appeared at 173.2 and 169.6 ppm, respectively, for the δ-VL/LLA system, those of PCL and PLLA at 173.5 and 169.5 ppm, respectively, for the ε-CL/LLA system, and those of PTMC and PLLA at 154.9 and 169.6 ppm, respectively, for the TMC/LLA system. Thus, these results strongly indicated that the polymer structures were confirmed as the diblock copolymers, poly(δ-valerolactone)-*block*-poly(L-lactide) (PVL-*b*-PLLA), poly(ε-caprolactone)-*block*-poly(L-lactide) (PCL-*b*-PLLA), and poly(trimethylene carbonate)-*block*-poly(L-lactide) (PTMC-*b*-PLLA) (Table 4.4, runs 24-26).

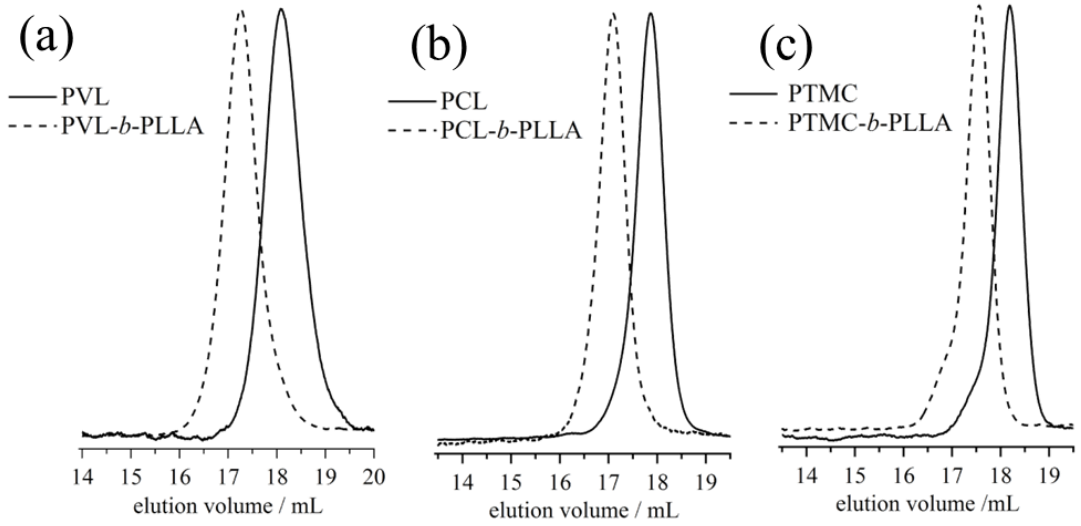

Figure 4.9. (a) SEC traces of (a) PVL (solid line) and PVL-*b*-PLLA (dashed line), (b) PCL (solid line) and PCL-*b*-PLLA (dashed line), and (c) PTMC (solid line) and PTMC-*b*-PLLA (flow rate, 0.8 mL min^{-1}; eluent, $CHCl_3$) (Table 4.4, runs 24-26).

Table 4.4. Block copolymerization of δ-valerolactone (δ-VL), ε-caprolactone (ε-CL), and trimethylene carbonate (TMC) with LLA using DPP and DMAP [a]

	run	monomer (M)	solvent	$[M]_0/[PPA]_0/[DPP]_0/[DMAP]_0$	time (h)	$[M]_0$ (mol L^{-1})	conv. (%) [b]	$M_{n,calcd}$ (g mol^{-1}) [c]	$M_{n,NMR}$ (g mol^{-1}) [b]	M_w/M_n [d]
24	First	δ-VL	toluene	50/1/1/0	1	3.0	98.5	5070	4440	1.16
	Second	LLA	toluene/CH_2Cl_2	50/1/3/6	141	1.5	91.3	11700	11600	1.16
25	First	ε-CL	toluene	50/1/1/0	3	3.0	99.4	5810	5270	1.14
	Second	LLA	toluene/CH_2Cl_2	50/1/3/6	168	1.5	98.0	12900	12600	1.12
26	First	TMC	toluene	50/1/1/0	16	3.0	98.5	5160	5440	1.10
	Second	LLA	toluene/CH_2Cl_2	50/1/3/6	74	1.7	88.0	11600	11000	1.10

[a] Initiator, 3-phenyl-1-propanol (PPA); temperature, room temp. [b] Determined by ^1H NMR in $CDCl_3$ [c] Calculated from $([M]_0/[PPA]_0) \times$ conv. $\times$ (M.W. of a monomer) + (M. W. of PPA). [d] Determined by SEC in $CHCl_3$ using PSt standards.

4.3 Conclusions

Diphenyl phosphate (DPP), a weak acid organocatalyst, performed the ring-opening polymerization (ROP) of lactones and cyclic carbonates, while no polymerization occurred for the L-lactide (LLA). To expand the scope of DPP, the author elucidated the co-catalysts for the ROP of LLA. The DPP/4-dimethylaminopyridine (DMAP)-catalyzed ROP of LLA showed the best results due to the bifuntional organocatalyst system of DPP and DMAP. These catalysts activated LLA and its polymer chain-end leading to production of well-defined poly(L-lactide) (PLLA). The binary system was versatile for the synthesis of end-fuctionalized PLLAs using functional alcohol initiators and diblock copolymers consisting of the PLLA segment with other polymer segments prepared by the DPP-catalyzed ROPs of ε-CL, δ-valerolactone (δ-VL), and trimethylene carbonate (TMC), which suggested that "dual" activation ability of DPP was changed to "bifunctional" activation ability of DPP/DMAP *in situ*.

4.4 Experimental Section

Materials. Toluene (>99.5 %; water content, <0.001 %, Kanto Chemical Co., Inc.) was distilled over sodium benzophenone ketyl under an argon atmosphere. Dichloromethane (CH_2Cl_2; >99.5 %, water content, <0.001 %, Kanto Chemical Co., Inc.), 3-phenyl-1-propanol (PPA; >98%, Tokyo Kasei Kogyo Co., Ltd. (TCI)), propargyl alcohol (PGA; >98%, TCI), *δ*-valerolactone (*δ*-VL; 99 %, Kanto Chemical Co., Inc.), and *ε*-caprolactone (*ε*-CL; 99 %, TCI) were distilled over CaH_2 under an argon atmosphere. 1,5-dioxepan-2-one (DXO; >98%, TCI) was dried by azeotropic distillation with toluene. 2-Hydroxyethyl methacrylate (HEMA; >95%, TCI) was distilled under reduced pressure. L-Lactide (LLA; >98%, TCI), trimethylene carbonate (TMC; >98%, TCI), and 4-dimethylaminopyridine (DMAP; 99+%, Wako Pure Chemical Industries, Ltd.) were purified by recrystallization from dry toluene prior to use. Methyl (*S*)-(-)-lactate (>98%, Merck), 2,3,4,5,6-pentafluorobenzyl alcohol (PFBA; >96%, TCI), diphenyl phosphate (DPP; >99%, TCI), benzoic acid (>99%, TCI), and a weak base anion exchange resin, Amberlyst A21 (Organo Co., Ltd.) were used as received. 6-Azido-1-hexanol (AHA)[12] and 4-vinylbenzyl alcohol (VBA)[13] were synthesized using previously reported methods. All other reagents were of synthetic grade and used without further purification.

Instruments. The number-average molecular weight ($M_{n,NMR}$) was determined from the ^1H NMR spectra recorded using a JEOL JNM-A400II instrument; the $M_{n,NMR}$ value was calculated by comparison between the methyne proton of polymer main-chains at 5.10-5.23 ppm and the benzyl methylene proton at 2.67 ppm. The polymerization was carried out in an MBRAUN stainless steel glove box equipped with a gas purification system (molecular sieves and copper catalyst) in a dry argon atmosphere (H_2O, O_2 < 1 ppm). The moisture and oxygen contents in the glove box were monitored by an MB-MO-SE 1 and MB-OX-SE 1, respectively. The size exclusion

chromatography (SEC) in $CHCl_3$ (0.8 mL·min^{-1}) was performed at 40 °C using a Jasco GPC-900 system equipped with a set of two Shodex KF-805L columns (linear, 8 mm × 300 mm). The polydispersity (M_w/M_n) of the polymers was calculated on the basis of a polystyrene calibration. Matrix-assisted laser desorption ionization time-of-flight mass spectrometry (MALDI-TOF MS) of the obtained polymers was performed using an Applied Biosystems Voyager-DE STR-H equipped with a 337-nm nitrogen laser (3 ns pulse width). One hundred shots were accumulated for the spectra at a 15 kV acceleration voltage in the reflector mode and calibrated using polystyrene (average M_n 3600, Waters Associates) as the internal standard. Samples for the MALDI-TOF MS were prepared by mixing PLLA (1.0 mg·L^{-1}, 10 μL), a matrix (dithranol, 10 mg·L^{-1}, 30 μL) and a cationizing agent (sodium iodide, 10 mg·L^{-1}, 10 μL) in THF. The MALDI target was spotted with 1.0 μL of solution and allowed to air-dry.

Polymerization of L-Lactide using Diphenyl Phosphate and 4-Dimetylaminopyridine. A typical procedure for the polymerization is as follows: LLA (216 mg, 1.50 mmol) was added to a stock solution of PPA (30.0 μL, 30.0 μmol) in CH_2Cl_2 at room temperature in the glove box. A CH_2Cl_2 stock solution of DPP (90.0 μL, 90.0 μmol) and DMAP (180 μL, 180 μmol) were then added to the solution to initiate the polymerization under an argon atmosphere. After 48 h, the polymerization was quenched by the addition of Amberlyst A21 and benzoic acid. Before the addition of the Amberlyst A21, the author obtained a portion of the polymerization mixtures and then added a small amount of triethylamine and benzoic acid to the mixtures for determining the monomer conversion that was directly determined from the ^{1}H NMR measurements of the polymerization mixtures. The polymer was isolated by reprecipitation in cold methanol. Yield, 54.1 %; $M_{n,NMR}$, 6650 g·mol^{-1}; M_w/M_n, 1.11; ^{1}H NMR ($CDCl_3$) δ (ppm), 1.58 (m, 3H × *n*, (-C*H*$_3$)$_n$), 1.97 (q, 2H, *J* = 6.8, ArCH$_2$C*H*$_2$-), 2.67 (t, 2H, *J* = 7.2, ArC*H*$_2$-), 4.15 (m, 2H,ArCH$_2$CH$_2$C*H*$_2$-), 4.36 (m, -C*H*(CH$_3$)OH), 5.10-5.23 (q, 1H × *n-1*, *J* = 7.6, (-C*H*(CH$_3$)O-)$_{n-1}$), 7.15-7.31 (m, 5H, aromatic).

Diblock Copolymerization of *δ*-Valerolactone, *ε*-Caprolactone, and Trimethylene Carbonate with L-Lactide. A typical procedure for the block copolymerization is as follows: Trimethylene carbonate (TMC; 51.0 mg, 500 μmol) was added to a stock solution of DPP (10.0 μL, 10.0 μmol) in toluene at room temperature in the glove box. A toluene stock solution of PPA (10.0 μL, 10.0 μmol) was then added to the solution to initiate the polymerization under an argon atmosphere. The polymerization was first stirred for 16 h, then the block copolymerization was started with 50 equiv. of LLA (72.1 mg, 500 μmol), 2 equiv. of DPP (5.00 mg, 20.0 μmol), 6 equiv. of DMAP (7.33 mg, 60.0 μmol) and CH_2Cl_2 (111 μL). Before the polymerization was quenched by the addition of Amberlyst A21 and benzoic acid after 74 h, to a portion of the polymerization mixture was added a small amount of triethylamine and benzoic acid to determine the monomer conversion, which was directly determined from the ^{1}H NMR measurement. The polymer was isolated by reprecipitation in cold methanol. Yield, 48.1 %; $M_{n,NMR}$, 11000 g·mol^{-1}; M_w/M_n, 1.10; ^{1}H NMR ($CDCl_3$) δ (ppm); 1.57 (q, J = 7.3, 3H × n, (-CH_3)$_n$), 1.95-2.12 (m, 2H, ArCH$_2$CH_2-; m, 2H × m, (-OCH$_2$CH_2-)$_m$), 2.76 (t, 2H, J = 6.5, ArCH_2-), 4.15 (m, 2H, ArCH$_2$CH$_2$CH_2-), 4.24 (t, 4H × m, (-OCH_2CH$_2$-)$_m$), 4.46 (m, -CH(CH$_3$)OH), 5.11-5.21 (q, 1H × n-1, J = 7.3, (-CH(CH$_3$)O-)$_{n-1}$), 7.13-7.29 (m, 5H, aromatic).

4.5 References and Notes

1. Dove, A. P.; Pratt, R. C.; Lohmeijer, B. G. G.; Waymouth, R. M.; Hedrick, J. L. *J. Am. Chem. Soc.* **2005**, *127*, 13798-13799.

2. Pratt, R. C.; Lohmeijer, B. G. G.; Long, D. A.; Lundberg, P. N. P.; Dove, A. P.; Li, H. B.; Wade, C. G.; Waymouth, R. M.; Hedrick, J. L. *Macromolecules* **2006**, *39*, 7863-7871.

3. Kan, S.; Jin, Y.; He, X.; Chen, J.; Wu, H.; Ouyang, P.; Guo, K.; Li, Z.; *Polym. Chem.,* **2013**, *4*, 5432-5439.

4. Koeller, S.; Kadota,J.; Deffieux, A.; Peruch,F.; Massip, S.; L*é*ger, J. –M.; Desvergne, J. –P.; Bibal, B. *J. Am. Chem. Soc.*, **2009**, *131*, 15088-15089.

5. Koeller, S.; Kadota, J.; Peruch, F.; Deffieux, A.; Pinaud, N.; Pianet, I.; Massip, S.; Léger, J.-M.; Desvergne, J.-P.; Bibal, B. *Chem. Eur. J.* **2010**, *16*, 4196-4205.

6. Alba, A.; Schopp, A.; De Souza Delgado, A. –P.; Cherif-Cheikh R.; Martin-Vaca B.; Bourissou, D. *J. Polym. Sci., Part A, Polym. Chem.,* **2010***, 48,* 959-965.

7. Thomas, C.; Peruch, F.; Deffieux, A.; Milet, A.; Desvergne, J. –P.; Bibal, B. *Adv. Synth. Catal.* **2011**, *353*, 1049-1054.

8. Thomas, C.; Peruch, F.; Bibal, B. *RSC Adv.* **2012**, ***2***, 12851-12856.

9. Coulembier, O.; Sanders, D. R.; Nelson, A.; Hollenbeck, A. N.; Horn, H. W.; Rice, J. E.; Fujiwara, M.; Dubois, P.; Hedrick, J. L. *Angew. Chem. Int. Ed.* **2009**, *48*, 5170-5173.

10. Kadota, J.; Pavlović, D.; Desvergne, J. -P.; Bibal, B.; Peruch, F.; Deffieux, A. *Macromolecules* **2010**, *43*, 8874-8879.

11. Coady, D. J.; Engler, A. C.; Horn, H. W.; Bajjuri, K. M.; Fukushima, K.; Jones, G. O.; Nelson, A.; Rice, J. E.; Hedrick, J. L. *Macro Lett.,* **2012**, *1*, 19-22.

12. Speers, A. E.; Adam, G. C.; Cravatt, B. F. *J. Am. Chem. Soc.* **2003**, *125*, 4686-4687.

13. Abramo, J. G.; Chapin, E.C. *J. Org. Chem.* **1961**, *26*, 2671–2673.

Chapter 5

Synthesis of Poly(*β*-butyrolactone) via Ring-Opening Polymerization Using Bis(4-nitrophenyl) Phosphate

5.1 Introduction

Aliphatic polyesters with biodegradable and biocompatible properties are some of the important green materials, which are synthesized using chemical and enzymatic methods.[1-5] Although poly(*δ*-valerolactone) (PVL), poly(*ε*-caprolactone) (PCL), poly(trimethylene carbonate) (PTMC), and polylactide were successfully produced by organocatalytic ring-opening polymerization (ROP) in above chapters, there is still useful aliphatic polyester.

For instance, poly(3-hydroxybutyrate) (P3HB), which is one of the enzymatically synthesized polyesters from renewable resources, possesses a good mechanical property comparable to polypropylene.[6-9] However, the high crystallinity of P3HB causes its low processability, consequently, there are many efforts, such as the enzymatic synthesis of copolyesters and blending with other polymers, to improve the physical property of P3HB for practical use.[8-11] Thus, the synthesis of poly(*β*-butyrolactone) (PBL) by the ring-opening polymerization (ROP) of *β*-butyrolactone (*β*-BL) has been studied as one of the alternative methods for producing P3HB, which provides control of the molecular weights and their distribution together with the syntheses of random and block copolyesters. Although there have been many attempts for the synthesis of PBL using metal-based catalysts,[12-17] the polymerizations using nonmetallic catalysts, i.e., organocatalysts, afford metal-free polyesters, whose property is suitable for application in the biomedical and electronic fields.[18-20]

The organocatalytic ROP of *β*-BL was insufficiently controlled because the high ring strain of *β*-BL caused cleavage through two ways, such as the *O*-acyl bond and *O*-alkyl bond cleavages. For example, the triazole carbine-catalyzed ROP of *β*-BL using an alcohol initiator afforded a PBL possessing the OH- and COOH-chain ends because the initiating species of an alcohoxy anion attacked *β*-BL with no selective bond cleavage.[21, 22] In addition, PBLs obtained with an alcohol initiator using other basic catalysts, such as guanidine, amidine, and

phosphazene, possessed catalyst residues at the α-chain-end by the initiation reaction between basic catalysts and *β*-BL and the crotonyl group at the ω-chain-end by the initiation reaction, such as the dehydration reaction of the hydroxyl group in the propagating chain-end.[23-25]

The polymerization using organic acids produced PBLs with well controlled structures in comparison to organic bases. For instance, Pohl and Bourissou et al. reported that trifluoromethanesulfonic acid was used as a very strong Brønsted acid for the ROP of *β*-BL with an alcohol initiator to afford the well-defined PBL having the initiator residue at the α-chain-end and the hydroxyl group at the ω-chain-end by the selective cleavage of the *O*-acyl bond.[26, 27] As mentioned in chapter 3, the author confirmed that diphenyl phosphate (DPP), one of the weak organic acids, was an effective organocatalyst for the ROPs of *δ*-valerolactone, *ε*-caprolactone (*ε*-CL), and trimethylene carbonate (TMC) to afford well-defined PVL, PCL, and PTMC without any undesirable reactions, in which DPP activated the monomers and hydroxyl groups in the intiators/propagating-chain-ends, i.e., a "dual activation" mechanism. Thus, of interest is to study the catalytic property of phosphoric acid for the ROP of *β*-BL in relation to the activation mechanisms. The author now report the ROP of *β*-BL using the phosphoric acids of DPP and bis(4-nitrophenyl) phosphate (BNPP) that has a greater acidic property compared to DPP, as shown in Scheme 5.1. The difference in the polymerization characteristics of *β*-BL between DPP and BNPP is discussed based on the "dual activation" mechanism. The end-functionalization of PBL was demonstrated using functional alcohols as the initiator, such as propargyl alcohol (PGA), *N*-(2-hydroxyethyl)maleimide (HEMI), 2,3,4,5,6-pentafluorobenzyl alcohol (PFBA), 4-vinylbenzyl alcohol (VBA), and 2-hydroxyethylmethacrylate (HEMA). In addition, the one-pot synthesis of diblock copolymers was carried out by the copolymerization of *β*-BL with *ε*-CL or TMC as second monomers.

Scheme 5.1. Ring-opening polymerization of β-butyrolactone (β-BL) using diphenyl phosphate (DPP) and bis(4-nitrophenyl) phosphate (BNPP)

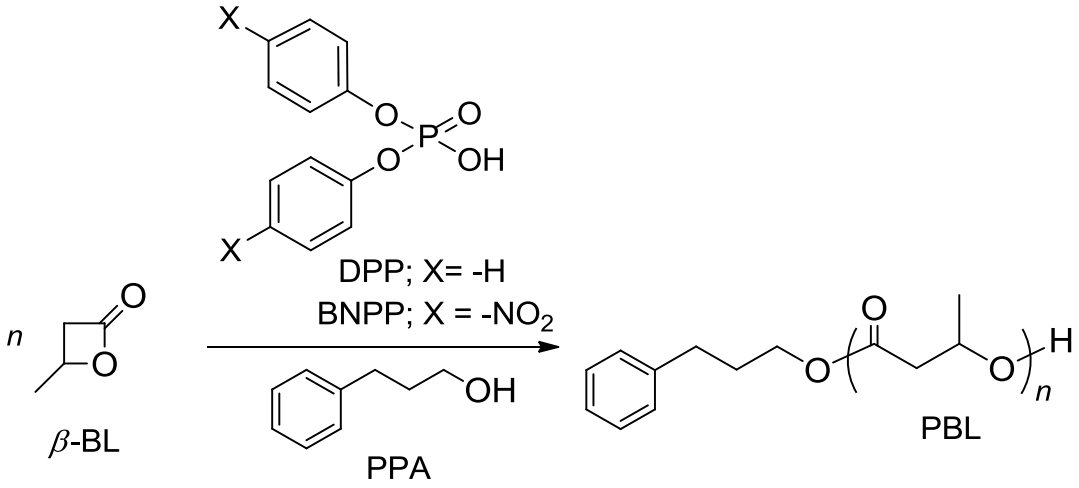

5.2 Results and Discussion

5.2.1 ROP of *β*-Butyrolactone (*β*-BL) Using DPP and Bis(4-nitrophenyl) Phosphate (BMPP). The ring-opening polymerization (ROP) of *β*-butyrolactone (*β*-BL) was carried out using 3-phenyl-1-propanol (PPA) in order to elucidate the catalytic performance of the diphenyl phosphate (DPP) and bis(4-nitrophenyl) phosphate (BNPP). Table 5.1 summarizes the results of the polymerizations with the initial monomer-to-initiator ratio ($[\beta\text{-BL}]_0/[\text{PPA}]_0$) of 50/1. The author first conducted the polymerization of *β*-BL using DPP to evaluate the catalytic ability (runs 1-3). The polymerization rate was very slow at room temperature even with a high loading amount of DPP, the $[\beta\text{-BL}]_0/[\text{DPP}]_0$ of 50/5 (run 1), and that with a low loading amount of DPP (the $[\beta\text{-BL}]_0/[\text{DPP}]_0$ of 50/1) was also slow at 70 °C (run 2). Although the monomer conversion, which was determined by the ^{1}H NMR measurement, was >99 % for 16 h (run 3), peaks due to the formation of oligomers were observed in the ^{1}H NMR and MALDI-TOF MS spectra. These results indicated that the low Brønsted acidity of DPP caused the low catalytic ability for the ROP of *β*-BL, thus bis(4-nitrophenyl) phosphate (BNPP) with a higher acidity than DPP was used, i.e., a pK_a of 1.77 for BNPP and 3.72 for DPP. [28, 29] The BNPP-catalyzed ROP of *β*-BL was also carried out with the initial ratio ($[\beta\text{-BL}]_0/[\text{PPA}]_0$) of 50/1 at 60 °C. The polymerization with the high loading amount of BNPP ($[\beta\text{-BL}]_0/[\text{BNPP}]_0$ = 50/1 for run 4) was heterogeneous due to the poor solubility of BNPP in toluene, resulting in the low monomer conversion of 39.0 % for 3 h, and that with the low amount of BNPP ($[\beta\text{-BL}]_0/[\text{BNPP}]_0$ = 50/0.3 for run 5) produced a polymer with the $M_{n,NMR}$ of 2,030 g mol^{-1} at the low monomer conversion of 47.4 % for 6 h. The polymerization with the $[\beta\text{-BL}]_0/[\text{BNPP}]_0$ of 50/0.5 (run 6) smoothly proceeded and the monomer conversion was 84.7 % for 4.5 h. In addition, the obtained polymer was well controlled and the $M_{n,NMR}$ of 3,830 mol^{-1} agreed with the $M_{n,calcd}$ of 3,780 mol^{-1} and the M_w/M_n value was as low as 1.19.

Thus, the author confirmed the time dependence of the polymerization for run 6 by the ^{1}H NMR and SEC measurements. The monomer conversion steadily increased with the increasing polymerization time until 1.0 h, and then the monomer consumption rate was extremely slow and the monomer conversion finally reached 97.2 % after 40 h, as shown in Figure 5.1a. The SEC trace shifted to the high molecular weight region with the increasing monomer conversion, and the broad peak in the low molecular weight region increased due to side reactions, such as the crotonylation and back biting reaction, and the amount of the low molecular weight products was ca. 10 % of all products based on the peak areas. To analyze the side-reactions, the reaction mixture was separated into the polymeric and oligomeric products by dialysis against methanol using a membrane with the cut-off of 1000 Da. The polymer structure is precisely analyzed in a later section. The oligomeric products were identified as cyclic oligomers derived from the back biting reaction, the PPA-initiated PBL having the crotonyl group at the ω-chain-end, and the H_2O-initiated PBL (H_2O was derived from the crotonylation). Therefore, the author quenched the polymerization at the monomer conversion of 80 – 85 % in order to prevent any undesirable side reactions.

Table 5.1. Ring-opening polymerization (ROP) of *β*-butyrolactone (*β*-BL) with 3-phenyl-1-propanol using diphenyl phosphate (DPP) and bis(4-nitrophenyl) phosphate (BNPP) [a]

run	$[M]_0$	catalyst	$[cat.]_0$ /$[PPA]_0$	temp. (°C)	time (h)	conv. (%) [b]	$M_{n,calcd}$ (g mol^{-1}) [c]	$M_{n,NMR}$ (g mol^{-1}) [b]	M_w/M_n [d]
1	4.0		5.0	r.t.	260	32.4	1530	n.d. [e]	1.52
2	4.0	DPP	1.0	70	95	15.8	820	770	n.d. [e]
3	8.0		5.0	100	16	>99.9	4400	n.d. [e]	1.76
4	8.0		1.0 [f]	60	3	39.0	1820	1670	1.31
5	8.0	BNPP	0.3	60	6	47.4	2180	2030	1.31
6	8.0		0.5	60	4.5	84.7	3780	3830	1.19 [g]

[a] Initiator, 3-phenyl-1-propanol (PPA); temperature, room temp.; solvent, toluene; $[\beta\text{-BL}]_0/[PPA]_0$, 50/1. [b] Determined by ^{1}H NMR in $CDCl_3$. [c] Calculated from $([\beta\text{-BL}]_0/[PPA]_0) \times$ conv. × (M.W. of *β*-BL) + (M. W. of PPA). [d] Determined by SEC in $CHCl_3$ using PSt standards for crude product. [e] Not determined. [f] BNPP was partly insoluble in toluene. [g] Determined after purification.

For the polymerization time up to 4.5 h, the $M_{n,NMR}$ of PBL linearly increased with the reaction time, the $M_{n,NMR}$ values of the PBL fairly agreed with the $M_{n,calcd}$ ones, and the M_w/M_n of PBL showed relatively low values ranging from 1.14 to 1.19, as shown in Figure 5.1b. Thus, the BNPP-catalyzed ROP of *β*-BL proceeded through a controlled/living mechanism to afford a well-defined PBL except for the late stage of the polymerization. Finally, the polymer with the $M_{n,NMR}$ of 3,830 g mol^{-1} and the M_w/M_n of 1.19 was obtained for 4.5 h.

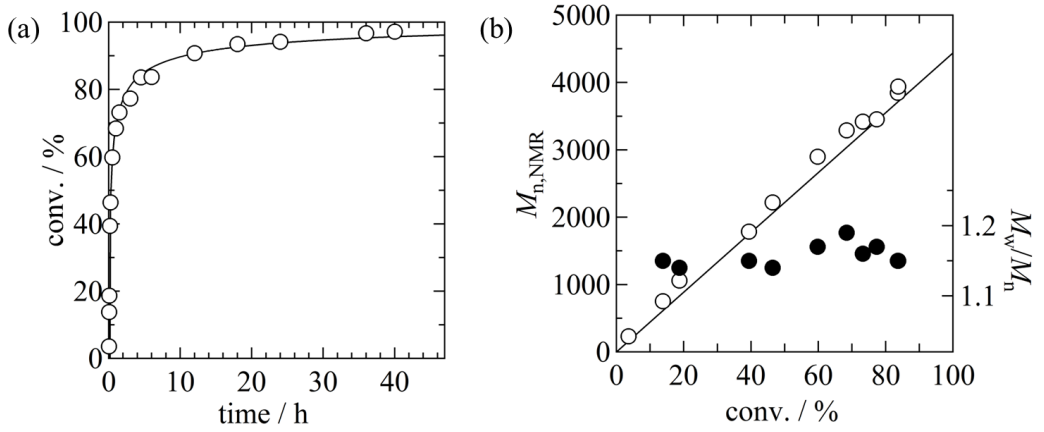

Figure 5.1. (a) Kinetic plots for the polymerization of β-BL at 60 °C in toluene ([β-BL]$_0$/[PPA]$_0$/[BNPP]$_0$ = 50/1/0.5 and [β-BL]$_0$ = 8.0 mol•L^{-1}) and (b) dependence of $M_{n,NMR}$ (○), M_w/M_n (●), and $M_{n,calcd}$ (solid line) on monomer conversion (conv.) until 4.5 h.

The BNPP-catalyzed ROP of β-BL was carried out by varying the [β-BL]$_0$/[PPA]$_0$ ratio from 30 to 150 (runs 7-9). Table 5.2 lists the polymerization results along with run 6. All the monomer conversions were >80 %, and the $M_{n,NMR}$ values of the obtained PBLs linearly increased from 2,240 to 10,650 g mol^{-1} with the increasing initial ratio of [β-BL]$_0$/[PPA]$_0$, which fairly agreed with the molecular weights ($M_{n,calcd}$s) calculated from the initial ratios of [β-BL]$_0$/[PPA]$_0$ and the monomer conversions. The SEC traces of the obtained PBLs are relatively narrow with the polydispersity index (M_w/M_n) of ca. 1.20, as shown in Figure 5.2, though the M_w/M_n value slightly increased to 1.39 for the polymer with the highest $M_{n,NMR}$ of 10,650 g mol^{-1}.

Table 5.2. ROP of β-BL with PPA using BNPP [a]

run	$[\beta\text{-BL}]_0/[\text{PPA}]_0/[\text{BNPP}]_0$	time (h)	conv. (%) [b]	$M_{n,calcd}$ (g mol^{-1}) [c]	$M_{n,NMR}$ (g mol^{-1}) [b]	M_w/M_n [d]
7	30/1/0.3	4	80.5	2220	2240	1.20
6	50/1/0.5	4.5	84.7	3780	3830	1.19
8	100/1/1	9	84.2	7380	7370	1.26
9	150/1/1.5	9.5	81.5	10670	10650	1.39

[a] Temperature, room temp.; solvent, toluene; $[\beta\text{-BL}]_0$ = 8.0 mol·L^{-1}. [b] Determined by ^{1}H NMR in $CDCl_3$ [c] Calculated from $([\beta\text{-BL}]_0/[\text{PPA}]_0)$ × conv. × (M.W. of β-BL) + (M. W. of PPA). [d] Determined by SEC in $CHCl_3$ using PSt standards after purification.

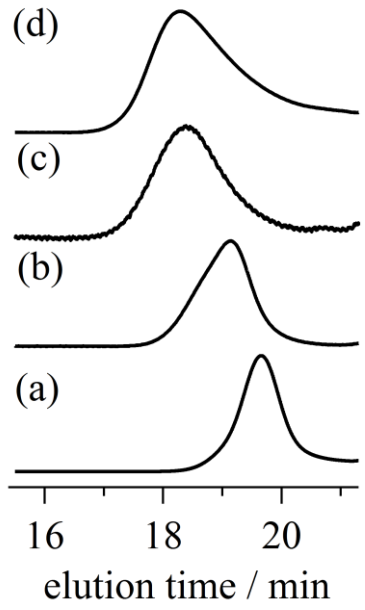

Figure 5.2. SEC traces of obtained PBLs with the molar ratio of β-BL and PPA ($[\beta\text{-BL}]_0/[\text{PPA}]_0$) of (a) 30, (b) 50, (c) 100, and (d) 150 (eluent, $CHCl_3$; flow rate, 1.0 mL min^{-1}).

5.2.2 Characterization of Poly(*β*-butyrolactone) (PBL) Structure. The chemical structure of the obtained polymer was revealed by the ^{1}H NMR and MALDI-TOF MS measurements (Table 5.1, run 6). The peaks at 1.26, 2.42-2.63 and 5.24 ppm due to the polymer main chain and at 1.94, 2.67, 4.09, and 7.16-7.30 ppm due to the initiator residue are observed in the ^{1}H NMR spectrum, as shown in Figure 5.3. In addition, the signal of the methine proton adjacent to the OH terminal group appeared at 4.20 ppm, meaning that the ROP of *β*-BL definitely proceeded through the *O*-acyl cleavage. Furthermore, one series of peaks perfectly agreed with the molecular weight of the polymer from *β*-BL possessing the PPA residue and the hydroxyl chain-end in the MALDI-TOF MS measurement, as shown in Figure 5.4; e.g., for the 30-mer, the measured value of 2741.05 corresponded to the calculated one of 2741.19, as shown in Figures 5.4b and 5.4c. These results indicated that the BNPP-catalyzed ROP of *β*-BL should proceed with the *O*-acyl cleavage of *β*-BL without the crotonylation, leading to well-defined PBLs with high molecular weights.

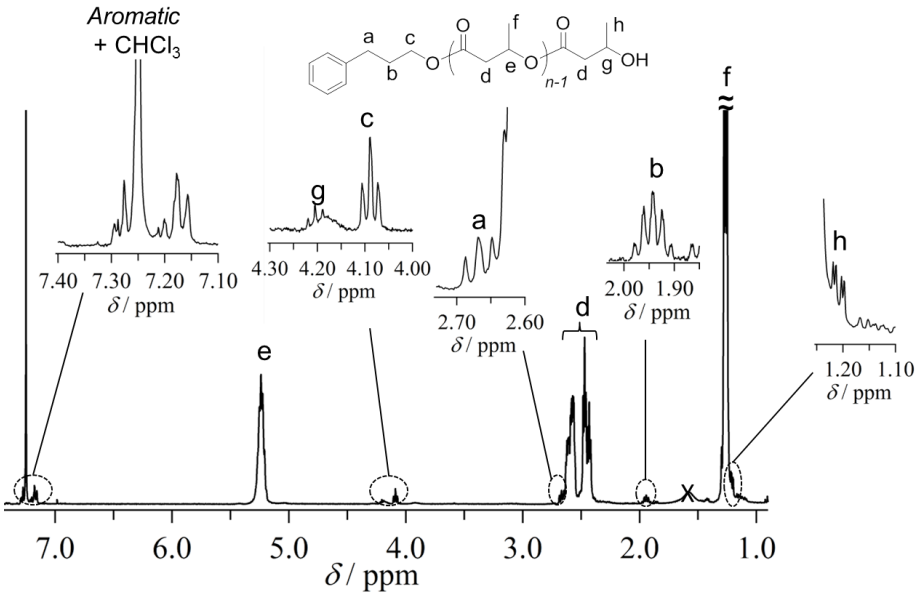

Figure 5.3. ^{1}H NMR spectrum of PBL initiated from 3-phenyl-1-propanol in $CDCl_3$ (Table 5.1, run 6).

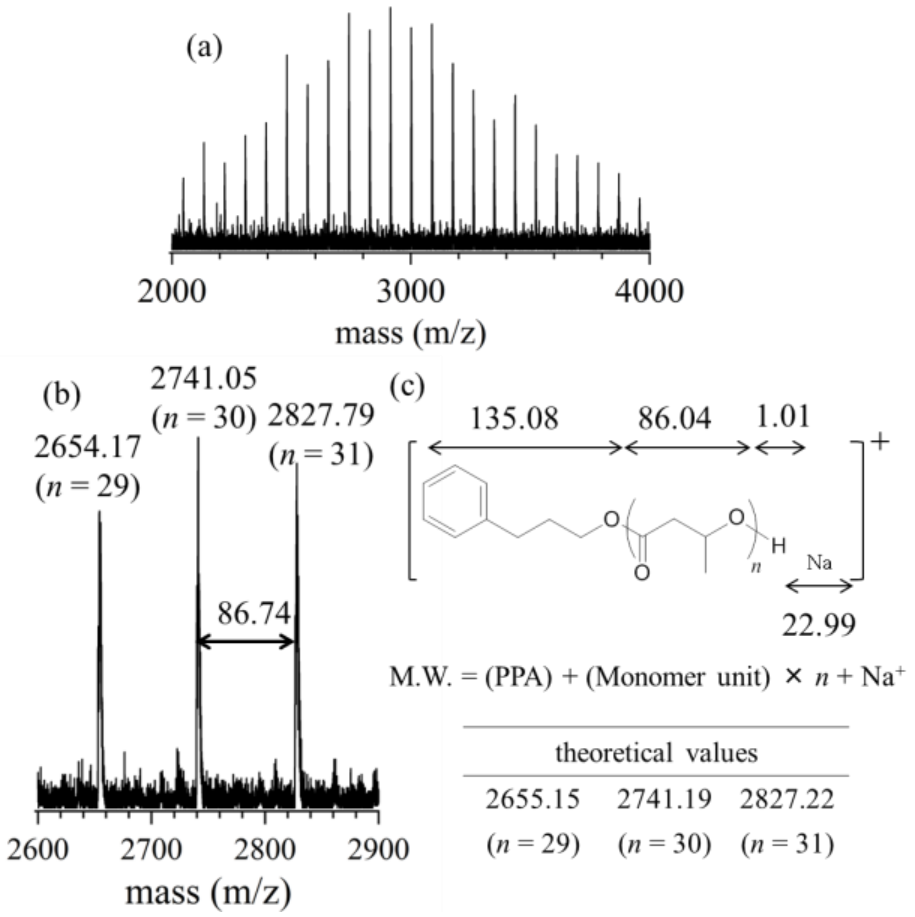

Figure 5.4. MALDI-TOF MS spectrum of PBL (Table 5.1, run 6).

5.2.3 Dual Activation Property of BNPP for ROP of *β*-BL. Phosphoric acid has the dual activation ability due to two substrate recognition sites, such as the Brønsted acidic site and Brønsted basic site. The hydroxyl proton of phosphoric acid acted as the Brønsted acid for capturing electrophilic components through hydrogen bonding, whereas the phosphoryl oxygen acted as the Brønsted base for accepting the proton of other substrates. The ROP of cyclic esters generally proceeds through the Fisher esterification, in which the nucleophilic oxygen of an alcohol attacked the carbonyl carbon of the monomer through the dual activation of the propagating chain-end and the monomer, as shown in Scheme 5.2.

Scheme 5.2. Dual activation of (a) *β*-BL and (b) PBL Chain-end by BNPP

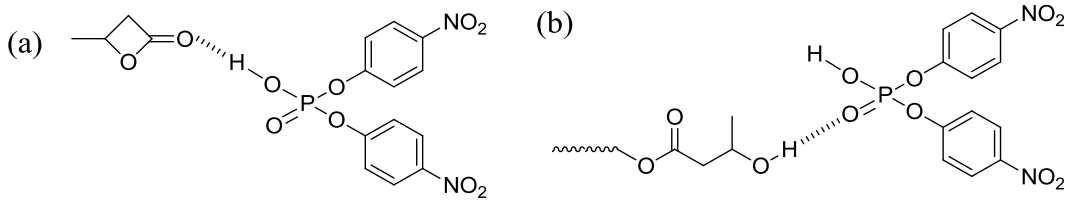

The activation mechanism of the BNPP-catalyzed ROP of *β*-BL was clarified by NMR measurements. The ^{13}C NMR spectra of *β*-BL were measured in the absence/presence of BNPP (the [*β*-BL]/[BNPP] ratio of 0.5) to confirm the monomer activation ability. The chemical shifts at 166.92 ppm due to the carbonyl carbon is observed downfield shifted to 167.03 ppm, as shown in Figures5.5a and 5.5b, implying that the acidic hydroxyl proton of BNPP activated the carbonyl group of *β*-BL. In addition, the ^{1}H NMR spectra were measured in the absence/presence of BNPP using ethyl DL-3-hydroxybutyrate as a PBL chain-end model; the hydroxyl proton signal shifts from 2.49 to 6.60 ppm in the presence of BNPP, as shown in Figures 5.5c and 5.5e, meaning that the nucleophilicity of the hydroxyl group in the propagating chain-end was activated by the interaction with the phosphoryl oxygen of BNPP. These results strongly indicated that BNPP has the dual activation ability for the monomer along with its polymer chain-end, as shown in Schemes 5.2a and 5.2b, respectively, which

played an important role in the controlled/living BNPP-catalyzed ROP of *β*-BL. The BNPP-catalyzed ROP of *β*-BL proceeded through the dual activation mechanism, as shown in Scheme 3, to afford the well-defined PBL though the acidity of BNPP with the pK_a of 1.77 is extremely weak compared to TfOH with the pK_a of -14.[30]

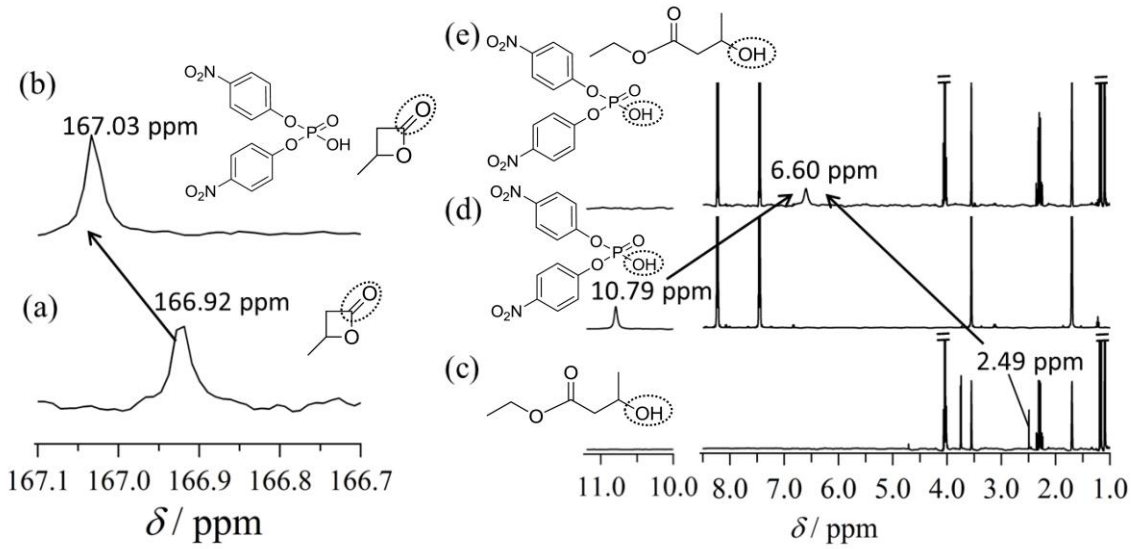

Figure 5.5. ^{13}C NMR spectra of the carbonyl carbon signals for (a) *β*-BL and (b) the 1:2 mixture of *β*-BL with BNPP and ^{1}H NMR spectra of the hydroxyl proton signals for (c) ethyl DL-3-hydroxybutyrate, (d) BNPP, and (e) the 1:1 mixture of ethyl DL-3-hydroxybutyrate with BNPP in THF-d_8.

Scheme 5.3. A proposed mechanism for ROP of β-BL with PPA using BNPP

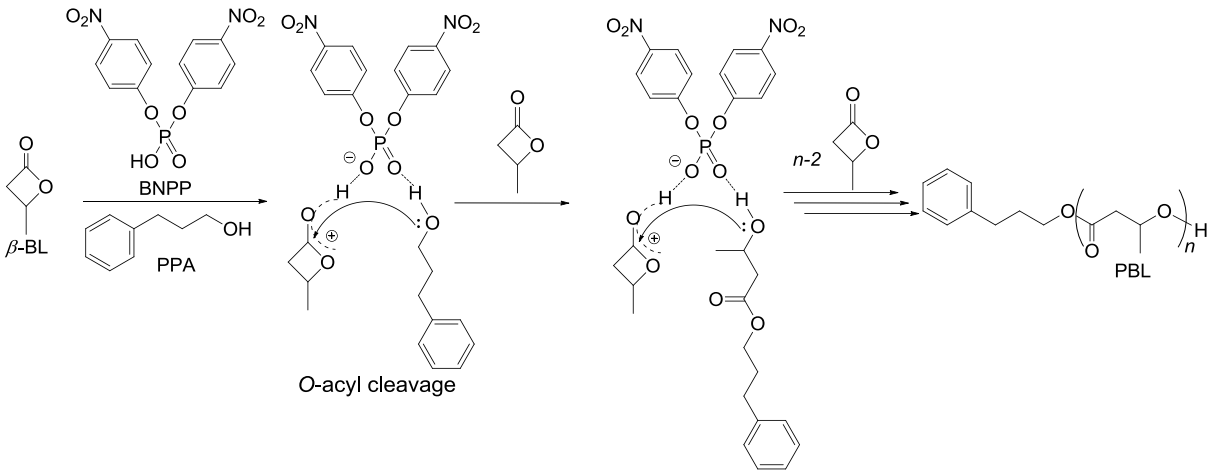

5.2.4 Synthesis of End-functionalized PBL Using Functional Alcohols.

The synthesis of end-functionalized PBLs was carried out by the BNPP-catalyzed ROP of *β*-BL using functional initiators, such as propargyl alcohol (PGA), *N*-(2-hydroxyethyl)maleimide (HEMI), 2,3,4,5,6-pentafluorobenzyl alcohol (PFBA), 2-hydroxyethyl methacrylate (HEMA), and 4-vinylbenzyl alcohol (VBA), as shown in Scheme 5.4. The end-functionalized PBLs having ethynyl, maleimide, and pentafluorophenyl groups, are applicable for further modification through the click reaction and those having methacryloyl and styryl groups are useful as marcromonomers leading to further graft copolymers. All the BNPP-catalyzed ROPs of *β*-BL using PGA, HEMI, PFBA, HEMA, and VBA proceeded in a well-controlled manner to afford the corresponding PBLs with predictable molecular weights and narrow molecular weight distributions of 1.17-1.20, as listed in Table 5.3. The $M_{n,NMR}$ values were 3,890 g mol^{-1} for PGA, 4,030 g mol^{-1} for HEMI, 4,270 g mol^{-1} for PFBA, 3,890 g mol^{-1} for HEMA, and 3,640 g mol^{-1} for VBA, which fairly agreed with the calculated ones ($M_{n,calcd}$) of 3,600, 3,740, 3,780, 3,780, and 3,680 g mol^{-1}, respectively. Furthermore, the structures of the functional chain-end groups were confirmed by the ^{1}H NMR spectra; the signal at 4.67 ppm due to the methylene protons linked to the ethynyl group for the PGA-initiated PBL, those at 6.72, 4.24, and 3.78 ppm due to the maleimide protons for the HEMI-initiated PBL, those at 6.12, 5.59, 4.33, and 1.94 ppm due to the methacryloyl vinyl protons for the HEMA-initiated PBL, those at 6.69, 5.77, and 5.09 ppm due to the styryl vinyl protons for the VBA-initiated PBL, and the signal at 53.5 ppm due to the benzyl carbon was confirmed for the PFBA-initiated PBL.

Scheme 5.4. Synthesis of end-functionalized PBLs by BNPP-Catalyzed ROP of *β*-BL with propargyl alcohol (PGA), *N*-(2-hydroxyethyl)maleimide (HEMI), 2,3,4,5,6-pentafluorobenzyl alcohol (PFBA), 2-hydroxyethyl methacrylate (HEMA), and 4-vinylbenzyl alcohol (VBA)

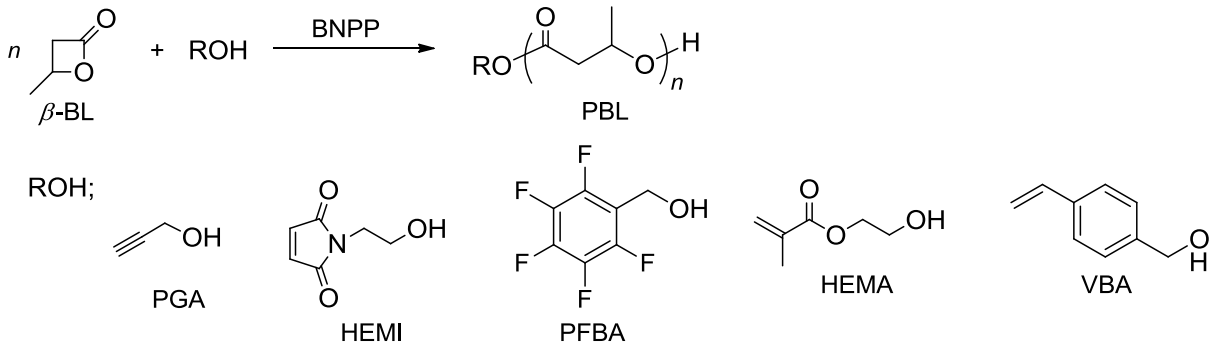

Table 5.3. BNPP-Catalyzed ROP of *β*-BL using functional initiators (FIs) [a]

run	functional initiator (FI)	conv. (%) [b]	$M_{n,calcd}$ (g mol^{-1}) [c]	$M_{n,NMR}$ (g mol^{-1}) [b]	M_w/M_n [d]
10	PGA	82.3	3600	3890	1.17
11	HEMI	83.5	3740	4030	1.20
12	PFBA	83.2	3780	4270	1.19
13	HEMA	84.7	3780	3890	1.19
14	VBA	82.3	3680	3640	1.19

[a] Temperature, 60 °C.; time, 4.5 h; solvent, toluene; $[\beta\text{-BL}]_0/[FI]_0/[BNPP]_0$, 50/1/0.5; $[\beta\text{-BL}]_0$, 8.0 mol·L^{-1}. [b] Determined by ^{1}H NMR in $CDCl_3$ [c] Calculated from $([\beta\text{-BL}]_0/[FI]_0)$ × conv. × (M.W. of *β*-BL) + (M. W. of FI). [d] Determined by SEC in $CHCl_3$ using PSt standards.

5.2.5. Synthesis of Diblock Copolymers with PBL. To expand the scope and limit of BNPP-catalyzed ROP, other cyclic monomres such as ε-caprolactone (ε-CL), trimethylene carbonate (TMC), and L-lactide (LLA), were utilized, as shown in Scheme 5.4. Table 5.4 summarized the polymerization results, for lactone and carbonate, polymerizations proceeded at room temperature affording polymers with controlled molecular weights and narrow polydispersity indices, which were similar results of DPP-catalyzed polymerization as the author revealed in chapter 3. For the polymerization of LLA, BNPP effectively catalyzed and produced well-defined poly(L-lactide) (PLLA) at 90 °C, whereas DPP and other acidic catalyst were insufficient because of its low acidity. Thus the results showed BNPP has the versatility for the ROPs of cyclic monomers compared with low acidic catalysts.

Table 5.4. BNPP-catalyzed ROP of ε-caprolactone (ε-CL), trimethylene carbonate (TMC), and L-lactide (LLA) [a]

run	Monomer (M)	time (h)	conv. (%) [b]	$M_{n,calcd}$ (g mol^{-1}) [c]	$M_{n,NMR}$ (g mol^{-1}) [b]	M_w/M_n [d]
15	ε-CL	4	98.3	5750	6000	1.07
16	TMC	17	98.5	5160	5120	1.09
17 [e]	LLA	24	84.2	6200	6360	1.13

[a] Temperature, room temp; solvent, CH_2Cl_2; $[M]_0/[PPA]_0/[BNPP]_0$, 50/1/1; $[M]_0$, 1.0 mol·L^{-1}. [b] Determined by ^{1}H NMR in $CDCl_3$ [c] Calculated from ($[M]_0/[PPA]_0$) × conv. × (M.W. of LLA) + (M. W. of FI). [d] Determined by SEC in THF using PSt standards. [e] Temperature, 90 °C; solvent, toluene; $[M]_0/[PPA]_0/[BNPP]_0$, 50/1/0.5; $[M]_0$, 4.0 mol·L^{-1}.

The BNPP-catalyzed ROP was applied to other cyclic monomers, such as ε-CL and TMC, for further well-defined polymers. Thus, diblock copolymers were synthesized consisting of the PBL segment with the polyester or polycarbonate segments by the sequential ROP method, as shown in Scheme 5.5. After the first BNPP-catalyzed ROP of β-BL using PPA with the [β-

$BL]_0/[PPA]_0[BNPP]_0$ of 50/1/0.5, 30 equivalents of ε-CL or TMC were continuously polymerized as the second monomer. The SEC trace of the first ROP of β-BL shifted to the higher molecular weight region while maintaining a narrow polydispersity, as shown in Figure 5.6; the $M_{n,NMR}$ values increased from 3,710 g mol^{-1} (M_w/M_n, 1.20) to 7,230 g mol^{-1} (1.16) for the β-BL/ε-CL system, and from 3,830 g mol^{-1} (1.21) to 7,170 g mol^{-1} (1.21) for the β-BL/TMC system. For the ^{1}H NMR measurement, the peaks due to the PPA residue and the PBL main chain were observed along with the appearance of peaks due to the poly(ε-caprolactone) (PCL) or poly(trimethylene carbonate) (PTMC) as the second polymer segment. In addition, only two peaks due to the carbonyl carbons of PBL and PCL appeared at 169.2 and 173.6 ppm, respectively, for the β-BL/ε-CL system, and those of PBL and PTMC at 169.2 and 155.0 ppm, respectively, for the β-BL/TMC system, as shown in the ^{13}C NMR spectra. The polymer structures were confirmed as the diblock copolymers of poly(β-butyrolactone)-*block*-poly(ε-caprolactone) (PBL-*b*-PCL) and poly(β-butyrolactone)-*block*-poly(trimethylene carbonate) (PBL-*b*-PTMC). These results strongly indicated that the chain-end of PBL was the hydroxyl group through the *O*-acyl cleavage of β-BL, and BNPP exhibited a catalytic ability for the second monomers after the first ROP.

Scheme 5.5. Synthesis of Poly(*β*-butyrolactone)-*block*-Poly(*ε*-caprolactone) (PBL-*b*-PCL) and Poly(*β*-butyrolactone)-*block*-Poly(trimethylene carbonate) (PBL-*b*-PTMC) by BNPP-catalyzed ROP of *β*-BL with *ε*-CL and TMC

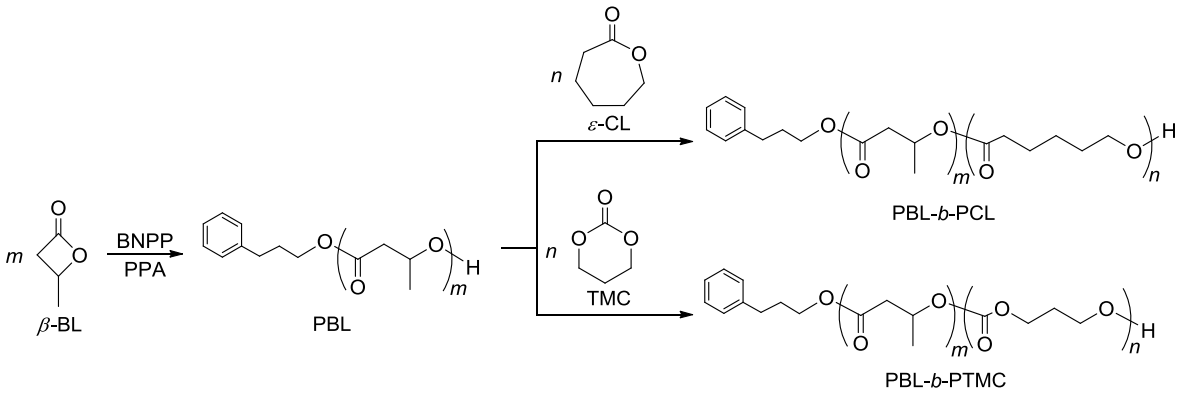

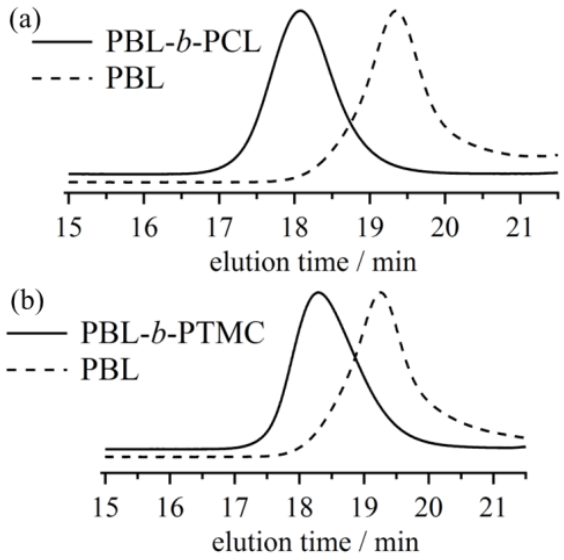

Figure 5.6. SEC traces of (a) PBL and PBL-*b*-PCL and (b) PBL and PBL-*b*-PTMC (eluent, $CHCl_3$; flow rate, 1.0 mL min^{-1}).

5.3 Conclusions

To expand the scope and limit of phosphoric acid-catalyzed ring-opening polymerization (ROP), the author demonstrated bis(4-nitrophenyl) phosphate (BNPP) as an efficient organocatalyst for the controlled/living ring-opening polymerization (ROP) of *β*-butyrolactone (*β*-BL). The introduction of the nitro group into diphenyl phosphate (DPP) enhanced the acidity of BNPP, resulting in a suitable catalytic ability for the ROP of *β*-BL. BNPP possessed a dual activation ability for *β*-BL along with its polymer chain-end leading to the selective *O*-acyl cleavage of *β*-BL, and the polymer structure and molecular weight were controlled though the acidity of BNPP was weaker than TfOH. The BNPP-catalyzed ROP system was versatile for the synthesis of end-fuctionalized poly(*β*-butyrolactone)s (PBLs) using functional alcohol initiators having clickable and vinyl moieties. Furthermore, the diblock copolymers containing PBL could be produced by the BNPP-catalyzed ROP of *β*-BL with the sequential addition of *ε*-caprolactone or trimethylene carbonate as a second monomer, thanks to the maintaining chain-end structure of PBL and catalytic ability of BNPP.

5.4 Experimental Section

Materials. Toluene (>99.5 %; water content, <0.001 %, Kanto Chemical Co., Inc.) was distilled over sodium benzophenone ketyl under an argon atmosphere. 3-phenyl-1-propanol (PPA; >98%, Tokyo Kasei Kogyo Co., Ltd. (TCI)), propargyl alcohol (PGA; >98%, TCI), and *ε*-caprolactone (*ε*-CL; 99 %, TCI) were distilled over CaH_2 under an argon atmosphere. *β*-Butyrolactone (*β*-BL; 98 %, Sigma Aldrich) was distilled twice over CaH_2 under an argon atmosphere. 2-Hydroxyethyl methacrylate (HEMA; >95%, TCI) was distilled under reduced pressure. Trimethylene carbonate (TMC; >98%, TCI) was purified by recrystallization from dry toluene prior to use. 6-Azido-1-hexanol (AHA),[31] *N*-(2-hydroxyethyl)maleimide (HEMI),[23] and 4-vinylbenzyl alcohol (VBA)[32] were synthesized using previously reported methods. Ethyl DL-3-hydroxybutyrate (>98%, TCI), 2,3,4,5,6-pentafluorobenzyl alcohol (PFBA), diphenyl phosphate (DPP; >99%, TCI), bis(4-nitrophenyl) phosphate (BNPP; >98%, TCI), and a weak base anion exchange resin, Amberlyst A21 (Organo Co., Ltd.) were used as received. All other reagents were of synthetic grade and used without further purification.

Instruments. The number-average molecular weight ($M_{n,NMR}$) was determined from the ^{1}H NMR spectra recorded using a JEOL JNM-A400II instrument. The polymerization was carried out in an MBRAUN stainless steel glove box equipped with a gas purification system (molecular sieves and copper catalyst) in a dry argon atmosphere (H_2O, O_2 < 1 ppm). The moisture and oxygen contents in the glove box were monitored by an MB-MO-SE 1 and MB-OX-SE 1, respectively. The SEC in THF (1.0 mL·min^{-1}) was performed at 40 °C using a Jasco GPC-900 system equipped with a set of two Shodex KF-804L columns (linear, 8 mm × 300 mm). The polydispersity (M_w/M_n) of the polymers was calculated on the basis of a polystyrene calibration. Matrix-assisted laser desorption ionization time-of-flight mass spectrometry (MALDI-TOF MS) of the obtained polymers was performed using an Applied Biosystems

Voyager-DE STR-H equipped with a 337-nm nitrogen laser (3 ns pulse width). One hundred shots were accumulated for the spectra at a 25 kV acceleration voltage in the reflector mode and calibrated using polystyrene (average M_n 3600, Waters Associates) as the internal standard. Samples for the MALDI-TOF MS were prepared by mixing PBL (1.0 mg), a matrix (2,5-dihydroxybenzoic acid, 15 mg) and a cationizing agent (sodium trifluoroacetate, 1.0 mg) in THF (1.0 mL). The MALDI target was spotted with 0.5 μL of solution and allowed to air-dry.

Polymerization of *β*-Butyrolactone Using Bis(4-nitrophenyl) Phosphate. A typical procedure for the polymerization is as follows: *β*-BL (246 μL, 3.00 mmol) was added to a stock solution of PPA (60.0 μL, 60.0 μmol) in toluene at room temperature in the glove box. A toluene stock solution of BNPP (10.2 mg, 30.0 μmol) was then added to the solution and heated in an oil bath at 60 °C to initiate the polymerization under an argon atmosphere. After 4.5 h, the polymerization was quenched by the addition of Amberlyst A21. Before the addition of the Amberlyst A21, the author obtained a portion of the polymerization mixtures and then a small amount of triethylamine was added to the mixtures for determining the monomer conversion that was directly determined from the ^{1}H NMR measurements of the polymerization mixtures. The polymer was dialyzed against methanol for 1 day. Yield, 27.9 %; $M_{n,NMR}$, 3810 g·mol^{-1}; M_w/M_n, 1.19; ^{1}H NMR ($CDCl_3$) δ (ppm), 1.21, (m, 3H, -CH(C*H*$_3$)OH) 1.26 (m, 3H × *n-1*, (-C*H*$_3$)$_{n-1}$), 1.94 (q, 2H, *J* = 7.2, ArCH$_2$C*H*$_2$-), 2.42-2.63 (m, 2H, (-COC*H*$_2$-)$_n$), 2.67 (t, 2H, *J* = 7.2, ArC*H*$_2$-), 4.09 (t, 2H, *J* = 6.4, ArCH$_2$CH$_2$C*H*$_2$-), 4.19 (m, 1H, -C*H*(CH$_3$)OH), 5.24 (m, 1H × *n-1*, (-C*H*(CH$_3$)O-)$_{n-1}$), 7.16-7.30 (m, 5H, aromatic).

5.5 References and Notes

1. R. A. Gross, and B. Kalra, *Science* **2002**, *297*, 803-807.
2. C. Jerome, and P. Lecomte, *Adv. Drug Deliv. Rev.* **2008**, *60*, 1056-1076.
3. M. I. Sabir, X. Xu, and L. Li, *J. Mater. Sci.* **2009**, *44*, 5713-5724.
4. P. Dubois, O. Coulembier, and J.-M. Raquez, Eds., *Handbook of Ring-Opening Polymerizaion*, WHILEY-VCH, Weinheim, Germany, **2009**.
5. M. Okada, *Prog. Polym. Sci.* **2002**, *27*, 87-133.
6. P. J. Barham, A. Keller, E. L. Otun, and P. A. Holmes, *J. Mater. Sci.* **1984**, *19*, 2781-2794.
7. C. S. K. Reddy, R. Ghai, R. Rashmi, and V. C. Kalia, *Bioresource Technology* **2003**, *87*, 134-146.
8. K. Sudesh, H. Abe, and Y. Doi, *Prog. Polym. Sci.* **2000**, *25*, 1503-1555.
9. W. Amass, A. Amass, and B. Tighe, *Polymer International* **1998**, *47*, 89-144.
10. A.-C. Albertsson, and I. K. Varma, *Biomacromolecules* **2003**, *4*, 1466-1486.
11. O. Coulembier, P. Degee, J. L. Hedrick, and P. Dubois, *Prog. Polym. Sci.* **2006**, *31*, 723-747.
12. S. Slomkowski, and S. Penczek, *Macromolecules* **1976**, *9*, 367-369.
13. Z. Jedlinski, M. Kowalczuk, W. Glowkowski, J. Grobelny, and M. Szwarc, *Macromolecules* **1991**, *24*, 349-352.
14. L. R. Rieth, D. R. Moore, E. B. Lobkovsky, and G. W. Coates, *J. Am. Chem. Soc.* **2002**, *124*, 15239-15248.
15. J. W. Kramer, D. S. Treitler, E. W. Dunn, P. M. Castro, T. Roisnel, C. M. Thomas, and G. W. Coates, *J. Am. Chem. Soc.* **2002**, *124*, 15239-15248.

16. A. L. Borgne, V. Vincens, M. Jourlard, and N. Spassky, *Makromolekulare Chemie. Macromolecular Symposia* **1993**, *73*, 37-46.
17. J. E. Kemnitzer, S. P. McCarthy, and R. A. Gross, *Macromolecules* **1993**, *26*, 1221-1229.
18. M. K. Kiesewetter, E. J. Shin, J. L. Hedrick, and R. M. Waymouth, *Macromolecules* **2010**, *43*, 2093-2107.
19. N. E. Kamber, W. Jeong, R. M. Waymouth, R. C. Pratt, B. G. G. Lohmeijer, and J. L. Hedrick, *Chem. Rev.* **2007**, *107*, 5813-5840.
20. A. P. Dove, *Macro Lett.* **2012**, *1*, 1409-1412.
21. Coulembier, L. Mespouille, J. L. Hedrick, R. M. Waymouth, and P. Dubois, *Macromolecules* **2006**, *39*, 4001-4008.
22. Coulembier, X. Delva, J. L. Hedrick, R. M. Waymouth, and P. Dubois, *Macromolecules* **2007**, *40*, 8560-8567.
23. C. G. Jaffredo, J.-F. Carpentier, and S. M. Guillaume, *Polym. Chem.* **2013**, *4*, 3837-3850.
24. C. G. Jaffredo, J. –F. Carpentier, and S. M. Guillaume, *Macromol. Rapid Commun.* **2012**, *33*, 1938-1944.
25. C. G. Jaffredo, J. –F. Carpentier, and S. M. Guillaume, *Macromolecules* **2013**, *46*, 6765-6776.
26. F. A. Jaipuri, B. D. Bower, and N. L. Pohl, *Tetrahedron: Asymmetry* **2003**, *14*, 3249-3252.
27. A. Couffin, B. Martin-Vaca, D. Bourissou, and C. Navarro, *Polym. Chem.* **2014**, *5*, 161-168.
28. pK_a of BNPP was determined by previously reported methods. See ref 29.
29. P. Christ, A. G. Lindsay, S. S. Vormittag, J. M. Neudörfl, A. Berkessel, and A. M. C. O'Donoghue, *Chem. Eur. J.* **2011**, *17*, 8524-8528.

30. S. E. Denmark, D. Kalyani, and W. R. Collins, *J. Am. Chem. Soc.* **2010**, *132*, 15752-15765.
31. W. H. Heath, F. Palmieri, J. R. Adams, B. K. Long, J. Chute, T. W. Holcombe, S. Zieren, M. J. Truitt, J. L. White, and C. G. Willson, *Macromolecules* **2008**, *41*, 719−726.
32. J. G. Abramo, and E. C. Chapin, *J. Org. Chem.* **1961**, *26*, 2671–2673.

Chapter 6

Chiral Phosphoric Acid-Catalyzed Enantiomer-Selective Ring-Opening Polymerization of *rac*-Lactide

6.1 Introduction

Chiral Brønsted acids have been widely utilized for a number of enantioselective organic transformations via activation of a variety of functional groups.[1-3] Among the reported chiral Brønsted acids, binaphthol (BINOL)-derived monophosphoric acids ((*R*)-**1** in Figure 6.1),[2,3] which represent an important and widely applicable class of organocatalysts, have emerged as a powerful tool for enantioselective transformations, and significant progress has been made in their utilization as asymmetric-inducing agents via activation of various prochiral substrates.[4] The high enantioselectivities have been achieved by the desirable features of the BINOL-derived phosphoric acids as a chiral Brønsted acid catalyst;[3a] the ring structure of the phosphate ester with the substituents (G) at the 3,3'-position of the binaphthyl backbone as well as the acid and base dual function of the OH group and the phosphoryl oxygen, respectively, even for monofunctional phosphoric acid catalysts. An appropriate chiral environment for the enantioselective transformations can be created by these sterically, but also electronically adjustable substituents (G) coupled with the acid and base dual function.

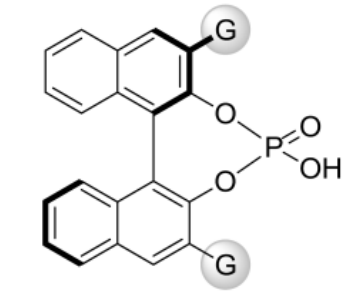

(*R*)-BINOL-derived
monophosphoric acid ((*R*)-**1**)

Figure 6.1. Structure of binaphthol (BINOL)-derived monophosphoric acid

For the polymer synthesis, organocatalytic asymmetric polymerization have been attracted attention, the accessible study is ring-opening polymerization of *rac*-lactide. As mentioned in

Chapter 1, PLA had been synthesized using organometallic catalyst/initiator having chiral or achiral ligand. On the other hand, several organocatalysts have been adopted for synthesis of stereoregulated polylactide (PLA).[5-9] For tailoring the physical properties including biodegradability and biocompatibility, the stereochemistry critically affected because the crystallinity and thermal property of polymeric materials changed. Whereas most of organocatalysts have the ability to polymerize *racemic* mixture of L-lactide (LLA) and D-lactide (DLA) leading to atactic PLA without any stereo control, some of metal-based catalysts were sufficient to produce stereocontrolled PLA, as shown in Figure 6.2.[10-17] For instance, Spassky introduced chiral Schiff-base into the Al complex for polymerization of *racemic*-lactide (*rac*-LA), which was first success of enantiomer-selective polymerization via kinetic resolution method.[12] The catalyst performed enantiomorphic site-control leading to kinetic resolution polymerization with a 20:1 preference for the polymerization of DLA against LLA, meaning that the selectivity factor s (= k_D/k_L)[13] was 20. Inspired by Spaskky's method, chiral and achiral Schiff-base system were widely reported, in particular, Feijen et al. demonstrated (*R*,*R*)-cyclohexanediamine Schiff-base complex showed relatively high enantiomer selectivity against LLA (k_L/k_D = 14).[14] These catalysts of *racemic* mixture formed stereoblock PLA via polymer exchange mechanism.[15, 16] In addition, achiral Al-based complex also produced isotacitic stereoblock PLA from *rac*-LA by chain-end control (P_m up to 0.79).[17, 18] Therefore, the organometallic catalysts successfully controlled stereochemistry of PLA via selective polymerization of *rac*-LA, but the contamination of the metal residue in biodegradable product was inevitable, which could causes the environmental problem.

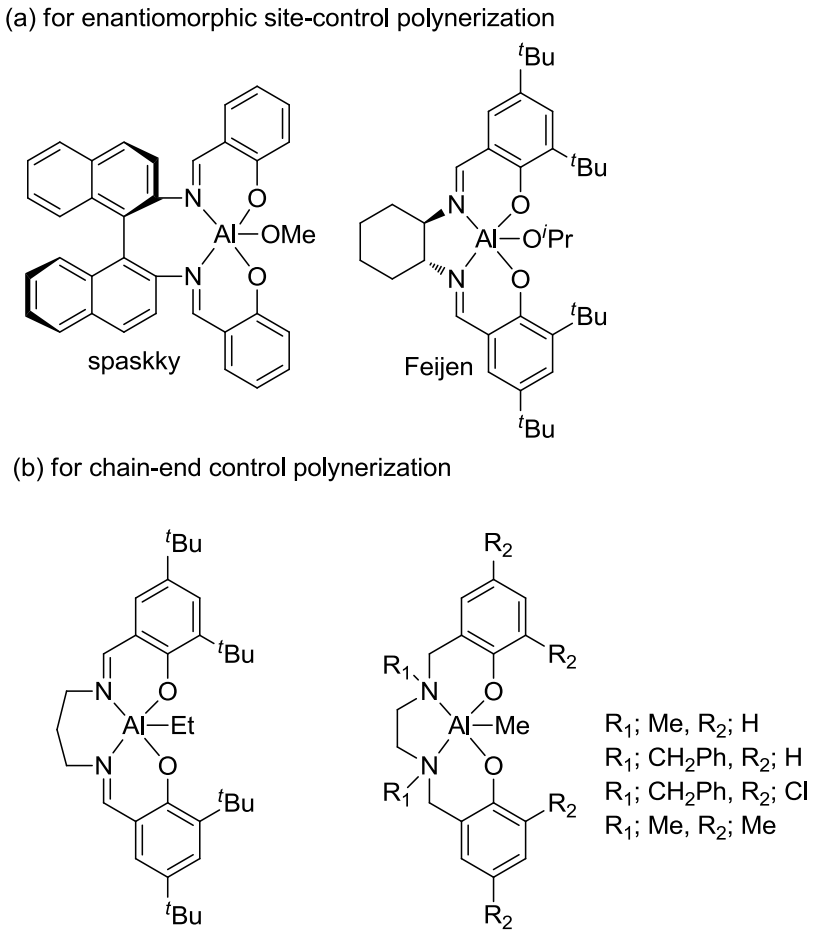

Figure 6.2. Organometalic catalysts for stereocontrolled ring-opening polymerization

For organocatalytic synthesis of stereocontrolled PLA, several challenges were mainly reported by Hedrick, e.g., *N*-heterocyclic carbene exhibited efficient stereo selectivity for ROP of *rac*-LA leading to isotactic PLA via chain-end control mechanism (P_m up to 0.90).[5] The phosphazene base-catalysed ROP of LA also utilized for the stereoselective polymerization without kinetic resolution (P_m up to 0.95).[6] Thus most of organocatalytic polymerization stereoselectively proceeded by chain-end control due to the coordination of the catalyst at the chain-end. On the other hand, kinetic resolution is one of the efficient methods to produce stereocomrtolled polymer via enantiomer-selective polymerization. As the only one example, cinchona alkaloid showed less enantiomer selectivity with the maximum selectivity factor

(k_L/k_D) of 4.4 at a 48.4 % monomer conversion.[8] Thus the challenging tasks still remained in the field of organocatalytic enantiomer-selective polymerization. To achieve the enantiomer-selective polymerization with a high selectivity, the author focused on the kinetic resolution method using chiral BINOL-derived monophosphoric acids ((*R*)-**1**), as shown in Scheme 6.1.

Scheme 6.1. Enantiomer-selective polymerization of *rac*-lactide catalyzed by chiral phosphoric acid

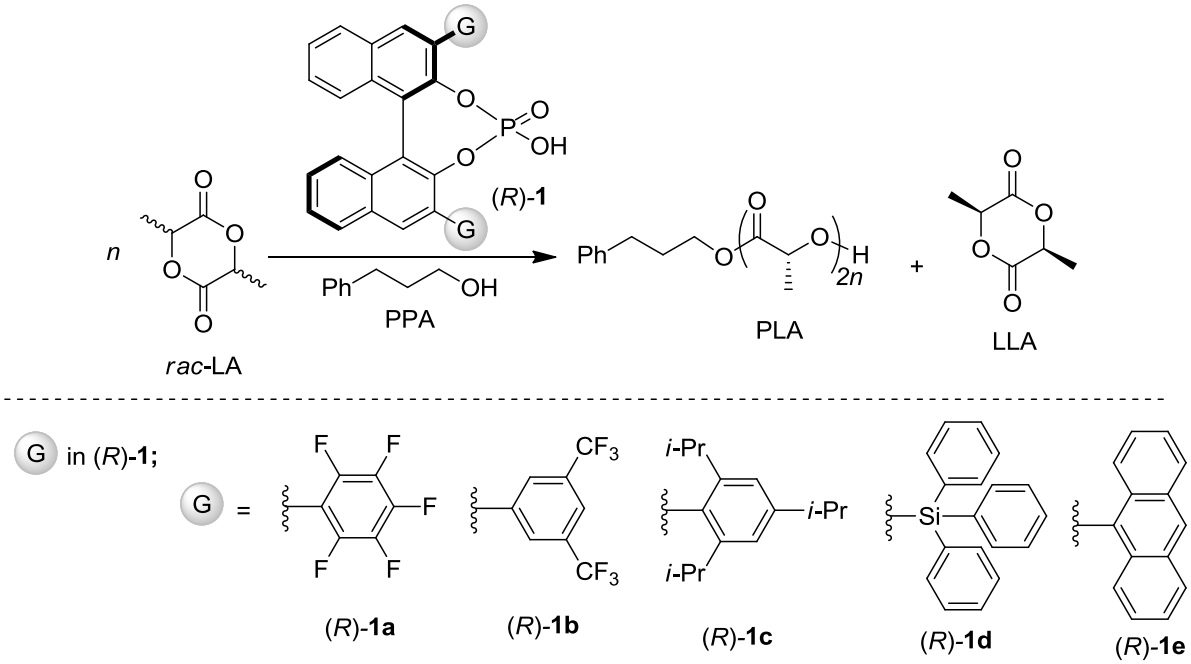

6.2 Results and Discussion

6.2.1 Enantiomer-Selective ROP of *rac*-LA Using Chiral Phosphoric Acid as an Organocatalyst. In order to obtain a high enantiomer-selectivity for the ring-opening polymerization (ROP) of *rac*-lactide (*rac*-LA) using (*R*)-**1**, the author first evaluated the substituent (G) effect of (*R*)-**1** (Scheme 6.1). The polymerization was conducted using 3-phenyl-1-propanol (PPA) as the initiator and (*R*)-**1a-c** as a catalyst with the initial monomer-to-initiator ratio of $[rac\text{-LA}]_0/[\text{PPA}]_0$ = 50 (Table 6.1, runs 3, 8, and 10). All the polymerizations homogeneously proceeded at 75 °C and the monomer conversions reached ca. 50 % within 18 h. After quenching the polymerization, the residual monomer was recovered as the hexane/isopropanol soluble part and the enantiomeric excess (*ee*) of the unreacted monomer was determined by a chiral HPLC measurement. The chromatograms strongly suggested that D-lactide (DLA), one of the enantiomers, was preferentially polymerized by the effect of these catalysts, resulting that the calculated *ee* values were 80.6, 62.3, and 0.09 for the (*R*)-**1a**, **1b**, and **1c**-catalyzed system, respectively (Figure 6.3). These results indicated that the electronic nature of the substituent (G) strongly influenced the *ee* compared to the steric hindrance; the highest *ee* was achieved by (*R*)-**1a**. Actually, other chiral phosphoric acid having bulky substituent ((*R*)-**1d, 1e**) showed less or no enantiomer-selectivity (Table 6.1, runs 11 and 12), meaning that steric hindrance less influenced the ROP of *rac*-LA. On the other hand, the acidity of chiral phosphoric acids strongly enhanced the enantiomer-selectivity, i.e., highly acidity of (*R*)-**1a** (pK_a = 1.76)[19] led preferred results compared with that using (*R*)-**1b** (pK_a = 2.63).[20]

Table 6.1. Enantiomer-selective ring-opening polymerization (ROP) of *rac*-lactide (*rac*-LA) using (*R*)-**1** as an organocatalyst [a]

run	catalyst	[*rac*-LA]$_0$ /[PPA]$_0$	temp (°C)	time (h)	conv. (%) [b]	$M_{n,calcd}$ (g mol^{-1}) [c]	$M_{n,NMR}$ (g mol^{-1}) [b]	M_w/M_n [d]	*ee* (%) [e]	k_D/k_L [f]
1 [g]	(*R*)-**1a**	50	60	24	51.4	3840	1780	1.16	24.4	1.99
2 [g]		50	70	24	52.1	3890	4130	1.11	35.6	2.73
3		50	75	18	49.0	3670	3730	1.13	80.6	28.3
4		50	80	15	49.2	3680	3810	1.08	74.8	17.3
5		50	90	12	54.4	4060	3950	1.11	74.9	9.60
6		100	75	90	50.0	7340	7290	1.09	73.1	13.9
7 [g]	(*R*)-**1b**	50	70	24	49.9	3730	3610	1.13	22.2	1.92
8		50	75	18	45.7	3430	3310	1.16	62.3	12.6
9 [g]	(*R*)-**1c**	50	70	24	50.4	3770	4170	1.11	5.22	1.16
10		50	75	18	56.1	4180	3660	1.06	0.09	1.00
11	(*R*)-**1d**	50	75	72	37.2	2800	3000	n.d. [h]	0.00	1.00
12	(*R*)-**1e**	50	75	15	39.2	3000	1800	n.d. [h]	12.0	1.63

[a] Solvent, toluene; initiator (I), 3-phenyl-1-propanol; [*rac*-LA]$_0$/[PPA]$_0$/[(*R*)-**1**]$_0$, 50/1/1; [*rac*-LA]$_0$, 3.0 mol L^{-1}. [b] Determined by ^{1}H NMR in $CDCl_3$. [c] Calculated from ([*rac*-LA]$_0$/[PPA]$_0$) × conv. × (M.W. of *rac*-LA) + (M.W. of PPA). [d] Determined by SEC in $CHCl_3$ using PSt standards. [e] Enantiomeric excess of unreacted monomer measured by chiral HPLC. [f] Calculated from {ln[(1-conv.)(1-*ee*)]}/{ln[(1-conv.)(1+*ee*)]}. [g] Partially insoluble in toluene. [h] Not determined.

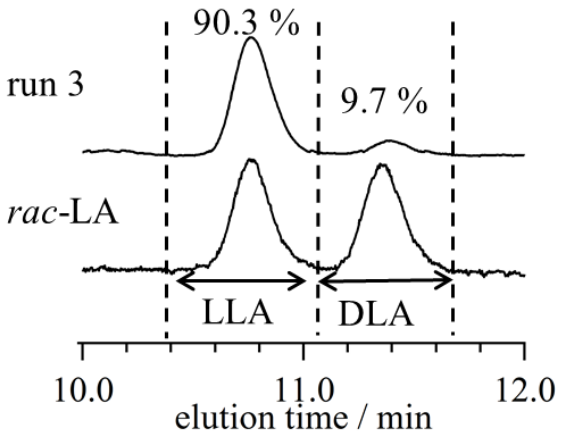

Figure 6.3. HPLC chromatograms of unreacted monomer (Table 6.2, run 3, upper) and *rac*-LA as a reference (lower) determined by UV (254 nm) detector (Column, Chiralpak IA; flow rate, 0.5 mL min^{-1}; eluent, hexane/isopropanol = 7/3; temperature; 25 °C).

For achieving high enantiomer-selectivity, the author carried out the ROP of *rac*-LA using (*R*)-**1a** at various temperatures, as listed in Table 6.1 runs 1-5. Based on the results, the *ee* strongly depended on the reaction temperature, and the high *ee* of 80.6 was observed at 75 °C, i.e., the enantiomer-selectivity was decreased with increasing of reaction temperature between 75 °C and 90 °C, which was same result as metal-catalysed enantiomer-selective polymerization. For considering the increase of selectivity between 70 °C and 75 °C, the solubility of monomer and catalyst critically influenced; actually, the polymerization heterogeneously proceeded at 60 °C and 70 °C leading to less controlled molecular weight accompanied with low enantiomer-selectivity. Thus the suitable reaction temperature should be selected for good solubility and enantiomer-selectivity. For the polymerization at 75 °C, the k_D/k_L was calculated to be 28.3, which was higher than the value obtained from the enantiomer-selective polymerization of *rac*-LA using a metal catalyst;[13-15] for instance, the chiral Schiff-base complex of Al as the representative metal catalysts led to a $k_D/k_L = 20$ via a kinetic resolution mechanism. Therefore, the (*R*)-**1a**-catalyzed enantiomer-selective ROP

could compete with the metal complex-catalyzed ROP, i.e., the chiral phosphoric acid–catalyzed system opened the door for the novel enantiomer-selective ROP as well as enantioselective organic transformations.

The kinetic study also supported the selective polymerization of DLA; the slope of time vs $\ln([LA]_0/[LA])$ plots for the ROP of DLA had more sharp angles compared to those of LLA and *rac*-LA (Figure 6.4). The result implied that the polymerization of DLA was faster than that of LLA because the catalytic ability of (*R*)-**1a** was different against each monomer.

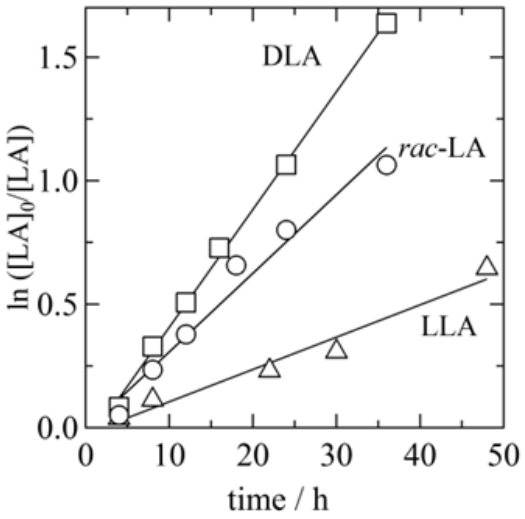

Figure 6.4. Kinetic plots for the polymerization of LLA, *rac*-LA and DLA at 75 °C in toluene with $[LA]_0/[PPA]_0/[(R)\text{-}\mathbf{1a}]_0 = 50/1/1$ and $[LA]_0 = 3.0$ mol L^{-1}.

6.2.2 Stereochemistry of the Obtained Poly(lactide) (PLA). For determining the chemical structure of the obtained polymer, the author measured the ^{1}H and ^{13}C NMR spectra (Figure 6.5). For ^{1}H NMR measurement, the characteristic peaks due to the polymer main chain and chain-end were clearly observed at 7.14 to 7.29, 5.10 to 5.23, 4.34, 4.14, 2.66, 1.95, and 1.57 ppm, respectively, which supported the fact that the chemical structure of the obtained polymer was assigned to the polylactide (PLA). Additionally, ^{13}C NMR spectrum also revealed the exact structure and showed isotactic enrichment of PLA (P_m up to 0.93),[21] which was elucidated by *mrm* tetrad peak of methine region, as shown in Figure 6.6. This result suggested that the obtained polymer was mainly composed of DLA. Size exclusion chromatography (SEC) for the obtained polymers showed monomodal shapes with the narrow polydispersity indices of 1.08-1.13 (Figure 6.7).

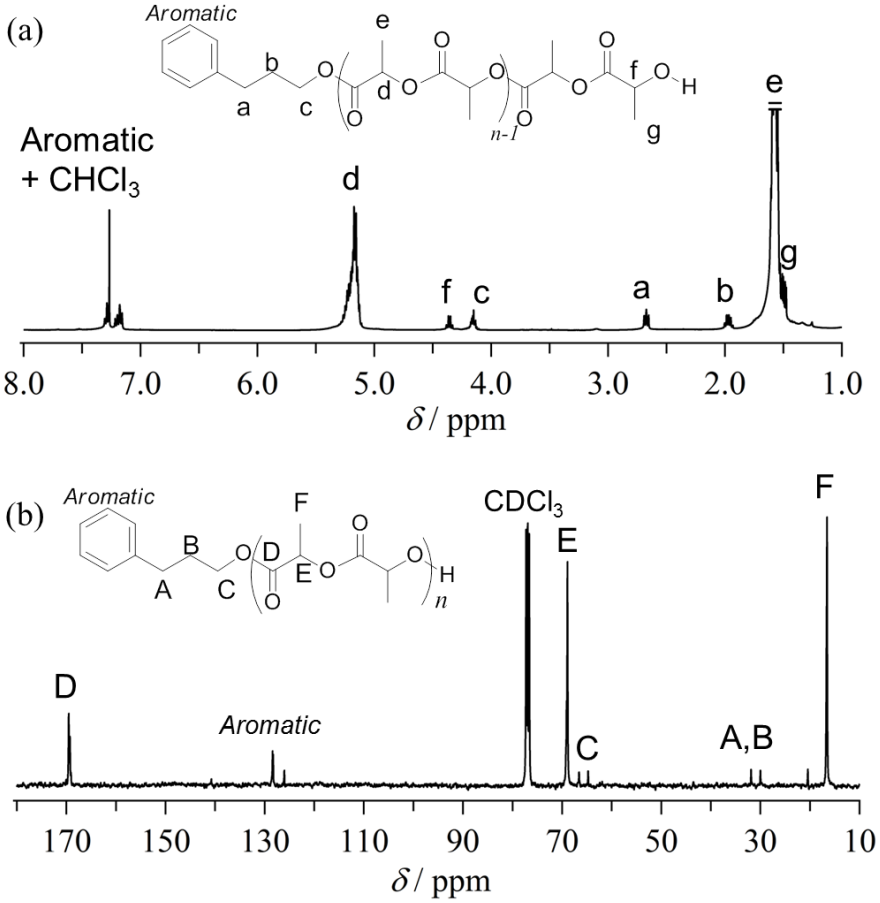

Figure 6.5. (a) ^{1}H (b) and ^{13}C NMR spectra of the obtained PLA (Table 6.2, run 6) ($CDCl_3$).

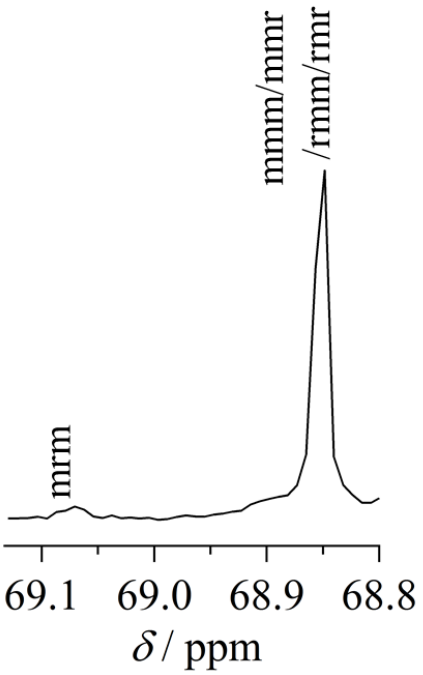

Figure 6.6. Methine region of ^{13}C NMR spectrum of the obtained PLA prepared with [*rac*-LA]$_0$/[PPA]$_0$ = 50 at 75 °C (conv., 37.1%; P_m, 0.93) (100 MHz, $CDCl_3$).

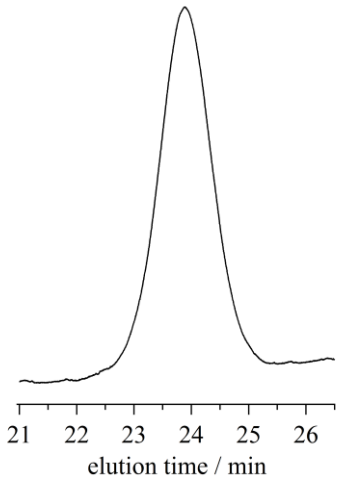

Figure 6.7. SEC trace of the obtained PLA (Table 6.2, run 6) (eluent, $CHCl_3$; flow rate, 0.8 mL min^{-1}).

In order to clarify the catalytic ability of (*R*)-**1a** under different polymerization conditions, the ROP of *rac*-LA was carried out at [*rac*-LA]$_0$/[PPA]$_0$ = 100 (Table 6.2, run 10). The *ee* of the unreacted monomer at a ca. 50 % monomer conversion was 73.1 % and the k_D/k_L was 13.9,

which suggested that the resulting polymer mainly consisted of DLA units and enantiomer-selective polymerization proceeded in different [*rac*-LA]$_0$/[PPA]$_0$ ratio. Furthermore, the tacticity of PLA was elucidated by the methine peaks in the homonuclear decoupled ^{1}H NMR and ^{13}C NMR spectra (Figure 6.8). The peaks were assigned to the appropriate tetrad conformation and the *mmm* tetrad peak proved the production of the highly isotactic PLA. As shown in Figure 6.8, the P_m for the obtained PLA was determined to be 0.73. More importantly, the number-average molecular weight ($M_{n,NMR}$) of the obtained polymer fairly well agreed with the calculated value ($M_{n,calcd}$); the $M_{n,NMR}$ and $M_{n,calcd}$ values were 3730 g mol^{-1} and 3670 g mol^{-1} for run 6., and 7290 g mol^{-1} and 7340 g mol^{-1} for run 10, respectively (Table 6.2). These results strongly suggested that the polymerization proceeded with not only an enantiomer-selective but also controlled/living fashion.

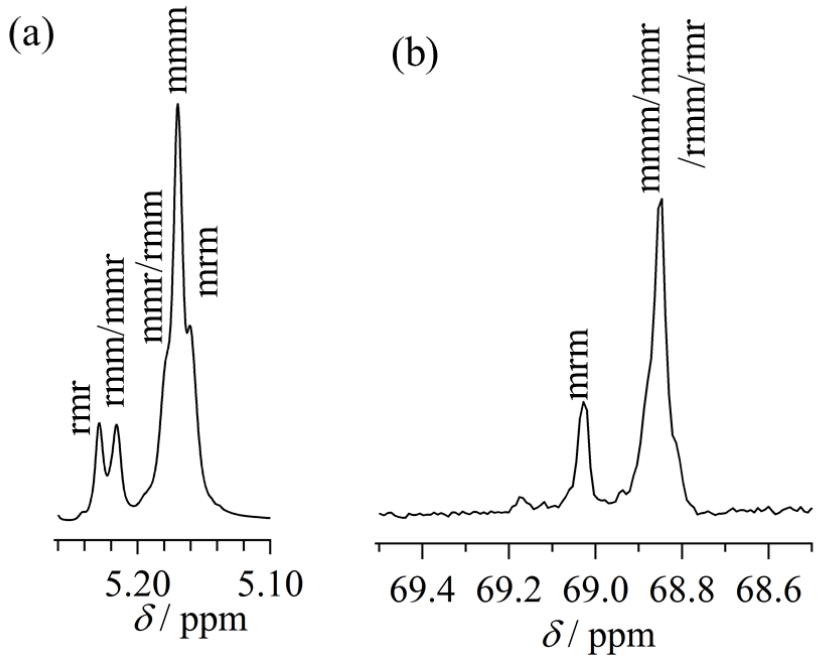

Figure 6.8. Methine region of (a) homonuclear decoupled ^{1}H NMR and (b) ^{13}C NMR spectra of the obtained polylactide prepared with [*rac*-LA]$_0$/[PPA]$_0$ = 50 at 75 °C (conv., 50.0 %; P_m, 0.73) ($CDCl_3$).

6.2.3 Mechanism of Chiral Phosphoric Acid-Catalyzed Enantiomer-Selective Polymerization. Chiral phosphoric acids were applied for wide range of asymmetric organic transformations because the characteristic features effectively worked for selective activation. Phosphoric acids have the two substrate recognition sites, i.e., Brønsted acidic site and Brønsted basic site; the hydroxyl proton has relatively strong acidity and acted as Brønsted acid for capturing the electrophilic components through H-bonding whereas the phosphoryl oxygen acted as Brønsted base for accepting the proton of the substrate. Thus the dual activation ability was the key role to achieve asymmetric reactions. In addition, chiral environment was constructed by ring structure of binaphtyl backbone and enantioselectivity was influenced by the 3,3'-substituents.

For the ROP of cyclic esters, fundamental reaction was Fisher esterification; nucleophilic oxygen of an alcohol attacked to the carbonyl carbon of the reactant via the activation of alcohol and/or carbonyl group. For phosphoric acid-catalyzed system, the polymerization should proceeded through dual activation of the carbonyl group of the monomer and hydroxyl group of the propagating chain-end, as shown in Scheme 6.2.

Scheme 6.2. The proposed polymerization mechanism of dual activation by (*R*)-**1a**

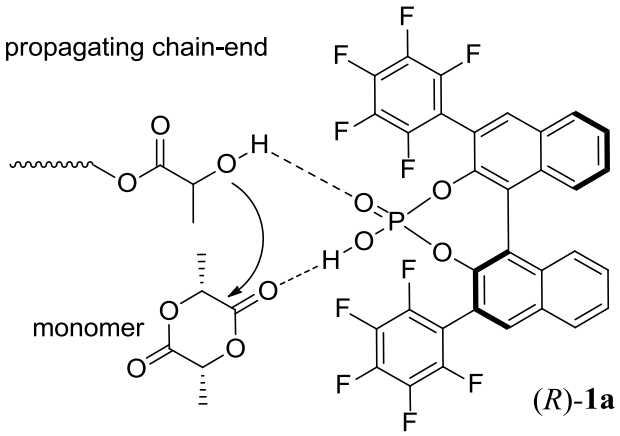

In order to clarify the catalytic performance of (*R*)-**1a**, the ^{13}C NMR spectra of LLA and DLA were measured in the absence/presence of (*R*)-**1a** ([LA]/[(*R*)-**1a**] = 1.0 and 3.0) (Figure 6.9).[22-24] The chemical shift for the carbonyl carbon of DLA at 166.55 ppm shifted to lower field at 166.58 and 166.61 ppm for [LA]/[(*R*)-**1a**] = 1.0 and 3.0, respectively, corresponding to the interaction between DLA and (*R*)-**1a**, whereas upper field shift was observed for LLA in the presence of (*R*)-**1a**. Thus the carbonyl activation of DLA was strongly suggested and the polymerization of DLA was preferentially induced by the enantiomer-selective monomer activation. The carbonyl activation of DLA was also investigated by IR spectroscopy with the [LA]/[(*R*)-**1a**] ratio was 1/1; the carbonyl vibration was observed at lower wavenumber after the addition of catalyst (Figure 6.10).

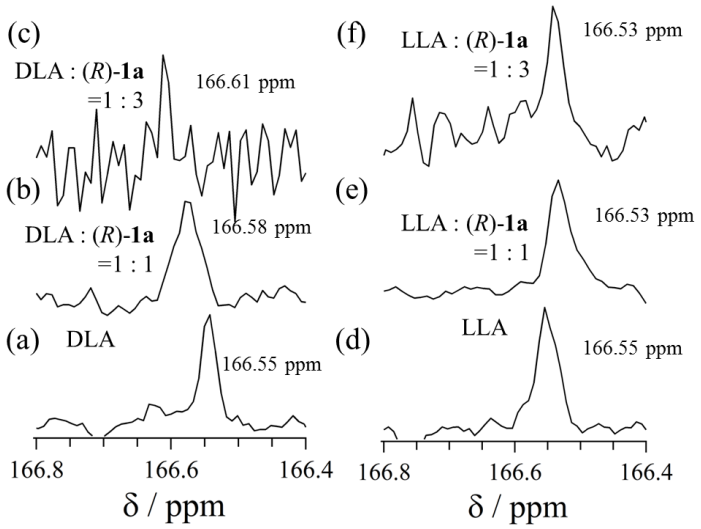

Figure 6.9. ^{13}C NMR spectra of the carbonyl carbon signals of (a) DLA, (b) a 1:1 mixture of DLA and (*R*)-**1a**, (c) 1:3 mixture of DLA and (*R*)-**1a**, (d) LLA, (e) a 1:1 mixture of LLA and (*R*)-**1a**, and (f) 1:3 mixture of LLA and (*R*)-**1a** at 75 °C in toluene-d_8.

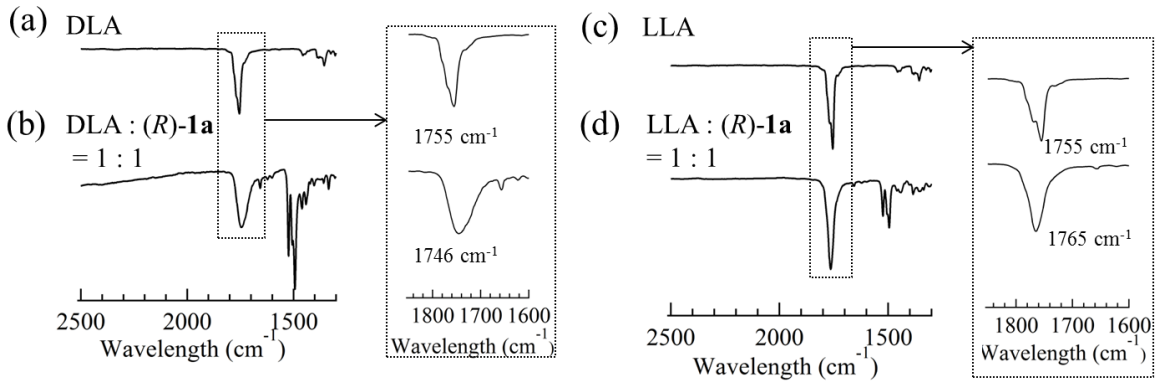

Figure 6.10. IR spectra of (a) DLA, (b) a 1:1 mixture of DLA and (*R*)-**1a**, (c) LLA and (d) a 1:1 mixture of LLA and (*R*)-**1a**.

On the other hand, the activation of the propagating chain-end was observed by the ^{1}H NMR and IR analysis for methyl (*R*)-DL-lactate, which was used as a model of the polymer chain-end, with/without (*R*)-**1a**. For ^{1}H NMR measurement, hydroxyl proton signal was shifted to lower field due to the activation in the presence of (*R*)-**1a** (Figure 6.11). The IR spectroscopy also supported the results because the hydroxyl group appeared at lower wavenumber compared with that of the original methyl DL-lactate (Figure 6.12), which implied that the phosphoryl oxygen acted as proton acceptor and the hydroxyl proton of the propagating chain-end was activated through H-bonding.

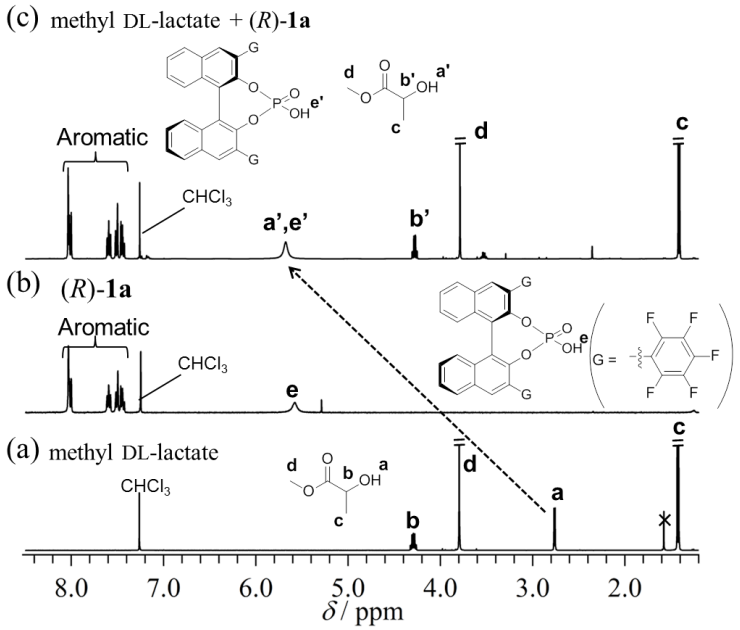

Figure 6.11. ^{1}H NMR spectra of the hydroxyl proton signals for (a) methyl DL-lactate, (b) (*R*)-**1a**, and (c) the 1:1 mixture of methyl DL-lactate with (*R*)-**1a** (400 MHz, $CDCl_3$).

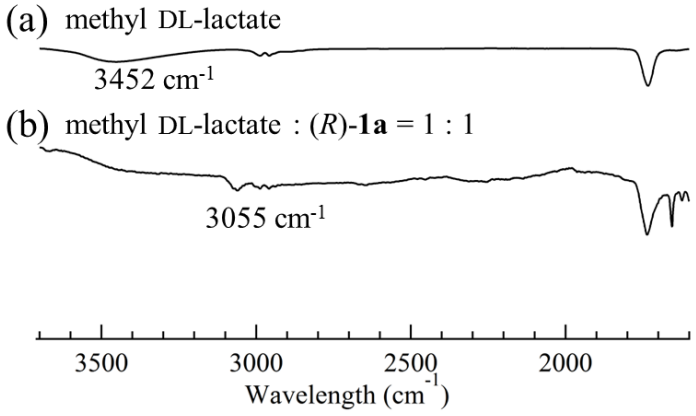

Figure 6.12. IR spectra of (a) (a) methyl DL-lactate and (b) the 1:1 mixture of methyl DL-lactate with (*R*)-**1a**.

Therefore, the polymerization mechanism was assigned to the enantiomer-selective monomer activation accompanied with chain-end activation, which indicated that (*R*)-**1a**

preferentially promoted the polymerization of DLA via dual activation due to the function of Brønted acidic site and Brønsted basic site of the catalyst.

6.3 Conclusions

In conclusion, the author achieved the high enantiomer-selectivity for the polymerization of *rac*-lactide (*rac*-LA) using chiral phosphoric acid, which is one of the well-known organocatalysts. Actually, the ring-opening polymerization (ROP) of D-lactide (DLA) preferentially proceeded using (*R*)-**1a** at 75 °C, and the selectivity factor (k_D/k_L) was 28.3 at a 49.0 % monomer conversion. To the best of our knowledge, this was highest value for the enantiomer-selective ROP of *rac*-LA. For the reaction mechanism, the polymerization should have proceeded by dual activation of the monomer and chain-end due to the function of the chiral phoshphoric acid catalyst, and the selective activation contributed to achieve the high k_D/k_L. This strategy for the organocatalytic enantiomer-selective ROP promises to be a new method for synthesizing various stereocontrolled polymers via the selective activation of a monomer and/or propagating chain-end.

6.4 Experimental Section

Materials. Toluene (>99.5 %; water content, <0.001 %, Kanto Chemical Co., Inc.) was distilled over sodium benzophenone ketyl under an argon atmosphere. *rac*-Lactide (*rac*-LA; >98%, Tokyo Kasei Kogyo Co., Ltd. (TCI)), L-lactide (LLA; >98%, TCI) and D-lactide (DLA; >99%, Musashino Chemical Co. Ltd.) were purified by two recrystallizations from dry toluene before use. 3-Phenyl-1-propanol (PPA; >98%, TCI) was distilled over CaH_2 under an argon atmosphere. (*R*)-3,3'-bis(pentafluorophenyl)-1,1'-binaphtyl-2,2'-diyl-hydrogenphosphate ((*R*)-**1a**) was synthesized via previously reported technique.[25] (*R*)-3,3'-bis[3,5-bis(trifluoromethyl)phenyl]-1,1'-binaphtyl-2,2'-diyl-hydrogenphosphate ((*R*)-**1b**; 95%, Sigma Aldrich), (*R*)-3,3'-bis(2,4,6-triisopropylphenyl)-1,1'-binaphtyl-2,2'-diyl-hydrogenphosphate ((*R*)-**1c**; >97.5%, Sigma Aldrich), (*R*)-3,3'-bis(triphenylsilyl)-1,1'-binaphtyl-2,2'-diyl-hydrogenphosphate ((*R*)-**1d**; >96%, Sigma Aldrich), (*R*)-3,3'-bis(9-anthracenyl)-1,1'-binaphtyl-2,2'-diyl-hydrogenphosphate ((*R*)-**1e**; 95%, Sigma Aldrich), and a weak base anion exchange resin, Amberlyst A21 (Organo Co., Ltd.) were used as received. All other reagents were of synthetic grade and used without further purification.

Instruments. The number-average molecular weight ($M_{n,NMR}$) was determined from the ^1H NMR spectra recorded using a JEOL JNM-A400II instrument. The polymerization was carried out in an MBRAUN stainless steel glove box equipped with a gas purification system (molecular sieves and copper catalyst) in a dry argon atmosphere (H_2O, O_2 <1 ppm). The moisture and oxygen contents in the glove box were monitored by an MB-MO-SE 1 and an MB-OX-SE 1, respectively. The size exclusion chromatography (SEC) was performed at 40 °C in $CHCl_3$ (0.8 mL·min^{-1}) using a Jasco GPC-900 system equipped with a set of two Shodex KF-805L columns (linear, 8 mm × 300 mm). The polydispersity index (M_w/M_n) of the

polymers was calculated on the basis of a polystyrene calibration. The preparative SEC was performed in $CHCl_3$ (3.5 mL·min^{-1}) at 23 °C using a JAI LC-9201 equipped with a JAI JAIGEL-3H column (20 mm × 600 mm; exclusion limit, 7 × 10^4) and a JAI RI-50s refractive index detector.

Polymerization of *rac*-lactide (*rac*-LA) catalyzed by *(R)*-3,3'-bis(pentafluorophenyl)-1,1'-binaphtyl-2,2'-diyl-hydrogenphosphate (*(R)*-1).

A typical procedure for the polymerization is as follows: rac-LA (288 mg, 2.0 mmol) and *(R)*-1 (13.6 mg, 20.0 μmol) were added in toluene (0.646 mL), a stock solution of PPA (20.0 μL, 20.0 μmol) then added to initiate the polymerization under an argon atmosphere at 75 °C in oil bath. After 90 h, the polymerization was quenched by the addition of Amberlyst A21. Before the addition of the Amberlyst A21, the author obtained a portion of the polymerization mixtures and then added a small amount of triethylamine to the mixtures for determining the monomer conversion that was directly determined by the ^{1}H NMR measurements of the polymerization mixtures. The polymer was isolated by preparative SEC (eluent, $CHCl_3$) to remove the remaining residue. Yield, 34.1 %; $M_{n,NMR}$, 7,340 g·mol^{-1}; M_w/M_n, 1.09; ^{1}H NMR ($CDCl_3$) δ (ppm), 1.57 (m, 3H × *n*, $(\text{-}CH_3)_n$), 1.95 (q, 2H, *J* = 8.8, $ArCH_2CH_2$-), 2.66 (t, 2H, *J* = 8.0, $ArCH_2$-), 4.14 (m, 2H, $ArCH_2CH_2CH_2$-), 4.34 (q, 1H, *J* = 6.8, -$CH(CH_3)OH$), 5.10-5.25 (m, 1H × *n-1*, , $(\text{-}CH(CH_3)O\text{-})_{n-1}$), 7.13-7.30 (m, 5H, aromatic).

HPLC measurement

For determining of the enantiomer ratio of unreacted monomer after the polymerization, the recovered materials were measured by chiral HPLC. The quenched compounds were evaporated to remove the solvent, and the unreacted monomer was collected as hexane/isopropanol = 1/1 soluble part. The HPLC measurement for the unreacted monomer was carried out using hexane/isopropanol (7/3) (column, Chiralpak IA; flow, 0.5 mL·min^{-1})

and the enantiomeric excess (*ee*) of unreacted monomer was determined from the ratio of peak areas. The selectivity factor (k_D/k_L) was equated as k_D/k_L = {ln[(1-conv.)(1-*ee*)]}/{ln[(1-conv.)(1+*ee*)]}.

6.5 References and Notes

1. For reviews on chiral Brønsted acid catalysis, see: a) Akiyama, T. *Chem. Rev.* **2007**, *107*, 5744-5758; b) Akiyama, T.; Itoh, J.; Fuchibe, K. *Adv. Synth. Catal.* **2006**, *348*, 999-1010; c) Taylor, M. S.; Jacobsen, E. N. *Angew. Chem. Int. Ed.* **2006**, *45*, 1520-1543; d) Doyle, A. G.; Jacobsen, E. N. *Chem. Rev.* **2007**, *107*, 5713-5743; e) Yamamoto, H.; Payette, N. In *Hydrogen Bonding in Organic Synthesis* (Ed.: Pihko, P. M.), Wiley-VCH: Weinheim, **2009**, pp 73-140; f) Kampen, D.; Reisinger, C. M.; List, B. *Top. Curr. Chem.* **2010**, *291*, 395-456.
2. For seminal studies, see: a) Akiyama, T.; Itoh, J.; Yokota, K.; Fuchibe, K. *Angew. Chem. Int. Ed.* **2004**, *43*, 1566-1568; b) Uraguchi, D.; Terada, M. *J. Am. Chem. Soc.* **2004**, *126*, 5356-5357.
3. For reviews on BINOL-derived phosphoric acids, see: a) Terada, M. *Chem. Commun.* **2008**, 4097-4112; b) Terada, M. *Synthesis* **2010**, 1929-1982; c) Terada, M. *Bull. Chem. Soc. Jpn.* **2010**, 101-119; d) Zamfir, A.; Schenker, S.; Freund, M.; Tsogoeva, S. B. *Org. Biomol. Chem.* **2010**, *8*, 5262-5276; e) Terada, M. *Curr. Org. Chem.* **2011**, *15*, 2227-2256; f) Akiyama, T. in *Science of Synthesis, Asymmetric Organocatalysis 2, Brønsted Base and Acid Catalysts, and Additional Topics*, (Ed.: Maruoka, K.), Georg Thieme Verlag KG, New York, **2012**, pp.169-217; g) Terada, M.; Momiyama, N. in *Science of Synthesis, Asymmetric Organocatalysis 2, Brønsted Base and Acid Catalysts, and Additional Topics,* (Ed.: Maruoka, K.), Georg Thieme Verlag KG, New York, **2012**, pp.219-278.
4. For the activation of a racemic mixture of chiral substrates, see: a) Hoffmann, S.; Nicoletti, M.; List, B. *J. Am. Chem. Soc.* **2006**, *128*, 13074-13075; b) Cheng, X.; Goddard, R.; Buth, G.; List, B. *Angew. Chem., Int. Ed.* **2008**, *47*, 5079-5081; c) Akiyama, T.; Katoh,

T.; Mori, K. *Angew. Chem., Int. Ed.* **2009**, *48*, 4226-4228; d) Han, Z.-Y.; Xiao, H.; Gong, L.-Z. *Bioorg. Med. Chem. Lett.* **2009**, *19*, 3729-3732; e) Sun, F.-L.; Zheng, X.-J.; Gu, Q.; He, Q.-L.; You, S.-L. *Eur. J. Org. Chem.* **2010**, 47-50; f) Čorić, I.; Müller, S.; List, B.; *J. Am. Chem. Soc.* **2010**, *132*, 17370-17373. Also see, g) Terada, M.; Machioka, K.; Sorimachi, K. *Angew. Chem. Int. Ed.* **2009**, *48*, 2553-2557; h) Terada, M.; Toda, Y. *J. Am. Chem. Soc.* **2009**, *131*, 6354-6355; i) Rueping, M.; Nachtsheim, B. J. *Synlett* **2010**, 119-122; j) Terada, M.; Moriya, K.; Kanomata, K.; Sorimachi, K. *Angew. Chem. Int. Ed.* **2011**, *50*, 12586-12590; k) Terada, M.; Yamanaka, T.; Toda, Y. *Chem. Eur. J.* **2013**, *41*, 13658-13662.

5. Dove, A. P.; Li, H.; Pratt, R. C.; Lohmeijer, B. G. G.; Culkin, D. A.; Waymouth, R. M.; Hedrick, J. L. *Chem. Commun.***2006**, 2881-2883.

6. Zhang, L.; Nederberg, F.; Messman, J. M.; Pratt, R. C.; Hedrick, J. L.; Wade, C. G. *J. Am. Chem. Soc.* **2007**, *129*, 12610-12611.

7. Pratt, R. C.; Lohmeijer, B. G. G.; Long, D. A.; Lundberg, P. N. P.; Dove, A. P.; Li, H. B.; Wade, C. G.; Waymouth, R. M.; Hedrick, J. L. *Macromolecules* **2006**, *39*, 7863-7871.

8. Miyake, G. M.; Chen, E. Y. X. *Macromolecules*, **2011**, *44*, 4116-4124.

9. Zhang, L.; Pratt, R. C.; Nederberg, F.; Horn, H. W.; Rice, J. E.; Waymouth, R. M.; Wade, C. G.; Hedrick, J. L. *Macromolecules* **2010**, *43*, 1660-1664.

10. Thomas, C. M. *Chem. Soc. Rev.* **2010**, *39*, 165-173.

11. Stanford, M. J.; Dove, A. P. *Chem. Soc. Rev.* **2010**, *39*, 486-494.

12. Spassky, N.; Wisniewski, M.; Pluta, C.; Le Borgne, A. *Macromol. Chem. Phys.* **1996**, *197*, 2627-2637.

13. k_L/k_D or k_D/k_L is the selectivity factor, which is defined as the ratio of the relative rates of reaction for the two enantiomers.

14. Zhong, Z.; Dijkstra, P. J.; Feijen, J. *Angew. Chem., Int. Ed.* **2002**, *41*, 4510- 4513.

15. Ovitt, T. M.; Coates, G. W. *J. Polym. Sci., Part A: Polym. Chem.* **2000**, *38*, 4686-4692.

16. Ovitt, T. M.; Coates, G. W. *J. Am. Chem. Soc.* **2002**, *124*, 1316-1326.

17. Nomura, N.; Ishii, R.; Akakura M.; Aoi, K. *J. Am. Chem. Soc.* **2002**, *124*, 5938-5939.

18. Hormnirun, P. ; Marshall, E. L., Gibson, V. C.; White, A. J. P.; Williams, D. J. *J. Am. Chem. Soc.* **2004**, *126*, 2688-2689.13, 14

19. pK_a of (*R*)-**1a** was determined by previously reported methods. See ref 20.

20. Christ, P.; Lindsay, A. G.; Vormittag, S. S.; Neudörfl, J.-M.; Berkessel, A.; O'Donoghue, A. M. C. *Chem. Eur. J.* **2011**, *17*, 8524-8528.

21. The probability of meso linkage (P_m) was equated from the methie region of ^{13}C NMR spectrum: [*mmm*] = $P_m(P_m+1)/2$; [*mmr*] = $P_m(1-P_m)/2$; [*rmm*] = $P_m(1-P_m)/2$; [*rmr*] = $(1-P_m)^2/2$; [*mrm*] = $(1-P_m)/2$.

22. Coulembier, O.; Sanders, D. P.; Nelson, A.; Hollenbeck, A. N.; Horn, H. W.; Rice, J. E.; Fujiwara, M.; Dubois, P.; Hedrick, J. L. *Angew. Chem. Int. Ed.* **2009**, *48*, 5170-5173.

23. Chen, J.; Kan, S.; Xia, H.; Zhou, F.; Chen, X.; Jiang, X.; Guo, K.; Li, Z. *Polymer* **2013**, *54*, 4177-4182.

24. Kan, S.; Jin, Y.; He, X.; Chen, J.; Wu, H.; Ouyang, P.; Guo, K.; Li, Z. *Polym. Chem.* **2013**, *4*, 5432-5439.

25. N. Momiyama, H. Nishimoto, M. Terada, *Org. Lett.,* **2011**, *13*, 2126-2129.

Chapter 7

Conclusions

In this thesis, the author describes the efficient catalytic ability of an organic acid for the ring-opening polymerization of cyclic monomers such as *δ*-valerolactone, *ε*-caprolactone, trimethylene carbonate, lactide, and *β*-butyrolactone. Super Brønsted acid-catalyzed ring-opening polymerizations were conducted to evaluate the effect of the catalyst acidity for monomer activation and the results showed that tuning the acidity of the catalysts is sufficient to expand the applicable monomers. On the other hand, simultaneous activation (dual activation and bifunctional activation) of the monomer and initiator/propagating chain-end was the focus. Diphenyl phosphate has two activation sites in one molecule and the polymerizations of *δ*-valerolactone, *ε*-caprolactone, and trimethylene carbonate proceeded via a dual activation. The L-lactide was also polymerized in the presence of diphenyl phosphate/4-dimethylaminopyridine via bifunctional activation, which was generated by the addition of 4-dimethylaminopyridine as the co-catalyst. All the polymerizations showed a controlled/living nature and the versatility of diphenyl phosphate was proved by the synthesis of functionalized polymers and diblock copolymers. Furthermore, the introduction of a nitro group to diphenyl phosphate enhanced the acidity leading to the successful controlled polymerization of *β*-butyrolactone via dual activation. Dual activation with an acidity enhancement was also sufficient to polymerize *ε*-caprolactone and L-lactide. As another substituent effect, the chiral phosphoric acid, which consisted of a binaphthyl group and phosphoric acid, showed an enantiomer-selectivity during the polymerization of *rac*-lactide. The polymerization of D-lactide preferentially proceeded with maximum selectivity factor of 28.3. Therefore, the author first discovered the versatility of the organic acid-catalyzed polymerization of cyclic monomers, which should contribute to future studies for developing the organocatalytic synthesis of a wide-range of polymers.

A summary of this thesis is as follows:

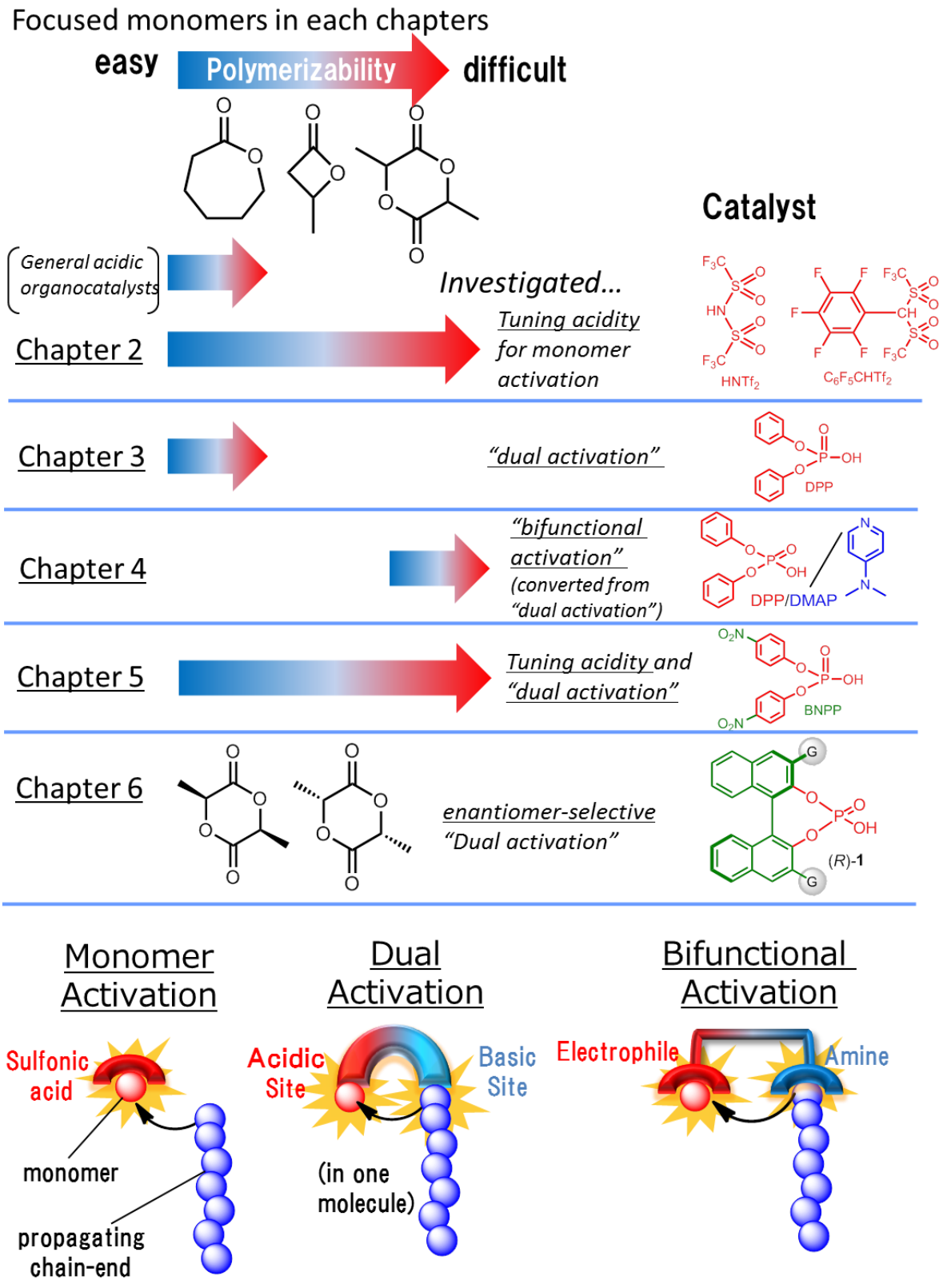

Chart 7.1. Overview and summary of the thesis.

In chapter 2, the super Brønsted acid, such as triflimide and pentafluorophenylbis(triflyl)methane, showed a strong monomer activation ability leading to the production of poly(δ-valerolacton) and poly(ε-caprolactone) with a shorter polymerization time and low catalyst loading. The molecular weight was controlled up to 10000 g mol^{-1}, and polydispersity indices were relatively narrow. In addition, the extreme acidity of triflimide was sufficient to activate and polymerize other cyclic monomers such as the lactide and β-butyrolactone, which were less polymerizable by the acid-catalyzed ROP. The NMR measurement supported the fact that the monomer activation using an organic acid whereas another activation was not confirmed. Furthermore, end-functionalized polyesters could be produced using functional initiators having polymerizable and clickable group.

In chapter 3, to approach the organic acid-catalyzed ROP from another direction, the author focused on the combination of the Brønsted acid/base activation of diphenyl phosphate. The diphneyl phosphate-catalyzed polymerization of δ-valerolactone, ε-caprolactone, and trimethylene carbonate proceeded in a controlled/living nature via dual activation of the monomer and propagating chain-end. The high molecular weight polyesters could be obtained under moderate conditions, and poly(trimethylene carbonate) was synthesized without decarboxylation due to its lower acidity. The end-functionalized polymers were also produced using the functional initiators, and the side-chain functionalized polycarbonates were obtained via the ROP of functionalized trimethylene carbonate. The polymerization of the cyclic ester-ether, which is an analog of ε-caprolactone, afforded the poly(ester-ether) with controlled weight. Furthermore, the one-pot diblock copolymerization of δ-valerolactone, ε-caprolactone, and trimethylene carbonate successfully proceeded regardless of the monomer addition order.

In chapter 4, based on the findings in chapter 3, the ring-opening polymerization of the lactide is described. In the presence of diphenyl phosphate with 4-dimethylaminopyridine, the polymerization of L-lactide proceeded and the obtained poly(L-lactide) had a controlled molecular weight and narrow polydispersity index whereas only the diphenyl phosphate could not produce the poly(L-lactide). NMR measurements revealed that the 1:1 mixture of diphenyl phosphate and 4-dimethylaminopyridine activated the monomer and another 4-dimethylaminopyridine activated the propagating chain-end. These results strongly suggested that the mechanism of the polymerization was bifunctional activation due to the combination of diphenyl phosphate and 4-dimethylaminopyridine. The system was also used for the synthesis of the end-functionalized poly(L-lactide)s using functional initiators. Furthermore, the diphenyl phosphate-catalyzed ROP could be easily reformed for the diphenyl phosphate/4-dimethylaminopyridine catalyzed ROP *in situ*, which successfully produced the diblock copolymers consisting of poly(δ-valerolactone), poly(ε-caprolactone), and poly(trimethylene carbonate) with poly(L-lactie) in one-pot.

In chapter 5, the possibility of tuning the phosphate catalysts by introduction of a nitro group was described. Bis(4-nitrophenyl) phosphate, which has a nitro group at the 4-position of the phenyl group on the diphenyl phosphate, showed a high acidity. The enhanced acidity is adequate to activate the β-butyrolactone, thus the polymerization was conducted under carefully optimized conditions. Although the polymerization should be quenched at an ca. 80 % monomer conversion to inhibit any side-reactions, the resultant polymer had a controlled molecular weight and exact structure. The dual activation mechanism was obviously confirmed by the NMR measurement. This system was sufficient to polymerize the

ε-caprolactone, trimethylene carbonate, and L-lactide under their own specific polymerization conditions.

In chapter 6, the enantiomer-selective polymerization of *rac*-lactide was evaluated using chiral phosphoric acid. The introduction of an axial chirality derived from the binaphthyl backbone constructed a chiral environment and the 3,3'-position of the substituent on the binaphthyl group strongly affected the selectivity. During the polymerization, the D-lactide was preferentially polymerized via kinetic resolution with the maximum selectivity factor of 28.3 at 75 °C using chiral phosphoric acid having a pentafluorophenyl group, whereas that having a bulky component showed a lower selectivity. These results suggested that the electron withdrawing group of the substituent strongly influenced the k_D/k_L compared to the steric hindrance. The obtained polymer was a well-defined polylactide with a controlled molecular weight and narrow polydispersity index, which indicated that the controlled/living polymerization occurred. In addition, isotactic enrichment of the resultant polymer that supported the enantiomer-selective polymerization occurred (the probability of meso linkage up to 0.93). The selective polymerization of the D-lactide was derived from the dual activation mechanism, i.e., enantiomer-selective monomer activation with chain-end activation, which was assigned by the NMR and IR analyses.